TRANSLATION OF SALIVARY GLAND CANCER TUMOR BIOLOGY TO THE CLINIC

GERBEN LASSCHE

Translation of salivary gland cancer tumor biology to the clinic

Gerben Lassche

The research presented in this thesis was carried out at the Radboud Institute for Health Sciences, Radboud University Medical Centre.
This work was financially supported by:

- The Dutch Salivary Gland Cancer Patient Network (Patiëntenvereniging Speekselklierkanker)
- The Radboud Oncology Fund (ROF)
- Bayer B.V. (reference number RD-SOP-1257)

ISBN: 978-94-6469-154-2
Cover & lay out: Bregje Jaspers | ProefschriftOntwerp.nl
Print: ProefschriftMaken | www.proefschriftmaken.nl

Translation of salivary gland cancer tumor biology to the clinic

Proefschrift ter verkrijging van de graad van doctor
aan de Radboud Universiteit Nijmegen
op gezag van de rector magnificus prof. dr. J.H.J.M. van Krieken,
volgens besluit van het college voor promoties
in het openbaar te verdedigen op

dinsdag 24 januari 2023
om 16:30 uur precies

door

Gerben Lassche
geboren op 2 mei 1994
te Arnhem

Promotoren:
Prof. dr. C.M.L. van Herpen
Prof. dr. J.A. Schalken

Copromotor:
Dr. G.W.C.T. Verhaegh

Manuscriptcommissie:
Prof. dr. M.M. van den Heuvel (voorzitter)
Prof. dr. A. Skálová (Univerzita Karlova, Tsjechië)
Prof. dr. V. Vander Poorten (UZ Leuven, België)

Contents

CHAPTER 1

General introduction and outline of this thesis

Adapted from:

Advances and challenges in precision medicine in salivary gland cancer

Gerben Lassche, Wim van Boxtel, Marjolijn J.L. Ligtenberg, Adriana C.H. van Engen – van Grunsven, Carla M.L. van Herpen

Cancer Treat Rev. 2019;80:101906.

&

Systemic therapy in the management of recurrent or metastatic salivary duct carcinoma: A systematic review

Maike J.M. Uijen, Gerben Lassche, Adriana C.H. van Engen – van Grunsven, Yuichiro Tada, Gerald W. Verhaegh, Jack A. Schalken, Chantal M.L. Driessen, Carla M.L. van Herpen

Cancer Treat Rev. 2020;89:102069

General introduction

Chapter outline

In this chapter, first an introduction on salivary gland cancer (SGC) and a description of the clinical unmet need in systemic treatment for SGC is given, with a brief overview of usage of chemotherapy and immunotherapy in SGC. Next, an overview of the known genomic aberrations (*i.e.,* genetic mutations and gene amplifications) and protein expression profiles for the most frequently occurring local recurrent or metastatic (R/M) SGC subtypes is given. Those aberrations are possible targets for (personalized) therapy. Subsequently, the remaining knowledge gaps and the implications of these druggable targets for future studies and personalized treatments is discussed. Next, for the aggressive subtype of salivary duct carcinoma (SDC), systemic therapy options, including hormonal therapy, are summarized in detail and an unmet need for selecting the right patients amenable for such treatments is highlighted. Finally, the overall paucity in research models for SGC is described. The recent establishment of 3D-organoid models in other cancers are presented and the potential utility for translational research are highlighted, if these models would be available for SGC.

1. Introduction to salivary gland cancer

Humans have three pairs of major salivary glands, the parotid gland, the submandibular gland and the sublingual gland, and several hundreds of minor salivary glands spread throughout the oral cavity (Figure 1) (1). In both the major and the minor salivary glands SGC can arise. SGC is a heterogeneous group of malignancies comprising approximately 6.5% of cases within head and neck cancer (2). This makes it a rare cancer, with an estimated age-standardized annual incidence of less than 2/100.000 in most countries (3). The most recent World Health Organization classification of Head and Neck Tumours distinguishes 22 histopathological subtypes of SGC, which makes each subtype even rarer (Table 1) (4). Recognition of, and differentiation between these different subtypes is notoriously difficult and different subtypes exhibit different clinical features adding up to the complexity of the disease (5). For localized and resectable disease, surgical resection with or without postoperative radiotherapy is the cornerstone of (curative) treatment (6). In case of R/M disease, palliative systemic treatment is challenging, but urgently needed given the poor prognosis of the disease at this stage. For all types of SGC with distant metastases combined (71% of the patients presenting with recurrent disease) the median overall survival is 15 months with overall survival rates at 1, 3 and 5 years of 54.5%, 28.4% and 14.8%, respectively (7). These numbers, however, vary widely between different subtypes. For example, in adenoid cystic carcinoma (AdCC) median overall survival of several years in distant metastatic disease has been reported (8, 9). This contrasts

with salivary duct carcinoma (SDC), an aggressive subtype of SGC, in which median overall survival for R/M disease receiving best supportive care is only 5 months (10).

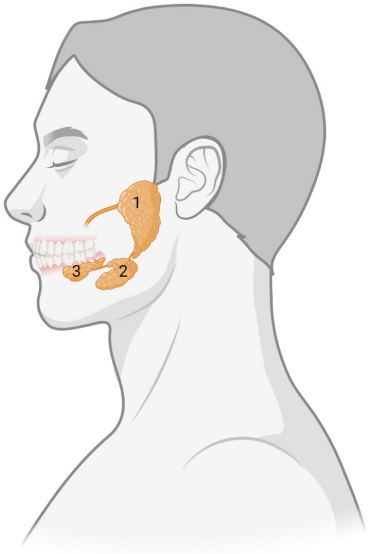

Figure 1: the major salivary glands: 1. Parotid gland; 2. Submandibular gland; 3. Sublingual gland. Created with BioRender.com.

Table 1: Salivary gland cancer subtypes according to WHO classification of head and neck tumours, 4th edition, 2017 (4). Subtypes are ordered following this WHO classification.

Salivary gland cancer subtypes	
1. Mucoepidermoid carcinoma	12. Carcinoma ex pleomorphic adenoma
2. Adenoid cystic carcinoma	13. Secretory carcinoma
3. Acinic cell carcinoma	14. Sebaceous adenocarcinoma
4. Polymorphous adenocarcinoma	15. Carcinosarcoma
5. Clear cell carcinoma	16. Undifferentiated carcinoma
6. Basal cell adenocarcinoma	17. Large cell neuroendocrine carcinoma
7. Intraductal carcinoma	18. Small cell neuroendocrine carcinoma
8. Adenocarcinoma, not otherwise specified	19. Lymphoepithelial carcinoma
9. Salivary duct carcinoma	20. Squamous cell carcinoma
10. Myoepithelial carcinoma	21. Oncocytic carcinoma
11. Epithelial-myoepithelial carcinoma	22. Sialoblastoma *(uncertain malignant potential)*

Systemic treatment of salivary gland cancers

Systemic therapy in oncology can be divided into 4 modalities: classic chemotherapy, hormonal therapy, immunotherapy and targeted therapy. For all subtypes that frequently progress to the R/M stage, targeted therapy options are summarized in section 2 of this chapter and classic chemotherapy and immunotherapy options are summarized in the following paragraph. For salivary duct carcinoma, the only subtype in which hormonal therapy is frequently given, all 4 treatment modalities will be discussed in-depth in section 3 of this chapter.

The clinicopathological diversity of SGC justifies therapy tailored to the specific SGC subtype, highlighting the importance of adequate pathological examination (e.g., subtype, stage, growth pattern), preferably performed by a salivary gland expert pathologist. However, rarity of SGC and its extensive heterogeneity hinders large-scale patient accrual in prospective trials and difficulties in correct histopathological subtyping of SGC endanger homogeneity of cohorts. Therefore, performance of clinical trials in SGC is challenging. This is reflected by the limited number of studies performed on classic chemotherapeutic agents and immunotherapy in SGC.

In R/M AdCC, chemotherapy at best has moderate effects, objective responses in patients treated with single-agent chemotherapy (several agents) were only observed in 18 of 141 (13%) patients enrolled in clinical trials (8). Vinorelbine or mitoxantrone can be recommended as single agents based on their favorable response rates and toxicity profiles. For combination chemotherapy, cisplatin with an anthracycline is most frequently used in AdCC, with cyclophosphamide + doxorubicin + cisplatin (CAP) as most common combination (8, 11). Evidence for the efficacy of chemotherapy in other SGC subtypes is very scarce. For R/M SDC, retrospective analyses of 18 patients treated with carboplatin in combination with paclitaxel revealed 7 responses (median progression free survival (PFS) 6.5 months (95% confidence interval (CI) 3.6-9.3)) (11, 12). In R/M mucoepidermoid carcinoma (MEC), responses on cisplatin alone or in combination with other agents (e.g., CAP, or cisplatin + gemcitabine) and paclitaxel as monotherapy were observed in small patient cohorts (3 responses on paclitaxel monotherapy in 14 patients in the largest MEC cohort). CAP, paclitaxel monotherapy and gemcitabine or vinorelbine in combination with cisplatin has led to responses in adenocarcinoma not otherwise specified (NOS) (11). Overall, use of chemotherapy in R/M SGC is poorly studied and in general is not effective enough to drastically change outcomes in most R/M SGC.

Comparable to classic chemotherapeutic agents, immunotherapy in SGC thus far only has limited effects. The SGC subtype heterogeneity is also reflected in the immunological microenvironment of the several subtypes. For instance, the tumor mutational burden (TMB), and thus the amount of neoepitopes recognizable by the immune system, differs.

SDC has much higher TMB than AdCC and myoepithelial carcinoma and especially AdCC is an immune-excluded subtype (13). Results obtained in clinical studies should therefore be interpreted per subtype.

Prospective clinical studies with immune modulating agents in SGC are restricted to checkpoint inhibitors, anti-PD-L1 (programmed death-ligand 1), anti-PD-1 (programmed cell death protein 1) or anti-CTLA-4 (cytotoxic T-lymphocyte-associated protein 4), either as monotherapy or combined. Regarding PD-L1 inhibitors, 3 studies investigated use of pembrolizumab. In a randomized phase 2 study evaluating efficacy of pembrolizumab with or without radiation for 20 AdCC patients with disease progression, no objective responses were seen outside of the radiation field (stable disease (SD) in 60% of cases) (14). When pembrolizumab was combined with vorinostat, in 25 SGC patients 4 responses were seen (2 acinic cell carcinomas, 1 AdCC and 1 lymphoepithelioma-like carcinoma) (15). Pembrolizumab monotherapy in 26 SGC patients led to 3 responses, with a median duration of response of 4 months (16). For evaluation of efficacy of nivolumab (anti-PD-1) monotherapy or nivolumab combined with ipilimumab (anti-CTLA-4) in SGC, only congress abstracts are available. Nivolumab monotherapy has limited efficacy: 9% of 50 AdCC patients and 4% of 52 non-AdCC patients experienced a response. The primary endpoint of this study, the 6-months non-progression rate was 33.3% for AdCC patients and 14% for non-AdCC patients (17). When nivolumab was combined with ipilimumab in 2 out of 32 AdCC patients responses were seen (6%, with a duration of 18.4 and 7.8 months) and in 5 out of 32 non-AdCC patients (16%, with a duration ranging from 15.7-29.5 months) (18, 19). Thus, immunotherapy with checkpoint inhibition in SGC only has limited efficacy, especially in AdCC. However, subgroups of SGC patients might benefit from checkpoint inhibition.

The limited benefit of chemotherapy and immunotherapy emphasize that there is an unmet need for new therapeutic strategies for patients with R/M SGC. The paucity of treatment options may be reduced by cataloging tumor characteristics and unraveling genetic aberrations in search for possible targets for systemic therapies. By doing so, SGC patients could also benefit from the therapeutic advances made in more common malignancies, especially since the body of evidence for presence of several targets amenable with targeted therapies in different histological subtypes is increasing. In the next 2 sections of this chapter current literature on possible targets for systemic therapy are summarized for the most frequently occurring R/M SGC subtypes.

2. Possible targets amenable for targeted therapy in different SGC subtypes

Mucoepidermoid Carcinoma

Mucoepidermoid carcinoma (MEC) is the most common histological subtype of SGC and comprises approximately 30% of SGCs arising in the minor salivary glands, and 26-47% of SGCs arising in the major salivary glands (4, 20-22). Compared to other histological subtypes, MEC has a rather good prognosis with 75.2% (95% CI 73.8-76.7%) overall survival at 5 years, although survival highly depends on pathological grade and stage. For high grade disease (26%), 5-year overall survival drops to 48.5% (95% CI 45.4-51.9%) and to 39.4% (95% CI 34.3-45.2%) in case of N2 stage (23). Distant metastases are more prevalent in high grade disease, but remain rare: 3.2% of the high-grade cases at presentation in a large retrospective database study (24). Overall, risk of distant metastasis was found to be 16% at 10 years (5).

In 38-82% of MECs (all grades) gene fusions involving the *MAML2* gene are observed (table 2) (25). This *MAML2* gene fuses with *CRCT1* as a result of a t(11;19)(q21;p13) translocation in most cases, and in a smaller number of cases with *CRTC3* as a result of a t(11;15)(q21;q26) translocation (4, 26, 27). This *MAML2* gene rearrangement is highly specific and could therefore serve as a diagnostic tool in atypical histopathological cases (25, 28). *MAML2* gene rearrangement has also been proposed as a favorable prognostic marker, although current insights dispute this (25, 29-31). *CRTC1* and *MAML2* are members of different transcriptional coactivator families that regulate CREB-mediated transcription and Notch signaling, respectively. Downstream, the *CRTC1-MAML2* gene fusion causes upregulation of the epidermal growth factor receptor (EGFR) ligand amphiregulin (AREG), thereby supporting tumor growth (32). This upregulation could serve as potential key for systemic therapy with EGFR-inhibitors. On immunohistochemistry (IHC) EGFR is overexpressed in 46% of the cases (table 3) (33). In several case reports (with a total of 5 patients, also including MECs arising in the lungs) responses on EGFR-inhibitors (cetuximab, gefitinib or erlotinib), alone or in combination with radiotherapy or chemotherapy, were observed in MEC. For EGFR-inhibitor monotherapy in 3 reported cases partial responses (PR) were seen with gefitinib and erlotinib and one complete response (CR) was observed with gefitinib. (34-38). Of note, *EGFR* gene mutation or amplification status was assessed, and some responding patients did not have a mutation or amplification. However, fusion gene analysis for *CRTC1-MAML2* was not performed. All identified clinical studies (including case reports) on EGFR-inhibitors in MEC are listed in table 3.

In conclusion, evidence of clinical benefit of an EGFR-inhibitor in MEC patients is anecdotal and requires further evaluation. Especially in patients with the highly specific *CRCT1-MAML2* gene rearrangement EGFR therapy is attractive based on preclinical work, as this gene fusions is pivotal in tumor survival through AREG-EGFR signaling (32).

Table 2: Prevalence of common genetic alterations (>10%) in different histological subtypes of salivary gland cancer

Subtype	Altered genes	Prevalence	Potential therapeutic target	References
Mucoepidermoid carcinoma	*CRTC1-MAML2,CRTC3-MAML2* rearrangements	38-82%	EGFR	Luk et al (25)
Adenoid cystic carcinoma	*MYB, MYBL1, NFIB* rearrangements (most often *MYB-NFIB* fusion)	88%	IGFR1R, INSR, MET, EGFR	Fujii et al (39)
		48-57%		Ho et al (40)
	NOTCH1 mutation	14%	NOTCH1	Ferarrotto et al (41)
	Mutations in genes of PI3K-pathway	30%	PI3K-pathway	Ho et al (40)
Polymorphous adenocarcinoma	*PRKD1* p.E710D	50-73%	Unknown	Piscuoglio et al (42)
				Weinreb et al (43)
Clear cell carcinoma	*EWSR1* rearrangements (most often *EWSR1-ATF1* fusion)	82-87%	Unknown	Antonescu et al (44)
				Shah et al (45)
Intraductal carcinoma	*RET* rearrangements	47%	Unknown	Skalova et al (46)
				Weinreb et al (47)
Adenocarcinoma NOS	*PIK3CA*	20%	PI3K-pathway	Wang et al (48)
	CDKN2A	17%		
	CDKN2B	12%		
	HRAS	14%		
Salivary duct carcinoma	*TP53*	53-68%	PI3K-pathway	Shimura et al (49)
	PIK3CA	18-26%		Schmitt et al (50)
	HRAS	16%		
Myoepithelial carcinoma	*EWSR1* rearrangements	39%[1]	Unknown	Skalova et al (51)
Epithelial-myoepithelial carcinoma	*MYB* rearrangements	18%	IGFR1R, INSR MET, EGFR	Bishop et al (52)
	HRAS	Up to 33%		Chiosea et al (53)
	KRAS	18%		Fonseca et al (54)
Carcinoma ex pleomorphic adenoma	*HMGA2* or *PLAG1* rearrangements	86%	Unknown	Katabi et al (55)
Secretory carcinoma	*ETV6-NTRK3* gene fusion	~100%	TRK	Boon et al (56)
				Skalova et al (57)

1. percentage of EWSR1 rearrangements in myoepithelial carcinoma with prominent clear cell component.

Adenoid Cystic Carcinoma

AdCC represents approximately a quarter of all SGCs and is the most common histological subtype observed in patients with distant metastatic disease (60%) (11, 58). Of patients with AdCC of the head and neck region, approximately 42% will develop distant metastases, predominantly located in the lungs and in most cases occurring within 5 years after diagnosis, although development of distant metastasis after many years is possible. Median survival in case of distant metastatic disease ranges between 14 and 36 months. Longer duration of survival is reported, especially when metastases are only located in the lungs (median between 25 and 54 months). Growth pattern and gene mutations are important prognostic factors. Patients with a solid tumor growth pattern have poorer prognosis compared to patients with a cribriform or tubular tumor growth pattern (9). A *NOTCH1* gene mutation confers a shorter overall survival compared to patients in whom the *NOTCH1* gene is not mutated (41).

A major pitfall in studying AdCC is the often rather indolent growth of AdCC, also in metastatic disease. High percentages of stable disease reported in studies may be due to the natural tumor growth characteristics rather than treatment effects, especially if progressive disease is not an inclusion criterion. Besides this, dedifferentiation and solid growth pattern are of prognostic importance but difficult to recognize, adding up to heterogeneity of study groups.

A high percentage (up to 90%) of AdCC have shown KIT overexpression by IHC (Table 3). Targeting c-KIT with imatinib therefore seemed promising, but failed to show results in the vast majority of cases (table 4). Response rate on dasatinib (which amongst others targets c-KIT) in KIT positive AdCC patients was also disappointing with 2.5% PR, although evidence of progressive disease was an inclusion criterion and 50% of the patients reached SD with a median PFS of 4.8 months (95%-CI 1.8-6.9) (8, 11, 59). Positivity for epidermal growth factor receptor (EGFR) is also frequently observed on IHC in AdCC (24-85%, different scoring systems), providing a potential target for anti-EGFR therapy (33, 60). This has been studied with single-agent cetuximab, gefitinib and lapatinib (61-63). Of these three agents, the study on lapatinib included only AdCC patients with disease progression and with confirmed EGFR expression. No responses were observed, but 79% reached SD (47% ≥6 months) (table 4) (61). Approximately 76% of AdCCs are immunohistochemically positive for vascular endothelial growth factor (VEGF), which could be targeted with VEGF-inhibitors (64). Trials using such agents in AdCC patients have been performed, with very limited benefit (11, 65). However, an overall response rate of 15.6% (75% SD) with a median PFS of 17.5 months in AdCC patients with progressive disease treated with the multi-tyrosine kinase inhibitor lenvatinib (inhibiting VEGFR1-3, FGFR1-4, KIT, RET and PDGFRα) has been reported recently (Table 4) (66).

In the genomic landscape of AdCC, which has an overall low somatic mutation rate, a large proportion of AdCC patients harbor gene fusions in the *MYB, MYBL1* or *NFIB* genes (88%). In approximately half of the cases (48-57%) a *MYB-NFIB* gene fusion is observed whereas a *MYBL1-NFIB* fusion is less prevalent (39, 40). These gene fusions lead to overexpression of the *MYB* or the *MYBL1* gene and are likely oncogenic drivers (67). *In vitro* studies of AdCC cells harboring a *MYB-NFIB* translocation showed activation of IGF1R, INSR, MET and EGFR, which could be synergistically targeted with linsitinib (IGF1R inhibitor), crizotinib (ALK and MET inhibitor) and gefitinib (EGFR inhibitor) to decrease cell proliferation. Inhibition of IGFR1R also seems pivotal in downregulation of *MYB-NFIB* expression (68). Possible new treatment strategies could therefore consist of a combination of these multiple targeted agents or specifically aiming at downregulation of *MYB-NFIB* in AdCC tumors harboring this gene fusion (*e.g.* with linsitinib). Unfortunately, however, tumor growth of an *in vivo* AdCC tumor model was not inhibited by linsitinib treatment alone (68, 69). Monoclonal antibodies targeting IGF1R, such as figitumumab, are currently not registered. Regarding figitumumab, one AdCC case with a minor response upon figitumumab (initially combined with dacomitinib, a pan-human EGFR inhibitor) is described, although it was not described whether this patient had a *MYB-NFIB* gene fusion (70). The combination of figitumumab with dacomitinib showed also significant growth inhibition in 4 out of 6 AdCC xenograft avatar mice (3 out of 6 on figitumumab monotherapy). The simultaneously reported phase I trial on this combination also included patients with AdCC, but results were not reported separately (71).

An activating *NOTCH1* mutation is found in 9-26% of AdCC patients (activating *NOTCH2* and *NOTCH3* are less common, in 2-6% and 4% respectively), and can be detected in R/M tumors more often compared to primary tumors (41, 72). In tumors with activating *NOTCH1* mutations IHC for Notch1 intracellular domain (NICD1, a downstream protein in the Notch signaling cascade) is positive. However, in *NOTCH1* wild-type tumors, activation of the Notch-pathway has also been observed, indicated by 49% NICD1 positivity on IHC in these wild-type tumors (41). Some authors even found 98% NICD1 positivity in all AdCC patients (73). Possibly the *MYB-NFIB* gene fusion described above could also lead to activation of the Notch-pathway in the absence of an activating *NOTCH1* mutation (74). Targeting the Notch-pathway, using specific Notch(1)-inhibitors, has been scarcely studied in AdCC. Treatment with the Notch1-inhibitor brontictuzumab led to PR in 2 out of 12 and SD in 3 out of 12 AdCC patients enrolled in a phase 1 trial (75). In an expansion of a phase I study on crenigacestat, another Notch-inhibitor, a cohort of 22 AdCC patients (64% positive on IHC, mutation status not given) were enrolled and received the recommended phase 2 dose. One patient had an unconfirmed PR and SD was observed in 68% (evidence of disease progression not required for inclusion); median PFS was 5.3 months (95%-CI 2.4-not ended) (76). Of note, *NOTCH1* wild-type tumors with activation of the Notch-pathway on IHC failed to show

tumor growth inhibition in a xenografted mouse model upon exposure on a Notch1-inhibitor (brontictuzumab) (41). Currently, one phase 2 trial on the Notch-inhibitor AL101 in AdCC patients with a known *NOTCH* mutation is active (NCT03691207), and preliminary results of this trial presented at ASCO 2022 show a response rate of 14.8% (77). Another phase I/IIA trial on the Notch-inhibitor CB-103 is also including AdCC patients (*NOTCH* mutation confirmation not required, NCT03422679).

Different mutations in genes encoding the PI3K-pathway have also been identified in AdCC (each distinct mutation occurs in less than 8% of AdCCs, but 30% of AdCC harbor a gene mutation important in this pathway), which might entail therapeutic options to patients bearing such mutations (40). Besides this, in 53-67% of AdCC cases c-MET positivity on IHC is seen, which can be targeted with cabozantinib (78, 79). One trial reported on efficacy of cabozantinib in c-MET positive AdCC patients. In this trial an objective response in 1 out of 15 AdCC patients was observed, although significant toxicity was seen, which was the reason to close the study prematurely (80). In table 4 information on clinical trials in AdCC is summarized.

Besides these targeted drugs, the transmembrane glycoprotein prostate-specific membrane antigen (PSMA) is often expressed on the cell surface of AdCC cells and could serve as a genuine theranostic marker. Radiolabeled PSMA-ligands, such as ^{68}gallium-PSMA-HBED-CC have been used in combination with positron emission tomography/computed tomography (PET/CT) as diagnostic tool in AdCC, with relevant radioligand uptake in the majority (93%) of the AdCC tumors (81). Analogous to prostate cancer patients, PSMA-positive AdCC patients may benefit from therapy with ^{177}lutetium-labeled PSMA-ligands, and currently one trial is ongoing (NCT04291300) (82).

In conclusion, exploring possible actionable mutations could be a feasible strategy to select a targeted therapy in AdCC patients (table 2 and 3). Although phase 2 evidence is lacking, preclinical data indicates that strategies targeting IGF1R alone or in combination with MET or EGFR inhibition could be fruitful in patients with *MYB-NFIB* gene fusions (approximately 48-57% of the cases). The use of Notch-inhibitors in patients with an activation of the Notch-pathway (activating *NOTCH1*-mutation in 14%, NICD on IHC 49-98%) seems a promising strategy (table 4), as well as ^{177}Lutetium-PSMA therapy. Confirmation by additional clinical trials however is warranted.

Table 3: Frequently overexpressed protein targets in different SGC subtypes

Subtype	Overexpression (determined by IHC)	Prevalence (%)	Possible drug for therapy	References
Mucoepidermoid carcinoma	EGFR	46%	Cetuximab Gefitinib Lapatinib	Cros et al (33)
Adenoid cystic carcinoma	c-KIT	65-90%	Imatinib Dasatinib	Alfieri et al (11)
	c-MET	53-67%	Cabozantinib	Suzuki et al (79) Bell et al (78)
	EGFR	24-85%	Cetuximab Gefitinib Lapatinib	Vered et al (60) Cros et al (33)
	VEGF	76% (moderate and high staining)	Anti-VEGF	Zhang et al (64)
	NICD	49-98%	Brontictuzumab Crenigacestat	Ferraroto et al (41) Sajed et al (73)
Salivary duct carcinoma	AR	78-96%	ADT	Boon et al (83) Takase et al (84)
	HER2	29-46%	Trastuzumab, pertuzumab	Boon et al (83) Schmitt et al (50) Takase et al (84)
	EGFR	53%	Cetuximab Gefitinib Lapatinib	Schmitt et al (50)
Epithelial-myoepithelial carcinoma	FGFR1	86%	FGFR1 inhibitors	Fonseca et al (54)
	c-KIT	69-83%	Imatinib Dasatinib	Seethela et al (85) Cros et al (33)

Due to the heterogeneous character of the carcinoma component of CXPA, CXPA is not included in this table (see full text). Abbreviations: EGFR=epidermal growth factor receptor, VEGF=vascular endothelial growth factor, NICD=NOTCH intracellular domain, AR=androgen receptor, ADT=androgen deprivation therapy, HER2= human epidermal growth factor receptor 2, FGFR1= fibroblast growth factor receptor 1, FGFR2=fibroblast growth factor receptor 1.

Acinic cell carcinoma

Acinic cell carcinoma (approximately 10% of all SGC) most commonly arises in the major salivary glands (90.9%). Most patients present in an early stage (78.2%) and metastatic disease at presentation is very rare (<1%) (58, 86). Distant metastases occur in 19% of the cases (87). Prognosis of patients is generally good, with even a 20-year disease specific survival of 64.3% for patients with stage IV disease, which includes, but is not restricted to distant metastatic disease (86). Noteworthy is that these numbers stem from a large retrospective database study from 1973 to 2009. In 2010 (mammary analogue) secretory carcinoma ((MA)SC), which was formerly frequently classified as acinic cell carcinoma, has been described as a separate entity with an excellent prognosis (see below). Therefore, data regarding acinic cell carcinoma going back further than 2010 may be biased (27, 88).

It has been demonstrated that a subset of 4% of acinic cell carcinomas possesses aberrations in the *MSANTD3* gene, of which the majority is a fusion with *HTN3* resulting in the *HTN3-MSANTD3* fusion gene. However, the role of this gene fusion in oncogenesis is unknown. It has not been described in other tumors and *MSANTD3* overexpression does not seem to enhance cell proliferation (89, 90). Therefore, it remains speculative whether the proteins encoded by this fusion gene are valuable targets for systemic therapy, and currently no drug of such kind is available nor is being developed. In summary, no targeted therapy is available for acinic cell carcinoma. However, we do advice *NTRK* gene fusion analysis in acinic cell carcinoma patients because secretory carcinoma is often misclassified as acinic cell carcinoma. Secretory carcinomas harbor *NTRK* fusion genes and respond extremely well to targeted therapy (see below). *NTRK* gene fusion analysis should be performed using next-generation sequencing techniques or fluorescent in-situ hybridization, as pan-TRK immunohistochemistry in SGC is highly unreliable (91).

Polymorphous adenocarcinoma

Polymorphous adenocarcinoma (PAC) is an entity in which the histopathological landscape has been redesigned in the most recent version of the WHO classification of head and neck tumors (27). PAC consists mostly of tumors formerly described as polymorphous low-grade adenocarcinoma (PLGA) and it controversially also contains the far less prevalent cribriform adenocarcinoma of the minor salivary gland (CAMSG). Between PAC and CAMSG, there might be differences in clinical behavior (92). PAC (PLGA/CAMSG) is the second most common intraoral SGC and in most cases arises from the minor salivary glands. Prognosis of PAC, both PLGA and CAMSG, is generally good. For PLGA, 5- and 10-year disease specific survival are 98.6% and 96.4%, respectively, and distant metastases are rare, with only 4.3% at presentation (92-94). The highly specific hotspot mutation *PRKD1* p.E710D, which is likely to be activating, is found in 50-73% of PLGA (42, 43). *PRKD1* abnormalities have also been found in the majority of CAMSG (95). This specific *PRKD1* p.E710D mutation is not found

in other cancers and therapy targeting this activating mutation does not yet exist (43). In the rare occasion systemic therapy is required to counter progression in patients with PAC, the genomic landscape does not yet reveal promising targeted therapy options.

Adenocarcinoma, not otherwise specified (NOS)

By its very nature adenocarcinoma NOS is a residual group of malignancies that cannot be classified into one of the other subtypes. The reported proportion of SGC constituted by adenocarcinoma NOS ranges between 4.3-17.8%, although arguably these numbers overestimate the real prevalence due to misclassification (58, 96). It is unknown whether recently made diagnostic advances such as molecular characterization (see table 2) would lead to reduction of this rest group, as recent series on adenocarcinomas NOS are lacking. This impedes interpretation of results on expression profiles. However, it is reasonable to perform at least IHC for androgen receptor (AR) and fluorescence *in situ* hybridization (FISH) for human epidermal growth factor receptor 2 (HER2) in all poorly differentiated adenocarcinomas as AR positive cases should probably be regarded and treated as SDC. The proportion of AR and HER2 positivity in adenocarcinoma NOS has been reported to be as high as 21% for both targets, which might thus be an overestimation. Nevertheless, androgen deprivation therapy or therapy with anti-HER2 agents is reasonable in AR or HER2 positive patients (also see SDC) (97). Indeed, patients classified as adenocarcinoma NOS have been included in trials investigating androgen deprivation therapy (ADT) in SGC patients, however results of this small subset were not reported separately (98). A wide spectrum of genomic alterations has been described in adenocarcinoma NOS. These include genomic alterations in the PI3K-pathway (36.5%), cyclin dependent kinases (34.6%) and *RAS* family (17.3%) (48). Evidence of use of these targets in systemic treatment in adenocarcinoma is virtually absent, although responses in adenocarcinoma NOS have been described after treatment with trastuzumab in a HER2-positive tumor and after treatment with sorafenib in another case (99, 100).

Salivary duct carcinoma

Possible targets amenable for targeted therapy in salivary duct carcinoma are discussed in detail and summarized in part 2 of this introduction and in tables 4 and 5.

Carcinoma ex pleomorphic adenoma

Carcinoma ex pleomorphic adenoma (CXPA) is not a stand-alone diagnosis and the most recent version of the WHO highlights the importance of describing the subtype of the carcinoma component of CXPA; most often this is adenocarcinoma NOS, AdCC, MEC or SDC (and many other subtypes or a mixture have been described less frequently) (4, 27, 101, 102). Of all malignant SGC 5-15% is reported to be CXPA. Broad ranges of 5-year survival (25-75%) and several factors influencing survival have been reported (101, 103). In the genomic

landscape of CXPA, gene fusions of *HMGA2* and more often *PLAG1* with several partner genes are frequently found: up to 86% of CXPA shows rearrangements in either one of these genes (55, 102). Although of diagnostic importance, the role of these gene fusions in CXPA and therefore their possible utility as aim for targeted therapy is unknown (102). CXPA's heterogeneity is also resembled in the wide spectrum of overexpressed growth factors and receptors that have been described. These include FGF(R)-2, TGFβ-1, TGFα, HGF-A, c-MET, IGFR-1, EGFR and HER2, providing possible valuable entry points for systemic therapy (101). For instance, responses to trastuzumab based chemotherapy and trastuzumab-emtansine were described in HER2 positive CXPA (104, 105). The possible targets for systemic therapy of other histological subtypes of SGC described in this review highlight the importance of adequate description of the carcinoma component of CXPA as this might reveal promising approaches for treatment.

Secretory carcinoma

Secretory carcinoma (SC), previously named mammary analogue secretory carcinoma (MASC), is a relatively new entity that was first described in the salivary glands in 2010 (27, 57). In retrospect, most cases of what is now called secretory carcinoma were initially classified as acinic cell carcinoma and also as polymorphous adenocarcinoma or adenocarcinoma NOS (56). SC is rare, is most often found in the parotid gland (58-68%) and behaves relatively indolent with a good prognosis. R/M disease is rare (estimated 5- and 10-years survival 95%) (56, 106). The genetic hallmark of SC is a *ETV6-NTRK3* gene fusion as a result of a t(12;15)(p13;q25) translocation, although other gene fusions with *ETV6* have been described (for instance *ETV6-MET* and *ETV6-RET*) (107, 108). *NTRK* gene fusions are known oncogenic drivers and have been described in other tumor types (109). This *ETV6-NTRK3* gene fusion therefore provides a promising target for systemic therapy, and the body of evidence for efficacy of TRK-inhibitors (e.g. larotrectinib, entrectinib, repotrectinib, LOXO-195) in patients with *NTRK* gene fusions is expanding (109). A recent study evaluating the efficacy of larotrectinib in *NTRK* fusion positive SGC patients included 13 patients with (MA)SC and reported a response rate of 92%; median progression free survival rate after 2 years was 78% (110). Responses in patients with MASC have also been observed for entrectinib and repotrectinib (second line) in case reports (111, 112) and in a phase 1-2 trial PR was seen in all 6 of the evaluable SC patients (113). A phase I/II trial evaluating LOXO-195 in second line in which SGC patients can be included is active (not recruiting) (NCT03215511). Whether *NTRK* gene fusions are present in other subtypes of SGC is currently unknown, but treatment with TRK-inhibitors is a very promising treatment option for patients with advanced SC (table 4).

Table 4: Targeted therapy trials in patients with different histological subtypes of SGC

Subtype	Study type	Target	Drug(s)	N	Response	Prior target identification[1]	References
Mucoepidermoid carcinoma	Case reports	EGFR	Cetuximab, gefitinib, erlotinib[4]	5x1	PR 40%, CR 40%, PR/PD 20%	Variable	Grisanti et al, Han et al, Lee et al, Li et al, Milanovic et al (34-38)
	Phase II	EGFR	Cetuximab	2	n.a.[5]	No	Locati et al (63)
	Phase II	EGFR	Gefitinib	2	n.a.[5]	No	Jakob et al (62)
	Phase II	EGFR/ERBB2	Lapatinib	2	n.a.[5]	Yes	Agulnik et al (61)
Adenoid cystic carcinoma[4]	Phase II[2]	c-KIT	Imatinib	71 (6 trials)	RR 2.8%, SD 48%	Variable	Laurie et al (8)
	Randomized Phase II	VEGFR1-3	Axitinib	6	PR 17%, SD 50%	No	Locati et al (65)
	Phase II	VEGFR1-3	Axitinib	33	PR 9%, SD 76%, PD 12%	No	Ho et al (114)
	Phase II	VEGFR1-3	Axitinib (A) vs observation (O) + crossover to axitinib	27/27	A: SD 100% O: SD 52%, PD 48% O after crossover: PR 12%, SD 81%, PD 8%	No	Kang et al (115)
	Phase I[3]	NOTCH1	Brontictuzumab	12	PR 17%, SD 25%	Yes	Ferrarotto et al (75)
	Phase II[3]	EGFR	Cetuximab	23	SD 87%	No	Locati et al (63)
	Phase I expansion[3]	NOTCH1	Crenigacestat	22	Unconfirmed PR 5%, SD 68%	No	Even et al (76)
	Phase II	c-KIT	Dasatinib	40	2.5% PR, 50% SD	Yes	Wong et al (59)
	Phase II[3]	EGFR	Gefitinib	18	PR/CR 0%	No	Jakob et al (62)
	Phase II	EGFR/ERBB2	Lapatinib	21	SD 79%	Yes	Agulnik et al (61)
	Phase II	VEGF KIT FGFR2	Lenvatinib	33	PR 15.6%, SD 75%	No	Tchekmedyian et al (66)
	Phase II I[3]	VEGF KIT FGFR2	Lenvatinib	26	PR 12%, SD 54%	No	Locati et al (116)

(Table continues on next page)

	Phase II[3]	Various	Sorafenib	19	PR 11%, SD 68%, PD 21%	No	Thomson et al (117)
	Phase II	Various	Sunitinib	13	SD 85%, PD 15%	No	Chau et al (118)
Salivary duct carcinoma	See Table 5 and Table 6						
Poorly differentiated carcinoma	Phase II	Various	Sorafenib	1	PR	No	Locati et al (100)
	Phase II	VEGFR1-3	Axitinib	5	PR 20%	No	Locati et al (65)
Secretory carcinoma	Phase II	TRK	Larotrectinib	13	PR 85%	Yes	Le et al (110)
	Case reports	TRK	Entrectinib Repotrectinib	2x1	PR	Yes	Drilon et al (111) Drilon et al (112)
	Phase I-II	TRK	Entrectinib	6	PR 100%	Yes	Doebele et al (113)

1. This column lists whether the targeted agent was only administered to patients with the known genetic aberration, upregulation or protein overexpression at which was aimed.
2. One trial combined imatinib with cisplatin.
3. Evidence of disease progression not required.
4. Cetuximab was combined with either chemotherapy or radiotherapy.
5. Proportion of responding patients with the specific histological subtype not specified.

Abbreviations: N=number, EGFR=epidermal growth factor receptor, VEGF=vascular endothelial growth factor, FGFR2=fibroblast growth factor receptor 2, HER2=human epidermal growth factor receptor 2, TRK=tropomyosin receptor kinase, CR=complete response, PR=partial response, SD=stable disease, PD=progressive disease.

Practical guidelines for SGC patients requiring systemic therapy

Pivotal in choosing the right systemic therapy is an adequate pathological diagnosis to determine the exact histological subtype. Since SGC is rare and there are many types of salivary gland neoplasms with overlapping histomorphological features, pathological review by an expert salivary gland pathologist is recommended. Further work-up depends on the subtype, as is summarized in figure 2. For some subtypes little or no clinical evidence is available hampering making hard recommendations for additional immunohistochemical staining or molecular evaluation to identify therapeutic targets. For these subtypes we advocate immunohistochemical staining for AR and evaluation of HER2 expression, preferably by immunohistochemical staining and FISH. Besides this, regular use of a next generation sequencing panel which includes frequently affected genes in other cancers which are currently targetable with anticancer drugs (e.g., *PIK3CA, BRAF, NRAS, MET)* is recommended. Regarding the different gene fusions, which are often not present in commercially available panels, it is important to test specifically for the presence of *NTRK* gene fusions, as this has great implications for individual patients. Other gene fusions are of diagnostic and potentially (in the future) of therapeutic value. To guide treatment decisions, these gene fusions are therefore currently of less importance than *NTRK* gene fusions.

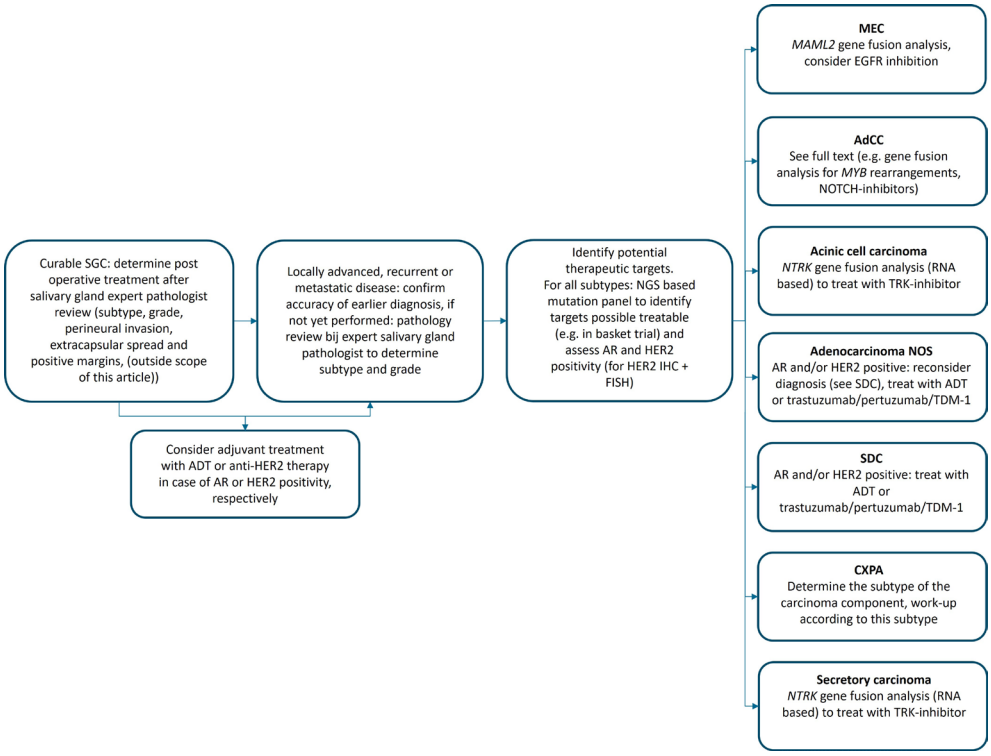

Figure 2: flow chart of work up for patients with SGC requiring systemic therapy to rationalize targeted therapy options. See full text for more elaborate description of targets (possibly) amenable for systemic therapy sorted by subtype. Abbreviations: SGC=salivary gland cancer, NGS=next-generation sequencing, AR=androgen receptor, HER2=human epidermal growth factor receptor 2, ICH=immunohistochemistry, FISH=fluorescence in situ hybridization, MEC= mucoepidermoid carcinoma, AdCC=adenoid cystic carcinoma NOS=not otherwise specified, SDC=salivary duct carcinoma, ADT=androgen deprivation therapy, TDM-1=trastuzumab-emtansine, CXPA=carcinoma ex pleomorphic adenoma.

3. Treatment options in salivary duct carcinoma

SDC is an aggressive subtype of SGC, representing 4-10% of all SGC (50, 58, 119). Overall survival at 3, 5 and 10-years is poor: 70.5% (95%-CI 61.4-77.8%), 43% (95%-CI 33-52%) and 26% (95%-CI 15-37%), respectively (83, 119). Of the SDC patients treated with curative intent, 54% will develop locoregional recurrences and/or distant metastases. In patients with distant metastases, spread to lungs (54%) and bones (46%) was seen most, but a high percentage of brain metastasis was also observed (18%) (83). Given this dismal prognosis and high prevalence of distant metastasis, systemic therapy is often required. Available evidence for systemic therapy options for SDC is summarized and grouped for hormonal therapy, targeted therapy (HER2 and other targets), chemotherapy and immunotherapy (Tables 5 and 6).

Hormonal therapy

One phase 2 trial studied the efficacy of combined androgen blockade (CAB) with leuprorelin acetate and bicalutamide in 36 patients (of which 64% with metastatic disease and 36% with unresectable locally advanced or locoregional recurrent disease) with advanced AR-positive SGC (94% SDC) (98). The results were not reported separately for the SDC patients. Objective responses occurred in 42% of the patients (CR: 11%, PR: 31%). The clinical benefit rate, defined as CR, PR, or SD ≥24 weeks, was 75% with a median PFS of 8.8 months and overall survival OS of 30.5 months (no survival data in historical cohort with other treatments reported).
Another phase 2 trial reported on efficacy of abiraterone combined with prednisone and a luteinizing hormone-releasing hormone (LHRH) analogue as second line therapy for CAB-resistant SGC. The majority of included patients suffered from SDC, but efficacy was not reported separate for these patients. In 5 out of 23 included patients PR and in 10 patients SD was seen, with a median PFS of 3.7 months (120).

Three case series reported on a total of sixty AR-positive SDC patients that received androgen deprivation therapy (ADT) (10, 121, 122). Patients were treated with either monotherapy (LHRH analogues or the AR antagonists: enzalutamide or bicalutamide), or CAB (LHRH analogue and bicalutamide). In the largest of these studies, objective response was seen in 18% of the patients, all PR (10). In the other two studies objective responses were seen in 53% and 50% (121, 122). Only the largest study reported the clinical benefit rate and compared survival to a historical best supportive care group. The clinical benefit rate (CR, PR or SD) was 50%. The median OS in ADT treated SDC patients was 17 months, compared to 5 months in the best supportive care group. Additionally, this study reported on eleven SDC patients that received second line ADT (LHRH analogue, either as monotherapy, or combined with bicalutamide and/or a 5-alfa-reductase-inhibitor), after progression on first line ADT. The ten evaluable patients showed no objective response, but six patients had SD (60%) with a median duration of 9 months (10).

Furthermore, use of ADT in SDC was described in case reports in a total of twelve patients (123-132). Positive results were described in six patients (1 CR, 2 PR, 1 SD ≥6 months, 1 clinical improvement, 1 response on positron-emission tomography (PET) imaging). In addition, one patient was treated with a combination of hormone therapy and chemotherapy; this patient received bicalutamide, leuprolide and paclitaxel, which resulted in PR that was ongoing at 6 months (133).

HER2 targeted therapy

Fifty-seven SDC patients, of which 86% had distant metastases, were treated with the combination of trastuzumab and docetaxel in a phase 2 study including HER2-positive SDC patients (134). Objective responses were seen in 70% of the patients (14% CR and 56% PR) with a clinical benefit rate of 84% (CR, PR and SD ≥24 weeks). PFS and OS were 8.9 months and 39.7 months, respectively. Another study (case series) evaluated the combination of trastuzumab with paclitaxel and carboplatin and in five HER2-positive SDC patients, all with distant metastases (135). The objective response rate was 60% (1 CR and 2 PR) with a median duration of response of 18 months.

In case reports, a total of twelve patients received a combination of trastuzumab with docetaxel/paclitaxel (104, 123, 124, 136-141). Two patients had CR (17%) and eight patients had PR (67%). Duration of responses varied between 3 and 32 months. Additionally, six patients received a combination of trastuzumab, docetaxel/paclitaxel and carboplatin, which led to 3 PR and 3 CR; little was reported on the duration of the responses (48, 137, 142-145).

The combination of trastuzumab and pertuzumab in combination with different types of chemotherapy was given in six SDC patients (123, 131, 132, 146). The combination of trastuzumab and pertuzumab with chemotherapy (*N*=6) led to 3 CR, 1 PR, 1 SD and 1 response on PET imaging. Some durations were still ongoing but ranged from 3-17 months.

HER2 targeted therapy was given as monotherapy in three SDC patients. One patient with a parapharyngeal lymph node metastasis received trasGEX (second-generation monoclonal antibody of trastuzumab) in a phase 1 trial and achieved CR, without progression at 53 months follow-up (147). Two patients received trastuzumab monotherapy, leading to 1 CR, with ongoing duration at 18 months, and 1 SD for 5 months (140, 148). Additionally, four case reports described SDC patients treated with trastuzumab-emtansin (T-DM1) (123, 131, 132, 136). Two patients achieved PR (duration: 8 and 14 months), the other reports mentioned a clinical response of 12 months and an ongoing CR based on PET imaging at 29 months of follow-up.

Targeted therapy (other targets than AR and HER2)

Five prospective targeted therapy trials, which included SDC patients, focused on tyrosine kinase inhibitors (61, 149-152). In all these studies, SDC patients comprised ≤10% of the total study population. No case series were identified reporting on targeted therapy in SDC patients, only several case reports using drugs targeting BRAF, EGFR, VEGFR and some other targets have been reported.

BRAF:

The efficacy of vemurafenib was examined in a basket study for solid tumors with BRAF mutations (151). This study included one SDC patient, which achieved CR lasting for 8 months. Furthermore, one case report described the treatment combination of dabrafenib and trametinib in one SDC patient with a BRAF V600E mutation (128). The patient showed marked improvement of osseous metastases, but progression occurred at 13 months.

EGFR:

Two phase 2 trials in SGC patients studied the effect of EGFR inhibitors (gefitinib, lapatinib) (61, 149). In both trials no objective responses were observed in the entire study population. The trial of gefitinib (*N*= 37) included three SDC patients. In the non-AdCC cohort (total of 18 patients) four patients did have SD ≥9 months, but it is unclear if these were SDC patients (149). None of the four SDC patients treated with lapatinib had SD >6 months (61). In a case report, lapatinib resulted in a complete resolution of skin lesions, with progression after 18 months (136).

VEGFR:

The effect of sorafenib and nintedanib (VEGFR inhibitors) was studied in two phase 2 trials in SGC patients (150, 152). Of the two SDC patients in the trial with sorafenib, one had a PR. The other patient did not have an objective response (150). No objective responses were observed in the nintedanib trial. In the only SDC patient in this trial SD was achieved for 7.3 months (152).

Other targets

One phase 2 trial reported on efficacy of cabozantinib in 4 evaluable SDC patients, of which one experienced a PR for 40 weeks, although significant toxicity was seen in this trial, and therefore prematurely closed (80). In one case report treatment with cabozantinib for two *NCOA-RET* gene fusion positive SDC patients was evaluated. Both patients experienced clinical improvement with no specification of the duration. One case report mentioned treatment with a combination of trastuzumab, lapatinib and bevacizumab, leading to a PR in a single SDC patient. Besides one asymptomatic bone metastasis treated with radiation, the patient had no signs of further progression at 25 months (137). The combination of

temsirolimus and bevacizumab was given to two SDC patients; one patient showed a visual response of skin lesions, and the other patient had a PR for 3 months (153). One study reported on different targeted therapy approaches in three separate patients (154). Three PR were observed: one in a patient treated with a combination of BRAF- and MEK-inhibitors, one in a patient treated with a PI3K-inhibitor, and one in a patient treated with TORC1/2 inhibitor with durations of 5, 12 and 3.7 months, respectively.

Chemotherapy

In total, three SDC patients received chemotherapy in prospective clinical trials (155, 156). Two received CAP (cyclophosphamide, doxorubicin and cisplatin) and one patient was treated with gemcitabine and cisplatin. CAP resulted in one PR and one SD; gemcitabine combined with cisplatin resulted in PR. Little was reported regarding the duration of the responses (table 5). Three case series reported on the effect of chemotherapy in SDC patients. A total of 40 SDC patients were treated with chemotherapy in these studies. In two studies patients were treated with a combination of carboplatin and a taxane (docetaxel/paclitaxel) (12, 157). The combination of carboplatin and paclitaxel (*N*=18) resulted in objective responses in 39% of the patients, and the combination of carboplatin with docetaxel (*N*=12) resulted in objective response in 50%. One study reported on the use of several different chemotherapeutics in 10 SDC patients, mainly platinum-based regimes (122). One patient (10%) achieved CR (treatment schedule unclear), but there were no other objective responses reported.

Table 5: Prospective clinical trials in SDC patients

Study	Design	Patient characteristics	Drugs	Only SDC	*N* of SDC patients (% of total number)	Disease stage*	Prior systemic therapy*	Response*	Median Survival (PFS, OS)*	Remarks
Hormone therapy										
Fushimi et al.(98)	Phase 2	SGC AR+	leuprorelin + bicalutamide	N	34 (94%)	NR	NR	NR	NR	Results total study (N=36): CR: 4 (11%) PR: 11 (31%) SD: 16 (44%) PD: 5 (14%) ORR: 42% (26%-59%) CBR: 75% (58%-88%) (includes SD>24 weeks) PFS: 8.8 mo, OS: 30.5 mo
Locati et al.	Phase II	SGC AR+	Abiraterone + prednison + LHRH analogue	N	19 (79%)	Castration resistant	ADT: all chemo 12 (50% of all patients)	NR	NR	Results total study (N=23) CR: 0 PR: 5 (21%) SD: 10 (42%) PD: 9 (38%) ORR: 5 (21%) CBR: 15 (63%) PFS: 3.7 mo, OS: 22.5 mo
HER2 targeted therapy										
Takahashi et al.(134)	Phase 2	SDC HER2+	docetaxel + trastuzumab	Y	57 (100%)	LR: 8 (14%) DM: 49 (86%)	chemo: 20 (35%) ADT: 3 (5%)	CR: 8 (14%) PR: 32 (56%) SD: 14 (25%) PD: 3 (5%)	PFS: 8.9 mo OS: 39.7 mo	ORR: 70% (57%-82%) CBR: 84% (72%-93%) (includes SD>24 weeks) 14 pts received other treatment after 6 cycli.
Fiedler et al.(147)	Phase 1	Solid tumors HER2+	trasGEX	N	1 (3%)	LR: 1 (100%)	NR	CR: 1 (100%)	PFS: 53 mo**	

(Table continues on next page)

Targeted therapy (other targets than AR and HER2)										
Agulnik et al.(61)	Phase 2	SGC EGFR+ and/or erbB2+	lapatinib	N	4 (10%)	NR	NR	NR	NR	No objective responses in trial SD>6 mo: 13/40 pts, but no SDC.
Jakob et al.(149)	Phase 2	SGC	gefitinib	N	3 (8%)	NR	NR	NR	NR	No objective responses in trial Non-AdCC cohort: 4 pts SD >9 mo, unclear if SDC.
Locati et al.(150)	Phase 2	SGC	sorafenib	N	2 (5%)	NR	NR	PR: 1 (50%)	NR	Other SDC patient unclear if PD or SD.
Hyman et al.(151)	Phase 2 basket	Solid tumors BRAF V600 mutation	vemurafenib	N	1 (1%)	NR	NR	CR: 1 (100%)	PFS: 8 mo	
Kim et al.(152)	Phase 2	SGC	nintedanib	N	1 (5%)	NR	chemo: 1 (100%)	SD: 1 (100%)	PFS: 7.3 mo OS: 10.1 mo**	No objective responses in trial.
Van Boxtel et al. (80)	Phase 2	SGC	Cabozantinib	N	5 (20%)	LR + DM: 2 (40%) DM: 3 (60%)	ADT: 2 (40%) Anti-HER2: 3 (60%) Chemo: 1 (20%)	PR: 1 (20% SD: 3 (60%) NE: 1 (20%)	PFS: 7.2 mo OS: 14.2 mo	
Chemotherapy										
Licitra et al.(155)	Phase 2	SGC	CAP	N	2 (9%)	LR: 1 (50%) DM: 1 (50%)	NR	PR: 1 (50%) SD: 1 (50%)	PR: PFS: 6 mo, OS: 12 mo SD: PFS: NR, OS: 16 mo	
Laurie et al.(156)	Phase 2	SGC	gemcitabine + cisplatin	N	1 (3%)	NR	NR	PR: 1 (100%)	NR	

AR: androgen receptor, CAP: cyclophosphamide, doxorubicin and cisplatin, CBR: clinical benefit rate, CR: complete response, DM: distant metastases, EGFR: epidermal growth factor receptor, erbB2+: refers to HER2 positivity, HER2: human epidermal growth factor receptor 2, LHRH: luteinizing hormone-releasing hormone, LR: locoregional, mo: months, N: no, NE: not evaluable, NR: not reported, ORR: overall response rate, OS: overall survival, PD: progressive disease, PFS: progression free survival, PR: partial response, pts: patients, SD: stable disease, SDC: salivary duct carcinoma, SGC: salivary gland cancer, trasGEX: second generation monoclonal antibody of trastuzumab, Y: yes.
*only SDC patients are reported.
**(response) ongoing at time of report.

Table 6: Retrospective clinical studies in which ≥5 SDC patients were included

Study	Design	Patient characteristics	Drugs	Only SDC	*N* of SDC patients (% of total number)	Disease stage*	Prior systemic therapy*	Response*	Median Survival (PFS, OS)*	Remarks
Hormone therapy										
Boon et al.(10)	Case series	SDC AR+	bicalutamide +/- goserelin	Y	35 (100%)	LR: 2 (6%) DM: 33 (94%)	no	CR: 0 (0%) PR: 6 (18%) SD: 11 (32%) PD: 17 (50%)	PFS: 4 mo OS: 17 mo	Evaluable: 34/35 pts CBR: 50% Median PFS for pts with PR or SD: 11 mo. 11 pts later received second line ADT (goserelin +/- bicalutamide +/- 5-ARI) Evaluable pts: 10/11 pts. SD: 6 (60%) with median PFS of 9 mo. PD: 4 (40%) CBR: 60%
Viscuse et al.(122)	Case series	SGC AR+	leuprolide +/- bicalutamide or bicalutamide or enzalutamide	N	17 (85%)	NR	no	CR or PR: 9 (53%)	NR	Study included 35 pts, 20 received ADT (17 SDC), 14 chemo (10 SDC) See row below.
Locati et al.(121)	Case series	SGC AR+	bicalutamide + triptorelin	N	8 (47%)	DM: 8 (100%)	chemo: 3 (38%)	CR: 2 (25%) PR: 2 (25%) SD: 3 (37.5%) PD: 1 (12.5%)	NR	Duration responses: CR: 11 and 39 mo PR: 6 and 7 mo SD: 8, 10 and 23 mo
HER2 targeted therapy										
Limaye et al.(135)	Case series	SDC HER2+	paclitaxel + trastuzumab + carboplatin	Y	5 (100%)	DM: 5 (100%)	chemo: 1 (20%)	CR: 1 (20%) PR: 2 (40%) SD: 0 (0%) PD: 2 (40%)	DoR: 18 mo	Study also reports on 8 pts in adjuvant setting.

(Table continues on next page)

Chemotherapy										
Nakano et al.(12)	Case series	SGC	paclitaxel + carboplatin	N	18 (47%)	NR	chemo: 2 (11%)	Objective response: 7 (39%)	NR	Objective response was not further specified.
Okada et al.(157)	Case series	SGC	carboplatin + docetaxel	N	12 (50%)	NR	yes: 9 (75%)	CR: 2 (17%) PR: 4 (33%) SD: 3 (25%) PD: 3 (25%)	PFS: 8.0 mo OS: 32.6 mo	Disease stage NR, but target lesions: LR: 3 (35%) DM: 8 (67%)
Viscuse et al.(122)	Case series	SGC	chemo	N	10 (71%)	NR	no	CR: 1 (10%) PR: 0 SD: NR	NR	Different chemo combinations were given. SD: 3/14 pts, unclear if SDC

ADT: androgen deprivation therapy, AR: androgen receptor, CBR: clinical benefit rate, CR: complete response, DoR: duration of response, DM: distant metastases, HER2: human epidermal growth factor receptor 2, LR: locoregional, mo: months, N: no, NR: not reported, OS: overall survival, PFS: progression free survival, PR: partial response, pts: patients, SD: stable disease, SDC: salivary duct carcinoma, SGC: salivary gland cancer, Y: yes, 5-ARI: 5-alfa-reductase-inhibitor.

*only SDC patients are reported.

**(response) ongoing at time of report.

Additional SDC case reports mentioned the effect of different combinations of chemotherapy in seven patients (124, 128, 138, 140, 158). Three out of these seven patients had PR (one on CAP, one with cisplatin+vinorelbine, one with cisplatin+docetaxel). In addition, in one case report first line treatment of cisplatin and 5-fluorouracil combined with cetuximab was given, leading to a CR that lasted 3 months. As second line cisplatin and 5-fluorouracil (5-FU) were replaced by tegafur-gimeracil-oteracil potassium (which also contains a 5-FU prodrug), which led to SD ongoing at 7 months (159).

Immunotherapy

One case report describing the use of immunotherapy in a SDC patient has been published. This patient received nivolumab as second line therapy (128). Dosage and efficacy were not reported; the patient stayed on therapy for 3 months and treatment was discontinued due to severe fatigue.

4. SGC tumor models for basic and translational research applications

As mentioned above, SGC is a rare and heterogeneous disease, as 22 different subtypes with highly variable clinicopathological characteristics can be distinguished. This complicates the development and clinical testing of new treatments. Especially for the subtypes which frequently develop recurrent/metastatic disease and in which systemic therapy is required, such as AdCC, MEC and SDC, development of new therapies is urgently needed. To perform fundamental and translational research, appropriate SGC tumor models, such as cell lines, patient-derived xenografts (PDXs) or organoids, representing the three major SGC sub-types are required.

Several cell line models for the three major SGC subtypes have been described: two AdCC cell lines, one with (160) and one without (161) the pathognomonic *MYB-NFIB* gene fusion, several MEC cell lines including lines that retained the characteristic *CRTC1-MAML2* gene fusion (162, 163) and one SDC cell line that expresses AR (164). Although of great value in cancer research, cell lines in general have several drawbacks, that include extensive adaptation and selection of tumor cells to the 2D culture environment, which makes the recapitulation of heterogeneity of the tumor it was derived from questionable, lack of differentiation in a 3D context, and the absence of surrounding stromal cells (165).

PDX models effectively tackle several of these drawbacks, as tumor heterogeneity is retained and the stromal compartment of the tumor remains present in the first passages, but PDXs have other drawbacks. This includes limited take rates in experimental animals (in general immunocompromised mice) and possible host-specific tumor evolution (165). Besides this,

PDX engraftment is labor and resource intensive, and tumor formation may take weeks or even months to take place. Despite these drawbacks, several PDX models have been described for AdCC and have been used for preclinical drug testing (166-170). PDX models have also been described for MEC and acinic cell carcinoma (171).

Patient-derived tumor organoids (PDOs) have been shown to be an excellent platform to capture tumor heterogeneity, to facilitate differentiation in a 3D context and study cancer biology, and to perform drug screening assays (165, 172). A representative and in-depth characterized tumor organoid biobank can be used for drug screening purposes to provide new therapeutic leads. Furthermore, such organoids form the basis to build more complex tissue models and have the potential to become (immuno-) therapeutic personalized tumor avatars. Tumor organoids are cell culture models of typically epithelial tumors, commonly embedded in a 3-dimensional extracellular matrix. Derived from adult cancer stem cells and grown in basement membrane extract, establishing organoids as epithelial monocultures has been successful for a range of cancer types and with relatively comparable conditions: with both common and some tissue-specific growth factors (173). PDOs thus lack most of the abovementioned drawbacks of cell lines and PDX models but share advantages with PDXs and cell lines (165). Although basic organoid cultures do not contain stromal or immune cells, it has been proven feasible to co-culture these cells with organoids (174-177).

Unfortunately, however, such an organoid model has thus far not been established for SGC. If SGC PDOs would be available as a stable platform, fundamental and translational research into SGC would become possible, this being of great importance for the development of new therapeutic leads.

Outline of this thesis

This thesis aims to translate aspects of the tumor biology of SGC to clinically meaningful insights, that will eventually improve treatment choice for SGC patients.

In **Part 1** the genetic background of different subtypes of salivary gland cancer will be investigated. In **Chapter 2** tumor material of a large cohort of SGC patients, suffering from a variety of SGC subtypes, is subjected to next-generation sequencing on DNA and RNA level. Genetic aberrations that can be targeted with genetically matched therapies are described.

In **Chapter 3** the preliminary results of an autopsy study in 4 SGC patients are presented. In these 4 patients the burden of disease is extensively mapped and sampled. This study eventually aims to answer more fundamental questions on the SGC genetic background, regarding intra-tumor heterogeneity and clonal evolution. The first results of this study, proving feasibility of this approach, are presented in this chapter.

In **Part 2** pathway analysis is used to predict response to systemic therapy in SDC patient. In **Chapter 4** pathway analysis is used to predict the response to combined androgen blockade with an LHRH-agonist and bicalutamide. Besides activity levels of seven different pathways, the expression levels of the gene *SRD5A1* were quantified and assessed for their predictive and prognostic potential. In **Chapter 5** the results of therapy aimed at the HER2 receptor in SDC patients is described. Results of treatment with triple therapy, consisting of trastuzumab, pertuzumab and docetaxel and second line trastuzumab-emtansine is described, as is the use of pathway analysis to predict benefit of these treatments.

In **Part 3** the development and use of organoids models in SGC is described. In **Chapter 6** the results of the development of such a patient-derived organoid model is given, as are the first result of small-scale drug screens in the established models. The phenotypic and genotypic characterization of these models is also described in this chapter. In **Chapter 7** organoid culturing, drug screening and characterization results in one secretory carcinoma case harboring an *NTRK3* gene fusion is in-depth described. This highlights important challenges in correlating *in vivo* and *in vitro* therapy response using organoids.

Finally, in **Chapter 8** the presented work in this thesis is summarized, discussed and future perspectives are given.

References

1. de Paula F, Teshima THN, Hsieh R, Souza MM, Nico MMS, Lourenco SV. Overview of Human Salivary Glands: Highlights of Morphology and Developing Processes. Anat Rec (Hoboken). 2017;300(7):1180-8.
2. Carvalho AL, Nishimoto IN, Califano JA, Kowalski LP. Trends in incidence and prognosis for head and neck cancer in the United States: a site-specific analysis of the SEER database. International journal of cancer. 2005;114(5):806-16.
3. Forman D BF, Brewster DH, Gombe Mbalawa C, Kohler B, Piñeros M, Steliarova-Foucher E, Swaminathan R, Ferlay J, editors (2014). Cancer Incidence in Five Continents, Vol. X. IARC Scientific Publication No. 164. Lyon: International Agency for Research on Cancer.
4. El-Naggar A.K., Chan J.K.C., Grandis J.R., Takata T., Slootweg P.J. WHO classification of head and neck tumours, 4th edition. Lyon: IARC; 2017.
5. Terhaard CH, Lubsen H, Van der Tweel I, Hilgers FJ, Eijkenboom WM, Marres HA, et al. Salivary gland carcinoma: independent prognostic factors for locoregional control, distant metastases, and overall survival: results of the Dutch head and neck oncology cooperative group. Head & neck. 2004;26(8):681-92; discussion 92-3.
6. Sood S, McGurk M, Vaz F. Management of Salivary Gland Tumours: United Kingdom National Multidisciplinary Guidelines. The Journal of laryngology and otology. 2016;130(S2):S142-s9.
7. Nam SJ, Roh JL, Cho KJ, Choi SH, Nam SY, Kim SY. Risk Factors and Survival Associated with Distant Metastasis in Patients with Carcinoma of the Salivary Gland. Annals of surgical oncology. 2016;23(13):4376-83.
8. Laurie SA, Ho AL, Fury MG, Sherman E, Pfister DG. Systemic therapy in the management of metastatic or locally recurrent adenoid cystic carcinoma of the salivary glands: a systematic review. The Lancet Oncology. 2011;12(8):815-24.
9. van Weert S, Reinhard R, Bloemena E, Buter J, Witte BI, Vergeer MR, et al. Differences in patterns of survival in metastatic adenoid cystic carcinoma of the head and neck. Head & neck. 2017;39(3):456-63.
10. Boon E, van Boxtel W, Buter J, Baatenburg de Jong RJ, van Es RJJ, Bel M, et al. Androgen deprivation therapy for androgen receptor-positive advanced salivary duct carcinoma: A nationwide case series of 35 patients in The Netherlands. Head & neck. 2018;40(3):605-13.
11. Alfieri S, Granata R, Bergamini C, Resteghini C, Bossi P, Licitra LF, et al. Systemic therapy in metastatic salivary gland carcinomas: A pathology-driven paradigm? Oral oncology. 2017;66:58-63.
12. Nakano K, Sato Y, Sasaki T, Shimbashi W, Fukushima H, Yonekawa H, et al. Combination chemotherapy of carboplatin and paclitaxel for advanced/metastatic salivary gland carcinoma patients: differences in responses by different pathological diagnoses. Acta oto-laryngologica. 2016;136(9):948-51.
13. Linxweiler M, Kuo F, Katabi N, Lee M, Nadeem Z, Dalin MG, et al. The Immune Microenvironment and Neoantigen Landscape of Aggressive Salivary Gland Carcinomas Differ by Subtype. Clinical cancer research : an official journal of the American Association for Cancer Research. 2020;26(12):2859-70.
14. Mahmood U, Bang A, Chen YH, Mak RH, Lorch JH, Hanna GJ, et al. A Randomized Phase 2 Study of Pembrolizumab With or Without Radiation in Patients With Recurrent or Metastatic Adenoid Cystic Carcinoma. International

journal of radiation oncology, biology, physics. 2021;109(1):134-44.

15. Rodriguez CP, Wu QV, Voutsinas J, Fromm JR, Jiang X, Pillarisetty VG, et al. A Phase II Trial of Pembrolizumab and Vorinostat in Recurrent Metastatic Head and Neck Squamous Cell Carcinomas and Salivary Gland Cancer. Clinical cancer research : an official journal of the American Association for Cancer Research. 2020;26(4):837-45.
16. Cohen RB, Delord JP, Doi T, Piha-Paul SA, Liu SV, Gilbert J, et al. Pembrolizumab for the Treatment of Advanced Salivary Gland Carcinoma: Findings of the Phase 1b KEYNOTE-028 Study. American journal of clinical oncology. 2018.
17. Fayette J, Even C, Digue L, Geoffrois L, Rolland F, Cupissol D, et al. NISCAHN: A phase II, multicenter nonrandomized trial aiming at evaluating nivolumab (N) in two cohorts of patients (pts) with recurrent/metastatic (R/M) salivary gland carcinoma of the head and neck (SGCHN), on behalf of the Unicancer Head & Neck Group. Journal of Clinical Oncology. 2019;37(15_suppl):6083-.
18. Tchekmedyian V, Sherman EJ, Dunn L, Fetten JV, Michel LS, Kriplani A, et al. A phase II trial cohort of nivolumab plus ipilimumab in patients (Pts) with recurrent/metastatic adenoid cystic carcinoma (R/M ACC). Journal of Clinical Oncology. 2019;37(15_suppl):6084-.
19. Burman B, Sherman EJ, Dunn L, Fetten JV, Michel LS, Morris LGT, et al. A phase II trial cohort of nivolumab plus ipilimumab in patients (Pts) with recurrent/metastatic salivary gland cancers (R/M SGCs). Journal of Clinical Oncology. 2021;39(15_suppl):6002-.
20. Amini A, Waxweiler TV, Brower JV, Jones BL, McDermott JD, Raben D, et al. Association of Adjuvant Chemoradiotherapy vs Radiotherapy Alone With Survival in Patients With Resected Major Salivary Gland Carcinoma: Data From the National Cancer Data Base. JAMA otolaryngology-- head & neck surgery. 2016;142(11):1100-10.
21. Baddour HM, Jr., Fedewa SA, Chen AY. Five- and 10-Year Cause-Specific Survival Rates in Carcinoma of the Minor Salivary Gland. JAMA otolaryngology-- head & neck surgery. 2016;142(1):67-73.
22. Cheraghlou S, Kuo P, Mehra S, Agogo GO, Bhatia A, Husain ZA, et al. Adjuvant therapy in major salivary gland cancers: Analysis of 8580 patients in the National Cancer Database. Head and Neck-Journal for the Sciences and Specialties of the Head and Neck. 2018;40(7):1343-55.
23. Rajasekaran K, Stubbs V, Chen J, Yalamanchi P, Cannady S, Brant J, et al. Mucoepidermoid carcinoma of the parotid gland: A National Cancer Database study. Am J Otolaryngol. 2018;39(3):321-6.
24. Chen MM, Roman SA, Sosa JA, Judson BL. Histologic grade as prognostic indicator for mucoepidermoid carcinoma: a population-level analysis of 2400 patients. Head & neck. 2014;36(2):158-63.
25. Luk PP, Wykes J, Selinger CI, Ekmejian R, Tay J, Gao K, et al. Diagnostic and prognostic utility of Mastermind-like 2 (MAML2) gene rearrangement detection by fluorescent in situ hybridization (FISH) in mucoepidermoid carcinoma of the salivary glands. Oral surgery, oral medicine, oral pathology and oral radiology. 2016;121(5):530-41.
26. Noda H, Okumura Y, Nakayama T, Miyabe S, Fujiyoshi Y, Hattori H, et al. Clinicopathological significance of MAML2 gene split in mucoepidermoid carcinoma. Cancer science. 2013;104(1):85-92.

27. Seethala RR, Stenman G. Update from the 4th Edition of the World Health Organization Classification of Head and Neck Tumours: Tumors of the Salivary Gland. Head and neck pathology. 2017;11(1):55-67.
28. Bishop JA, Cowan ML, Shum CH, Westra WH. MAML2 Rearrangements in Variant Forms of Mucoepidermoid Carcinoma: Ancillary Diagnostic Testing for the Ciliated and Warthin-like Variants. The American journal of surgical pathology. 2018;42(1):130-6.
29. Birkeland AC, Foltin SK, Michmerhuizen NL, Hoesli RC, Rosko AJ, Byrd S, et al. Correlation of Crtc1/3-Maml2 fusion status, grade and survival in mucoepidermoid carcinoma. Oral oncology. 2017;68:5-8.
30. Seethala RR, Chiosea SI. MAML2 Status in Mucoepidermoid Carcinoma Can No Longer Be Considered a Prognostic Marker. The American journal of surgical pathology. 2016;40(8):1151-3.
31. Saade RE, Bell D, Garcia J, Roberts D, Weber R. Role of CRTC1/MAML2 Translocation in the Prognosis and Clinical Outcomes of Mucoepidermoid Carcinoma. JAMA otolaryngology-- head & neck surgery. 2016;142(3):234-40.
32. Chen Z, Chen J, Gu Y, Hu C, Li JL, Lin S, et al. Aberrantly activated AREG-EGFR signaling is required for the growth and survival of CRTC1-MAML2 fusion-positive mucoepidermoid carcinoma cells. Oncogene. 2014;33(29):3869-77.
33. Cros J, Sbidian E, Hans S, Roussel H, Scotte F, Tartour E, et al. Expression and mutational status of treatment-relevant targets and key oncogenes in 123 malignant salivary gland tumours. Annals of oncology : official journal of the European Society for Medical Oncology. 2013;24(10):2624-9.
34. Grisanti S, Amoroso V, Buglione M, Rosati A, Gatta R, Pizzocaro C, et al. Cetuximab in the treatment of metastatic mucoepidermoid carcinoma of the salivary glands: a case report and review of literature. Journal of medical case reports. 2008;2:320.
35. Han SW, Kim HP, Jeon YK, Oh DY, Lee SH, Kim DW, et al. Mucoepidermoid carcinoma of lung: potential target of EGFR-directed treatment. Lung cancer (Amsterdam, Netherlands). 2008;61(1):30-4.
36. Lee KW, Chan AB, Lo AW, Lam KC. Erlotinib in metastatic bronchopulmonary mucoepidermoid carcinoma. Journal of thoracic oncology : official publication of the International Association for the Study of Lung Cancer. 2011;6(12):2140-1.
37. Li S, Zhang Z, Tang H, He Z, Gao Y, Ma W, et al. Pathological complete response to gefitinib in a 10-year-old boy with EGFR-negative pulmonary mucoepidermoid carcinoma: a case report and literature review. The clinical respiratory journal. 2017;11(3):346-51.
38. Milanovic D, Jeremic B, Kayser G, Rischke HC, Pfeiffer J, Henke A. Relapsing high grade mucoepidermoid carcinoma. Long-lasting complete response following reirradiation and EGFR blockade. Strahlentherapie und Onkologie : Organ der Deutschen Rontgengesellschaft [et al]. 2012;188(6):518-22.
39. Fujii K, Murase T, Beppu S, Saida K, Takino H, Masaki A, et al. MYB, MYBL1, MYBL2 and NFIB gene alterations and MYC overexpression in salivary gland adenoid cystic carcinoma. Histopathology. 2017;71(5):823-34.
40. Ho AS, Kannan K, Roy DM, Morris LG, Ganly I, Katabi N, et al. The mutational landscape of adenoid cystic carcinoma. Nature genetics. 2013;45(7):791-8.
41. Ferrarotto R, Mitani Y, Diao L, Guijarro I, Wang J, Zweidler-McKay P, et al. Activating NOTCH1 Mutations Define a Distinct Subgroup of Patients With Adenoid Cystic Carcinoma Who Have

Poor Prognosis, Propensity to Bone and Liver Metastasis, and Potential Responsiveness to Notch1 Inhibitors. Journal of clinical oncology : official journal of the American Society of Clinical Oncology. 2017;35(3):352-60.

42. Piscuoglio S, Fusco N, Ng CK, Martelotto LG, da Cruz Paula A, Katabi N, et al. Lack of PRKD2 and PRKD3 kinase domain somatic mutations in PRKD1 wild-type classic polymorphous low-grade adenocarcinomas of the salivary gland. Histopathology. 2016;68(7):1055-62.
43. Weinreb I, Piscuoglio S, Martelotto LG, Waggott D, Ng CK, Perez-Ordonez B, et al. Hotspot activating PRKD1 somatic mutations in polymorphous low-grade adenocarcinomas of the salivary glands. Nature genetics. 2014;46(11):1166-9.
44. Antonescu CR, Katabi N, Zhang L, Sung YS, Seethala RR, Jordan RC, et al. EWSR1-ATF1 fusion is a novel and consistent finding in hyalinizing clear-cell carcinoma of salivary gland. Genes, chromosomes & cancer. 2011;50(7):559-70.
45. Shah AA, LeGallo RD, van Zante A, Frierson HF, Jr., Mills SE, Berean KW, et al. EWSR1 genetic rearrangements in salivary gland tumors: a specific and very common feature of hyalinizing clear cell carcinoma. The American journal of surgical pathology. 2013;37(4):571-8.
46. Skalova A, Vanecek T, Uro-Coste E, Bishop JA, Weinreb I, Thompson LDR, et al. Molecular Profiling of Salivary Gland Intraductal Carcinoma Revealed a Subset of Tumors Harboring NCOA4-RET and Novel TRIM27-RET Fusions: A Report of 17 cases. The American journal of surgical pathology. 2018;42(11):1445-55.
47. Weinreb I, Bishop JA, Chiosea SI, Seethala RR, Perez-Ordonez B, Zhang L, et al. Recurrent RET Gene Rearrangements in Intraductal Carcinomas of Salivary Gland. The American journal of surgical pathology. 2018;42(4):442-52.
48. Wang K, Russell JS, McDermott JD, Elvin JA, Khaira D, Johnson A, et al. Profiling of 149 Salivary Duct Carcinomas, Carcinoma Ex Pleomorphic Adenomas, and Adenocarcinomas, Not Otherwise Specified Reveals Actionable Genomic Alterations. Clinical cancer research : an official journal of the American Association for Cancer Research. 2016;22(24):6061-8.
49. Shimura T, Tada Y, Hirai H, Kawakita D, Kano S, Tsukahara K, et al. Prognostic and histogenetic roles of gene alteration and the expression of key potentially actionable targets in salivary duct carcinomas. Oncotarget. 2018;9(2):1852-67.
50. Schmitt NC, Kang H, Sharma A. Salivary duct carcinoma: An aggressive salivary gland malignancy with opportunities for targeted therapy. Oral oncology. 2017;74:40-8.
51. Skalova A, Weinreb I, Hyrcza M, Simpson RH, Laco J, Agaimy A, et al. Clear cell myoepithelial carcinoma of salivary glands showing EWSR1 rearrangement: molecular analysis of 94 salivary gland carcinomas with prominent clear cell component. The American journal of surgical pathology. 2015;39(3):338-48.
52. Bishop JA, Westra WH. MYB Translocation Status in Salivary Gland Epithelial-Myoepithelial Carcinoma: Evaluation of Classic, Variant, and Hybrid Forms. The American journal of surgical pathology. 2018;42(3):319-25.
53. Chiosea SI, Miller M, Seethala RR. HRAS mutations in epithelial-myoepithelial carcinoma. Head and neck pathology. 2014;8(2):146-50.
54. Fonseca I, Bell A, Wani K, Bell D. Global transcriptome and sequenome analysis of formalin-fixed salivary epithelial-myoepithelial carcinoma specimens. Genes, chromosomes & cancer. 2015;54(4):249-59.
55. Katabi N, Ghossein R, Ho A, Dogan S, Zhang L, Sung YS, et al. Consistent PLAG1 and

HMGA2 abnormalities distinguish carcinoma ex-pleomorphic adenoma from its de novo counterparts. Human pathology. 2015;46(1):26-33.

56. Boon E, Valstar MH, van der Graaf WTA, Bloemena E, Willems SM, Meeuwis CA, et al. Clinicopathological characteristics and outcome of 31 patients with ETV6-NTRK3 fusion gene confirmed (mammary analogue) secretory carcinoma of salivary glands. Oral oncology. 2018;82:29-33.

57. Skalova A, Vanecek T, Sima R, Laco J, Weinreb I, Perez-Ordonez B, et al. Mammary analogue secretory carcinoma of salivary glands, containing the ETV6-NTRK3 fusion gene: a hitherto undescribed salivary gland tumor entity. The American journal of surgical pathology. 2010;34(5):599-608.

58. Bjorndal K, Krogdahl A, Therkildsen MH, Overgaard J, Johansen J, Kristensen CA, et al. Salivary gland carcinoma in Denmark 1990-2005: a national study of incidence, site and histology. Results of the Danish Head and Neck Cancer Group (DAHANCA). Oral oncology. 2011;47(7):677-82.

59. Wong SJ, Karrison T, Hayes DN, Kies MS, Cullen KJ, Tanvetyanon T, et al. Phase II trial of dasatinib for recurrent or metastatic c-KIT expressing adenoid cystic carcinoma and for nonadenoid cystic malignant salivary tumors. Annals of oncology : official journal of the European Society for Medical Oncology. 2016;27(2):318-23.

60. Vered M, Braunstein E, Buchner A. Immunohistochemical study of epidermal growth factor receptor in adenoid cystic carcinoma of salivary gland origin. Head & neck. 2002;24(7):632-6.

61. Agulnik M, Cohen EW, Cohen RB, Chen EX, Vokes EE, Hotte SJ, et al. Phase II study of lapatinib in recurrent or metastatic epidermal growth factor receptor and/or erbB2 expressing adenoid cystic carcinoma and non adenoid cystic carcinoma malignant tumors of the salivary glands. Journal of clinical oncology : official journal of the American Society of Clinical Oncology. 2007;25(25):3978-84.

62. Jakob JA, Kies MS, Glisson BS, Kupferman ME, Liu DD, Lee JJ, et al. Phase II study of gefitinib in patients with advanced salivary gland cancers. Head & neck. 2015;37(5):644-9.

63. Locati LD, Bossi P, Perrone F, Potepan P, Crippa F, Mariani L, et al. Cetuximab in recurrent and/or metastatic salivary gland carcinomas: A phase II study. Oral oncology. 2009;45(7):574-8.

64. Zhang J, Peng B, Chen X. Expressions of nuclear factor kappaB, inducible nitric oxide synthase, and vascular endothelial growth factor in adenoid cystic carcinoma of salivary glands: correlations with the angiogenesis and clinical outcome. Clinical cancer research : an official journal of the American Association for Cancer Research. 2005;11(20):7334-43.

65. Locati LD, Cavalieri S, Bergamini C, Resteghini C, Alfieri S, Calareso G, et al. Phase II trial with axitinib in recurrent and/or metastatic salivary gland cancers of the upper aerodigestive tract. Head & neck. 2019;41(10):3670-6.

66. Tchekmedyian V, Sherman EJ, Dunn L, Tran C, Baxi S, Katabi N, et al. Phase II Study of Lenvatinib in Patients With Progressive, Recurrent or Metastatic Adenoid Cystic Carcinoma. Journal of clinical oncology : official journal of the American Society of Clinical Oncology. 2019:Jco1801859.

67. Brayer KJ, Frerich CA, Kang H, Ness SA. Recurrent Fusions in MYB and MYBL1 Define a Common, Transcription Factor-Driven Oncogenic Pathway in Salivary Gland Adenoid Cystic Carcinoma. Cancer discovery. 2016;6(2):176-87.

68. Andersson MK, Afshari MK, Andren Y, Wick MJ, Stenman G. Targeting the Oncogenic Transcriptional Regulator MYB in Adenoid Cystic Carcinoma by Inhibition of IGF1R/AKT Signaling. Journal of the National Cancer Institute. 2017;109(9).

69. Ness SA. Editorial: Targeting MYB Oncogene Expression in Adenoid Cystic Carcinoma. Journal of the National Cancer Institute. 2017;109(9).

70. Morelli MP, Calvo E, Ordonez E, Wick MJ, Viqueira BR, Lopez-Casas PP, et al. Prioritizing phase I treatment options through preclinical testing on personalized tumorgraft. Journal of clinical oncology : official journal of the American Society of Clinical Oncology. 2012;30(4):e45-8.

71. Calvo E, Soria JC, Ma WW, Wang T, Bahleda R, Tolcher AW, et al. A Phase I Clinical Trial and Independent Patient-Derived Xenograft Study of Combined Targeted Treatment with Dacomitinib and Figitumumab in Advanced Solid Tumors. Clinical cancer research : an official journal of the American Association for Cancer Research. 2017;23(5):1177-85.

72. Ho AS, Ochoa A, Jayakumaran G, Zehir A, Valero Mayor C, Tepe J, et al. Genetic hallmarks of recurrent/metastatic adenoid cystic carcinoma. J Clin Invest. 2019;129(10):4276-89.

73. Sajed DP, Faquin WC, Carey C, Severson EA, A HA, C AJ, et al. Diffuse Staining for Activated NOTCH1 Correlates With NOTCH1 Mutation Status and Is Associated With Worse Outcome in Adenoid Cystic Carcinoma. The American journal of surgical pathology. 2017;41(11):1473-82.

74. Ferrarotto R, Heymach JV. Taking it up a NOTCH: a novel subgroup of ACC is identified. Oncotarget. 2017;8(47):81725-6.

75. Ferrarotto R, Eckhardt G, Patnaik A, LoRusso P, Faoro L, Heymach JV, et al. A phase I dose-escalation and dose-expansion study of brontictuzumab in subjects with selected solid tumors. Annals of oncology : official journal of the European Society for Medical Oncology. 2018;29(7):1561-8.

76. Even C, Lassen U, Merchan J, Le Tourneau C, Soria JC, Ferte C, et al. Safety and clinical activity of the Notch inhibitor, crenigacestat (LY3039478), in an open-label phase I trial expansion cohort of advanced or metastatic adenoid cystic carcinoma. Investigational new drugs. 2019.

77. Ferrarotto R, Metcalf R, Rodriguez CP, Muzaffar J, Even C, Perez CA, et al. Results of ACCURACY: A phase 2 trial of AL101, a selective gamma secretase inhibitor, in subjects with recurrent/metastatic (R/M) adenoid cystic carcinoma (ACC) harboring Notch activating mutations (Notchmut). Journal of Clinical Oncology. 2022;40(16_suppl):abstr 6046.

78. Bell D, Ferrarotto R, Fox MD, Roberts D, Hanna EY, Weber RS, et al. Analysis and significance of c-MET expression in adenoid cystic carcinoma of the salivary gland. Cancer biology & therapy. 2015;16(6):834-8.

79. Suzuki K, Cheng J, Watanabe Y. Hepatocyte growth factor and c-Met (HGF/c-Met) in adenoid cystic carcinoma of the human salivary gland. Journal of oral pathology & medicine : official publication of the International Association of Oral Pathologists and the American Academy of Oral Pathology. 2003;32(2):84-9.

80. van Boxtel W, Uijen MJM, Krens SD, Dijkema T, Willems SM, Jonker MA, et al. Excessive toxicity of cabozantinib in a phase II study in patients with recurrent and/or metastatic salivary gland cancer. European journal of cancer (Oxford, England : 1990). 2022;161:128-37.

81. van Boxtel W, Lütje S, van Engen-van Grunsven ICH, Verhaegh GW, Schalken JA, Jonker MA, et al. (68)Ga-PSMA-HBED-CC PET/CT imaging

for adenoid cystic carcinoma and salivary duct carcinoma: a phase 2 imaging study. Theranostics. 2020;10(5):2273-83.

82. Ferdinandus J, Violet J, Sandhu S, Hofman MS. Prostate-specific membrane antigen theranostics: therapy with lutetium-177. Current opinion in urology. 2018;28(2):197-204.
83. Boon E, Bel M, van Boxtel W, van der Graaf WTA, van Es RJJ, Eerenstein SEJ, et al. A clinicopathological study and prognostic factor analysis of 177 salivary duct carcinoma patients from The Netherlands. International journal of cancer. 2018;143(4):758-66.
84. Takase S, Kano S, Tada Y, Kawakita D, Shimura T, Hirai H, et al. Biomarker immunoprofile in salivary duct carcinomas: clinicopathological and prognostic implications with evaluation of the revised classification. Oncotarget. 2017;8(35):59023-35.
85. Seethala RR, Barnes EL, Hunt JL. Epithelial-myoepithelial carcinoma: a review of the clinicopathologic spectrum and immunophenotypic characteristics in 61 tumors of the salivary glands and upper aerodigestive tract. The American journal of surgical pathology. 2007;31(1):44-57.
86. Biron VL, Lentsch EJ, Gerry DR, Bewley AF. Factors influencing survival in acinic cell carcinoma: a retrospective survival analysis of 2061 patients. Head & neck. 2015;37(6):870-7.
87. Neskey DM, Klein JD, Hicks S, Garden AS, Bell DM, El-Naggar AK, et al. Prognostic factors associated with decreased survival in patients with acinic cell carcinoma. JAMA otolaryngology--head & neck surgery. 2013;139(11):1195-202.
88. Vander Poorten V, Triantafyllou A, Thompson LD, Bishop J, Hauben E, Hunt J, et al. Salivary acinic cell carcinoma: reappraisal and update. European archives of oto-rhino-laryngology : official journal of the European Federation of Oto-Rhino-Laryngological Societies (EUFOS) : affiliated with the German Society for Oto-Rhino-Laryngology - Head and Neck Surgery. 2016;273(11):3511-31.
89. Andreasen S, Varma S, Barasch N, Thompson LDR, Miettinen M, Rooper L, et al. The HTN3-MSANTD3 Fusion Gene Defines a Subset of Acinic Cell Carcinoma of the Salivary Gland. The American journal of surgical pathology. 2018.
90. Barasch N, Gong X, Kwei KA, Varma S, Biscocho J, Qu K, et al. Recurrent rearrangements of the Myb/SANT-like DNA-binding domain containing 3 gene (MSANTD3) in salivary gland acinic cell carcinoma. PloS one. 2017;12(2):e0171265.
91. Solomon JP, Linkov I, Rosado A, Mullaney K, Rosen EY, Frosina D, et al. NTRK fusion detection across multiple assays and 33,997 cases: diagnostic implications and pitfalls. Modern pathology : an official journal of the United States and Canadian Academy of Pathology, Inc. 2019.
92. Vander Poorten V, Triantafyllou A, Skalova A, Stenman G, Bishop JA, Hauben E, et al. Polymorphous adenocarcinoma of the salivary glands: reappraisal and update. European archives of oto-rhino-laryngology : official journal of the European Federation of Oto-Rhino-Laryngological Societies (EUFOS) : affiliated with the German Society for Oto-Rhino-Laryngology - Head and Neck Surgery. 2018;275(7):1681-95.
93. Hernandez-Prera JC. Historical Evolution of the Polymorphous Adenocarcinoma. Head and neck pathology. 2018.
94. Patel TD, Vazquez A, Marchiano E, Park RC, Baredes S, Eloy JA. Polymorphous low-grade adenocarcinoma of the head and neck: A population-based study of 460 cases. The Laryngoscope. 2015;125(7):1644-9.
95. Weinreb I, Zhang L, Tirunagari LM, Sung YS, Chen CL, Perez-Ordonez B, et al. Novel PRKD gene

rearrangements and variant fusions in cribriform adenocarcinoma of salivary gland origin. Genes, chromosomes & cancer. 2014;53(10):845-56.

96. Deng R, Tang E, Yang X, Huang X, Hu Q. Salivary adenocarcinoma, not otherwise specified: a clinicopathological study of 28 cases. Oral surgery, oral medicine, oral pathology and oral radiology. 2012;113(5):655-60.

97. Locati LD, Perrone F, Losa M, Mela M, Casieri P, Orsenigo M, et al. Treatment relevant target immunophenotyping of 139 salivary gland carcinomas (SGCs). Oral oncology. 2009;45(11):986-90.

98. Fushimi C, Tada Y, Takahashi H, Nagao T, Ojiri H, Masubuchi T, et al. A prospective phase II study of combined androgen blockade in patients with androgen receptor-positive metastatic or locally advanced unresectable salivary gland carcinoma. Annals of oncology : official journal of the European Society for Medical Oncology. 2018;29(4):979-84.

99. Ghazali N, Parker L, Settle K, Lubek JE. Sustained response of HER2-positive metastatic salivary adenocarcinoma, not otherwise specified, treated with trastuzumab. Oral surgery, oral medicine, oral pathology and oral radiology. 2016;122(3):292-9.

100. Locati LD, Perrone F, Cortelazzi B, Bergamini C, Bossi P, Civelli E, et al. A phase II study of sorafenib in recurrent and/or metastatic salivary gland carcinomas: Translational analyses and clinical impact. European journal of cancer (Oxford, England : 1990). 2016;69:158-65.

101. Antony J, Gopalan V, Smith RA, Lam AK. Carcinoma ex pleomorphic adenoma: a comprehensive review of clinical, pathological and molecular data. Head and neck pathology. 2012;6(1):1-9.

102. Asahina M, Saito T, Hayashi T, Fukumura Y, Mitani K, Yao T. Clinicopathological effect of PLAG1 fusion genes in pleomorphic adenoma and carcinoma ex pleomorphic adenoma with special emphasis on histological features. Histopathology. 2019;74(3):514-25.

103. Hu YH, Li W, Zhang CY, Xia RH, Tian Z, Wang LZ, et al. Prognostic nomogram for disease-specific survival of carcinoma ex pleomorphic adenoma of the salivary gland. Head & neck. 2017;39(12):2416-24.

104. Kadowaki S, Yatabe Y, Hirakawa H, Komori A, Kondoh C, Hasegawa Y, et al. Complete Response to Trastuzumab-Based Chemotherapy in a Patient with Human Epidermal Growth Factor Receptor-2-Positive Metastatic Salivary Duct Carcinoma ex Pleomorphic Adenoma. Case reports in oncology. 2013;6(3):450-5.

105. Hassanieh I, Hilal L, Al Feghali KA, Khalifeh I, Youssef B. Trastuzumab Emtansine for the Treatment of HER-2 Positive Carcinoma Ex-pleomorphic Adenoma Metastatic to the Brain: A Case Report. Frontiers in oncology. 2018;8:274.

106. Khalele BA. Systematic review of mammary analog secretory carcinoma of salivary glands at 7 years after description. Head & neck. 2017;39(6):1243-8.

107. Rooper LM, Karantanos T, Ning Y, Bishop JA, Gordon SW, Kang H. Salivary Secretory Carcinoma With a Novel ETV6-MET Fusion: Expanding the Molecular Spectrum of a Recently Described Entity. The American journal of surgical pathology. 2018;42(8):1121-6.

108. Skalova A, Vanecek T, Martinek P, Weinreb I, Stevens TM, Simpson RHW, et al. Molecular Profiling of Mammary Analog Secretory Carcinoma Revealed a Subset of Tumors Harboring a Novel ETV6-RET Translocation: Report of 10 Cases. The American journal of surgical pathology. 2018;42(2):234-46.

109. Cocco E, Scaltriti M, Drilon A. NTRK fusion-positive cancers and TRK inhibitor therapy. Nature reviews Clinical oncology. 2018;15(12):731-47.

110. Le X, Baik C, Bauman J, Gilbert J, Brose MS, Grilley-Olson JE, et al. Larotrectinib Treatment for Patients With TRK Fusion-Positive Salivary Gland Cancers. Oncologist. 2022.

111. Drilon A, Li G, Dogan S, Gounder M, Shen R, Arcila M, et al. What hides behind the MASC: clinical response and acquired resistance to entrectinib after ETV6-NTRK3 identification in a mammary analogue secretory carcinoma (MASC). Annals of oncology : official journal of the European Society for Medical Oncology. 2016;27(5):920-6.

112. Drilon A, Ou SI, Cho BC, Kim DW, Lee J, Lin JJ, et al. Repotrectinib (TPX-0005) Is a Next-Generation ROS1/TRK/ALK Inhibitor That Potently Inhibits ROS1/TRK/ALK Solvent- Front Mutations. Cancer discovery. 2018;8(10):1227-36.

113. Doebele RC, Drilon A, Paz-Ares L, Siena S, Shaw AT, Farago AF, et al. Entrectinib in patients with advanced or metastatic NTRK fusion-positive solid tumours: integrated analysis of three phase 1-2 trials. The Lancet Oncology. 2020;21(2):271-82.

114. Ho AL, Dunn L, Sherman EJ, Fury MG, Baxi SS, Chandramohan R, et al. A phase II study of axitinib (AG-013736) in patients with incurable adenoid cystic carcinoma. Annals of oncology : official journal of the European Society for Medical Oncology. 2016;27(10):1902-8.

115. Kang EJ, Ahn MJ, Ock CY, Lee KW, Kwon JH, Yang Y, et al. Randomized Phase II Study of Axitinib versus Observation in Patients with Recurred or Metastatic Adenoid Cystic Carcinoma. Clinical cancer research : an official journal of the American Association for Cancer Research. 2021;27(19):5272-9.

116. Locati LD, Galbiati D, Calareso G, Alfieri S, Singer S, Cavalieri S, et al. Patients with adenoid cystic carcinomas of the salivary glands treated with lenvatinib: Activity and quality of life. Cancer. 2020;126(9):1888-94.

117. Thomson DJ, Silva P, Denton K, Bonington S, Mak SK, Swindell R, et al. Phase II trial of sorafenib in advanced salivary adenoid cystic carcinoma of the head and neck. Head & neck. 2015;37(2):182-7.

118. Chau NG, Hotte SJ, Chen EX, Chin SF, Turner S, Wang L, et al. A phase II study of sunitinib in recurrent and/or metastatic adenoid cystic carcinoma (ACC) of the salivary glands: current progress and challenges in evaluating molecularly targeted agents in ACC. Annals of oncology : official journal of the European Society for Medical Oncology. 2012;23(6):1562-70.

119. Otsuka K, Imanishi Y, Tada Y, Kawakita D, Kano S, Tsukahara K, et al. Clinical Outcomes and Prognostic Factors for Salivary Duct Carcinoma: A Multi-Institutional Analysis of 141 Patients. Annals of surgical oncology. 2016;23(6):2038-45.

120. Locati LD, Cavalieri S, Bergamini C, Resteghini C, Colombo E, Calareso G, et al. Abiraterone Acetate in Patients With Castration-Resistant, Androgen Receptor-Expressing Salivary Gland Cancer: A Phase II Trial. Journal of clinical oncology : official journal of the American Society of Clinical Oncology. 2021;39(36):4061-8.

121. Locati LD, Perrone F, Cortelazzi B, Lo Vullo S, Bossi P, Dagrada G, et al. Clinical activity of androgen deprivation therapy in patients with metastatic/relapsed androgen receptor-positive salivary gland cancers. Head & neck. 2016;38(5):724-31.

122. Viscuse PV, Price KA, Garcia JJ, Schembri-Wismayer DJ, Chintakuntlawar AV. First Line Androgen Deprivation Therapy vs. Chemotherapy for Patients With Androgen Receptor Positive Recurrent or Metastatic Salivary Gland

Carcinoma-A Retrospective Study. Frontiers in oncology. 2019;9:701.

123. Correa TS, Matos GDR, Segura M, Dos Anjos CH. Second-Line Treatment of HER2-Positive Salivary Gland Tumor: Ado-Trastuzumab Emtansine (T-DM1) after Progression on Trastuzumab. Case reports in oncology. 2018;11(2):252-7.

124. De Block K, Vander Poorten V, Dormaar T, Nuyts S, Hauben E, Floris G, et al. Metastatic HER-2-positive salivary gland carcinoma treated with trastuzumab and a taxane: a series of six patients. Acta Clin Belg. 2016;71(6):383-8.

125. de Cecio R, Cantile M, Fulciniti F, Collina F, Scognamiglio G, Longo F, et al. Metastatic salivary ductal carcinoma androgen receptor-positive with V600E BRAF gene mutation. International Journal of Clinical and Experimental Medicine. 2016;9(11):22463-9.

126. Elkrief A, Saleh R. Androgen deprivation therapy for metastatic salivary gland cancer. Cmaj. 2018;190(33):E985-E7.

127. Graham LJ, Meininger LJ. Salivary ductal adenocarcinoma with complete response to androgen blockade. Journal of Community and Supportive Oncology. 2018;16(4):e200-e1.

128. Lin VTG, Nabell LM, Spencer SA, Carroll WR, Harada S, Yang ES. First-Line Treatment of Widely Metastatic BRAF-Mutated Salivary Duct Carcinoma With Combined BRAF and MEK Inhibition. Journal of the National Comprehensive Cancer Network : JNCCN. 2018;16(10):1166-70.

129. Urban D, Rischin D, Angel C, D'Costa I, Solomon B. Abiraterone in metastatic salivary duct carcinoma. Journal of the National Comprehensive Cancer Network : JNCCN. 2015;13(3):288-90.

130. Yamamoto N, Minami S, Fujii M. Clinicopathologic study of salivary duct carcinoma and the efficacy of androgen deprivation therapy. Am J Otolaryngol. 2014;35(6):731-5.

131. Swed BL, Cohen RB, Aggarwal C. Targeting HER2/neu Oncogene Overexpression With Ado-Trastuzumab Emtansine in the Treatment of Metastatic Salivary Gland Neoplasms: A Single-Institution Experience. JCO precision oncology. 2019;3.

132. van Boxtel W, Boon E, Weijs WLJ, van den Hoogen FJA, Flucke UE, van Herpen CML. Combination of docetaxel, trastuzumab and pertuzumab or treatment with trastuzumab-emtansine for metastatic salivary duct carcinoma. Oral oncology. 2017;72:198-200.

133. Kuroda H, Sakurai T, Yamada M, Uemura N, Ono M, Abe T, et al. [Effective treatment by both anti-androgen therapy and chemotherapy for a patient with advanced salivary duct carcinoma]. Gan To Kagaku Ryoho. 2011;38(4):627-30.

134. Takahashi H, Tada Y, Saotome T, Akazawa K, Ojiri H, Fushimi C, et al. Phase II Trial of Trastuzumab and Docetaxel in Patients With Human Epidermal Growth Factor Receptor 2-Positive Salivary Duct Carcinoma. Journal of clinical oncology : official journal of the American Society of Clinical Oncology. 2019;37(2):125-34.

135. Limaye SA, Posner MR, Krane JF, Fonfria M, Lorch JH, Dillon DA, et al. Trastuzumab for the treatment of salivary duct carcinoma. The oncologist. 2013;18(3):294-300.

136. Almquist D, Umakanthan JM, Ganti AK. Sequential HER2-Targeted Therapy in Salivary Ductal Carcinoma With HER2/neu Overexpression and a Concomitant ERBB2 Mutation. JCO Precision Oncology. 2018(2):1-5.

137. Falchook GS, Lippman SM, Bastida CC, Kurzrock R. Human epidermal receptor 2-amplified salivary duct carcinoma: regression with dual human epidermal receptor 2 inhibition and anti-vascular endothelial growth factor combination treatment. Head & neck. 2014;36(3):E25-7.

138. Gibo T, Sekiguchi N, Gomi D, Noguchi T, Fukushima T, Kobayashi T, et al. Targeted therapy with trastuzumab for epidermal growth factor receptor 2 (HER2)-positive advanced salivary duct carcinoma: A case report. Molecular and clinical oncology. 2019;11(2):111-5.

139. Krishnamurthy J, Krishnamurty DM, Baker JJ, Zhen W, Lydiatt D, Ganti AK. Salivary duct carcinoma responding to trastuzumab-based therapy: case report and review of the literature. Head & neck. 2013;35(12):E372-5.

140. Nashed M, Casasola RJ. Biological therapy of salivary duct carcinoma. The Journal of laryngology and otology. 2009;123(2):250-2.

141. Ueki Y, Tada Y, Togashi T, Kawakita D, Nagao T, Sato Y. Pathological response of salivary duct carcinoma to trastuzumab and docetaxel therapy. International cancer conference journal. 2016;5(3):150-3.

142. Kaidar-Person O, Billan S, Kuten A. Targeted therapy with trastuzumab for advanced salivary ductal carcinoma: case report and literature review. Medical oncology (Northwood, London, England). 2012;29(2):704-6.

143. Prat A, Parera M, Reyes V, Peralta S, Cedres S, Andreu J, et al. Successful treatment of pulmonary metastatic salivary ductal carcinoma with trastuzumab-based therapy. Head & neck. 2008;30(5):680-3.

144. Thorpe LM, Schrock AB, Erlich RL, Miller VA, Knost J, Le-Lindqwister N, et al. Significant and durable clinical benefit from trastuzumab in 2 patients with HER2-amplified salivary gland cancer and a review of the literature. Head & neck. 2017;39(3):E40-e4.

145. Iguchi F, Taniguchi Z, Kusano J, Takahashi Y, Murai N. [A case of metastatic salivary duct carcinoma successfully treated with trastuzumab-based targeted therapy]. Nihon Jibiinkoka Gakkai Kaiho. 2014;117(8):1108-14.

146. Park JC, Ma TM, Rooper L, Hembrough T, Foss RD, Schmitt NC, et al. Exceptional responses to pertuzumab, trastuzumab, and docetaxel in human epidermal growth factor receptor-2 high expressing salivary duct carcinomas. Head & neck. 2018;40(12):E100-e6.

147. Fiedler W, Stoeger H, Perotti A, Gastl G, Weidmann J, Dietrich B, et al. Phase i study of TrasGEX, a glyco-optimised anti-HER2 monoclonal antibody, in patients with HER2-positive solid tumours. ESMO Open. 2018;3 (4) (no pagination)(e000381).

148. Lee JS, Kwon OJ, Park JJ, Seo JH. Salivary duct carcinoma of the parotid gland: Is adjuvant HER-2-targeted therapy required? Journal of Oral and Maxillofacial Surgery. 2014;72(5):1023-31.

149. Jakob JA, Kies MS, Glisson BS, Kupferman ME, Liu DD, Lee JJ, et al. Phase II study of gefitinib in patients with advanced salivary gland cancers. Head & neck. 2015;37(5):644-9.

150. Locati LD, Perrone F, Cortelazzi B, Bergamini C, Bossi P, Civelli E, et al. A phase II study of sorafenib in recurrent and/or metastatic salivary gland carcinomas: Translational analyses and clinical impact. European Journal of Cancer. 2016;69:158-65.

151. Hyman DM, Puzanov I, Subbiah V, Faris JE, Chau I, Blay JY, et al. Vemurafenib in multiple nonmelanoma cancers with BRAF V600 mutations. New England Journal of Medicine. 2015;373(8):726-36.

152. Kim Y, Lee SJ, Lee JY, Lee SH, Sun JM, Park K, et al. Clinical trial of nintedanib in patients with recurrent or metastatic salivary gland cancer of the head and neck: A multicenter phase 2 study (Korean Cancer Study Group HN14-01). Cancer. 2017;123(11):1958-64.

153. Piha-Paul SA, Cohen PR, Kurzrock R. Salivary duct carcinoma: targeting the phosphatidylinositol 3-kinase pathway by blocking mammalian target of rapamycin with temsirolimus. Journal of clinical oncology : official journal of the American Society of Clinical Oncology. 2011;29(26):e727-30.

154. Nardi V, Sadow PM, Juric D, Zhao D, Cosper AK, Bergethon K, et al. Detection of novel actionable genetic changes in salivary duct carcinoma helps direct patient treatment. Clinical cancer research : an official journal of the American Association for Cancer Research. 2013;19(2):480-90.

155. Licitra L, Cavina R, Grandi C, Palma SD, Guzzo M, Demicheli R, et al. Cisplatin, doxorubicin and cyclophosphamide in advanced salivary gland carcinoma. A phase II trial of 22 patients. Annals of oncology : official journal of the European Society for Medical Oncology. 1996;7(6):640-2.

156. Laurie SA, Siu LL, Winquist E, Maksymiuk A, Harnett EL, Walsh W, et al. A phase 2 study of platinum and gemcitabine in patients with advanced salivary gland cancer: a trial of the NCIC Clinical Trials Group. Cancer. 2010;116(2):362-8.

157. Okada T, Saotome T, Nagao T, Masubuchi T, Fushimi C, Matsuki T, et al. Carboplatin and docetaxel in patients with salivary gland carcinoma: A retrospective study. In Vivo. 2019;33(3):843-53.

158. Yamamoto H, Uryu H, Segawa Y, Tsuneyoshi M. Aggressive invasive micropapillary salivary duct carcinoma of the parotid gland. Pathology international. 2008;58(5):322-6.

159. Kawahara K, Hiraki A, Yoshida R, Arita H, Matsuoka Y, Yamashita T, et al. Salivary duct carcinoma treated with cetuximab-based targeted therapy: A case report. Molecular and clinical oncology. 2017;6(6):886-92.

160. Warner KA, Oklejas AE, Pearson AT, Zhang Z, Wu W, Divi V, et al. UM-HACC-2A: MYB-NFIB fusion-positive human adenoid cystic carcinoma cell line. Oral oncology. 2018;87:21-8.

161. Li J, Perlaky L, Rao P, Weber RS, El-Naggar AK. Development and characterization of salivary adenoid cystic carcinoma cell line. Oral oncology. 2014;50(10):991-9.

162. Warner KA, Adams A, Bernardi L, Nor C, Finkel KA, Zhang Z, et al. Characterization of tumorigenic cell lines from the recurrence and lymph node metastasis of a human salivary mucoepidermoid carcinoma. Oral oncology. 2013;49(11):1059-66.

163. Noguchi K, Kanda S, Yoshida K, Funaoka Y, Yamanegi K, Yoshikawa K, et al. Establishment of a patient-derived mucoepidermoid carcinoma cell line with the CRTC1-MAML2 fusion gene. Molecular and clinical oncology. 2022;16(3):75.

164. Li J, Mitani Y, Rao PH, Perlaky L, Liu B, Weber RS, et al. Establishment and genomic characterization of primary salivary duct carcinoma cell line. Oral oncology. 2017;69:108-14.

165. Drost J, Clevers H. Organoids in cancer research. Nat Rev Cancer. 2018;18(7):407-18.

166. Acasigua GA, Warner KA, Nör F, Helman J, Pearson AT, Fossati AC, et al. BH3-mimetic small molecule inhibits the growth and recurrence of adenoid cystic carcinoma. Oral oncology. 2015;51(9):839-47.

167. Jiang Y, Gao R, Cao C, Forbes L, Li J, Freeberg S, et al. MYB-activated models for testing therapeutic agents in adenoid cystic carcinoma. Oral oncology. 2019;98:147-55.

168. Sun B, Wang Y, Sun J, Zhang C, Xia R, Xu S, et al. Establishment of patient-derived xenograft models of adenoid cystic carcinoma to assess pre-clinical efficacy of combination therapy of a PI3K inhibitor and retinoic acid. Am J Cancer Res. 2021;11(3):773-92.

169. Warner KA, Nör F, Acasigua GA, Martins MD, Zhang Z, McLean SA, et al. Targeting MDM2

for Treatment of Adenoid Cystic Carcinoma. Clinical cancer research : an official journal of the American Association for Cancer Research. 2016;22(14):3550-9.

170. Takada K, Aizawa Y, Sano D, Okuda R, Sekine K, Ueno Y, et al. Establishment of PDX-derived salivary adenoid cystic carcinoma cell lines using organoid culture method. International journal of cancer. 2021;148(1):193-202.

171. Keysar SB, Eagles JR, Miller B, Jackson BC, Chowdhury FN, Reisinger J, et al. Salivary Gland Cancer Patient-Derived Xenografts Enable Characterization of Cancer Stem Cells and New Gene Events Associated with Tumor Progression. Clinical cancer research : an official journal of the American Association for Cancer Research. 2018;24(12):2935-43.

172. Bleijs M, van de Wetering M, Clevers H, Drost J. Xenograft and organoid model systems in cancer research. Embo j. 2019;38(15):e101654.

173. Larsen BM, Kannan M, Langer LF, Leibowitz BD, Bentaieb A, Cancino A, et al. A pan-cancer organoid platform for precision medicine. Cell Rep. 2021;36(4):109429.

174. Dijkstra KK, Cattaneo CM, Weeber F, Chalabi M, van de Haar J, Fanchi LF, et al. Generation of Tumor-Reactive T Cells by Co-culture of Peripheral Blood Lymphocytes and Tumor Organoids. Cell. 2018;174(6):1586-98.e12.

175. Neal JT, Li X, Zhu J, Giangarra V, Grzeskowiak CL, Ju J, et al. Organoid Modeling of the Tumor Immune Microenvironment. Cell. 2018;175(7):1972-88.e16.

176. Zhao H, Jiang E, Shang Z. 3D Co-culture of Cancer-Associated Fibroblast with Oral Cancer Organoids. J Dent Res. 2021;100(2):201-8.

177. Tsai S, McOlash L, Palen K, Johnson B, Duris C, Yang Q, et al. Development of primary human pancreatic cancer organoids, matched stromal and immune cells and 3D tumor microenvironment models. BMC cancer. 2018;18(1):335.

PART 1:
Unraveling tumor genetics of salivary gland cancer

CHAPTER 2

Identification of fusion genes and targets for genetically matched therapies in a large cohort of salivary gland cancer patients

Gerben Lassche, Sjoerd van Helvert, Astrid Eijkelenboom, Martijn J.H. Tjan, Erik A.M. Jansen, Patricia H.J. van Cleef, Gerald W. Verhaegh, Eveline J. Kamping, Katrien Grünberg, Adriana C.H. van Engen-van Grunsven, Marjolijn J.L. Ligtenberg, Carla M.L. van Herpen

Cancers (Basel). 2022;27;14(17):4156

Abstract

Introduction

Salivary gland cancer (SGC) is a rare cancer for which systemic treatment options are limited. Therefore, it is important to characterize its genetic landscape in search for actionable aberrations, such as NTRK gene fusions. This research aimed to identify these actionable aberrations by combining NGS-based analysis of RNA (gene fusions) and DNA (single and multiple nucleotide variants, copy number variants, microsatellite instability and tumor mutational burden) in a large cohort of SGC patients.

Methods

RNA and DNA were extracted from archival tissue of 121 patients with various SGC subtypes. Gene fusion analysis was performed using a customized RNA-based targeted NGS panel. DNA was sequenced using a targeted NGS panel encompassing 523 cancer related genes. Cross-validation of NGS-based NTRK fusion detection and pan-TRK immunohistochemistry (IHC) was performed.

Results

Fusion transcripts were detected in 50% of the cases and included both known (MYB-NFIB, MYBL1-NFIB, CRTC1-MAML2) and previously unknown fusions (including transcripts involving RET, BRAF or RAD51B). Only one NTRK fusion transcript was detected, in a secretory carcinoma case. Pan-TRK IHC (clone EPR17341) was false positive in 74% of cases. The proportion of patients with targets for genetically matched therapies differed among subtypes (salivary duct carcinoma: 82%, adenoid cystic carcinoma 28%, mucoepidermoid carcinoma 50%, acinic cell carcinoma 33%). Actionable aberrations were most often located in PIK3CA (N= 18, 15%), ERBB2 (N=15, 12%), HRAS and NOTCH1 (both N=9, 7%).

Conclusion

Actionable genetic aberrations were seen in 53.7% of all SGC cases on the RNA and DNA level, with varying percentages between subtypes.

Introduction

Precision medicine has gained great momentum in clinical oncology practice over the past decade. This is highlighted by the rapidly increasing number of basket trials being performed, in which cancer patients are treated with therapeutic interventions targeting specific aberrations present in the patients' tumor (1). Recent reports of such basket trials indicate that tumor responses can be elicited in patient groups lacking other standard treatment options (2, 3). Hence, it is a promising approach to treat patients based on specific genetic aberrations which drive the tumor, especially for treatment of patients suffering from rare cancers, because it takes advantage of knowledge obtained in more common malignancies. Moreover, in rare cancers, the conventional route of drug registration is often hampered by difficulties in performing phase III trials.

Salivary gland cancer (SGC) is a rare cancer for which limited treatment options are available in the palliative treatment setting (4). Adding to the complexity of studying SGC is its subdivision into 22 different subtypes that highly differ in clinicopathological characteristics and genetic hallmarks (4-6). This merits recognition of the different subtypes as separate entities and treating them as such, but also emphasizes the importance of characterizing the molecular landscape to identify potential actionable genetic aberrations.

A common feature in the molecular landscape of SGC is the presence of gene fusions, which are believed to be dominant drivers of cancer progression (7, 8). Chromosomal rearrangements that have previously been identified in SGC are *MYB*- or *MYBL1-NFIB* gene fusions in adenoid cystic carcinoma (AdCC), *CRTC1*- or *CTRC3-MAML2* gene fusions in mucoepidermoid carcinoma (MEC), *PLAG1* or *HMGA2* gene fusions in carcinoma ex pleomorphic adenoma (CXPA) and *ETV6-NTRK3* gene fusions in secretory carcinoma (8-14). *NTRK* gene fusions are of particular interest due to recent registration of targeted therapies for *NTRK* fusion-positive cancers. *NTRK* rearrangements are found in a wide variety of cancer types and they can result in the expression of ligand-independent and/or constitutive active oncogenic fusion proteins (15). The resulting activated downstream signaling is believed to be a strong driver for these cancers, indicated by impressive response rates seen in *NTRK* gene fusion-positive cancer patients after treatment with selective TRK inhibitors, such as larotrectinib (71% response rate, with a median duration of response 35 months) and entrectinib (57% response rate with a median duration of response of 10 months) (16, 17).

Various types of genetic aberrations are actionable with matched therapies. It is therefore pivotal to also test for single and multiple nucleotide variants and copy number variants in SGC. This research aims to comprehensively assess the prevalence of actionable aberrations, including gene fusions, in a large cohort of SGC patients. An RNA-based targeted next-

generation sequencing (NGS) panel was used for gene fusion detection and targeted DNA-based NGS panel analysis was used to detect single and multiple nucleotide variants, copy number variants, tumor mutational burden and microsatellite instability in 121 SGCs. The combined approach revealed the presence of gene fusions in half of the cases, including several fusions not previously described in SGC, and the presence of targets for genetically matched therapies in 28.3-81.8% of cases, depending on the SGC subtype.

Methods

Patient selection and material acquisition

Patients participating in the Radboud university medical center biobank for SGC were included in this study. This cohort was supplemented with patients visiting the outpatient clinics of the departments of otorhinolaryngology, maxillofacial surgery, or medical oncology of the tertiary referral center Radboudumc university medical center, who were suffering from, AdCC, salivary duct carcinoma (SDC), MEC or acinic cell carcinoma (AciCC). Formalin-fixed paraffin-embedded (FFPE) tissue that was not older than five years had to be available. This study was approved by the institutional review board and all patients provided written informed consent (file numbers 2017-3679 and 2019-5476). FFPE material of these patient was retrieved from pathological archives, partially by the Nationwide Network and Registry of Histo- and Cytopathology in the Netherlands (PALGA) (18). Clinicopathological characteristics were retrospectively collected from the medical records.

DNA and RNA extraction

DNA and RNA were extracted from 6 µm FFPE sections, 5-10 sections per case. Adjacent 4 µm sections were stained with hematoxylin and eosin (HE) for estimation of tumor cell percentage and annotation of the tissue area containing tumor cells. The annotated tissue was manually macrodissected from the 6 µm sections. RNA was isolated using the Reliaprep FFPE Total RNA Miniprep system (Promega, Madison, WI, USA) according to manufacturers' protocol. Genomic DNA was extracted using Chelex-100 and 400µg proteinase K as previously described (19). Nucleic acid concentrations were measured using the Qubit dsDNA Broad Range and RNA HS kits (Thermo Fisher Scientific, Waltham, MA, USA).

Detection of RNA gene fusion transcripts

Anchored multiplex PCR technology was used to detect RNA gene fusion transcripts. Up to 250 ng total RNA was used for preparation of cDNA. Open-ended target-enriched NGS libraries were subsequently prepared using the FusionPlex® kit according to the manufacturer s instructions (Invitae, San Francisco, CA, USA). A custom designed targeted gene panel was used (Radboudv1), which includes 56 genes relevant for, but not limited to,

differential diagnosis of SGC and therapeutic targeting (Supplementary Table 1). Pooled FusionPlex® libraries were combined with TSO500 libraries for sequencing. Demultiplexing was performed using an in-house bioinformatic workflow and data was thereafter analyzed using Archer Analysis software (ArcherDX, Boulder, CO, USA) version 6.2.7. Analysis QC was based on the percentage of reads mapped on RNA. Analyses with ≥50% RNA reads were classified as 'good quality', 20-50% as 'mediocre' and <20% as 'fail'. The minimum average unique RNA start sites per gene-specific primer 2 for control genes was set at 10.

DNA next generation sequencing

Presence of single and multiple nucleotide variants, copy number variants (CNVs), tumor mutational burden (TMB) and microsatellite instability (MSI) was assessed using the TruSight Oncology 500 panel (TSO500, Illumina, San Diego, CA, USA), which contains 523 cancer related genes with a total genomic content of 1.94 Mb (Supplementary Table 2). Preparation of NGS libraries was performed according to the manufacturers' instructions, as described before (20). During library preparation, unique molecular identifier ligation and two-step hybridization capture-based target enrichment was used, allowing sensitive detection of mutations. Sequencing was performed using a NextSeq500 (Illumina, San Diego, CA, USA) with a high output cassette.

NGS data (TSO500) is available in the European Genome-Phenome Archive after reasonable request (Study ID EGAS00001006232).

Pan-TRK immunohistochemistry

TRK expression was detected in FFPE tissue sections with pan-TRK immunohistochemistry (IHC). The rabbit monoclonal antibody EPR17341 (Abcam, Cambridge, MA, USA), targeting a conserved epitope on the TRKA, TRKB and TRKC proteins, was used on a semi-automatic Labvision immunostainer 480 or 360 (Thermo Fisher Scientific, Waltham, MA, USA) in a dilution of 1:25. Detection was performed using EnVision FLEX High Ph, HRP rabbit/mouse (DAKO Agilent, Santa Clara, CA, USA). Healthy appendix tissue was used as a positive control. Scoring was performed by an expert SGC pathologist (AvEvG). Samples were divided in four categories after comparing to the negative and positive control: negative, weak/dubious, moderate and positive. In case of tissue shortage, priority was given to NGS over IHC analysis.

***NTRK1*, *NTRK2* and *NTRK3* fluorescence *in situ* hybridization**

Fluorescence *in situ* hybridization (FISH) was performed for cases with discordant results in pan-TRK IHC and gene fusion analysis (only when RNA-NGS QC was mediocre or fail). Dual-color break apart probes targeting *NTRK1* (z-2167-200), *NTRK2* (z-2205-200) and *NTRK3* (z-2206-200) were used according to manufacturer's instruction (ZytoVision, Bremerhaven, Germany). Fifty nuclei were scored by two independent researchers, using a Leica DMRBE (Leica, Wetzlar, Germany) fluorescence microscope. Samples were considered

positive if >50% of nuclei scored positive (1 yellow, 1 green and 1 red signal), and dubious if 10-50% of nuclei scored positive. Dubious results were considered positive if >15% of nuclei scored positive after scoring by the second researcher.

TSO500 data analysis

Sequencing data of the TSO500 panel was processed using the TSO500 Local App Version 2.0.0.70 (Illumina, San Diego, CA, USA). GRCh37/hg19 was used as reference genome. This pipeline calls variants along with their allele frequencies and reports total and non-synonymous tumor mutational burden (TMB) and the percentage of microsatellite instable sites (MSI). Non-synonymous TMB values are further used in this study and referred to as TMB. Cases were considered MSI high if the percentage of unstable sites was ≥25% and uncertain with 10-25% unstable sites. Called variants were filtered by excluding synonymous variants, variants in non-coding regions outside of splice sites (including the 3' and 5' untranslated region (UTR)) and variants that have a prevalence >0.1% in the general population (assessed by crosschecking the variant in the Exome Aggregation Consortium database (version 0.2). Variants were assessed in a subset of genes (Supplementary Table 3), that were mainly selected because mutations in these genes could lead to treatment with currently registered drugs or in basket trials (such as the Drug Rediscovery protocol, NCT02925234). Single and multiple nucleotide somatic variants were rated in a five-tier classification of pathogenicity: 1. benign (single nucleotide polymorphisms (SNPs)), 2. likely benign, 3. variant of unknown/uncertain significance (VUS), 4. likely pathogenic or 5. pathogenic, as recommended by the American College of Medical Genetics and Genomics and the Association for Molecular Pathology (21). Determination of pathogenicity was performed by a clinical scientist in molecular pathology (SvH). Variants classified as likely pathogenic and pathogenic were included for further analysis. Copy number variants were determined by calculating the relative coverage per gene, followed by comparison to coverage data obtained from healthy tissues, as previously reported (22). In general, a minimum of 50% tumor cells was required for analysis of copy number losses. Bi-allelic deletions were assessed for all tumor suppressor genes in the virtual panel, except for *TP53*. For the same tumor suppressor genes, loss of heterozygosity (LOH) was assessed only when a (likely) pathogenic mutation was detected. Actionability of the genes of the virtual panel is defined in Supplementary Table 3. Regarding gene fusions, activating *ABL1, ALK, BRAF, EGFR, FGFR1-3, MAML2, MET, NRG1, NTRK1-3, RET* and *ROS1* fusions were considered potentially actionable.

Data analysis

All patients for whom one or both NGS panels were performed (FusionPlex® RadboudV1 or TSO500) were included in the analysis. Cases were considered *NTRK* gene fusion positive based on results obtained from RNA NGS or FISH.

Descriptive statistics were used to summarize clinical data, analyzed using SPSS version 25.0 (IBM Crop. Armonk, NY, USA). Survival curves were constructed in Python version 3.8.8 with the Matplotlib, Pandas and Lifelines packages, using Kaplan-Meier estimates. 95%-confidence intervals (CI) for median survival were calculated using the exponential Greenwood formula. Oncoplots were created using maftools package in R version 4.1.2.

Results

Included patients comprise diverse subtypes of salivary gland cancer

A total of 139 patients were included in this study and NGS data was acquired for 121 patients. In total 118 FusionPlex® RadboudV1 and 119 TSO500 panels were performed (both panels were performed for 116 patients). The primary tumor was the tissue source in 71 cases (58.7%), a local recurrence in 7 cases (5.8%) and a metastatic site in 43 cases (35.5%). Absence of tumor material or material of insufficient quality was the reason for inability to perform NGS in the other cases.

The 121 patients included in the analysis consisted of 46 AdCC patients, 44 SDC patients, 16 MEC patients, 9 AciCC patients and 6 patients with other subtypes (1 secretory carcinoma, 1 polymorphic adenocarcinoma (PAC), 1 adenocarcinoma NOS, 1 myoepithelial carcinoma, 1 epithelial/myoepithelial carcinoma and 1 mixed PAC/myoepithelial carcinoma).

For all 121 patients, median age at diagnosis was 57 years (range 17-90) and 47.9% was male. Most patients suffered from SGC in one of the major salivary glands (66.9%). The primary tumor was located outside the salivary glands in 9.9% of the cases (e.g. lacrimal gland or bronchus). At diagnosis, 15.7% presented with metastatic disease, and in 18.2% of cases the initial treatment intent was palliative. Of the patients treated with curative intent, 63.6% developed recurrent/metastatic disease during follow-up. During disease, 47.1% of the patients received systemic therapy (with a median of one line of systemic therapy). Table 1 lists clinical characteristics for the grouped cohort and per subtype.

After median follow-up of 40 months (range 2-378) Kaplan-Meier estimates indicated a median overall survival of 86 months from initial diagnosis (95%-CI 58-233 months) for all subtypes grouped. The median overall survival of all stages in AdCC patients was 195 months (95%-CI 58-not evaluable (NE)), in SDC patients 72 months (95%-CI 47-81 months), in MEC patients 283 months (95%-CI 49-283), in AciCC patients 207 months (95%-CI 9-207) and in the miscellaneous group 46 months (3-NE) (Figure 1).

Table 1: Clinicopathological characteristics of the included patients. AdCC: adenoid cystic carcinoma, SDC: salivary duct carcinoma, MEC: mucoepidermoid carcinoma, AciCC: acinic cell carcinoma, misc.: miscellaneous; R/M: recurrent/metastatic

		All (N=121)	AdCC (N=46)	SDC (N=44)	MEC (N=16)	AciCC (N=9)	Misc. (N=6)
	N (%)						
Age at diagnosis							
	Median (range)	57 (17-90)	53 (21-83)	63 (35-90)	53 (17-72)	56 (45-71)	67 (48-79)
Gender							
	Male	58 (47.9)	15 (32.6)	28 (63.6)	8 (50)	5 (55.6)	2 (33.3)
	Female	63 (52.1)	31 (67.4)	16 (36.4)	8 (50)	4 (44.4)	4 (66.7)
Location primary tumor							
	Major salivary gland	81 (66.9)	21 (45.7)	42 (95.5)	6 (37.5)	9 (100.0)	3 (50.0)
	Minor salivary gland	28 (23.1)	16 (34.8)	1 (2.3)	8 (50.0)	0 (0.0)	3 (50.0)
	Other	12 (9.9)	9 (19.6)	1 (2.3)	2 (12.5)	0 (0.0)	0 (0.0)
T-stage at diagnosis							
	1-2	39 (32.3)	6 (13.0)	16 (36.4)	10 (62.5)	4 (44.4)	3 (50.0)
	3-4	56 (46.3)	27 (58.7)	21 (47.7)	4 (25.0)	2 (22.2)	2 (33.3)
	Tx	26 (21.5)	13 (28.3)	7 (15.9)	2 (12.5)	3 (33.3)	1 (16.7)
N-stage at diagnosis							
	0	52 (43.0)	27 (58.7)	8 (18.2)	7 (43.8)	5 (55.6)	5 (83.3)
	1-3	44 (36.4)	7 (15.2)	28 (63.6)	7 (43.8)	1 (11.1)	1 (16.7)
	Nx	25 (20.7)	12 (26.1)	8 (18.2)	2 (12.5)	3 (33.3)	0 (0.0)
M-stage at diagnosis							
	0	100 (82.6)	36 (78.3)	39 (88.6)	14 (87.5)	7 (77.8)	4 (66.7)
	1	19 (15.7)	8 (17.4)	5 (11.4)	2 (12.5)	2 (22.2)	2 (33.3)
	Mx	2 (1.7)	2 (4.3)	0 (0.0)	0 (0.0)	0 (0.0)	0 (0.0)

(Table continues on next page)

Initial treatment intent							
	Curative	99 (83.5)	35 (76.1)	39 (88.6)	14 (87.5)	7 (77.8)	4 (66.7)
	Palliative	22 (18.2)	11 (23.9)	5 (11.4)	2 (12.5)	2 (22.2)	2 (33.3)
R/M disease after initial curative treatment (n=99)							
	Yes	63 (63.4)	28 (80.0)	24 (61.5)	6 (42.9)	4 (57.1)	1 (25%)
	No	36 (36.4)	7 (20.0)	15 (38.5)	8 (57.1)	3 (42.9)	3 (75%)
Underwent surgery primary tumor							
	Yes	101 (83.5)	36 (78.3)	38 (86.4)	15 (93.8)	8 (88.9)	4 (66.7)
	No	20 (16.5)	10 (21.7)	6 (13.6)	1 (6.3)	1 (11.1)	2 (33.3)
Palliative systemic therapy							
	Yes	57 (47.1)	18 (39.1)	28 (63.6)	4 (25.0)	5 (55.6)	2 (33.3)
	No	64 (52.9)	28 (60.9)	16 (36.4)	12 (75.0)	4 (44.4)	4 (66.7)
Lines of systemic therapy							
	Median (range)	1 (1-7)	1 (1-4)	2 (1-5)	2 (1-7)	2 (1-2)	1 (1)
First line systemic therapy							
	Chemotherapy	18 (14.9)	11 (23.9)	2 (4.5)	2 (12.5)	3 (33.3)	0 (0.0)
	Targeted	12 (9.9)	6 (13.0)	1 (2.3)	2 (12.5)	1 (11.1)	2 (33.3)
	Hormonal	17 (14.0)	0 (0.0)	16 (36.4)	0 (0.0)	1 (11.1)	0 (0.0)
	Immunotherapy	1 (0.8)	0 (0.0)	1 (2.3)	0 (0.0)	0 (0.0)	0 (0.0)
	Combination	8 (6.6)	0 (0.0)	8 (18.2)	0 (0.0)	0 (0.0)	0 (0.0)
	Other	1 (0.8)	1 (2.2)	0 (0.0)	0 (0.0)	0 (0.0)	0 (0.0)

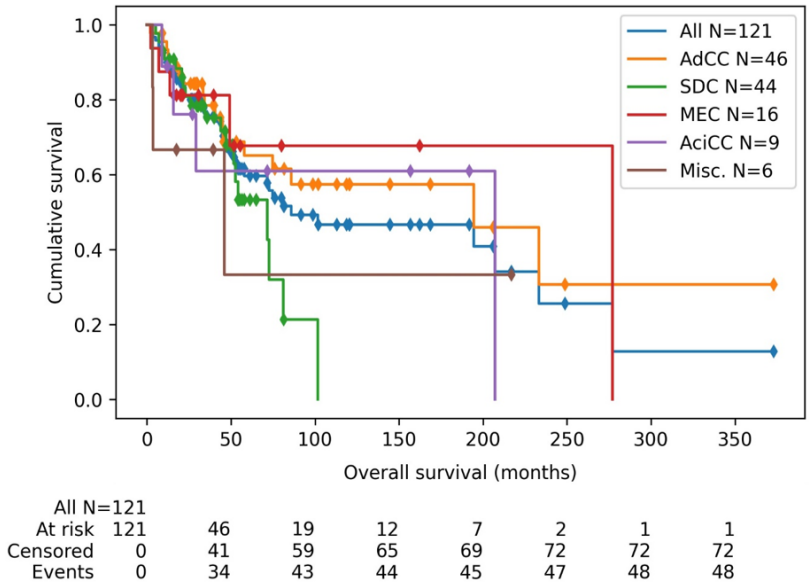

Figure 1: Kaplan-Meier curve of overall survival (from initial diagnosis until death), sorted per subtype and grouped for all subtypes together. All included patients are plotted, which is a mixed group regarding disease stage. Abbreviations: AdCC: adenoid cystic carcinoma, SDC: salivary duct carcinoma, MEC: mucoepidermoid carcinoma, ACiCC: acinic cell carcinoma, misc.: miscellaneous.

Half of SGC cases harbor gene fusions with varying incidence among subtypes

To detect relevant gene fusions in this cohort of mixed subtypes, a customized NGS panel was used (FusionPlex® RadboudV1). 115 of the 118 analyses were of sufficient quality. A fusion transcript was detected in 50.4% (58 out of 115) of these patients (Figure 2). The incidence varied per subtype, with detection of a fusion transcript in AdCC patients in 33 out of 44 (75.0%), in SDC in 12 out of 42 cases (28.6%), in MEC in 6 out of 15 (40.0%), in AciCC 3 out of 8 (37.5%) and 4 out of 6 (66.7%) in the miscellaneous group (Figure 2).

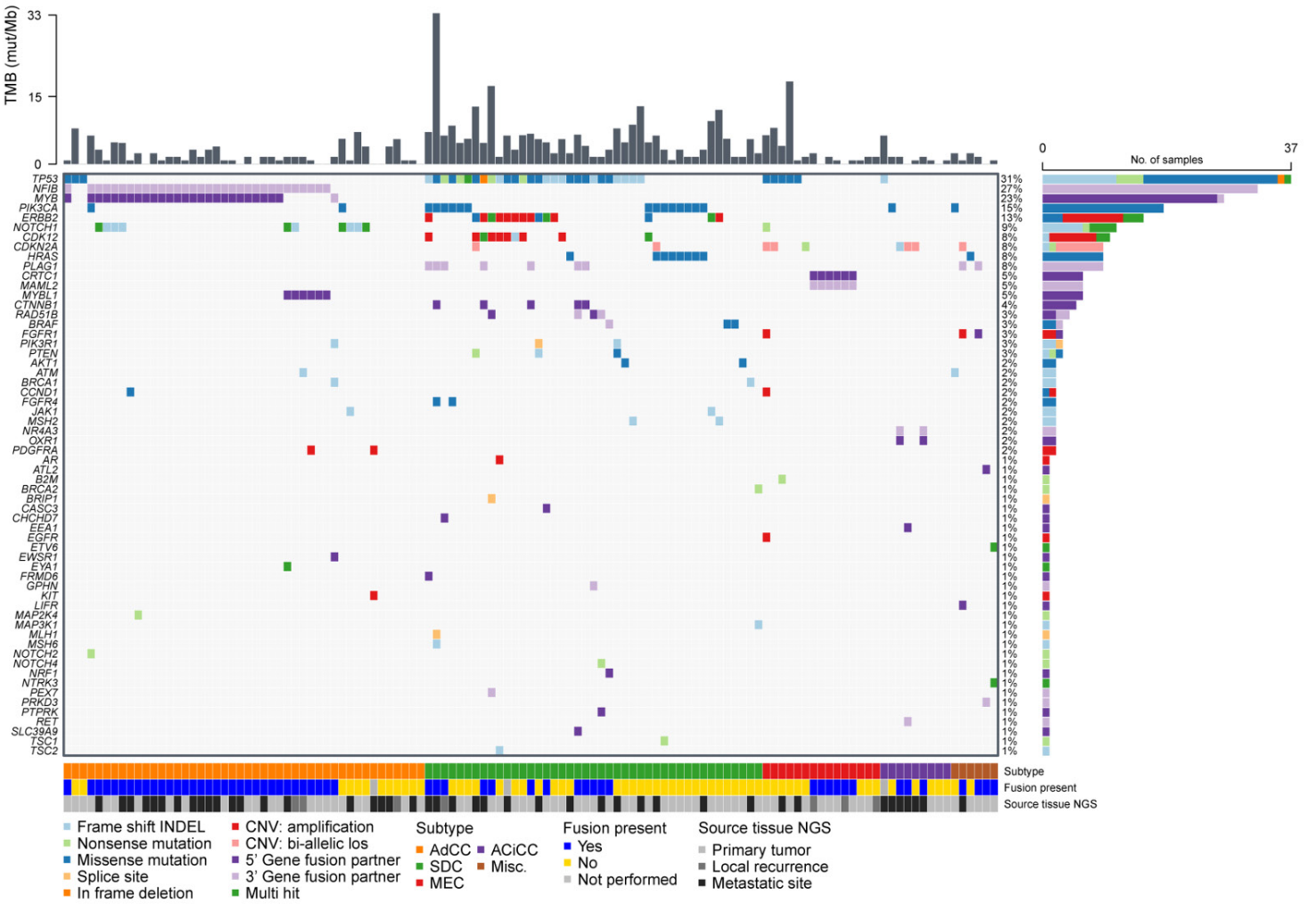

Figure 2: Oncoplot of all gene fusions, copy number variants and small variants that are assessed as pathogenic or likely pathogenic. AdCC: adenoid cystic carcinoma, SDC: salivary duct carcinoma, MEC: mucoepidermoid carcinoma, AciCC: acinic cell carcinoma, misc.: miscellaneous.

Frequent detection of *MYB*- and *MYBL1*-*NFIB* fusion transcripts in AdCC

In AdCC, all identified fusion transcripts involved *MYB* or *MYBL1,* fused to *NFIB* (N=33) and fusions involving these genes were exclusive to AdCC cases. Fusions with *MYB* or *MYBL1* gene as 5' partner and *NFIB* as 3' partner were detected most frequently (N=32, Figure 2 and Figure 3). In most of these cases (N=22) one or more alternative fusion transcripts involving the same genes were detected, with different breakpoints, indicating alternative or aberrant splicing of the fusion transcripts. One in-frame *EWSR1-MYB* fusion transcript was detected, with *MYB* as 3' partner, leaving the *MYB* coding sequence largely intact (fusion of exon 8 of *ESWR1* (NM_005243.3) and exon 2 of *MYB* (NM_005243.3)). This fusion has been described before in a myelofibrosis case and is believed to lead to upregulation of *MYB* (23).

All *MYB* and *MYBL1* fusion transcripts contained the DNA binding and (the majority of) the transactivation domain (Figure 3). Apparently, presence of these domains in the context of NFIB 3'UTR or its downstream genomic region are sufficient to serve as a driver. The contribution of the *NFIB* coding sequence appeared negligible in most cases, as in the majority of cases only a minor part of the *NFIB* open reading frame was retained in the fusion transcripts (Figure 3).

Three AdCC cases harbored an insertion in between *MYB/MYBL1* and *NFIB*. In one case *MYBL1* exon 12 was fused to exon 2 of the *EYA1* gene (NM_000503.5, both genes are located in close proximity to each other on chromosome 8, 8q13.1 and 8q13.3, respectively) and *EYA1* exon 6 fused to *NFIB* exon 3 into a triple gene fusion. In the second case, exon 2 of *PDE7B* (NM_018945.3) was inserted between exon 14 of *MYB* and exon 3 of *NFIB,* resulting in an open reading frame. The third case contained an insertion of 51 nucleotides (aligning to chromosome 8) in between exon 9 of *MYB* and exon 9 of *NFIB,* resulting in an out of frame fusion transcript.

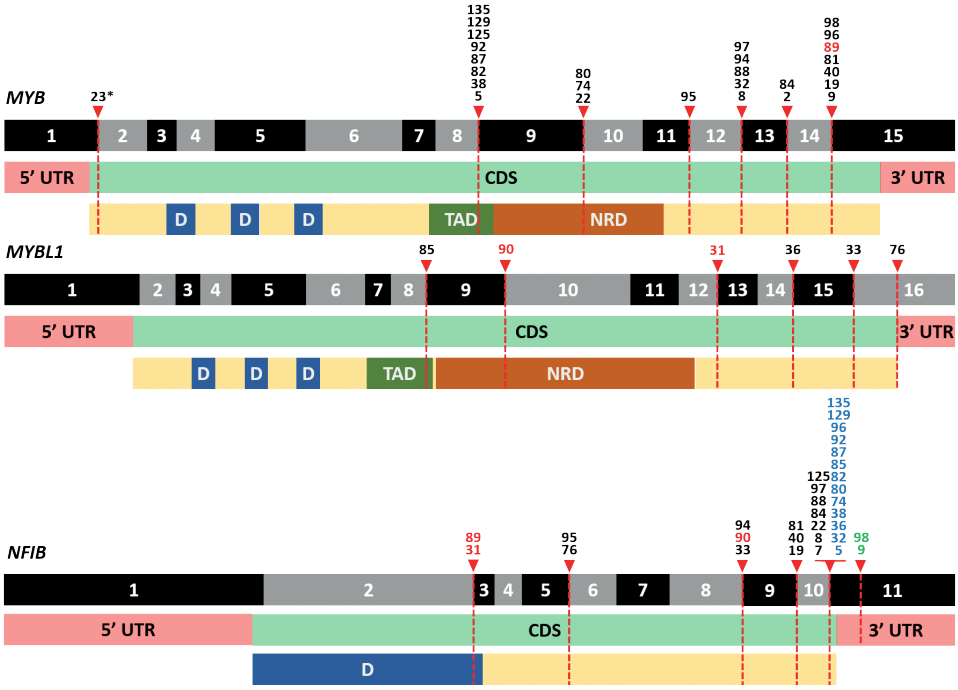

Figure 3: Overview of identified breakpoints in the *MYB*, *MYBL1* and *NFIB* genes and their location in functional domains of the proteins encoded by these genes. Numbers indicate unique cases. Used reference sequences are NM_005375.4 (*MYB*), NM_001080416.4 (*MYBL1*) and NM_001190737.2 (*NFIB*) and functional domains are derived from UniProt. The last exon and 3'UTR of each gene is not up to scale. In cases where more than one fusion transcript involving the same two genes was identified, the breakpoint of the dominant transcript (highest number of reads) is depicted. Red numbers: cases with an insertion between *MYB/MYBL1* and *NFIB.* Blue numbers: breakpoints mapped to exon 10 of *NFIB* transcript NM_001282787.1, which is absent in NM_001190737.2. Green numbers: cases with breaking point in 3' UTR, lacking last amino acids of NFIB (exact breaking point not up to scale). *MYB as 3' partner. Abbreviations: UTR: untranslated region, CDS: coding DNA sequence, D: DNA-binding.

A plethora of both known and new fusion transcripts was detected in non-AdCC cases

Fusion transcripts involving *PLAG1* as 3' partner, frequently seen in SGC arising from pleomorphic adenomas (CXPA), were detected in SDC (N=7), myoepithelial carcinoma (N=1) and a case with mixed PLGA/myoepithelial histology (9). In 8 out of these 9 cases earlier diagnostic pathology did reveal that these tumors did arise from pleomorphic adenomas. In the only case in which CXPA origin could not be confirmed, only biopsy material was available for diagnostic pathology, which might lead to missing the pleomorphic adenoma origin. The complete coding sequence of *PLAG1* was retained in all fusion transcripts. Presumably the *PLAG1* start codon is used, as in 8 out of 9 cases the start codon of the 5' partner is not present in the fusion transcript and in the other case the start codon of the 5' partner is followed by

2 non-coding exons of *PLAG1*. The 5' fusion partner genes were *CTNNB1* (N=5), *CHCHD7, FGFR1, FRMD6* or *LIFR* (N=1 each) (Figure 2).

CRTC1-MAML2 fusion transcripts were detected in 6 cases (all in-frame). As expected, they were all detected in MEC (5 low grade, 1 intermediate grade) (12). In 2 AciCC cases an *OXR1-NR4A3* fusion transcript was identified, which contained a short 5' sequence of *OXR1* fused to the complete coding sequence of *NR4A3*. Analogous to *PLAG1*-type translocations, this could result in a pathogenic effect due to exchange of regulatory sequences, rather than formation of a chimeric fusion protein. In line with these findings, enhancer hijacking has been shown to result in overexpression of the oncogenic *NR4A3* (24), although *OXR1* as fusion partner has not yet been described.

In 4 cases (all SDC) fusion transcripts involving *RAD51B* were detected, twice as 5' and twice as 3' fusion partner. These fusions probably lead to inactivation of *RAD51B*. It has been shown that even in the presence of a wild type allele this can lead to homologous recombination deficiency due to haploinsufficiency (25). In one of these cases, a second fusion transcript involving *PLAG1* was detected (Supplementary Table 4).

Regarding *NTRK* gene fusions, only one *ETV6-NTRK3* fusion transcript was detected in the secretory carcinoma case (as was the reciprocal *NTRK3-ETV6* transcript). No other fusion transcripts involving either one of the *NTRK* genes were detected.

Four other in-frame fusion transcripts were detected once: an *ATL2D-PRKD3* fusion transcript was detected in a PAC case and an *EEA1-RET* fusion transcript in an AciCC case (in-frame, kinase domains of *RET* retained). In one SDC, an in-frame *CASC3-ERBB2* fusion transcript was detected with retained *ERBB2* kinase domain. These genes are both located in close proximity on chromosome 17. This case was shown to harbor an *ERBB2* amplification in the TSO500 analysis. In an SDC case an *NRF1-BRAF* fusion transcript was detected, which has been described before in other tumor types and is believed to lead to activation of downstream MAPK signaling (26).

Pan-TRK immunohistochemistry is false positive in the majority of SGC cases

To enable treatment with TRK-inhibitors in case of incurable recurrent or metastatic disease detection of *NTRK* fusions is pivotal, for which pan-TRK IHC is often used as initial screening prior to NGS. To assess performance of this screening in SGC, pan-TRK IHC was performed in 108 cases. Compared to the negative control, weak cytoplasmatic IHC positivity was observed frequently, as was positive myoepithelium in AdCC cases (Supplementary Figure 1). Out of the 108 cases, 28 were negative (25.9%) and the other cases were scored as positive (clearly positive (N=11, 10.2%), weakly/dubious positive (N=47, 43.5%) or moderately

positive (N=22, 20.4%)). Of the AdCC cases 82.5% scored positive, in SDC cases 77.5%, in MEC cases 53.3%, in AciCC cases 37.5% and in the miscellaneous group including the secretory carcinoma case with the *ETV6-NTRK3* gene fusion all cases scored positive.

FISH was performed for 19 of 24 cases with a positive TRK-IHC and NGS data of mediocre quality. All the *NTRK1, NTRK2* and *NTRK3* FISH samples were scored negative, although 2 cases had a dubious *NTRK1* result (Supplementary Figure 2). Polysomy was detected frequently.

With the NGS and FISH results combined, an *NTRK* gene fusion was detected in 1 out of 118 cases (the secretory carcinoma case). Of the 80 cases that did not score negative on IHC, 79 cases were false positive, leading to an overall false positivity rate of pan-TRK IHC of 73.8% (79 out of 107). Given the overall low prevalence of *NTRK* gene fusions, sensitivity of IHC to detect *NTRK* gene fusions could not be assessed reliably.

High TMB and MSI are rare in SGC

To assess actionability with immune checkpoint inhibitors, TMB and microsatellite status were assessed. At least 1.2 megabases of coding regions were sequenced in each of the 119 TSO500 panels (46 AdCC cases, 43 SDC cases, 15 MEC cases, 9 AciCC cases and 6 miscellaneous cases). Median exon coverage ranged from 80-904 (median 308) unique reads and the median percentage of exon coverage with at least 100 unique reads was 96.6% (Supplementary Figure 3).

The median TMB for all subtypes grouped was 1.6 mut/Mb and ranged from 0.0-33.4 mut/Mb. The median TMB was highest in SDC cases with 4.8 mut/Mb. In AdCC median TMB was 1.6 mut/Mb, in MEC cases 1.6 mut/Mb, in AciCC cases 0.8 mut/Mb and in the miscellaneous group 1.2 mut/Mb (Figure 4A). Three tumors qualified as TMB-high, with 17.3 and 33.4 mut/Mb (SDC) and 18.3 mut/Mb (MEC).

Microsatellite status was determined by the percentage of unstable sites for MSI. Initially, no MSI was detected, with a median percentage of unstable sites in all subtypes grouped of 2% (range 0-11%, Figure 4B). One SDC case scored uncertain with 11% (12 of 106) unstable sites. In this case an *MLH1* mutation with LOH was detected and MLH1 IHC confirmed loss of nuclear MLH1 proteins. The same case also harbored the highest TMB (33.4 mut/Mb).

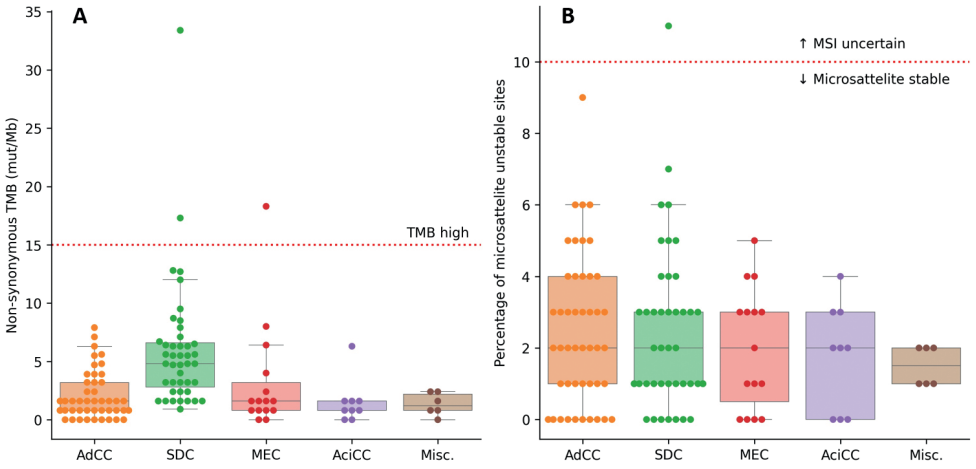

Figure 4: **A**: Non-synonymous tumor mutational burden (TMB), sorted per subtype. **B**: percentage of microsatellite instable sites (MSI), sorted per subtype. Dotted lines indicate thresholds for tumors with high TMB and with potential MSI. Abbreviations: SDC: salivary duct carcinoma, AdCC: adenoid cystic carcinoma, MEC: mucoepidermoid carcinoma, AciCC: acinic cell carcinoma, misc.: miscellaneous.

Pathogenic small nucleotide variants are most frequent in SDC

Single nucleotide and small insertion and/or deletion variants identified within a virtually defined panel of 61 genes (focusing on but not restricted to genes that may direct treatment decisions, Supplementary Table 3) were assessed for their pathogenicity. In total, 381 variants were assessed, of which 125 were classified as pathogenic or likely pathogenic somatic mutations, identified in 72 different cases (60.5%). These 125 (likely) pathogenic variants were located in 28 different genes (Figure 2). Mutations in *TP53, PIK3CA* and *NOTCH1* were most frequently observed. Twelve *NOTCH1* mutations were activating (i.e., truncating mutations deleting the PEST domain), as was the only *NOTCH2* mutation (27, 28). All were detected in AdCC cases. Four truncating *NOTCH1* mutations, detected in 3 cases (2 AdCC and 1 MEC), were considered inactivating, as too much of the open reading frame was lost. Nevertheless, they were classified as likely pathogenic because *NOTCH1* is also described as a tumor suppressor (29).

Copy number variants are mostly restricted to *ERBB2* amplifications in SDC

Gene amplifications were observed in 17 cases, mostly in SDC (N=13), but also in AdCC (N=2), MEC (N=1) and myoepithelial carcinoma (N=1) (Figure 2, Supplementary Figure 4). The most frequently amplified gene was *ERBB2* (N=11), often co-occurring with amplification of the nearby gene *CDK12* (N=8) (Figure 2, Supplementary Figure 4). AR amplification was seen in a primary tumor specimen (SDC) that was resected from a hormone-naïve patient,

indicating that the amplification was not a result of therapy-driven resistance. Bi-allelic loss of *CDKN2A* was seen in 7 cases (SDC, MEC and AciCC two cases each and one myoepithelial carcinoma case, Figure 2).

DNA and RNA analysis reveals actionable targets in the majority of SGC cases

The results of the FusionPlex® RadboudV1 and TSO500 were combined to estimate the fraction of SGC tumors that harbor a (potentially) actionable genetic aberration. Such aberrations (defined in Supplementary Table 3) were identified in 53.7% of all SGC cases. This varied per subtype: 28.3% for AdCC, 81.8% for SDC, 50.0% for MEC, 33.3% for AciCC and 83.3% for the miscellaneous group (Figure 5). In most subtypes the majority of actionable aberrations were single nucleotide variants or insertions/deletions, except for MEC, in which gene fusions *(MAML2)* were the most common potentially actionable aberration (Figure 5). Putatively actionable aberrations were most often located in *PIK3CA* (N= 18, 14.9%), *ERBB2* (N=15, 12.4%), *HRAS* and *NOTCH1* (both N=9, 7.4%). Actionable *ERRB2* aberrations were exclusive to SDC and actionable *NOTCH1* mutations to AdCC. *PIK3CA* and *HRAS* aberrations were most often seen in SDC (Figure 2).

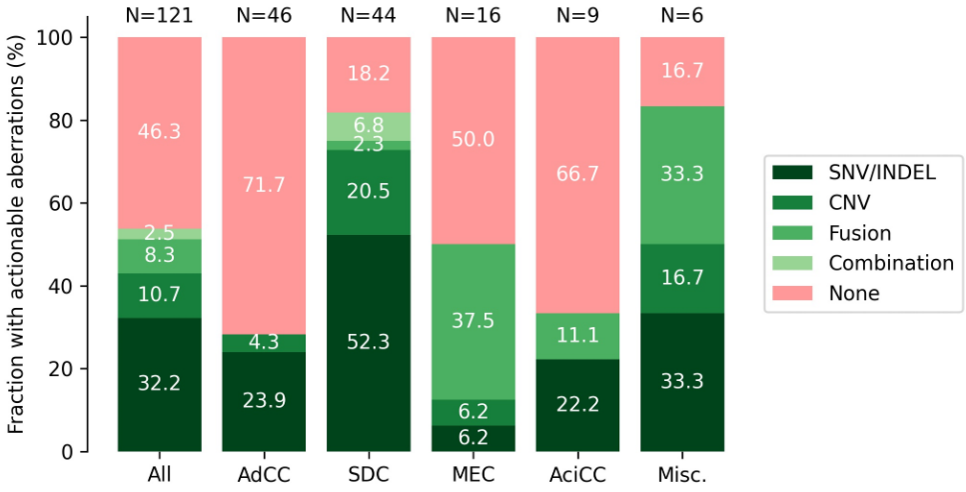

Figure 5: Fraction of cases with putatively actionable aberrations, split per subtype and type of aberration. The SNV/INDEL group for SDC contains one SDC case on which actionability was based solely on high TMB and one SDC case with MSI. Abbreviations: SDC: salivary duct carcinoma, AdCC: adenoid cystic carcinoma, MEC: mucoepidermoid carcinoma, AciCC: acinic cell carcinoma, misc.: miscellaneous; SNV: single nucleotide variant, INDEL: insertion/deletion; CNV: copy number variant; TMB: tumor mutational burden; MSI: microsatellite instability.

Discussion

In this study we comprehensively assessed the genetic landscape of different subtypes of SGC, with a focus on gene fusions and actionable aberrations. The fraction of patients with actionable genetic tumor aberrations differs among SGC subtypes, ranging from 28.3% in AdCC to 81.8% in SDC in this cohort. Gene fusions were identified in half of all SGC cases. Except for the only secretory carcinoma case in this study (a SGC subtype known to harbor *NTRK3* fusions), no *NTRK* gene fusions were detected in other SGC subtypes (14).

Because *NTRK* gene fusions are highly relevant with respect to systemic treatment options, the gene fusion analysis was focused on detection of these translocations. In two recent studies from the same group, the fractions of SGCs with *NTRK* gene fusions were 5.08% and 5.29% (13 out of 256 and 12 out of 227 cases respectively) (30, 31). The first study however did not report on the SGC histological subtype and in the second study 11 out of 12 *NTRK* positive cases were secretory carcinomas, and one was SDC. Together with our findings, this suggests that *NTRK* gene fusions in SGC are mostly restricted to secretory carcinoma. The prevalence of *NTRK* fusions in other SGC subtypes do not seem to be higher than in other cancers (0.28% pan-cancer, 95%-confidence interval 0.22-0.35%) (30, 31). Given the low prevalence of *NTRK* fusions and the high cost of detection by NGS techniques, pan-TRK IHC is often used as a fast and inexpensive screening method. Prior studies on usefulness of pan-TRK IHC (using the same EPR17341 antibody) reported sensitivities ranging between 87.9-100% and specificities between 81.1%-95.2% in all cancers, although with lower specificity for SGC (52% specificity, 88.9% sensitivity) (31, 32). We observed false positivity of pan-TRK IHC for *NTRK* gene fusion detection in 74.8% of cases, mostly due to weak cytoplasmic staining, especially in the myoepithelium of AdCC tumors. Up to approximately 100-fold higher *NTRK3* (protein alias TRKC) expression in AdCC compared to normal salivary gland tissue has been reported in the absence of activating mutations, supporting our observation (33). This TRKC overexpression possibly leads to oncogenic downstream TRK-signaling due to autocrine production of the TRKC ligand neurotrophin-3 (33). The consequence of this TRKC overexpression to efficacy of TRK-inhibition in AdCC patients is unknown. The sensitivity of pan-TRK IHC could be improved by more stringent scoring criteria, such as requirements that all tumor cells should score positive or that positivity should not be restricted to myoepithelial cells only. This however might lead to missing *NTRK* fusion positive cases (i.e., reduced sensitivity) (34). In our opinion, the results of this study and existing literature advocate for not using IHC as screening for *NTRK* fusion detection in SGC. In cases in which *NTRK* gene fusions are suspected (i.e., secretory carcinoma is in the differential diagnosis) gene fusion analysis or *NTRK3* FISH should be performed.

Gene fusions were identified in half of all cases in our cohort. The most common rearrangements were fusions between the *MYB* or *MYBL1* genes and *NFIB* in AdCC. These fusions lead to overexpression of *MYB* or *MYBL1* in a mutually exclusive way (35). Both *MYB* and *MYBL1* encode transcription factors that exert interchangeable effects on target gene expression (36). The DNA-binding domains and (majority of) the transactivating domain of *MYB* or *MYBL1* were preserved in all cases (Figure 2), in line with a previous report (35). The negative regulatory domain was (partially) lost in some cases, but not in all, suggesting that loss of this domain is not solely responsible for the overexpression of *MYB* or *MYBL1*. Regarding *MYB* fusions, it has been shown that juxtaposition of super-enhancers downstream of *NFIB* near the *MYB* locus drive the *MYB* expression. MYB protein can bind to these super-enhancers, thereby creating a positive feedback loop driving AdCC (37). In the biphasic nature of AdCC, consisting of basal myoepithelial and luminal ductal epithelial cells in AdCCs with tubular or cribriform growth patterns, *MYB* seems to drive different regulatory programs in these cell types by interplay with TP63 and NOTCH signaling (37). Occurrence of *NOTCH* gain-of-function mutations can lead to tipping of this balance, resulting in a solid growth pattern with loss of myoepithelial cells, which is associated with markedly poorer prognoses (27, 37). Our results again emphasize the importance of *MYB/MYBL1* gene fusions in AdCC tumor biology and their specificity to AdCC.

In this study we focused on targets for genetically matched therapies by analyzing a subset of genes in the sequencing panel (Supplementary Table 3). Thereby we estimated the fraction of patients harboring a potentially actionable genetic aberration per subtype (Figure 5). This included aberrations that would allow targeted treatment in basket trials (such as the Drug Rediscovery protocol, NCT02925234) (2). However, the true benefit of such a treatment remains inconclusive. In addition, we included some aberrations for which targeted treatment in clinical trials is probably possible in the near future. This included *MAML2* gene fusions (targetable with EGFR inhibitors) and activating *NOTCH* mutations (targetable with for instance γ-secretase inhibitors). The actionability of the presented genetic aberrations thus varies with time, as it is influenced by the availability of clinical trials and approval of new drugs. The reported fractions of patients should therefore be considered as a snapshot, highlighting the current potential treatment options for SGC. The reported fraction of 53.7% of patients with actionable aberrations however matches a recent study, which identified actionable aberrations in 53% of rare cancer patients by whole genome sequencing (38). A second recent study also matches several of our observations, including a markedly higher proportions of SDC patients with actionable aberrations compared to AdCC patients (39) . In the latter study actionable aberrations were identified in a lower percentage (27%) of the cases. This could be attributed to the use of a smaller NGS panel compared to our study, which also could not detect gene fusions. In addition, a high proportion of sequenced tumors in this study were AdCCs, which harbor the lowest amount of actionable aberrations.

A limitation of this study is that only one sample per patient was sequenced, which was the primary tumor in the majority of cases (58.7%). Possible heterogeneity between different disease sites could therefore not be assessed. In AdCC it is for instance known that the genomic landscape can differ significantly between primary tumors and recurrent/metastatic sites (40). Over time the genomic landscape can also alter. Sequencing of paired samples located at different disease sites, sampled over time or pre- and posttreatment could overcome this and aid in assessing clinical relevance of actionable aberrations.

The results of this study advocate treatment of SGC patients with genetically matched therapies, and some of the patients included in this study did indeed benefit from such treatments. Description of the different therapies that were given and the treatment outcomes are beyond the scope of this study. Nevertheless, future clinical trials using genetically matched therapies in SGC patients are warranted.

In conclusion, we identified previously described and novel gene fusions in half of all SGC cases, but no *NTRK* gene fusions in other subtypes than secretory carcinoma. Pan-TRK IHC false positivity is observed in 73.8% of SGC cases and is therefore not useful as initial screening for *NTRK* gene fusions in SGC. Of all SGC patients 53.7% harbors an actionable genetic aberration, possibly leading to therapeutic options, but this highly varies across subtypes. This highlights the potential of molecular diagnostics to select systemic treatment in SGC.

Acknowledgements

We thank PALGA, the nationwide network and registry of histo- and cytopathology in the Netherlands, for their role in tumor material acquisition.

References

1. Park JJH, Hsu G, Siden EG, Thorlund K, Mills EJ. An overview of precision oncology basket and umbrella trials for clinicians. CA Cancer J Clin. 2020;70(2):125-37.
2. van der Velden DL, Hoes LR, van der Wijngaart H, van Berge Henegouwen JM, van Werkhoven E, Roepman P, et al. The Drug Rediscovery protocol facilitates the expanded use of existing anticancer drugs. Nature. 2019;574(7776):127-31.
3. Hainsworth JD, Meric-Bernstam F, Swanton C, Hurwitz H, Spigel DR, Sweeney C, et al. Targeted Therapy for Advanced Solid Tumors on the Basis of Molecular Profiles: Results From MyPathway, an Open-Label, Phase IIa Multiple Basket Study. Journal of clinical oncology : official journal of the American Society of Clinical Oncology. 2018;36(6):536-42.
4. Lassche G, van Boxtel W, Ligtenberg MJL, van Engen-van Grunsven ACH, van Herpen CML. Advances and challenges in precision medicine in salivary gland cancer. Cancer Treat Rev. 2019;80:101906.
5. El-Naggar A.K., Chan J.K.C., Grandis J.R., Takata T., Slootweg P.J. WHO classification of head and neck tumours, 4th edition. Lyon: IARC; 2017.
6. Witte HM, Gebauer N, Steinestel K. Mutational and immunologic Landscape in malignant Salivary Gland Tumors harbor the potential for novel therapeutic strategies. Critical reviews in oncology/hematology. 2022;170:103592.
7. Mertens F, Johansson B, Fioretos T, Mitelman F. The emerging complexity of gene fusions in cancer. Nat Rev Cancer. 2015;15(6):371-81.
8. Bubola J, MacMillan CM, Demicco EG, Chami RA, Chung CT, Leong I, et al. Targeted RNA sequencing in the routine clinical detection of fusion genes in salivary gland tumors. Genes, chromosomes & cancer. 2021;60(10):695-708.
9. Asahina M, Saito T, Hayashi T, Fukumura Y, Mitani K, Yao T. Clinicopathological effect of PLAG1 fusion genes in pleomorphic adenoma and carcinoma ex pleomorphic adenoma with special emphasis on histological features. Histopathology. 2019;74(3):514-25.
10. Fujii K, Murase T, Beppu S, Saida K, Takino H, Masaki A, et al. MYB, MYBL1, MYBL2 and NFIB gene alterations and MYC overexpression in salivary gland adenoid cystic carcinoma. Histopathology. 2017;71(5):823-34.
11. Ho AS, Kannan K, Roy DM, Morris LG, Ganly I, Katabi N, et al. The mutational landscape of adenoid cystic carcinoma. Nature genetics. 2013;45(7):791-8.
12. Luk PP, Wykes J, Selinger CI, Ekmejian R, Tay J, Gao K, et al. Diagnostic and prognostic utility of Mastermind-like 2 (MAML2) gene rearrangement detection by fluorescent in situ hybridization (FISH) in mucoepidermoid carcinoma of the salivary glands. Oral surgery, oral medicine, oral pathology and oral radiology. 2016;121(5):530-41.
13. Seethala RR, Stenman G. Update from the 4th Edition of the World Health Organization Classification of Head and Neck Tumours: Tumors of the Salivary Gland. Head and neck pathology. 2017;11(1):55-67.
14. Skalova A, Vanecek T, Sima R, Laco J, Weinreb I, Perez-Ordonez B, et al. Mammary analogue secretory carcinoma of salivary glands, containing the ETV6-NTRK3 fusion gene: a hitherto undescribed salivary gland tumor entity. The American journal of surgical pathology. 2010;34(5):599-608.

15. Cocco E, Scaltriti M, Drilon A. NTRK fusion-positive cancers and TRK inhibitor therapy. Nature reviews Clinical oncology. 2018;15(12):731-47.
16. Drilon AE, Farago AF, Tan DS-W, Kummar S, McDermott RS, Berlin J, et al. Activity and safety of larotrectinib in adult patients with TRK fusion cancer: An expanded data set. Journal of Clinical Oncology. 2020;38(15_suppl):3610-.
17. Doebele RC, Drilon A, Paz-Ares L, Siena S, Shaw AT, Farago AF, et al. Entrectinib in patients with advanced or metastatic NTRK fusion-positive solid tumours: integrated analysis of three phase 1-2 trials. The Lancet Oncology. 2020;21(2):271-82.
18. Casparie M, Tiebosch AT, Burger G, Blauwgeers H, van de Pol A, van Krieken JH, et al. Pathology databanking and biobanking in The Netherlands, a central role for PALGA, the nationwide histopathology and cytopathology data network and archive. Cell Oncol. 2007;29(1):19-24.
19. Eijkelenboom A, Kamping EJ, Kastner-van Raaij AW, Hendriks-Cornelissen SJ, Neveling K, Kuiper RP, et al. Reliable Next-Generation Sequencing of Formalin-Fixed, Paraffin-Embedded Tissue Using Single Molecule Tags. J Mol Diagn. 2016;18(6):851-63.
20. Kroeze LI, de Voer RM, Kamping EJ, von Rhein D, Jansen EAM, Hermsen MJW, et al. Evaluation of a Hybrid Capture-Based Pan-Cancer Panel for Analysis of Treatment Stratifying Oncogenic Aberrations and Processes. J Mol Diagn. 2020;22(6):757-69.
21. Richards S, Aziz N, Bale S, Bick D, Das S, Gastier-Foster J, et al. Standards and guidelines for the interpretation of sequence variants: a joint consensus recommendation of the American College of Medical Genetics and Genomics and the Association for Molecular Pathology. Genet Med. 2015;17(5):405-24.
22. Eijkelenboom A, Tops BBJ, van den Berg A, van den Brule AJC, Dinjens WNM, Dubbink HJ, et al. Recommendations for the clinical interpretation and reporting of copy number gains using gene panel NGS analysis in routine diagnostics. Virchows Archiv : an international journal of pathology. 2019;474(6):673-80.
23. Pierini T, Di Giacomo D, Pierini V, Gorello P, Barba G, Lema Fernandez AG, et al. MYB deregulation from a EWSR1-MYB fusion at leukemic evolution of a JAK2 (V617F) positive primary myelofibrosis. Mol Cytogenet. 2016;9(1):68.
24. Haller F, Bieg M, Will R, Körner C, Weichenhan D, Bott A, et al. Enhancer hijacking activates oncogenic transcription factor NR4A3 in acinic cell carcinomas of the salivary glands. Nat Commun. 2019;10(1):368.
25. Date O, Katsura M, Ishida M, Yoshihara T, Kinomura A, Sueda T, et al. Haploinsufficiency of RAD51B causes centrosome fragmentation and aneuploidy in human cells. Cancer Res. 2006;66(12):6018-24.
26. Isaacson AL, Guseva NV, Bossler AD, Ma D. Urothelial carcinoma with an NRF1-BRAF rearrangement and response to targeted therapy. Cold Spring Harb Mol Case Stud. 2019;5(3).
27. Ferrarotto R, Mitani Y, Diao L, Guijarro I, Wang J, Zweidler-McKay P, et al. Activating NOTCH1 Mutations Define a Distinct Subgroup of Patients With Adenoid Cystic Carcinoma Who Have Poor Prognosis, Propensity to Bone and Liver Metastasis, and Potential Responsiveness to Notch1 Inhibitors. Journal of clinical oncology : official journal of the American Society of Clinical Oncology. 2017;35(3):352-60.
28. Wang K, Zhang Q, Li D, Ching K, Zhang C, Zheng X, et al. PEST domain mutations in Notch receptors comprise an oncogenic driver segment in triple-negative breast cancer sensitive to a

γ-secretase inhibitor. Clinical cancer research : an official journal of the American Association for Cancer Research. 2015;21(6):1487-96.

29. Lobry C, Oh P, Aifantis I. Oncogenic and tumor suppressor functions of Notch in cancer: it's NOTCH what you think. J Exp Med. 2011;208(10):1931-5.
30. Rosen EY, Goldman DA, Hechtman JF, Benayed R, Schram AM, Cocco E, et al. TRK Fusions Are Enriched in Cancers with Uncommon Histologies and the Absence of Canonical Driver Mutations. Clinical cancer research : an official journal of the American Association for Cancer Research. 2020;26(7):1624-32.
31. Solomon JP, Linkov I, Rosado A, Mullaney K, Rosen EY, Frosina D, et al. NTRK fusion detection across multiple assays and 33,997 cases: diagnostic implications and pitfalls. Modern pathology : an official journal of the United States and Canadian Academy of Pathology, Inc. 2020;33(1):38-46.
32. Hechtman JF, Benayed R, Hyman DM, Drilon A, Zehir A, Frosina D, et al. Pan-Trk Immunohistochemistry Is an Efficient and Reliable Screen for the Detection of NTRK Fusions. The American journal of surgical pathology. 2017;41(11):1547-51.
33. Ivanov SV, Panaccione A, Brown B, Guo Y, Moskaluk CA, Wick MJ, et al. TrkC signaling is activated in adenoid cystic carcinoma and requires NT-3 to stimulate invasive behavior. Oncogene. 2013;32(32):3698-710.
34. Csanyi-Bastien M, Lanic MD, Beaussire L, Ferric S, François A, Meseure D, et al. Pan-TRK Immunohistochemistry Is Highly Correlated With NTRK3 Gene Rearrangements in Salivary Gland Tumors. The American journal of surgical pathology. 2021;45(11):1487-98.
35. Togashi Y, Dobashi A, Sakata S, Sato Y, Baba S, Seto A, et al. MYB and MYBL1 in adenoid cystic carcinoma: diversity in the mode of genomic rearrangement and transcripts. Modern pathology : an official journal of the United States and Canadian Academy of Pathology, Inc. 2018;31(6):934-46.
36. Brayer KJ, Frerich CA, Kang H, Ness SA. Recurrent Fusions in MYB and MYBL1 Define a Common, Transcription Factor-Driven Oncogenic Pathway in Salivary Gland Adenoid Cystic Carcinoma. Cancer discovery. 2016;6(2):176-87.
37. Drier Y, Cotton MJ, Williamson KE, Gillespie SM, Ryan RJ, Kluk MJ, et al. An oncogenic MYB feedback loop drives alternate cell fates in adenoid cystic carcinoma. Nature genetics. 2016;48(3):265-72.
38. Hoes LR, van Berge Henegouwen JM, van der Wijngaart H, Zeverijn LJ, van der Velden DL, van de Haar J, et al. Patients With Rare Cancers in the Drug Rediscovery Protocol (DRUP) benefit from Genomics - Guided Treatment. Clinical cancer research : an official journal of the American Association for Cancer Research. 2022.
39. Rack S, Feeney L, Hapuarachi B, Adderley H, Woodhouse L, Betts G, et al. Evaluation of the Clinical Utility of Genomic Profiling to Inform Selection of Clinical Trial Therapy in Salivary Gland Cancer. Cancers. 2022;14(5):1133.
40. Ho AS, Ochoa A, Jayakumaran G, Zehir A, Valero Mayor C, Tepe J, et al. Genetic hallmarks of recurrent/metastatic adenoid cystic carcinoma. J Clin Invest. 2019;129(10):4276-89.

Supplementary information

Supplementary Table 1: Genes incorporated in the FusionPlex® RadboudV1

Gene	NM Reference	Coverage (exons), 5' or 3'directionality not shown
ABL1	NM_005157	exon 1, 2, 3, 4
ABL2	NM_007314	exon 2, 3, 4, 5, 6
ALK	NM_004304	exon 2, 4, 6, 10, 16, 17, 18, 19, 20, 21, 22, 23, 26
BCOR	NM_001123385	exon 6, 7, 8, 12, 14, 15
	NM_017745	exon 8
BRAF	NM_004333	exon 1, 2, 3, 7, 8, 9, 10, 11, 12, 13, 15, 16
CAMTA1	NM_015215	exon 3, 8, 9, 10
CIC	NM_015125	exon 18, 19, 20
EGFR	NM_005228	exon 1, 7, 8, 9, 16, 19, 20, 24, 25
ERBB2	NM_004448	exon 4, 5, 23, 24, 25, 26
ERG	NM_004449	exon 2, 3, 4, 5, 6, 7, 8, 9, 10, 11
ETV6	NM_001987	exon 1, 2, 3, 4, 5, 6, 7
EWSR1	NM_005243	exon 4, 5, 6, 7, 8, 9, 10, 11, 12, 13, 14
FGFR1	NM_015850	exon 2, 3, 4, 5, 6, 7, 8, 9, 10, 11, 12, 17
FGFR2	NM_000141	exon 2, 5, 7, 8, 9, 10, 16, 17
FGFR3	NM_000142	exon 3, 5, 8, 9, 10, 16, 17
FOS	NM_005252	exon 1, 2, 3, 4
FOSB	NM_006732	exon 1, 2, 3
	NM_001114171	exon 1, 2, 3
FOXO1	NM_002015	exon 1, 2, 3
FUS	NM_004960	exon 3, 4, 5, 6, 7, 8, 9, 10, 11, 13, 14
GLI1	NM_005269	exon 4, 5, 6, 7
HMGA2	NM_003483	exon 1, 2, 3, 4, 5
JAZF1	NM_175061	exon 2, 3, 4
MALT1	NM_006785	exon 2, 3, 4, 5, 6, 7, 9, 10
MAML2	NM_032427	exon 2, 3
MET	NM_000245	exon 2, 4, 5, 6, 13, 14, 15, 16, 17, 21
MKL2	NM_014048	exon 11, 12, 13
MYB	NM_001130173	exon 7, 8, 9, 11, 12, 13, 14, 15, 16
MYBL1	NM_001080416	exon 6, 7, 8, 9, 10, 11, 12, 13, 14, 15, 16
	NM_001144755	exon 8
NCOA1	NM_147223	exon 12, 13, 14, 15
NCOA2	NM_006540	exon 11, 12, 13, 14, 15, 16
NFIB	NM_005596	exon 5, 6, 7, 8, 9
	NM_001190737	exon 9, 10
NR4A3	NM_173200	exon 3, 4

(Table continues on next page)

NR4A3	NM_006981	exon 4
	NM_013962	exon 1
NRG1	NM_004495	exon 1, 2, 3, 6
	NM_013957	exon 1, 4, 8
NTRK1	NM_002529	exon 2, 4, 6, 8, 10, 11, 12, 13, 14, 15
NTRK2	NM_006180	exon 5, 7, 9, 11, 12, 13, 14, 15, 16, 17
NTRK3	NM_002530	exon 4, 7, 10, 12, 13, 14, 15, 16
	NM_001007156	exon 15
PDGFB	NM_002608	exon 2, 3
PDGFRB	NM_002609	exon 8, 9, 10, 11, 12, 13, 14
PHF1	NM_024165	exon 1, 2, 3, 4, 5, 6, 7, 8
PLAG1	NM_002655	exon 1, 2, 3, 4
PPARG	NM_015869	exon 1, 2, 3
PRKD1	NM_002742	exon 7, 8, 9, 10, 11, 12, 13, 14, 15, 16, 17
PRKD2	NM_016457	exon 7, 8, 9, 10, 11, 12, 13, 14, 15, 16, 17
PRKD3	NM_005813	exon 7, 8, 9, 10, 11, 12, 13, 14, 15, 16, 17
	NM_133509	exon 11
RAD51B	NM_002877	exon 11
	NM_133510	exon 1, 2, 3, 4, 5, 6, 7, 8, 9, 10, 11
RAF1	NM_002880	exon 4, 5, 6, 7, 8, 9, 10, 11, 12
RET	NM_020975	exon 8, 9, 10, 11, 12, 13, 14
	NM_020630	exon 2, 4, 6
ROS1	NM_002944	exon 2, 4, 7, 31, 32, 33, 34, 35, 36, 37
SS18	NM_001007559	exon 4, 5, 6, 8, 9, 10, 11
STAT6	NM_001178078	exon 1, 2, 3, 4, 5, 6, 7, 15, 16, 17, 18, 19, 20
TFE3	NM_006521	exon 2, 3, 4, 5, 6, 7, 8, 10
THADA	NM_022065	exon 24, 25, 26, 27, 28, 29, 30, 36, 37
TMPRSS2	NM_005656	exon 1, 3, 4, 5, 6
	NM_001135099	exon 1, 2
USP6	NM_004505	exon 1, 2, 3
YWHAE	NM_006761	exon 5

Supplementary Table 2: Genes incorporated in TruSight Oncology 500 panel

TSO500 panel							
ABL1	*BIRC3*	*CIC*	*ERBB3*	*FGF8*	*HIST1H1C*	*IRF2*	*MCL1*
ABL2	*BLM*	*CREBBP*	*ERBB4*	*FGF9*	*HIST1H2BD*	*IRF4*	*MDC1*
ACVR1	*BMPR1A*	*CRKL*	*ERCC1*	*FGFR1*	*HIST1H3A*	*IRS1*	*MDM2*
ACVR1B	*BRAF*	*CRLF2*	*ERCC2*	*FGFR2*	*HIST1H3B*	*IRS2*	*MDM4*
AKT1	*BRCA1*	*CSF1R*	*ERCC3*	*FGFR3*	*HIST1H3C*	*JAK1*	*MED12*
AKT2	*BRCA2*	*CSF3R*	*ERCC4*	*FGFR4*	*HIST1H3D*	*JAK2*	*MEF2B*
AKT3	*BRD4*	*CSNK1A1*	*ERCC5*	*FH*	*HIST1H3E*	*JAK3*	*MEN1*
ALK	*BRIP1*	*CTCF*	*ERG*	*FLCN*	*HIST1H3F*	*JUN*	*MET*
ALOX12B	*BTG1*	*CTLA4*	*ERRFI1*	*FLI1*	*HIST1H3G*	*KAT6A*	*MGA*
ANKRD11	*BTK*	*CTNNA1*	*ESR1*	*FLT1*	*HIST1H3H*	*KDM5A*	*MITF*
ANKRD26	*C11orf30*	*CTNNB1*	*ETS1*	*FLT3*	*HIST1H3I*	*KDM5C*	*MLH1*
APC	*CALR*	*CUL3*	*ETV1*	*FLT4*	*HIST1H3J*	*KDM6A*	*MLL*
AR	*CARD11*	*CUX1*	*ETV4*	*FOXA1*	*HIST2H3A*	*KDR*	*MLLT3*
ARAF	*CASP8*	*CXCR4*	*ETV5*	*FOXL2*	*HIST2H3C*	*KEAP1*	*MPL*
ARFRP1	*CBFB*	*CYLD*	*ETV6*	*FOXO1*	*HIST2H3D*	*KEL*	*MRE11A*
ARID1A	*CBL*	*DAXX*	*EWSR1*	*FOXP1*	*HIST3H3*	*KIF5B*	*MSH2*
ARID1B	*CCND1*	*DCUN1D1*	*EZH2*	*FRS2*	*HLA-A*	*KIT*	*MSH3*
ARID2	*CCND2*	*DDR2*	*FAM123B*	*FUBP1*	*HLA-B*	*KLF4*	*MSH6*
ARID5B	*CCND3*	*DDX41*	*FAM175A*	*FYN*	*HLA-C*	*KLHL6*	*MST1*
ASXL1	*CCNE1*	*DHX15*	*FAM46C*	*GABRA6*	*HNF1A*	*KMT2B*	*MST1R*
ASXL2	*CD274*	*DICER1*	*FANCA*	*GATA1*	*HNRNPK*	*KMT2C*	*MTOR*
ATM	*CD276*	*DIS3*	*FANCC*	*GATA2*	*HOXB13*	*KMT2D*	*MUTYH*
ATR	*CD74*	*DNAJB1*	*FANCD2*	*GATA3*	*HRAS*	*KRAS*	*MYB*
ATRX	*CD79A*	*DNMT1*	*FANCE*	*GATA4*	*HSD3B1*	*LAMP1*	*MYC*
AURKA	*CD79B*	*DNMT3A*	*FANCF*	*GATA6*	*HSP90AA1*	*LATS1*	*MYCL1*
AURKB	*CDC73*	*DNMT3B*	*FANCG*	*GEN1*	*ICOSLG*	*LATS2*	*MYCN*
AXIN1	*CDH1*	*DOT1L*	*FANCI*	*GID4*	*ID3*	*LMO1*	*MYD88*
AXIN2	*CDK12*	*E2F3*	*FANCL*	*GLI1*	*IDH1*	*LRP1B*	*MYOD1*
AXL	*CDK4*	*EED*	*FAS*	*GNA11*	*IDH2*	*LYN*	*NAB2*
B2M	*CDK6*	*EGFL7*	*FAT1*	*GNA13*	*IFNGR1*	*LZTR1*	*NBN*
BAP1	*CDK8*	*EGFR*	*FBXW7*	*GNAQ*	*IGF1*	*MAGI2*	*NCOA3*
BARD1	*CDKN1A*	*EIF1AX*	*FGF1*	*GNAS*	*IGF1R*	*MALT1*	*NCOR1*
BBC3	*CDKN1B*	*EIF4A2*	*FGF10*	*GPR124*	*IGF2*	*MAP2K1*	*NEGR1*
BCL10	*CDKN2A*	*EIF4E*	*FGF14*	*GPS2*	*IKBKE*	*MAP2K2*	*NF1*
BCL2	*CDKN2B*	*EML4*	*FGF19*	*GREM1*	*IKZF1*	*MAP2K4*	*NF2*
BCL2L1	*CDKN2C*	*EP300*	*FGF2*	*GRIN2A*	*IL10*	*MAP3K1*	*NFE2L2*
BCL2L11	*CEBPA*	*EPCAM*	*FGF23*	*GRM3*	*IL7R*	*MAP3K13*	*NFKBIA*
BCL2L2	*CENPA*	*EPHA3*	*FGF3*	*GSK3B*	*INHA*	*MAP3K14*	*NKX2-1*

(Table continues on next page)

BCL6	*CHD2*	*EPHA5*	*FGF4*	*H3F3A*	*INHBA*	*MAP3K4*	*NKX3-1*
BCOR	*CHD4*	*EPHA7*	*FGF5*	*H3F3B*	*INPP4A*	*MAPK1*	*NOTCH1*
BCORL1	*CHEK1*	*EPHB1*	*FGF6*	*H3F3C*	*INPP4B*	*MAPK3*	*NOTCH2*
BCR	*CHEK2*	*ERBB2*	*FGF7*	*HGF*	*INSR*	*MAX*	*NOTCH3*
NOTCH4	*PDGFRB*	*POLE*	*RAD51B*	*RPTOR*	*SMC3*	*TAF1*	*TSC2*
NPM1	*PDK1*	*PPARG*	*RAD51C*	*RUNX1*	*SMO*	*TBX3*	*TSHR*
NRAS	*PDPK1*	*PPM1D*	*RAD51D*	*RUNX1T1*	*SNCAIP*	*TCEB1*	*U2AF1*
NRG1	*PGR*	*PPP2R1A*	*RAD52*	*RYBP*	*SOCS1*	*TCF3*	*VEGFA*
NSD1	*PHF6*	*PPP2R2A*	*RAD54L*	*SDHA*	*SOX10*	*TCF7L2*	*VHL*
NTRK1	*PHOX2B*	*PPP6C*	*RAF1*	*SDHAF2*	*SOX17*	*TERC*	*VTCN1*
NTRK2	*PIK3C2B*	*PRDM1*	*RANBP2*	*SDHB*	*SOX2*	*TERT*	*WISP3*
NTRK3	*PIK3C2G*	*PREX2*	*RARA*	*SDHC*	*SOX9*	*TET1*	*WT1*
NUP93	*PIK3C3*	*PRKAR1A*	*RASA1*	*SDHD*	*SPEN*	*TET2*	*XIAP*
NUTM1	*PIK3CA*	*PRKCI*	*RB1*	*SETBP1*	*SPOP*	*TFE3*	*XPO1*
PAK1	*PIK3CB*	*PRKDC*	*RBM10*	*SETD2*	*SPTA1*	*TFRC*	*XRCC2*
PAK3	*PIK3CD*	*PRSS8*	*RECQL4*	*SF3B1*	*SRC*	*TGFBR1*	*YAP1*
PAK7	*PIK3CG*	*PTCH1*	*REL*	*SH2B3*	*SRSF2*	*TGFBR2*	*YES1*
PALB2	*PIK3R1*	*PTEN*	*RET*	*SH2D1A*	*STAG1*	*TMEM127*	*ZBTB2*
PARK2	*PIK3R2*	*PTPN11*	*RFWD2*	*SHQ1*	*STAG2*	*TMPRSS2*	*ZBTB7A*
PARP1	*PIK3R3*	*PTPRD*	*RHEB*	*SLIT2*	*STAT3*	*TNFAIP3*	*ZFHX3*
PAX3	*PIM1*	*PTPRS*	*RHOA*	*SLX4*	*STAT4*	*TNFRSF14*	*ZNF217*
PAX5	*PLCG2*	*PTPRT*	*RICTOR*	*SMAD2*	*STAT5A*	*TOP1*	*ZNF703*
PAX7	*PLK2*	*QKI*	*RIT1*	*SMAD3*	*STAT5B*	*TOP2A*	*ZRSR2*
PAX8	*PMAIP1*	*RAB35*	*RNF43*	*SMAD4*	*STK11*	*TP53*	
PBRM1	*PMS1*	*RAC1*	*ROS1*	*SMARCA4*	*STK40*	*TP63*	
PDCD1	*PMS2*	*RAD21*	*RPS6KA4*	*SMARCB1*	*SUFU*	*TRAF2*	
PDCD1LG2	*PNRC1*	*RAD50*	*RPS6KB1*	*SMARCD1*	*SUZ12*	*TRAF7*	
PDGFRA	*POLD1*	*RAD51*	*RPS6KB2*	*SMC1A*	*SYK*	*TSC1*	

Supplementary Table 3: virtual TSO500 panel that mainly contains genes in which aberrations may lead to targeted treatment

Analyzed genes	TS/O/R[1]	Counted as targetable[2]
AR	O,R	No
AKT1	O	Mut/Amp
AKT2	O	Mut/Amp
AKT3	O	Mut/Amp
ALK	O,R	Fus[3]
ATM	TS	Bi-allelic inactivation
BARD1	TS	Bi-allelic inactivation
BRAF	O	Mut/Fus[3]
BRCA1	TS	Bi-allelic inactivation
BRCA2	TS	Bi-allelic inactivation
BRIP1	TS	Bi-allelic inactivation
B2M	R	No
CCND1	O	Amp
CDK12	TS,O	Bi-allelic inactivation
CDK4	O	Mut/Amp
CDK6	O	Amp
CDKN2A	TS	Bi-allelic inactivation
EGFR	O,R	Mut/Fus[3]
ERBB2	O	Mut/Amp
ERBB4	O	Mut
FANCL	TS	Bi-allelic inactivation
FGFR1	O	Mut/Amp/Fus[3]
FGFR2	O	Mut/Amp/Fus[3]
FGFR3	O	Mut/Amp/Fus[3]
FGFR4	O	Mut/Amp
HRAS	O	Mut
JAK1	R	No
JAK2	O,R	No
KIT	O,R	Mut/Amp
KRAS	O	Mut (only G12C)
MAP2K1	O	Mut
MAP2K2	O	Mut
MAP2K4	TS	Bi-allelic inactivation
MAP3K1	TS	Bi-allelic inactivation
MET	O	Mut/Amp/Fus[3]
MLH1	TS	Bi-allelic inactivation
MSH2	TS	Bi-allelic inactivation
MSH6	TS	Bi-allelic inactivation

(Table continues on next page)

NOTCH1	TS, O	Activating Mut
NOTCH2	O	Activating Mut
NOTCH3	O	Activating Mut
NOTCH4	TS, O	No
NRAS	O	Mut
PALB2	TS	Bi-allelic inactivation
PDGFRA	O	Mut/Amp
PDGFRB	O	Mut/Amp
PIK3CA	O	Mut
PIK3R1	TS	Bi-allelic inactivation/activating mutations
PIK3R2	TS	Bi-allelic inactivation
POLE	TS	No
PPP2R2A	TS	Bi-allelic inactivation
PTEN	TS	Bi-allelic inactivation
RAD51B	TS	Bi-allelic inactivation
RAD51C	TS	Bi-allelic inactivation
RAD51D	TS	Bi-allelic inactivation
RAD54L	TS	Bi-allelic inactivation
RAF1	O	No
RET	O	Mut/Fus[3]
TP53	TS	No
TSC1	TS	Bi-allelic inactivation
TSC2	TS	Bi-allelic inactivation
MSI	-	≥25% unstable sites; in case of 10-25% unstable sites, confirm with MMR IHC
TMB	-	≥15mut/Mb

1. TS: Tumor suppressor; O: Oncogene; R: Resistance gene.

2. Only (likely) pathogenic mutations were counted as targetable, scored following recommendations of the American College of Medical Genetics and Genomics and the Association for Molecular Pathology. Bi-allelic inactivation: mut and/or loss.

Abbreviations: Mut: mutation; Amp: amplification; Fus: fusion; MSI: microsatellite instability; MMR: mismatch repair; IHC: immunohistochemistry; TMB: tumor mutational burden.

3. Fusions are not detectable by the TSO500 panel, but fusions in these genes were detectable by the FusionPlex® RadboudV1 panel that was used too in this study. In this panel fusions in these genes were counted as actionable: *ABL1, ALK, BRAF, EGFR, FGFR1-3, MAML2 , MET, NRG1, NTRK1-3, RET* and *ROS1*.

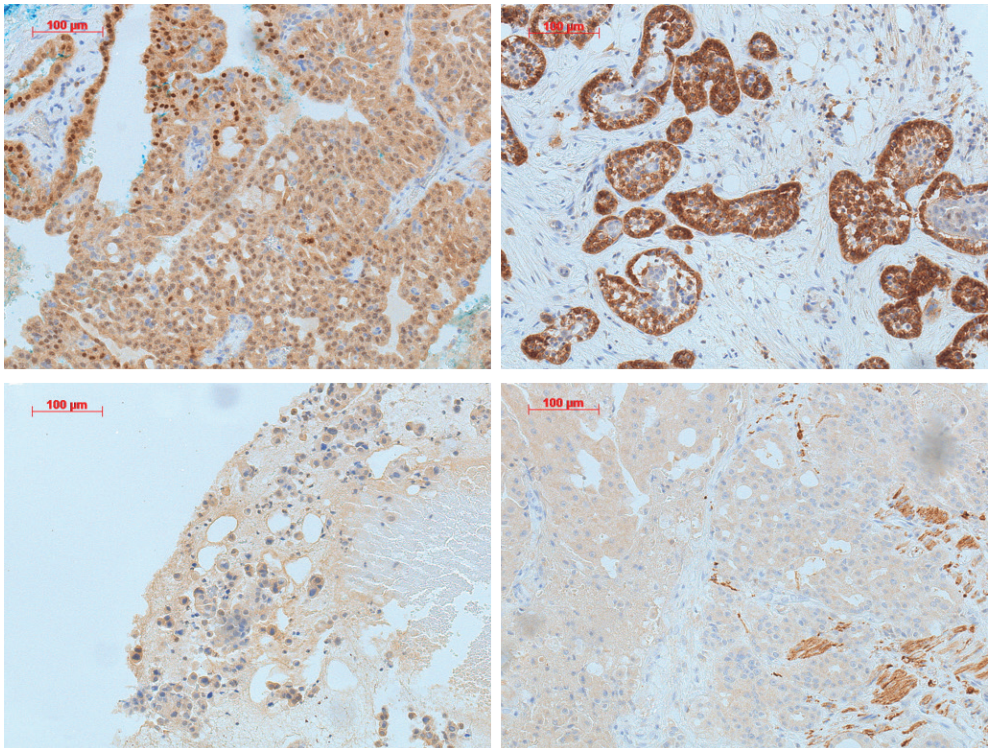

Supplementary Figure 1: Examples of pan-TRK immunohistochemistry (IHC). Top left: secretory carcinoma case harboring an *ETV6-NTRK3* gene fusion. Top right: AdCC case scored as positive. Bottom left: SDC case scored as moderate positive. Bottom right: SDC scored as weak/dubious positive.

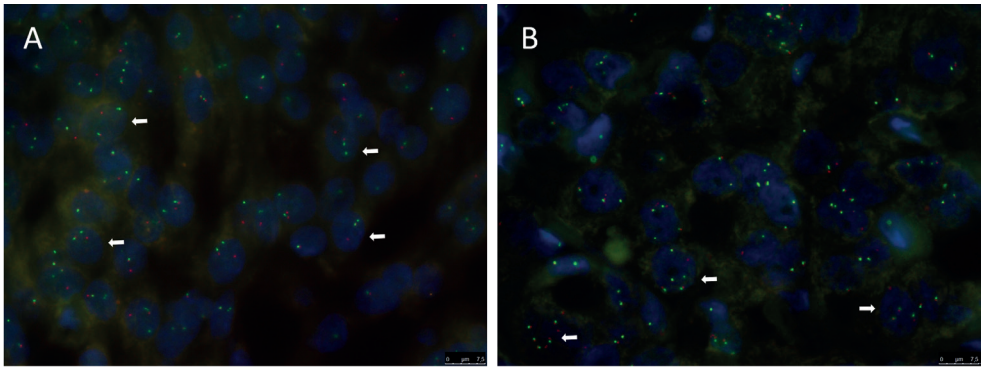

Supplementary Figure 2: Examples of *NTRK* FISH results. A: *NTRK3* FISH in a secretory carcinoma case harboring an *ETV6-NTRK3* gene fusion (examples of positive cells indicated with white arrows). B. *NTRK1* FISH in a SDC case without harboring a *NTRK* gene fusion, in which extensive polysomy is detected and FISH was scored as dubious (examples of cells with polysomy indicated with white arrows).

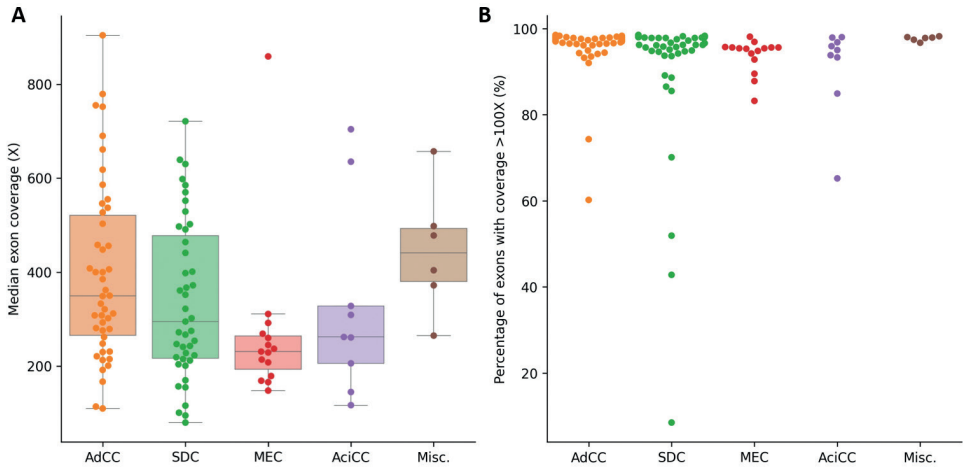

Supplementary Figure 3: Coverage metrics of TSO500 panel. A: median unique exon coverage, sorted per subtype. B: percentage of exons with unique coverage >100X, sorted per subtype. Abbreviations: SDC: salivary duct carcinoma, AdCC: adenoid cystic carcinoma, MEC: mucoepidermoid carcinoma, ACiCC: acinic cell carcinoma, misc.: miscellaneous.

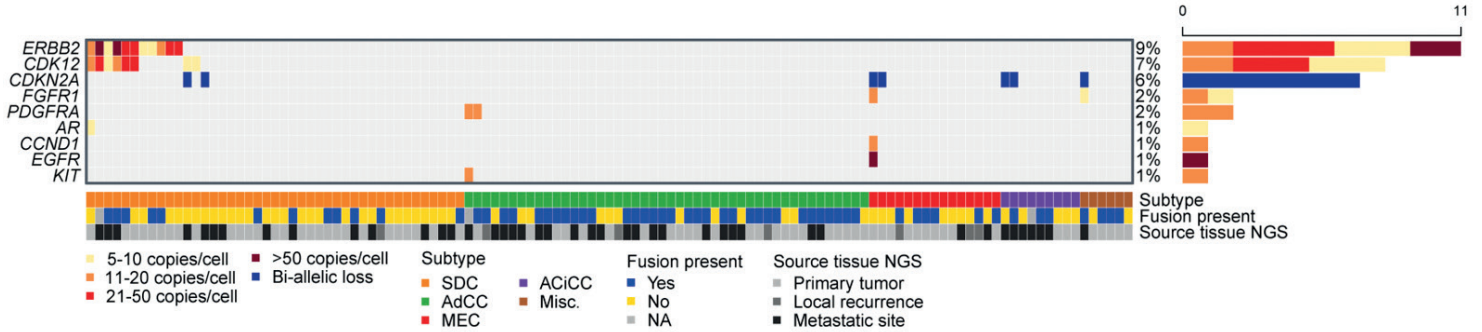

Supplementary Figure 4: Identified copy number variants, sorted for subtypes. Abbreviations: SDC: salivary duct carcinoma, AdCC: adenoid cystic carcinoma, MEC: mucoepidermoid carcinoma, AciCC: acinic cell carcinoma, Misc.: miscellaneous.

CHAPTER 3

Mapping intrapatient salivary gland cancer disease heterogeneity and clonal evolution: preliminary results of an obduction study

Gerben Lassche, Pui-Yuen Lee, Willemijn Klein, Adriana C.H. van Engen-van Grunsven, Sander Bervoets, Charlotte Kaffa, Jack A. Schalken, Gerald W. Verhaegh, Carla M.L. van Herpen

In preparation

Abstract

Introduction

Darwinian evolutionary processes during cancer development cause intra-tumor heterogeneity (ITH). Progression to metastatic disease has the potential to substantially add to ITH. This contributes to failure of targeted therapeutic interventions aimed at the eradication of metastases. Mapping of ITH is therefore crucial to gain insights in genetic changes and therapy failure in cancer. Here we present the preliminary results of an autopsy study to assess ITH in several subtypes end-stage metastasized salivary gland cancer (SGC).

Methods

Patients with metastasized SGC were enrolled in an autopsy program. Evolvement and burden of disease was assessed by comparison of ante and post-mortem imaging. During autopsy all internal organs were examined for tumor presence and samples of multiple tumor locations were snap frozen. A selection of samples was used for whole-genome sequencing (WGS).

Results

Autopsy of 4 SGC patients (2 adenoid cystic carcinoma, 1 salivary duct carcinoma, 1 myoepithelial carcinoma) was performed between 12 to 56 hours after death. A total of 169 samples of suspected tumor lesions were taken (20-58 per patient). In 138 out of these 169 samples cancer was confirmed by histopathology. Libraries of sufficient quality for subsequent WGS could be prepared in all 138 tumor samples. WGS was performed in 20 samples (3-7 per patient) with a mean WGS yield of 244Mbase/sample.

Conclusion

In all 4 SGC autopsy cases in this study it was feasible to acquire samples of sufficient quality for subsequent WGS. With future bioinformatic processing we aim to create phylogenetic trees and assess the spatial architecture of ITH in these different SGC patients, which will be a novelty in SGC.

Introduction

The complexity in cancer development can be explained by evolutionary processes of mutation, genetic drifts (*i.e.* introduction of changes in subclone frequency due to chance, a form of neutral evolution) and selection (1, 2). The clonal evolution of cancer, *i.e.* the process by which (epi)genetic alterations create diversity, is highly variable between tumor types and within single tumors (2, 3). In this process selective pressures forced by therapeutic agents also play a key role (4). Inherent to these evolutionary dynamics is the introduction of genetic intra-tumor heterogeneity (ITH) (4). Inversely, ITH can be used to infer the temporal order of mutation events and can thereby resolve the evolutionary history of a cancer (4).

The extent of ITH depends on tumor type and is inversely related to the tumor-mutational burden (TMB), where cancers with a high TMB, such as lung cancer or melanoma, in general have lower subclonal fractions of several types of genetic aberrations (4, 5). Pan-cancer ITH is however widespread, and even within single samples, mostly stemming from primary tumors, in 95.1% of the cases subclonal expansions can be identified (5). Thus, even in primary tumors clonal evolution already leads to substantial ITH.

Also during the complex process of metastasis substantial ITH arises (6). This heterogeneity in metastatic lesions can contribute to the failure of (targeted) therapeutic interventions. Delineation of the evolution and ITH in metastatic lesions is, therefore, pivotal for therapy development and treatment choices. Currently there are two main models for metastatic evolution: linear evolution, in which clones sequentially arise and dominate over time, or parallel evolution in which primary tumor and different metastases evolve in parallel (3, 6). The parallel evolution model gives rise to more genetic divergence between primary tumor and metastases, and seems to be more common pan-cancer (3, 5). Metastatic heterogeneity is however not only explained by these parallel or linear evolution models, other alternative seeding methods such as polyclonal seeding, primary tumor to metastasis reseeding and metastasis to metastasis reseeding can also play a role (6).

Every cancer thus has its own complex evolutionary history (5). For salivary gland cancer, a rare and diverse type of cancer, there is very little known about ITH and evolutionary processes. SGC is a very heterogeneous disease, and 22 different histopathological subtypes can be distinguished. Between these subtypes molecular landscape also highly differs (7). For instance, Adenoid cystic carcinoma (AdCC) and myoepithelial carcinoma have a low tumor mutational burden (TMB), whereas salivary duct carcinoma (SDC) has a markedly higher TMB (8). Whether these subtypes differ regarding ITH and tumor evolution is not known.

In this study we will delineate the evolutionary history of 4 salivary gland cancer (SGC) patients by multi-region whole-genome sequencing (WGS) combined with deep targeted sequencing in end-stage metastatic disease. By doing so, we aim to create a phylogenetic tree of tumor lesions in these patients and assess the spatial architecture of ITH. Preliminary results regarding feasibility of an autopsy program to reach this goal are presented in this manuscript.

Methods

Study inclusion

Four patients with metastasized SGC treated at the outpatient clinic of the department of medical oncology of the tertiary referral hospital Radboud university medical center entered a research autopsy program. The patients provided written informed consent to enter the program and consented to the Radboud biobank 'salivary gland cancer', both of which were approved by the institutional review board (case numbers 2017-3679 and 2019-5089).

Transportation and body cooling

Immediately after patients were declared death (all died at home), transportation to the Radboud university medical center took place, after which cooling to 2-5 °C commenced. Cooling was initiated within 6 hours after death occurred in all patients.

Post-mortem imaging

Post-mortem computed tomography (CT) scanning of the neck, thorax and abdomen was performed. If technically feasible (*i.e.* depending on the degree of rigor mortis) and no recent pulmonary ante-mortem imaging was available, intubation and inflation of the lungs took place during CT scanning for better visualization of pulmonary metastases (9). Elaborate magnetic resonance imaging (MRI) of the brain and face was performed if brain metastases were known or the primary salivary gland tumor or a locoregional recurrence was present. Post-mortem imaging was compared to ante-mortem imaging to identify fast growing metastases and to track metastas over time.

Rapid autopsy and tumor sampling

After imaging was completed, autopsy took place as soon as possible to prevent nucleic acid decay. All internal organs were examined for tumor presence. Bones were sampled if post-mortem imaging revealed presence of bone metastases. Brain autopsy was performed in 2 patients that gave an extra consent for this procedure. Tumor samples were taken of each disease location in different organs and in case multiple metastases were present in a single organ, representative samples were taken. In case of pulmonary metastases every invaded

lobe was representatively sampled. Several large metastases were sampled on both the core and the rim. In case the primary tumor or a locoregional recurrence was present this was sampled too. Healthy abdominal skin was sampled as germline control. Samples were snap-frozen to -80°C in Tissue-Tek OCT compound (Sakura).

Tumor purity estimation and sample selection for WGS library preparation
Cryosections of 4µm were fixated in paraformaldehyde and stained with hematoxylin and eosin (HE). Tumor purity was estimated and most viable areas with highest tumor purity were annotated. Punch biopsies of 2mm of all annotated areas were used for subsequent DNA isolation. All samples containing viable tumor and the healthy controls were used in this study.

DNA isolation, library preparation and whole-genome sequencing
DNA isolation, library preparation and sequencing took place at Hartwig Medical Foundation (Amsterdam, The Netherlands) according to previously published protocols (10). In short, samples were homogenized with Nuclease-free water using the Qiagen TissueLyzer. Samples were purified using the QIAsymphony and DSP DNA mini kit (Qiagen). Library preparation was done using the TruSeq Nano DNA library prep kit (Illumina, 8 PCR cycles) according to manufacturers' instructions with 50-200ng of Covaris sheared gDNA as input. Library concentrations were quantified by qPCR (KAPA) with a threshold of minimal 3nM.

A total of 24 samples and healthy controls were whole-genome sequenced (Illumina Novaseq S4 2x150bp V1.5) to a median coverage of 60X for tumor samples and 30X for healthy controls. Selection of samples was based on the optimal relation between tumor purity, concentration of prepared libraries, and spatial distribution of samples across different locations in the patients.

Planned bioinformatic analyses and deep sequencing of identified variants in all samples
Reads will be aligned to reference genome GRCh38 and tumor-normal comparison will take place to identify somatic variants using the Nextflow version of the HMF pipeline (version 5). The Somatic Alterations in Genome (SAGE version 3.0) algorithm is used as the somatic variant caller, which is specifically designed for the experiment design and sequencing strategy of the HMF laboratory. To determine driver mutations, the somatic variants are first filtered. Only variants that are not on the HMF Panel of Normal artefacts with enough coverage, are annotated using the gvanno toolkit (version 1.4.4). Identified drivers will be crosschecked in an independent somatic driver catalogue, such as OpenCRAVAT based on CHASMplus, HMFs Purple Driver Catalogue and/or CancerMine (as part of gvanno) (11-13). Drivers and other pathogenic small nucleotide variants of interest will be assessed for their (sub)clonality on all sampled tumor locations. To do so, a representative selection of the annotated somatic

variants is made, based on the intersection (performed by BCF Tools version 1.15) of somatic variants that are exonic, found consistently in all whole-genome sequenced locations and that are identified by the cancer annotation databases mentioned before or are of specific interest to the SGC subtype (such as activating *NOTCH* mutations in AdCC). Based on this selection, a single-molecule molecular inversion probes (smMIPs) panel customized per patient will be developed, and deep targeted sequencing will take place on DNA of all samples. This will give a robust assessment of the (sub)clonality of these variants per patient.

To acquire a complete insight of impactful somatic changes to the tumor genomes, a SV analysis is performed using GRIDSS (version 2.12.0) and the tumor purity and ploidy is investigated using HMF PURPLE (version 3.1). To project the development of the somatic changes (both CNVs and SNVs) over the multiple metastases an interactive phylogenetic tree will be constructed using PhyloWGS (version 1.0). To determine the actual metastasis driving mutation based on phylogenetic inference and to generate a report per sample, Treeomics (version 1.9) is used.

All analyses are based on open-source software, which is available on Github. Reference links to abovementioned tools are listed in Supplementary Table 1.

Data availability

All tumor specimens, DNA samples, prepared sequencing libraries and whole-genome sequencing data is available to the research community upon reasonable request.

Results

Case descriptions

Patient A, 57-year-old female, with a medical history of auto-immune hepatitis with primary biliary cirrhosis overlap, underwent a superficial parotidectomy after being analyzed for a lump in the left neck area. Pathologic evaluation revealed an AdCC with extensive perineural growth and extensive tumor growth in the resection margins. Post-operative radiotherapy to a total of 66Gy was given from the left parotid area to the skull base. Approximately one year after adjuvant radiotherapy was ended, the patient was diagnosed with asymptomatic pulmonary and pleural metastases. Over the course of the next six years the pulmonary metastases slowly progressed leading to increasing dyspnea and pain. Bilateral kidney metastases were seen on CT imaging and a locoregional metastasis emerged in the nasal vestibule. The patient opted out for palliative chemotherapy and no targets for genetically matched therapy were found with NGS of the primary tumor. Palliative radiotherapy was

given on painful pulmonary metastases. Eventually the patient passed away at the age of 64 years due to respiratory insufficiency caused by pulmonary metastases.

Ventilated post-mortem CT-scanning revealed very extensive disease load with several large confluent tumor masses in both lungs (Figure 1). Autopsy (starting 56 hours after cardiopulmonary arrest) confirmed this. Besides these pulmonary metastases, in both kidneys multiple metastases were seen, as was in the liver. Both the nose tip and the pericardium also harbored AdCC metastases.

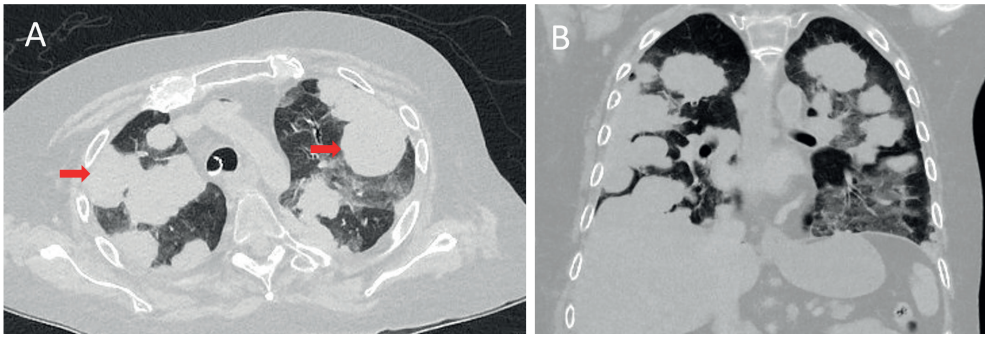

Figure 1: ventilated post-mortem CT-scan of the lungs of patient A, showing multiple large confluent AdCC metastases (arrows). **A:** transversal plane, **B:** coronal plane.

Patient B, a 53-year-old female with a medical history of hypertension was diagnosed with a T4N0 AdCC of the left mandibular gland, for which a combined mandibulectomy and neck dissection operation (commando procedure) was performed. Perineural growth was observed as well as solid growth, and the resection was irradical. The patient received adjuvant radiotherapy (70Gy). One-year post-operative the patient was diagnosed with metastatic disease in the retroperitoneal lymph nodes, lungs and lumbal vertebra. WGS of the tumor showed a *MYB-NFIB* gene fusion, but no targets for genetically matched therapy. Shortly after metastatic disease was diagnosed, the patient suffered from an epileptic seizure caused by multiple (>20) brain metastases, for which she received whole-brain radiotherapy (20Gy) and stereotactic radiotherapy on the two largest brain metastases (10Gy). She also received palliative radiotherapy on a bone metastasis in the pelvis (8Gy) and palliative systemic therapy with vinorelbine was started. Rapid cognitive decline and disease progression was seen, and the patient passed away approximately 8 months after metastatic disease was first diagnosed.

Post-mortem imaging confirmed the evident disease progression (Figure 4). During autopsy (starting 12 hours after cardiopulmonary arrest) several extensive AdCC metastases were seen in the brain, both lungs, the liver, both kidneys and adrenal glands, the thyroid, the

pancreas and bones. The kidney, adrenal gland and pancreatic metastases were not seen in the most-recent ante-mortem imaging (performed 5 months prior to death).

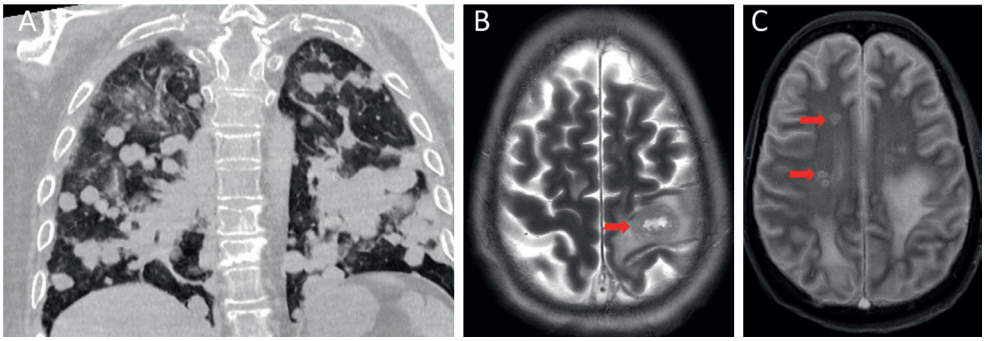

Figure 2: Post-mortem imaging of patient B. **A:** post-mortem CT-image of the lungs, coronal plane. Extensive AdCC metastases are visible in both lungs. **B:** T2-weighted transversal MRI image of the brain, showing a metastasis with edema in the left parietal lobe (arrow). **C**. FLAIR transversal MRI image showing multiple smaller intracranial metastases (arrows).

Patient C, a female complaining of a lump at the mandibular angle, was diagnosed at the age of 48 years with a pulmonary metastasized myoepithelial carcinoma ex pleomorphic adenoma of the left parotid gland. NGS of a needle biopsy of a pulmonary metastasis revealed presence of *LIFR-PLAG1* fusion, confirming the carcinoma ex pleomorphic origin, and loss of *CDKN2A*, upon which treatment with the CDK4/6 inhibitor ribociclib was initiated in a basket trial (NCT02925234). Before the first response evaluation took place, evident progression of the pulmonary and pleural metastases was seen and the patient died at the age of 48 years due to respiratory insufficiency caused by the metastases in combination with pleural effusion, 6 months after the myoepithelial carcinoma was diagnosed.

Post-mortem CT-scanning and MRI confirmed evident progression of the primary tumor to a final size of approximately 70-75mm, as well as extensive pulmonary and pleural metastases invading the majority of the lung parenchyma of both lungs (Figure 3). This was confirmed during autopsy (starting 24 hours after cardiopulmonary arrest), in which no extrapulmonary metastatic sites were identified.

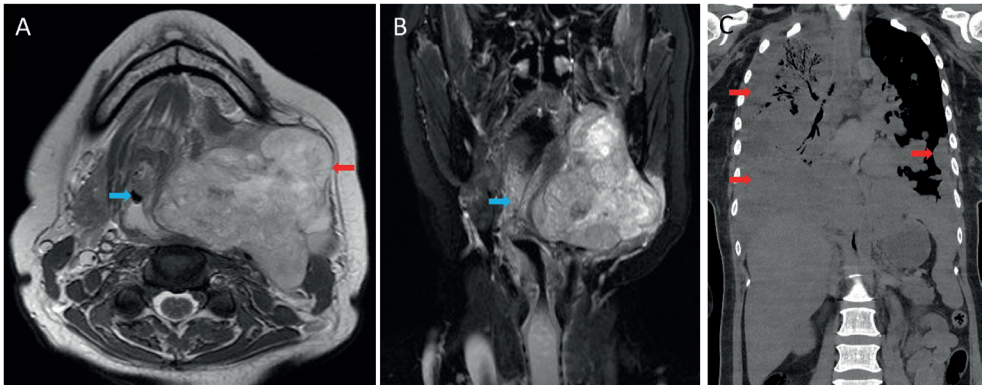

Figure 3: A: T2-weighted transversal image of post-mortem MRI of patient C, showing a large epithelial-myoepithelial carcinoma stemming from the deep lobe of the left parotid gland (red arrow), with compression on the trachea (blue arrow). **B:** T1- weighted fat-sat coronal MRI image of the parotid tumor. **C:** post-mortem CT-scan showing extensive pulmonary and pleural metastases in both lungs and close to absent air-containing parenchyma in the right lung (arrows).

The male **patient D** underwent a parotidectomy with a neck dissection of a T4aN2b SDC located in the left parotid at the age of 79 years. The patient had a medical history of an aneurysm of the abdominal aorta for which he had received an aortic bifurcation prosthesis. Post-operative radiotherapy to a maximal dose of 66Gy was given. Within 4 months after completion of the adjuvant radiotherapy follow-up imaging revealed metastases in lymph node (mediastinal and hilar), bone and lungs. Upon revision of the resection specimen, almost all tumor cells expressed the androgen receptor on immunohistochemistry. Her2 fluorescent in-situ hybridization was negative. The tumor harbored an activating *PIK3CA* (p.Q61R) and *HRAS* (p.H107R) mutation. Palliative combined androgen blockade (CAB) consisting of bicalutamide with gosereline was initiated. The first RECIST evaluation after 3 months of CAB showed a stable disease. After 16 months slow progression of pulmonary metastases was seen (progressive disease according to RECIST). Due to the slow growth, androgen deprivation therapy was continued until 31 months after start of therapy a vertebral metastasis led to a compression fracture. The patient received palliative radiotherapy (8Gy) on this vertebra and eventually passed away due to respiratory insufficiency caused by coronavirus disease (COVID-19) at the age of 82 years.

Post-mortem CT-scanning and autopsy (starting 37 hours after cardiopulmonary arrest) confirmed the presence of the ante-mortem diagnosed disease locations in the vertebra and lungs, as well as one new solitary liver metastasis. Extensive macroscopic and microscopic infiltrative changes consistent with the diagnosis COVID-19 pneumonia were visible in the lungs (Figure 2).

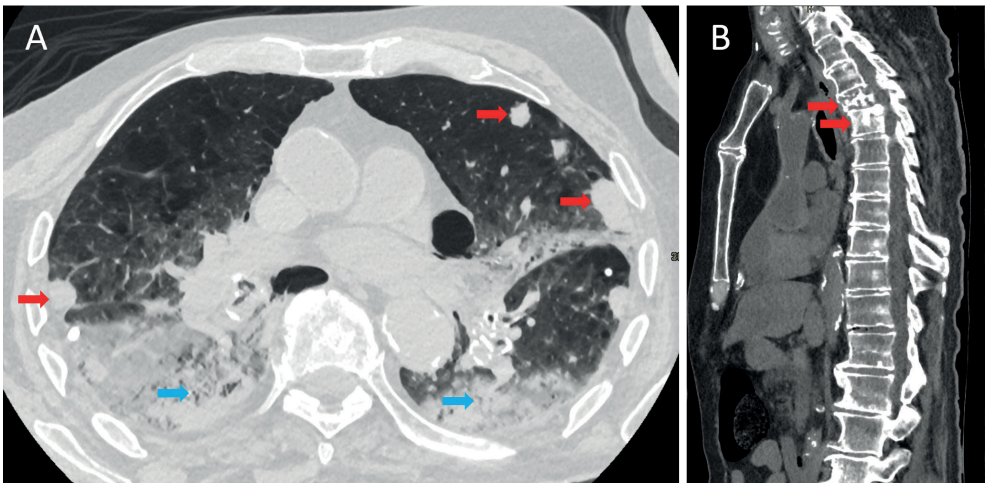

Figure 4: **A:** post-mortem CT-scan of the lungs of patient D, showing multiple SDC metastases in both lungs (red arrows), as well as ground glass opacification likely caused by COVID-19 pneumonia (blue arrows). **B:** post-mortem CT-scan of the thoracic spine demonstrating the pathologic aspect of Th4 and Th5 with sclerosis and collapse (arrows).

Tumor sampling

All patients died out-of-hospital. Autopsy took place within 56 hours after death in all patients. Cooling commenced within 6 hours in every patient. During autopsy, a total of 169 samples of suspected tumor lesions were taken (58, 44, 47 and 20 for patient A, B, C and D, respectively) as were healthy control samples for each patient (abdominal skin). In 138 out of the 169 suspected tumor samples, tumor presence was confirmed on HE sections, and sufficient non-necrotic tumor tissue was present to proceed to DNA isolation and library preparation (Table 1, Figure 5).

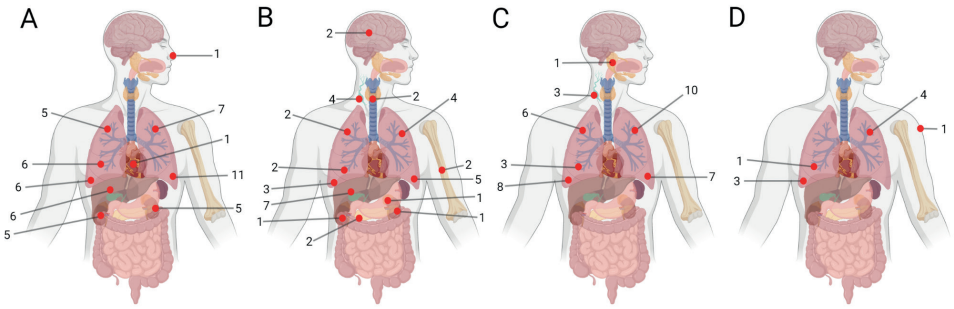

Figure 5: Overview of sampled tumor locations and number of samples taken at that location for patient A, B, C and D. Created with BioRender.com

Table 1: overview of samples used for DNA isolation and library preparations

Location	Patient A	Patient B	Patient C	Patient D
Primary tumor			1	
Locoregional recurrence	1			
Lymph nodes		4	3	
Right lung/pleura	17	7	17	4
Left lung/pleura	18	9	17	4
Liver	6	7		
Bones		2		
Brain		2		
Right kidney	5	1		
Left kidney	5	1		
Adrenal glands		1		
Thyroid		2		
Pancreas		2		
Pericardium	1			
Skin				1
Total	**53**	**38**	**38**	**9**

Library preparations and WGS

Yield after library preparations was high enough for subsequent WGS in all of these 138 tumor samples, with an average library concentration of 13.99nM. Of these 138 samples, 19 were whole-genome sequenced, as were the healthy controls of each patient (Table 2). Mean WGS yield was 245Mbase/sample (range: 207-323Mbase). Comparison of 2 samples taken from the lungs of patient D (one of the right lung and of the left lung) showed 39% overlap in somatic variants and substantial heterogeneity between these two locations (Supplementary Figure 1).

Table 2: overview of whole-genome sequenced samples

Location	Patient A	Patient B	Patient C	Patient D
Primary tumor			1	
Locoregional recurrence	1			
Right lung/pleura	1	1	2	1
Left lung/pleura	1	1	1	1
Liver	1	1		
Bones		1		
Brain		1		
Left kidney	1			
Adrenal glands		1		
Pancreas		1		
Pericardium	1			
Healthy control	1	1	1	1
Total	**7**	**8**	**5**	**3**

Discussion

In this study the preliminary results of an autopsy study to assess ITH and clonal evolution in different subtypes of salivary gland cancer are presented. This is the first report of autopsy results for further NGS analyses on patients with metastatic salivary gland cancer. We have shown that It is feasible to acquire tumor material with sufficient DNA quality to perform WGS in patients that died outside of the hospital. DNA from tumor material sampled from several organs as late as 56 hours after dead occurred were of sufficient quality for WGS. Besides this, several disease locations that were seen during autopsy were not identified on imaging prior to death.

Nucleic acid decay, caused by endogenous nuclease activity and hydrolytic attacks, commences at a stable rate immediately after death occurs (14). The quality of nucleic acid thus decreases as the post-mortal interval to sampling increases, and this is tissue type specific in healthy tissue (15). For tumor samples this is however less clear. A study investigating post-mortem RNA integrity number (RIN) indicated that for tumor derived RNA, this does not correlate with the post-mortal interval (most sampled <30 hours after death occurred) (15). And although RNA is in general less stable than DNA, it was feasible to perform RNA sequencing on post-mortem samples (15). Another study indicated that >75% of tissue sampled within 6 hours after cardiopulmonary arrest has a RIN ≥ 6, which is considered sufficient for RNA sequencing, in contrast to <25% of tissue sampled >23 hours after death (16). When sampled within hours, it is even proven feasible to perform whole-exome sequencing on very little

quantities of cell-free DNA derived from post-mortem blood samples (17). Besides this, after cardiopulmonary arrest takes place tissue and cells remains viable for a period of time, and this interval can be used to create patient-derived xenografts and organoids of deceased patients (18, 19).

It is thus feasible to extract high quality tumor tissue during autopsy. This is in line with our findings, in which in all included patients, multiple samples of sufficient quality for downstream WGS processing could be obtained out of a wide variety of organs, up to as much as 53 samples per patient. The post-mortal interval in our study could be as long as 56 hours, which is longer than most 'rapid autopsy' programs (18). After sampling, first tumor annotation took place, avoiding necrotic areas. Next, punch biopsies of the most viable and tumor cell rich areas were used for NGS library preparations, which might have resulted in the excellent success rate of library preparations of sufficient quality.

Multi-region sampling during autopsy and subsequent NGS entails the possibility to address fundamental questions in oncology regarding evolutionary dynamics, carcinogenesis and treatment resistance (18). Previous studies in more common cancers indeed used this multi-region sampling to address these fundamental questions in localized (20) and metastasized castration-resistant prostate cancer (21, 22), metastasized pancreatic cancer (23-25), metastasized renal carcinoma (26), primary endometrial carcinomas with abdominopelvic metastases (27) and metastatic colorectal cancer (28). This provides detailed information regarding ITH in these cancer types, which is pivotal to understand resistance mechanisms to therapy aimed at the eradication of metastatic disease.

Knowledge on genetic tumor heterogeneity in SGC is not available. Genetic characterization of this rare cancer is most often limited to single sample studies within a single subtype or focusing on a specific genetic aberration. Only 2 studies describe multi-regional characterization, both in AdCC. Liu *et al* show substantial ITH between primary tumor and tumor metastases (29, 30). Especially for the prognostically relevant mutations in *NOTCH* genes metastases were enriched compared to primary tumors (29, 31). Branched evolution with parallel dissemination was observed in all 8 investigated AdCC patients in one study on AdCC clonal evolution. Besides the primary tumor, in this study at most 2 metastatic samples were analyzed per patient (30).

Our study will expand the knowledge on ITH and clonal evolution in SGC, especially since patients suffering from three different subtypes participated in this study and AdCC patients with both aggressive and a more indolent disease course. The extent of samples taken is unprecedented in currently available literature, to our best knowledge. The planned targeted NGS using a customized smMIP) panel (using a workflow comparable to an earlier report)

on all sampled locations, up to as much as 53 samples for a single patient, will give a robust assessment of end-stage spatial ITH (32). The used WGS will extensively map the spectrum of germline and somatic mutation and can be used to assess the evolutionary history of these tumors, although the role of epigenetic changes remains to be elucidated.

In conclusion, this preliminary report on an autopsy study in 4 SGC patients proves that it is feasible to acquire samples of sufficient quality for subsequent WGS during autopsy performed within 56 hours after death occurs.

References

1. Greaves M, Maley CC. Clonal evolution in cancer. Nature. 2012;481(7381):306-13.
2. Turajlic S, Sottoriva A, Graham T, Swanton C. Resolving genetic heterogeneity in cancer. Nature Reviews Genetics. 2019;20(7):404-16.
3. Turajlic S, Swanton C. Metastasis as an evolutionary process. Science. 2016;352(6282):169-75.
4. McGranahan N, Swanton C. Clonal Heterogeneity and Tumor Evolution: Past, Present, and the Future. Cell. 2017;168(4):613-28.
5. Dentro SC, Leshchiner I, Haase K, Tarabichi M, Wintersinger J, Deshwar AG, et al. Characterizing genetic intra-tumor heterogeneity across 2,658 human cancer genomes. Cell. 2021;184(8):2239-54.e39.
6. Hunter KW, Amin R, Deasy S, Ha NH, Wakefield L. Genetic insights into the morass of metastatic heterogeneity. Nat Rev Cancer. 2018;18(4):211-23.
7. Lassche G, van Boxtel W, Ligtenberg MJL, van Engen-van Grunsven ACH, van Herpen CML. Advances and challenges in precision medicine in salivary gland cancer. Cancer Treat Rev. 2019;80:101906.
8. Morris LG, Linxweiler M, Kuo F, Katabi N, Nadeem Z, Dalin MG, et al. The immune microenvironment and neoantigen landscape of aggressive salivary gland carcinomas differ by subtype. Clinical cancer research : an official journal of the American Association for Cancer Research. 2020.
9. Germerott T, Preiss US, Ebert LC, Ruder TD, Ross S, Flach PM, et al. A new approach in virtopsy: Postmortem ventilation in multislice computed tomography. Leg Med (Tokyo). 2010;12(6):276-9.
10. Priestley P, Baber J, Lolkema MP, Steeghs N, de Bruijn E, Shale C, et al. Pan-cancer whole-genome analyses of metastatic solid tumours. Nature. 2019;575(7781):210-6.
11. Lever J, Zhao EY, Grewal J, Jones MR, Jones SJM. CancerMine: a literature-mined resource for drivers, oncogenes and tumor suppressors in cancer. Nature Methods. 2019;16(6):505-7.
12. Pagel KA, Kim R, Moad K, Busby B, Zheng L, Tokheim C, et al. Integrated Informatics Analysis of Cancer-Related Variants. JCO Clin Cancer Inform. 2020;4:310-7.
13. Sondka Z, Bamford S, Cole CG, Ward SA, Dunham I, Forbes SA. The COSMIC Cancer Gene Census: describing genetic dysfunction across all human cancers. Nature Reviews Cancer. 2018;18(11):696-705.
14. Tozzo P, Scrivano S, Sanavio M, Caenazzo L. The Role of DNA Degradation in the Estimation of Post-Mortem Interval: A Systematic Review of the Current Literature. Int J Mol Sci. 2020;21(10).
15. Fan J, Khanin R, Sakamoto H, Zhong Y, Michael C, Pena D, et al. Quantification of nucleic acid quality in postmortem tissues from a cancer research autopsy program. Oncotarget. 2016;7(41):66906-21.
16. Carithers LJ, Ardlie K, Barcus M, Branton PA, Britton A, Buia SA, et al. A Novel Approach to High-Quality Postmortem Tissue Procurement: The GTEx Project. Biopreserv Biobank. 2015;13(5):311-9.
17. Takai E, Maeda D, Li Z, Kudo-Asabe Y, Totoki Y, Nakamura H, et al. Post-mortem Plasma Cell-Free DNA Sequencing: Proof-of-Concept Study for the "Liquid Autopsy". Sci Rep. 2020;10(1):2120.
18. Iacobuzio-Donahue CA, Michael C, Baez P, Kappagantula R, Hooper JE, Hollman TJ. Cancer biology as revealed by the research autopsy. Nat Rev Cancer. 2019;19(12):686-97.

19. Risbridger GP, Clark AK, Porter LH, Toivanen R, Bakshi A, Lister NL, et al. The MURAL collection of prostate cancer patient-derived xenografts enables discovery through preclinical models of uro-oncology. Nat Commun. 2021;12(1):5049.

20. Boutros PC, Fraser M, Harding NJ, de Borja R, Trudel D, Lalonde E, et al. Spatial genomic heterogeneity within localized, multifocal prostate cancer. Nature genetics. 2015;47(7):736-45.

21. Gundem G, Van Loo P, Kremeyer B, Alexandrov LB, Tubio JMC, Papaemmanuil E, et al. The evolutionary history of lethal metastatic prostate cancer. Nature. 2015;520(7547):353-7.

22. Kumar A, Coleman I, Morrissey C, Zhang X, True LD, Gulati R, et al. Substantial interindividual and limited intraindividual genomic diversity among tumors from men with metastatic prostate cancer. Nat Med. 2016;22(4):369-78.

23. Campbell PJ, Yachida S, Mudie LJ, Stephens PJ, Pleasance ED, Stebbings LA, et al. The patterns and dynamics of genomic instability in metastatic pancreatic cancer. Nature. 2010;467(7319):1109-13.

24. Makohon-Moore AP, Zhang M, Reiter JG, Bozic I, Allen B, Kundu D, et al. Limited heterogeneity of known driver gene mutations among the metastases of individual patients with pancreatic cancer. Nature genetics. 2017;49(3):358-66.

25. Yachida S, Jones S, Bozic I, Antal T, Leary R, Fu B, et al. Distant metastasis occurs late during the genetic evolution of pancreatic cancer. Nature. 2010;467(7319):1114-7.

26. Gerlinger M, Rowan AJ, Horswell S, Math M, Larkin J, Endesfelder D, et al. Intratumor heterogeneity and branched evolution revealed by multiregion sequencing. The New England journal of medicine. 2012;366(10):883-92.

27. Gibson WJ, Hoivik EA, Halle MK, Taylor-Weiner A, Cherniack AD, Berg A, et al. The genomic landscape and evolution of endometrial carcinoma progression and abdominopelvic metastasis. Nature genetics. 2016;48(8):848-55.

28. Naxerova K, Reiter JG, Brachtel E, Lennerz JK, van de Wetering M, Rowan A, et al. Origins of lymphatic and distant metastases in human colorectal cancer. Science. 2017;357(6346):55-60.

29. Ho AS, Ochoa A, Jayakumaran G, Zehir A, Valero Mayor C, Tepe J, et al. Genetic hallmarks of recurrent/metastatic adenoid cystic carcinoma. J Clin Invest. 2019;129(10):4276-89.

30. Liu B, Mitani Y, Rao X, Zafereo M, Zhang J, Zhang J, et al. Spatio-Temporal Genomic Heterogeneity, Phylogeny, and Metastatic Evolution in Salivary Adenoid Cystic Carcinoma. Journal of the National Cancer Institute. 2017;109(10).

31. Ferrarotto R, Mitani Y, Diao L, Guijarro I, Wang J, Zweidler-McKay P, et al. Activating NOTCH1 Mutations Define a Distinct Subgroup of Patients With Adenoid Cystic Carcinoma Who Have Poor Prognosis, Propensity to Bone and Liver Metastasis, and Potential Responsiveness to Notch1 Inhibitors. Journal of clinical oncology : official journal of the American Society of Clinical Oncology. 2017;35(3):352-60.

32. Roepman P, de Bruijn E, van Lieshout S, Schoenmaker L, Boelens MC, Dubbink HJ, et al. Clinical Validation of Whole Genome Sequencing for Cancer Diagnostics. J Mol Diagn. 2021;23(7):816-33.

Supplementary information

Supplementary Table 1: reference links to open source software that will be used for the bioninformatic processing of WGS data

Tool	Github reference
Nextflow version of HMF pipeline	https://github.com/ErasmusMC-Bioinformatics/NextFlow-VC-pipeline
SAGE v3.0	https://github.com/hartwigmedical/hmftools/tree/master/sage
gvanno v1.4.4	https://github.com/sigven/gvanno
BCF Tools v1.15	https://github.com/samtools/bcftools
GRIDSS v2.12.0	https://github.com/PapenfussLab/gridss/releases
HMF Purple v3.1	https://github.com/hartwigmedical/hmftools/releases/tag/purple-v3.1
PhyloWGS v1.0	https://github.com/morrislab/phylowgs
Treeomics v1.9	https://github.com/reiterlab/treeomics

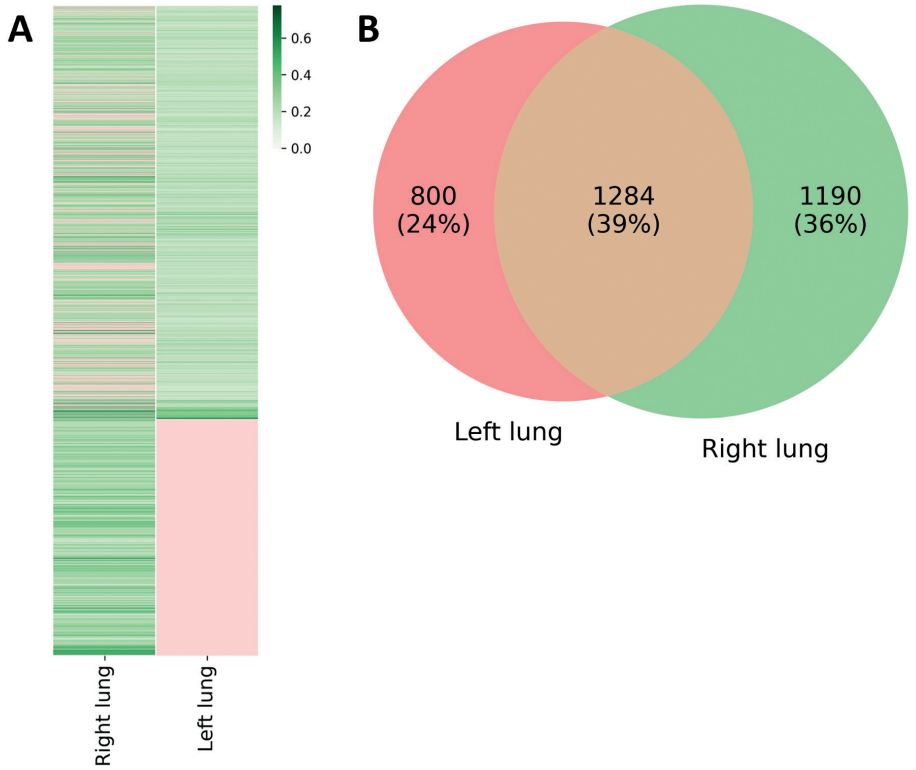

Supplementary Figure 1: difference in somatic variants presence between the right and left lung of patient 2, suffering from salivary duct carcinoma. A: Heatmap comparing variant allele frequencies of all somatic variants, B: Venn diagram showing overlap in variants in the right and left lung.

PART 2:

Biomarkers to predict response to systemic therapy in salivary duct carcinoma

CHAPTER 4

Predictive and prognostic biomarker identification in a large cohort of androgen receptor-positive salivary duct carcinoma patients scheduled for combined androgen blockade

Gerben Lassche, Yuichiro Tada, Carla M.L. van Herpen, Marianne A. Jonker, Toshitaka Nagao, Takashi Saotome, Hideaki Hirai, Natsuki Saigusa, Hideaki Takahashi, Hiroya Ojiri, Adriana C.H. van Engen-Van Grunsven, Jack A. Schalken, Chihiro Fushimi, and Gerald W. Verhaegh

Cancers (Basel). 2021;14;13(14):3527

Abstract

Introduction

Patients suffering from recurrent or metastatic (R/M) salivary duct carcinoma (SDC) are often treated with combined androgen blockade (CAB). However, CAB frequently fails, resulting in a worse prognosis. Therefore, biomarkers that can predict treatment failure are urgently needed.

Methods

mRNA from 76 R/M androgen receptor (AR)-positive SDC patients treated with leuprorelin acetate combined with bicalutamide was extracted from pre-treatment tumor specimens. AR, Notch, MAPK, TGFβ, estrogen receptor (ER), Hedgehog (HH), and PI3K signaling pathway activity scores (PAS) were determined based on the expression levels of target genes. Additionally, 5-alpha reductase type 1 (SRD5A1) expression was determined. These markers were related to clinical benefit (complete/partial response or stable disease ≥6 months) and progression-free and overall survival (PFS/OS).

Results

SRD5A1 expression had the highest general predictive value for clinical benefit and positive predictive value (PPV: 85.7%). AR PAS had the highest negative predictive value (NPV: 93.3%). The fitting of a multivariable model led to the identification of SRD5A1, TGFβ, and Notch PAS as the most predictive combination. High AR, high Notch, high ER, low HH PAS, and high SRD5A1 expression were also of prognostic importance regarding PFS and SRD5A1 expression levels for OS.

Conclusion

AR, Notch PAS, and SRD5A1 expression have the potential to predict the clinical benefit of CAB treatment in SDC patients. SRD5A1 expression can identify patients that will and AR PAS patients that will not experience clinical benefit (85.7% and 93.3% for PPV and NPV, respectively).

Introduction

Salivary duct carcinoma (SDC) is one of the 22 salivary gland cancer (SGC) subtypes, as recognized by the World Health Organization classification of head and neck tumors (1). SDC distinguishes itself from the other subtypes by its aggressive nature, with estimated 5 and 10 year overall survival rates as low as 43% and 26%, respectively (2). More than half of the patients treated with curative intent will eventually develop a locoregional recurrence or distant spread (2–4). In the case of metastatic disease, refraining from treatment with antineoplastic agents leads to a median overall survival (OS) of five months when best supportive care is given (5). This emphasizes the need for systemic, and preferably targeted, therapeutic approaches for these patients.

As a stand-alone treatment, chemotherapy generally only has limited potential in alleviating a dismal prognosis. A more promising treatment is targeting androgen receptor (AR) signaling or targeting the human epidermal growth factor receptor 2 (HER2) (6–9). HER2 is expressed in 29–46% of SDC cases, and trastuzumab combined with a taxane is a reasonable choice in patients expressing HER2 (8,9). The majority of patients, however, does not express HER2, but almost all SDC cases express the AR in the nucleus (78–96%). This provides the rational basis for therapy aimed to eliminate AR signaling. Androgen deprivation therapy (ADT) with luteinizing hormone-releasing hormone (LHRH) agonists has an established role in metastatic hormone-sensitive prostate cancer, and a combined androgen blockade (LHRH agonist combined with an AR antagonist) can improve treatment benefits compared to ADT monotherapy (10). Translating these treatment strategies to SDC is appealing, and the body of evidence demonstrating the beneficial effects of androgen-receptor targeting strategies in SDC is expanding (6–8). However, large-scale ressearch on the ideal AR pathway-targeting treatment regimen in SDC is lacking. Recently, combined androgen blockade (CAB) using the LHRH agonist leuprorelin acetate and non-steroidal AR-antagonist bicalutamide has been prospectively studied in a phase II study in SDC patients, leading to a response rate of 42% with a median progression-free survival (PFS) of 8.8 months and OS of 30.5 months (11). Additionally, retrospective studies have shown that various AR-targeting strategies (bicalutamide or enzalutamide with or without LHRH agonists) can lead to responses in SDC patients with response rates ranging from 18 to 53% (5,8,12,13). The large proportion of patients not responding to ADT or CAB and the poor prognosis of SDC patients emphasize the need for predictive biomarkers. The large number of non-responders also argues for the presence of intrinsic ADT resistance mechanisms, such as active tumor-driving signal transduction pathways other than AR signaling, which has yet to be explored.

Recently, a retrospective study aiming to identify intrinsic resistance mechanisms and biomarkers for response to ADT was published by our group (14). The quantification of

AR signaling in tumor samples of 30 SDC patients using a composite metric summarizing expression levels of AR target genes in a score called the AR pathway score was found to be predictive for clinical benefit (complete or partial response or stable disease >6 months) (15). Additionally, levels of SRD5A1 mRNA—which encodes the 5α-reductase type A1 enzyme that converts testosterone into the more potent androgen dihydrotestosterone (DHT)—were predictive for ADT response. Optimizing the cut-offs of the AR pathway activity score and SRD5A1 expression levels based on the receiver operating characteristic (ROC) curve in this cohort resulted in a sensitivity of 55.6% and a specificity of 95.2% for high AR pathway scores and 77.8% and 75.0%, respectively, for SRD5A1 expression. High SRD5A1 expression was also significantly associated with longer progression-free survival (2.8 months for low SRD5A1 expression versus 5.6 months for high expression; $p = 0.008$). Overall survival did not significantly differ between patients with low and high SRD5A1 expression levels (medians of 24.2 and 46.3 months, respectively; $p = 0.069$) (14).

In this study, we aimed to validate the predictive value and prognostic importance of the AR pathway activity score and SRD5A1 expression in an independent cohort of SDC patients with locally advanced, recurrent, or metastatic disease (R/M) that were treated with CAB. Additionally, we hypothesized that in patients not responding to ADT, other tumor-driving pathways might be in play. To explore this, the activity of tumor-driving pathways was quantified based on target gene mRNA levels, and the prognostic importance of the resulting pathway activity scores and their potential to tailor treatment decisions were assessed.

Methods

Cohort description

Tumor material and clinicopathological characteristics of AR-positive SDC patients initiating CAB treatment between 2012 and 2019 in the International University of Health and Welfare, Mita hospital (Tokyo, Japan) were collected. Some of these patients were treated in a phase II study evaluating efficacy of CAB in metastatic or locally advanced AR-positive salivary gland carcinoma (11). A publicly announced opt-out system for the residual use of patient material was used. This study and the international transfer of patient material was approved by the Institutional Ethics Review Board of the International University of Health and Welfare, Mita hospital (file number: 5-19-6).

All patients were treated with a subcutaneously administered dose of leuprorelin acetate of 3.75 mg every 4 weeks or 11.25 mg every 12 weeks combined with a daily oral dose of 80 mg bicalutamide. Response to treatment was evaluated with computed tomography scans or

magnetic resonance imaging at an interval of 6–8 weeks after CAB initiation until progressive disease (PD). Responses were scored according to RECIST criteria, v1.1.

Tumor material used for RNA extraction, immunohistochemistry and HER2 FISH
All tumor material used in this study was sampled prior to CAB initiation. Diagnoses of salivary duct carcinoma were confirmed by an expert head and neck pathologist (TN, HH, or ACHvEvG). Formalin-fixed paraffin-embedded (FFPE) material of the primary tumor was used; if not available, material of tumor-invaded lymph nodes or distant metastases was used. Hematoxylin and eosin-stained slides were used to estimate tumor cell percentages and to annotate tumor areas by an expert head and neck pathologist (ACHvEvG).

AR-status was assessed by immunohistochemistry (IHC). Heat-induced epitope retrieval on a 4 µm FFPE section was performed for 30 min in a 1 mmol/L EDTA solution, followed by incubation with an anti-AR antibody (AR441 ready-to-use BioCare Medical LLC, Pacheco, CA, USA). Diaminobenzide (DAB) was used as chromogen to detect immunoreactivity, and hematoxylin was used for counterstaining. AR positivity was defined as >1% of positive nuclei staining positive (11).

HER2 status was assessed by ERBB2 fluorescent in situ hybridization (FISH) according to standard ISH protocol using the PathVysion HER-2 DNA probe kit of Abbot (Vysis CEP17/ Vysis LSI Her2/neu)). HER2 FISH status was scored in accordance with the American Society of Clinical Oncology/College of American Pathologists (ASCO/CAP) guidelines for the evaluation of breast cancer (16). In addition to HER2 FISH, HER2 IHC was also performed using a polyclonal rabbit anti-human cerbB2 antibody (dilution 1:400, DAKO) to aid in the FISH scoring.

RNA isolation
For RNA extraction, tumor tissue was collected from the annotated tumor area of three 10 µm sections. RNA was extracted, eluted in 100 µL of buffer, and DNase-treated using VERSANT Tissue Preparation Reagents kit (Siemens, Munich, Germany) according to the manufacturer's instructions. RNA concentration was quantified using the Qubit RNA HS Assay Kit with a Qubit Fluorometer (Thermo Fisher, Waltham, MA, USA).

Pathway activity scores measurement
Seven different potential tumor-driving signaling pathway activities were measured and calculated using the Philips pathway activity profiling OncoSignal test (Philips Molecular Pathway Diagnostics, Eindhoven, The Netherlands): the androgen receptor pathway (AR), Notch signaling pathway (Notch), mitogen-activated protein kinase pathway (MAPK), transforming growth factor beta signaling pathway (TGFβ), estrogen receptor pathway (ER),

Hedgehog signaling pathway (HH), and phosphoinositide 3-kinase pathway (PI3K—the inverse of Forkhead Box-O (FOXO) signaling, in the absence of oxidative stress) (17,18). For each of these pathways, the output of this test was the odds of the transcription complex of this pathway being active vs. not active, expressed on a logarithmic scale and scaled to range from 0 to 100. Pathway activities scores were inferred from a defined set of target genes of each transcription complex. A Bayesian computational network considering the probabilistic relation between the target genes and transcription complex was used to calculate each pathway activity score. Each pathway model was calibrated with ground truth using samples with known active or inactive signaling. For instance, for AR-signaling, samples of the AR-positive human prostate cancer cell line LNCaP, treated with and without dihydrotestosterone, were used as ground truth values for active and inactive pathway activity state, respectively (15). This Bayesian approach of expressing the odds of a pathway being active or inactive based on quantitative measurements of target gene sets has previously been published and validated in several tissue types for different pathways (15,17-25). Target gene expression was quantified with one-step RT-qPCR, using SuperScript® III Platinum® One-Step qRT-PCR Kit (Invitrogen, Waltham, MA, USA) on FFPE-extracted RNA.

The AR pathway analysis was further optimized compared to the assay performed in the study by Van Boxtel et.al.; see Supplementary File S1 (14). In this study, activity scores calculated with the optimized assay were used.

cDNA synthesis and SRD5A1 expression quantification

FFPE-derived total RNA (500 ng) was used as input for cDNA synthesis using random hexamer primers and SuperScript II RT (Thermo Fisher Scientific, Waltham, MA). SYBR Green qPCR was performed using gene-specific primers (Supplementary Table S1) and a LightCycler 480 machine, according to the manufacturer's instructions (Roche, Basel, Switzerland). Relative SRD5A1 expression was assessed by normalization to housekeeping HPRT1 gene levels using the ΔΔCt method, essentially as described previously (14).

Statistical analysis

Baseline characteristics were described using descriptive statistics (median ± interquartile range (IQR) or mean ± standard deviation). Response to ADT treatment was scored in one of the four RECIST categories: complete response (CR), partial response (PR), stable disease (SD), or PD. Clinical benefit to ADT was defined as CR, PR, and SD ≥ 6 months, as in the previous study on AR pathway analysis in ADT-treated SDC patients (14). PFS was defined as the time from first CAB administration until PD or death, and OS was defined as the time from first CAB administration until death from any cause. For all analysis of SRD5A1 expression, a natural logarithmic transformation was performed. For categorical variables (e.g., HER2 status), Fisher's exact test or chi-square in case of >2 groups was used, and for

continuous variables, the Mann–Whitney U test was used to compare baseline differences in the group with and without clinical benefit. A p-value of 0.05 was considered statistically significant. Analyses were performed in SPSS version 25 (IBM Corp. Armonk, NY, USA) and R Studio version 3.5.3 (Rstudio PBC, Boston, MA, USA). Graphical work was created using Python version 3.8 with the Matplotlib, Pandas, Numpy, Seaborn, and Lifelines packages.

Univariable analysis

For each pathway and SRD5A1 expression data, an ROC curve was plotted and the area under the curve (AUC) was calculated. The value of the pathway activity score or SRD5A1 expression level resulting in the highest value of true positive rate minus false positive rate based on the ROC results was used as the cut-off for pathway activity score dichotomization to calculate negative (NPV) and positive predictive value (PPV), with the prevalence estimated as fraction of patients with clinical benefit. Subsequently, survival curves using Kaplan–Meier estimates were constructed after dichotomization using the median pathway activity score for all pathways and the cut-off found in the ROC analysis . The cut-off found in the ROC analysis optimally separated patients with and without clinical benefit, and clinical benefit was presumed to relate to survival, making this cut-off a rational choice to separate patients with short and long survival. A log-rank test was performed to compare differences in survival.

Multivariable analysis

Next, we aimed to fit a prediction model using different tumor-driving pathways as input to see whether a multicomponent model would more accurately predict clinical benefit. A multivariable logistic regression model was fitted using a forward selection strategy based on Akaike information criterion (AIC) to prevent overfitting (26). The predictiveness of the model with lowest AIC was assessed by ROC analysis.

For the AR pathway activity score and SRD5A1 expression levels, which were predictive in the earlier study by van Boxtel et al., a second analysis was performed to identify cut-off values for these scores optimized towards preventing false negatives (i.e., to identify a group of non-responders with minimal false-negatives) (14). The cut-offs for these scores were identified by the maximized value of a loss function calculating a total penalty for every cut-off in both scores, giving a penalty of 3 for a false negative outcome and a penalty of 1 for a false positive outcome. This procedure was cross-validated by splitting the dataset into a training set (two-third) and a test set (one-third), calculating both cut-offs on the training set and test predictiveness in the test set. Median sensitivity and specificity with IQR were calculated by repeating this procedure a thousand times.

Results

Patient cohort description and treatment outcome

Seventy-six patients with a median age of 65.2 years were treated with CAB and included in the analysis. Of these 76 patients, 93.4% were male, and the majority of the primary tumors were located in the parotid gland (68.4%). CAB was the first-line treatment in 75.0% of the patients (Table 1). Of the 76 ADT-treated patients, 5 (6.6%) experienced CR, 15 (19.7%) experienced PR, and 36 (47.4%) SD and 20 (26.3%) experienced PD as best response upon treatment with bicalutamide and leuprorelin, respectively. Clinical benefit, defined as CR, PR, or SD with PFS ≥ 6 months, was seen in 40 patients (52.6%). Baseline characteristics did not significantly differ between patients with and without clinical benefit, except for systemic treatments given post-CAB (Table 1). In the entire cohort, the median PFS was 28 weeks overall and 47 weeks in the group with clinical benefit. The median OS was 87 weeks in the entire cohort, 68 weeks in the group without clinical benefit, and 105 weeks in the group with clinical benefit.

Of these 76 patients, biopsies or surgical specimens sampled before the initiation of CAB were used for molecular analysis. These samples were taken from the primary lesion in 81.6%, lymph node metastases in 14.5%, and distant metastasis in 3.9% of the cases. RNA quality was sufficient for subsequent downstream pathway analysis for 72 (94.7%) of the samples. SRD5A1 expression could be determined in 75 (98.7%) of the samples.

Table 1: Baseline characteristics sorted for patients with and without clinical benefit

Characteristic, N (%)	***N* (%)**	**Number of Patients (*N* = 76)**		
		Clinical Benefit [1] (*N* = 40)	**No Clinical Benefit [1] (*N* = 36)**	**Difference**
Age at diagnosis				$p = 0.53$
	Median (range)	66.3 (46–83)	65.2 (42–81)	
Gender				$p = 0.18$
	Male	39 (97.5)	32 (88.9)	
	Female	1 (2.5)	4 (11.1)	
Location primary tumor				$p = 0.84$
	Parotid	28 (70.0)	24 (66.7)	
	Sublingual	0 (0)	0 (0)	
	Submandibular	9 (22.5)	10 (27.8)	
	Minor	3 (7.5)	2 (5.6)	
HER2 status [2]				$p = 0.075$
	Positive	7 (17.5)	13 (36.1)	
	Negative	33 (82.5)	23 (63.9)	
HER2 IHC				$p = 0.071$
	0	9 (22.5)	9 (25.0)	
	1+	17 (42.5)	9 (25.0)	
	2+	9 (22.5)	5 (13.9)	
	3+	5 (12.5)	13 (36.1)	
T-stage at diagnosis				$p = 1.0$
	1–2	18 (45.0)	15 (41.7)	
	3–4	22 (55.0)	20 (55.6)	
	Unknown	0 (0)	1 (2.7)	
N-stage at diagnosis				$p = 0.34$
	0	16 (40.0)	10 (27.8)	
	1–2	24 (60.0)	26 (72.2)	
M-stage at diagnosis				$p = 0.36$
	0	32 (80.0)	32 (88.9)	
	1	8 (20.0)	4 (11.1)	
R/M				$p = 0.41$
	Locally advanced/ recurrent	7 (17.5)	3 (8.3)	
	Metastatic	27 (67.5)	27 (75.0)	
	Both	6 (15.0)	6 (16.7)	

(Table continues on next page)

Table 1: Continued

Underwent surgery				$p = 1.0$
	Yes	34 (85.0)	31 (86.1)	
	No	6 (15.0)	5 (13.9)	
Postoperative radiotherapy				$p = 1.0$
	Yes	16 (40.0)	15 (41.7)	
	No	24 (60.0)	21 (58.3)	
CAB as first line				$p = 0.43$
	Yes	28 (70.0)	29 (80.6)	
	No	12 (30.0)	7 (19.4)	
Post-CAB systemic treatment				$p = 0.094$
	Yes	22 (55.0)	27 (75.0)	
	No	18 (45)	9 (25.0)	
Post-CAB anti-HER2				$p = 0.01$
	Yes	2 (5.0)	10 (27.8)	
	No	38 (95.0)	26 (72.2)	
Post-CAB chemotherapy				$p < 0.001$
	Yes	9 (22.5)	24 (66.7)	
	No	31 (77.5)	12 (33.3)	
Post-CAB platinum- based treatment				$p = 0.10$
	Yes	6 (15.0)	12 (33.3)	
	No	34 (85.0)	24 (66.7)	

Abbreviations: HER2: human epidermal growth factor receptor 2; T: tumor; N: nodal; M: metastasis; R/M: locally advanced, recurrent, or metastatic; CAB: combined androgen blockade. 1 Clinical benefit: CR, PR, or SD ≥6 months. 2 HER2 status according to ASCO/CAP guidelines.

Predictive value of pathway activity scores and SRD5A1 expression

Besides AR pathway activity, six other potential tumor-driving pathways were analyzed: Notch, MAPK, TGFβ, ER, HH, and PI3K. In addition, the expression levels of SRD5A1 mRNA were determined. Of all pathways, AR and Notch pathway activity scores were significantly higher in patients with clinical benefit ($p = 0.02$ and $p = 0.05$, respectively; Figure 1A and Table 2). The AR and Notch pathway activity scores did not correlate to each other (Pearson's correlation coefficient: $\rho = 0.14$). SRD5A1 expression was also significantly higher in the group with clinical benefit compared to the group without clinical benefit ($p < 0.001$; Figure 1B and Table 2).

Table 2: Pathway activity score differences between patients with and without clinical benefit

Pathway	Clinical Benefit (Mean [Range])	No Clinical Benefit (Mean [Range])	Difference
AR	57.5 [31.7–71.9]	52.8 [29.6–71.9]	$p = 0.02$
Notch	68.1 [58.8–79.3]	64.8 [52.2–76.0]	$p = 0.05$
MAPK	63.0 [47.8–73.2]	66.4 [50.7–84.9]	$p = 0.051$
TGFβ	66.2 [49.2–74.5]	68.2 [57.5–78.5]	$p = 0.26$
ER	35.3 [11.3–45.3]	33.3 [16.7–44.9]	$p = 0.097$
HH	25.9 [11.3–38.9]	26.8 [13.4–35.0]	$p = 0.44$
PI3K [1]	16.7 [6.5–32.9]	16.7 [6.5–28.8]	$p = 0.88$
SRD5A1 expression [2]	1.45 [−1.46–3.67]	0.42 [−1.18–2.39]	$p < 0.001$

Abbreviations: AR: androgen receptor pathway; Notch: Notch signaling pathway; MAPK: mitogen-activated protein kinase pathway; TGFβ: transforming growth factor beta signaling pathway; ER: estrogen receptor pathway; HH: hedgehog signaling pathway; PI3K: phosphoinositide 3-kinase pathway. 1. PI3K, as the inverse of Forkhead Box-O (FOXO) signaling, in the absence of oxidative stress. 2. Log-transformed value of SRD5A1 expression normalized to HPRT1.

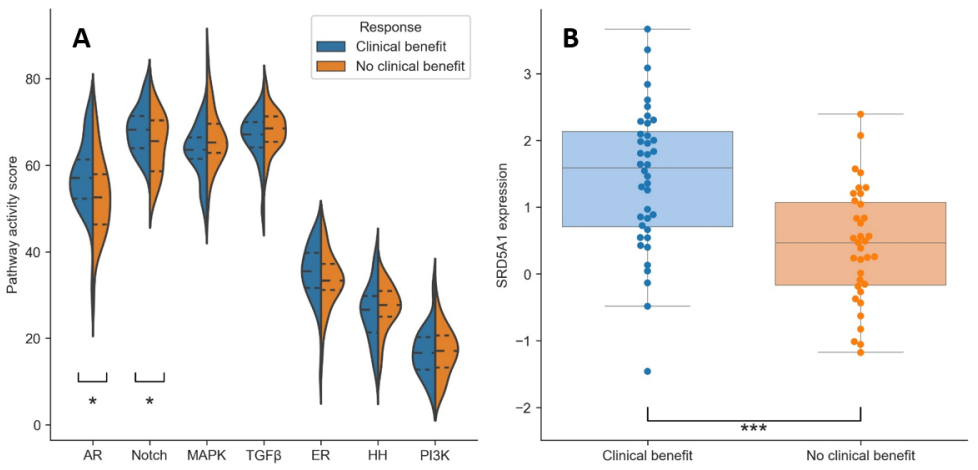

Figure 1: Violin plots of pathway activity scores (A) and dot/boxplot for SRD5A1 expression (B) for the patients with (blue) and without (orange) clinical benefit. Dotted lines in (A): quartiles. * = p < 0.05, *** = p < 0.001.

The corresponding AUC values of the ROC curves for the AR and Notch pathways were 0.66 (95% confidence interval (CI): 0.53–0.79) and 0.63 (95% CI: 0.50–0.77), respectively, and the corresponding AUC value for SRD5A1 expression was 0.78 (95% CI: 0.67–0.88) (Figure 2). The pathway activity score resulting in the highest value of true positive rate minus false positive rate was 47.8 for the AR pathway and 62.3 for the Notch pathway. These cut-off values for AR and Notch pathway activity resulted in a sensitivity of 97.4% and specificity of 38.2% for predicting clinical benefit for AR and 89.5% sensitivity and 38.2% specificity for Notch. Using the cut-off of 47.8 for AR pathway activity, 19.4% of the patients tested below this threshold. This corresponded to a PPV of 63.8% and an NPV of 92.9%. Using the cut-off of 62.3 for Notch pathway activity, 23.6% of the patients tested below this threshold, which corresponded to a PPV of 61.8% and an NPV of 76.5%. Regarding SRD5A1 expression, the optimal cut-off of the log-transformed expression value was 1.30, which resulted in 62.6% of the patients that tested below this threshold, a sensitivity of 60%, and a specificity of 88.6%, as well as a PPV of 85.7% and an NPV of 66.0%.

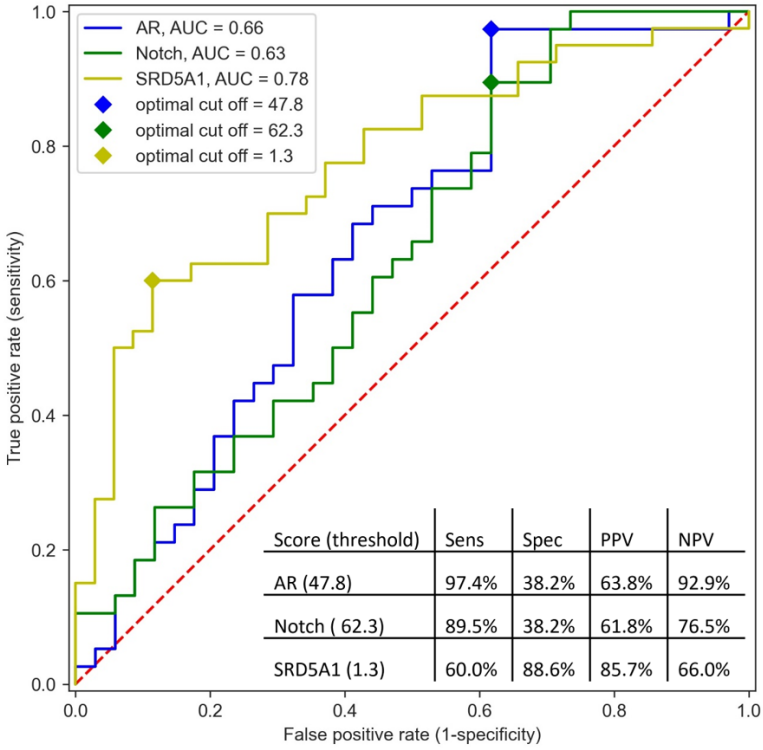

Figure 2: AUC curve of AR and Notch pathway activity scores and SRD5A1 expression levels. The optimal cut-off was defined as maximum value for true positive rate minus false positive rate. Abbreviations: Sens = sensitivity; Spec = specificity; PPV = positive predictive value; NPV = negative predictive value.

Clinical benefit prediction using multiple pathways and SRD5A1 expression

For the multivariable logistic regression, all patients with complete data regarding pathway activity scores and SRD5A1 expression levels were used (n N = 71; four samples did not pass quality check for pathway analysis, and one additional sample failed in SRD5A1 qPCR analysis). As a starting point for the multivariable logistic regression analysis, the model resulting from univariable logistic regression with the lowest AIC was used, indicating that the maximized value of the likelihood upon univariable logistic regression was highest in this model. AIC was lowest for SRD5A1 expression. All other pathways were added one after another, and the combination of two resulting in the lowest AIC was used as input for the next round (if the AIC was lower than the AIC of the previous round). This procedure was repeated until the AIC did not decrease anymore. Using this strategy, a model using SRD5A1 expression, TGFβ pathway activity score, and Notch pathway activity score as input was the most accurate in predicting clinical benefit, with an AUC of 0.81 (95% CI: 0.71–0.91). Using the cut-off value of this model resulting in the highest value of true positive rate minus false positive rate resulted in a sensitivity of 89.5%, a specificity of 63.6%, a PPV of 73.9%, and an NPV of 83.9%. Adding the AR pathway activity score to a regression model containing SRD5A1 expression had no added value.

When only using pathway activity scores (commercially available as composite test), excluding SRD5A1 levels, the model most accurately predicting clinical benefit consisted of AR, Notch, and MAPK pathway activity, with an AUC of 0.73 (95% CI: 0.61–0.84). The addition of HER2 status (determined according to ASCO/CAP guidelines), very commonly assessed in the diagnostic work-up of SDC, on top of the Notch/TGFβ pathway activity score into the model led to an AUC of 0.76 (95% CI: 0.64–0.87). The addition of HER2 status on top of the first model including SRD5A1 expression and Notch and TGFβ pathway activity scores had no added value.

Optimizing cut-offs of AR pathway activity score and SRD5A1 expression to prevent false negatives

In order to assess whether cut-offs for the AR pathway activity score and SRD5A1 expression could be optimized to identify a group of non-responders with minimal false negatives, a loss function was used. This function calculated the total amount of misclassifications for every combination of cut-offs in both scores, penalizing false negatives harder than false positives. By applying cut-offs for the AR pathway activity score and SRD5A1 expression found with this loss function in a subset of the data, these tests together could reach a median sensitivity of 93.3% (IQR: 9.1%) with a specificity of 37.5% (IQR: 19%) (Supplementary Figure S1). Given the prevalence of clinical benefit in the total dataset (53.5%), this sensitivity and specificity corresponded to a PPV of 63.2% and an NPV of 83.0%.

Prognostic value of pathway activity scores

Besides the value of the individual and combinations of pathway activity scores to predict response to ADT, the prognostic value on PFS and OS was assessed for each individual pathway and for SRD5A1 levels. All pathway scores and SRD5A1 expression levels were dichotomized on the median and plotted in a Kaplan–Meier plot, and a second dichotomization based on the cut-offs found in the ROC curve analysis was made for the AR and Notch pathway activity scores and the SRD5A1 expression. Results are summarized in Table 3, Figure 3, and Supplementary Figures 2 and 3 . High AR and Notch pathway activity scores and high SRD5A1 expression were significantly associated with better PFS when using the cut-off based on the ROC analysis optimally separating patients with and without clinical benefit. The median PFS in the groups scoring above and below this threshold was 31 (95% CI: 24–38) vs. 12 (95% CI: 11–13) ($p = <0.001$), respectively, for AR; 31 (95% CI: 24–39) vs. 18 (95% CI: 10–25) ($p = 0.003$), respectively, for Notch; and 47 (95% CI: 32–62) vs. 21 (95% CI: 13–29) ($p = 0.002$), respectively, for SRD5A1 expression (Figure 3 and Table 3). Dichotomization on the median also led to significant differences in PFS in these three scores (AR, Notch, and SRD5A1 expression; Table 3 and Supplementary Figure S2). Additionally, patients with high ER or low HH pathway activity dichotomized on the median also had significantly higher PFS ($p = 0.04$ and $p = 0.007$, respectively; Table 3 and Supplementary Figure S2).

For the prediction of OS, dichotomization on the median did not result in significant differences in survival (Table 3 and Supplementary Figure S3). When cut-offs were based on ROC analysis, only high SRD5A1 expression levels were significantly associated with OS (Figure 3). The median OS was 175 (96–254) weeks for patients scoring above the threshold and 97 (83–111) weeks for patients scoring below the threshold ($p = 0.04$; Table 3 and Figure 3).

Table 3: Prognostic value of pathway activity scores and SRD5A1 expression

Pathway	Median PFS in Weeks [95% CI]		
	Below Median Score	**Above Median Score**	**Difference [1]**
AR	23 [19–28]	36 [24–47]	$p = 0.035$
Notch	24 [19–28]	31 [19–43]	$p = 0.035$
MAPK	30 [20–40]	23 [13–33]	$p = 0.41$
TGFβ	30 [20–41]	23 [17–30]	$p = 0.40$
ER	24 [22–26]	35 [27–43]	$p = 0.039$
HH	30 [18–42]	24 [18.0–30]	$p = 0.007$
PI3K [2]	29 [23–35]	24 [16–32]	$p = 0.995$
SRD5A1	18 [5–31]	38 [34–42]	$p = 0.003$
	Below ROC cut-off	**Above ROC cut-off**	
AR	12 [11–13]	31 [24–38]	$p < 0.001$
Notch	18 [10–25]	31 [24–39]	$p = 0.003$
SRD5A1	21 [13–29]	47 [32–62]	$p = 0.002$
	Median OS in weeks [95% CI]		
	Below median score	**Above median score**	
AR	107 [66–147]	122 [81–163]	$p = 0.57$
Notch	122 [93–151]	112 [15–209]	$p = 0.84$
MAPK	112 [85–139]	126 [76–175]	$p = 0.74$
TGFβ	122 [72–172]	112 [71–154]	$p = 0.27$
ER	126 [87–165]	112 [75–149]	$p = 0.59$
HH	154 [68–241]	107 [83–130]	$p = 0.16$
PI3K[2]	121 [76–167]	105 [93–117]	$p = 0.73$
SRD5A1	97 [83–111]	168 [99–237]	$p = 0.11$
	Below ROC cut-off	**Above ROC cut-off**	
AR	154 [39–270]	112 [82–143]	$p = 0.87$
Notch	126 [85–166]	107 [79–135]	$p = 0.87$
SRD5A1	97 [82–111]	175 [96–254]	$p = 0.04$

1. Log-rank test. 2.PI3K, as the inverse of Forkhead Box-O (FOXO) signaling, in the absence of oxidative stress.

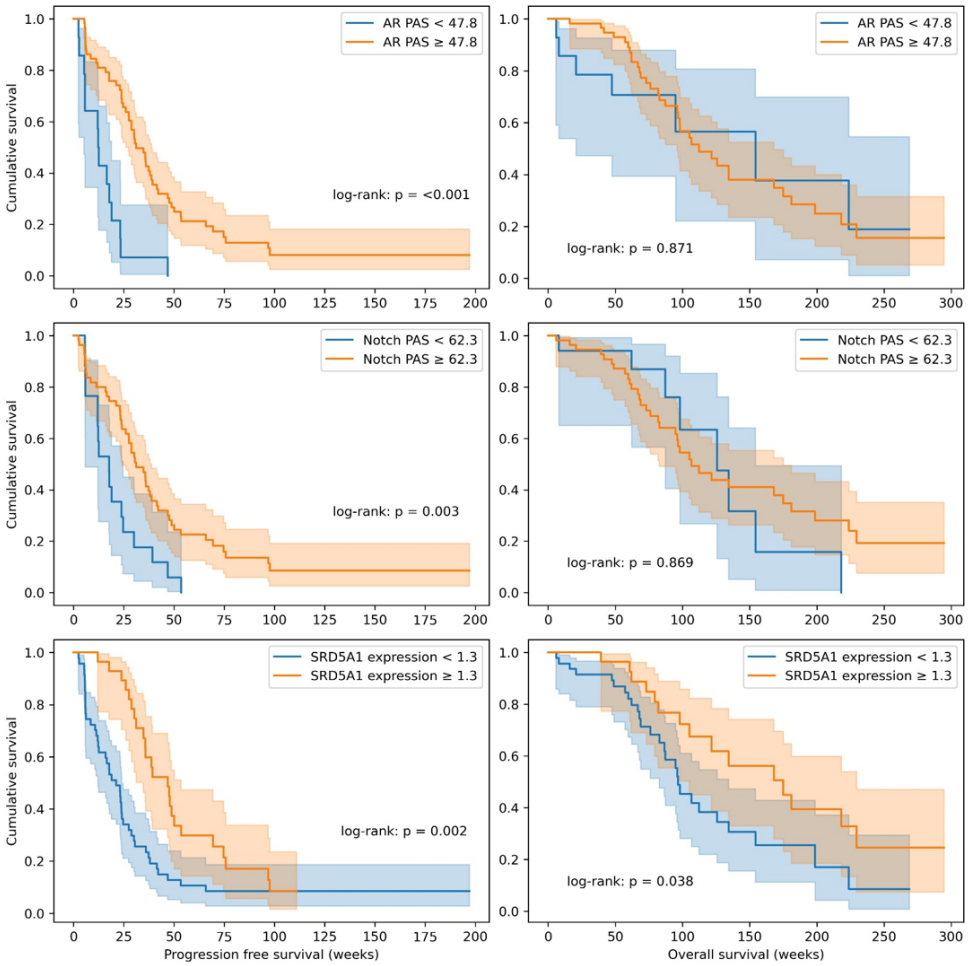

Figure 3: Kaplan–Meier curves of progression-free survival (left) and overall survival (right) for AR (androgen receptor) and Notch pathway activity scores (PAS) and SRD5A1 expression using cut-off values found in the ROC analysis.

Discussion

Patients suffering from R/M SDC, an aggressive AR-positive subtype of SGC, are often treated with agents targeting AR signaling. A significant proportion will, however, not benefit from this treatment (response rates between 18 and 53%), and their prognosis is poor (8). In this study, we aimed to predict the clinical benefit of combined AR blockade in a large cohort of SDC patients, especially focusing on the prediction of non-response (i.e., a test with a high NPV). Thus, the probability of activity of seven tumor-driving pathways and

expression levels of SRD5A1 mRNA were quantified. Of the seven signaling pathways, AR pathway activity was the best predictor of clinical benefit (AUC: 0.66; 95% CI: 0.53–0.79). At a threshold of 47.8, sensitivity was 97.4% and specificity was 38.2%. Using this threshold, 21% of the patients tested below this threshold, with a negative predictive value of 92.9%. SRD5A1 expression had the highest general predictive value for clinical benefit (AUC: 0.78; 95% CI: 0.67–0.88), with a markedly higher specificity compared to the AR pathway activity score (88.6% at optimal cut-off). The NPV of SRD5A1 expression was, however, lower than the AR pathway activity score (66.0% vs. 92.9%). Combining different pathway and gene expression scores in a multivariable model led to the identification of SRD5A1 expression combined with TGFβ and Notch pathway activity as the combination with the highest general predictive value (AUC: 0.81; 95% CI: 0.71–0.91). Besides the prediction of clinical benefit, high AR, Notch, ER, and SRD5A1 scores and a low HH score also predicted PFS. SRD5A1 expression was the only marker that was significantly associated with OS in this cohort (with a median OS of 175 weeks for patients with high SRD5A1 expression and 97 weeks for patients with low expression). The observation that very few markers could predict OS in contrast to PFS can be explained by the fact that the majority of patients received different types of systemic therapies after progressive disease on ADT, possibly influencing OS results.

The predictive and prognostic value of AR pathway activity and SRD5A1 expression were in line with our previous study in a smaller cohort of SDC patients treated with ADT (14). In the latter study, the ROC–AUC was 0.75 for the AR pathway activity score and 0.79 for SRD5A1 expression; the optimal cut-offs, using the same approach as in this study, were 52.9 and 2.75 (corresponding to a log-transformed value of 1.02), respectively. These cut-offs could not formally be validated in this study because both cohorts significantly differed regarding used treatment regimen. In the former study, only 7 out of 30 (23.3%) of the patients received CAB, whilst the remaining patients were only treated with the AR antagonist bicalutamide. This may explain the markedly lower clinical benefit rate (30%) in the work of Van Boxtel et al. versus 51.9% in this study. This is especially important when establishing the most important test metric in clinical practice, the NPV, because it is highly dependent on the prevalence of the outcome of interest in the total population. Though no formal validation could be performed, the findings of this study were in strong agreement with the findings of Van Boxtel et al. The found cut-offs in this study regarding the different tests slightly differed, especially the AR cut-off that was shifted upwards, due to a slightly different assay that was used. These cut-offs were optimized to this cohort of patients and are therefore likely to perform worse in an independent cohort. The validation of these cut-offs is required to robustly assess their predictiveness and enable the routine use of the predictive biomarker test in clinical practice.

The most important unmet clinical need in the management of SDC patients with recurrent or metastatic disease is to accurately identify patients that will not respond to CAB. This

treatment itself has relatively minor toxicities, but SDC has a very poor prognosis, thus emphasizing that losing valuable time on treatments that will not give any clinical benefit would do significant harm (8). The test that performed most optimally in this regard was the AR pathway test (univariable), which, with an NPV of 92.9%, was able to exclude 19.4% of the patients who did not respond to CAB. Using cut-offs for AR and SRD5A1 (optimized to prevent false negatives), a median sensitivity of 93.3% and a median specificity of 37.5% could be reached. Though only a fraction of the total number of non-responders can be identified, precious time is saved for those patients, allowing them to undergo other potentially effective treatments such as chemotherapy or HER2-targeting agents in the case of HER2-positive disease (8). This is valuable information for both the palliative SDC treatment and adjuvant ADT treatment of SDC patients with curative intent.

AR and Notch pathway activity scores and SRD5A1 expression were the only scores that significantly differed between patients with and without clinical benefit from CAB. In this anti-hormonal treatment-naïve cohort, CAB was the first-line treatment in the majority of cases. Hence, there is a sound biological rationale for the AR score to be predictive for response, as a higher AR pathway activity score is based on ligand-dependent transcriptional activation of known AR target genes. Though in our study, a low AR pathway activity score was indicative of the absence of clinical benefit from CAB in the vast majority of cases, a high pathway activity score was not necessarily associated with better clinical benefit in the responders. In that way, a high AR pathway activity score can be considered to be a default state and a prerequisite for response to CAB. This is in line with observations in prostate cancer, which is also highly dependent on AR-signaling for proliferation and progression (27). In prostate cancer, the AR pathway also often remains active in a castration-resistant state, and several studies have shown that AR-dependent resistance mechanisms have evolved (27–29). This is in line with the observation that high expression levels of SRD5A1 are prognostically beneficial and predictive for response to CAB. Steroid 5α-reductase 1, the enzyme encoded by SRD5A1, is involved in the intracellular conversion of testosterone into the more potent androgen, DHT (29). We hypothesize that high levels of SRD5A1 mRNA in SDC tissue are indicative of a high dependency on AR signaling for tumor proliferation, as well as that the deprivation of circulating androgens will hit these tumors hard, resulting in a better prognosis upon CAB treatment. The important role of SRD5A1 in SDC tumor proliferation leads to the hypothesis that blocking this key enzyme in intratumoral steroidogenesis using the 5α-reductase-1 inhibitor dutasteride could be beneficial. Early preclinical work has indicated that, especially in combi-nation with other AR-targeting drugs, dutasteride could be beneficial (14,30,31).

It is surprising that a higher probability of active Notch signaling is both indicative of response to CAB and associated with a better outcome (32). Active Notch signaling can give either tumor suppression or progression, but in adenoid cystic carcinoma (another subtype of

SGC that has a distinct molecular background), activating NOTCH mutations give markedly poorer prognoses (33–36). Besides this, in castration-resistant prostate cancer, Notch signaling contributes to enzalutamide resistance and therefore promotes tumor cell survival. It therefore seems that Notch signaling interacts with AR signaling, and downstream targets of Notch are known to regulate AR. In hormone therapy-naïve patients, high Notch pathway activity scores might therefore just be a proxy for the high activity of AR signaling, although AR and Notch pathway activity scores did not directly correlate in our cohort ($\rho = 0.14$) (37–39). The fact that the addition of AR after Notch signaling and SRD5A1 expression in our multivariable analysis did not add up to the predictiveness of the model also suggests that these two pathways interact in this hormone-naïve SDC cohort. Though NOTCH mutation status was unknown in our cohort, NOTCH1 mutations have previously been described in SDC, and the upregulation of downstream NOTCH target genes has also been previously reported, which indicates that NOTCH signaling might be of importance in SDC (40,41).

One of the strengths of this study was the large number of included patients, given the rarity of SDC, and the fact that all patients received a uniform treatment regimen. Besides this, the wide scope on potential tumor-driving pathways has provided novel insights in SDC tumor biology. However, a limitation of this study was that a control group of patients not receiving CAB in which pathway activities and SRD5A1 status was known was not available. Therefore, the prognostic value of the different biomarkers in non-treated patients remains unknown (42).

The validation of the predictive value of the found cut-offs of the AR pathway activity score, SRD5A1 expression, and the multivariable model is needed, especially since the number of total covariates used for the analysis was rather high for the number of patients, thus bearing the risk of overfitting. Ideally, this would be done in a randomized controlled trial in which biomarker-positive and negative (based on the calculated cut-offs in this study) patients would be treated with and without CAB. The latter could be considered unethical given the expanding body of evidence showing clinical benefit from CAB in SDC patients and the sparsity in other treatment options. Furthermore, the rarity of the disease hampers the large-scale patient accrual that would be required (8,11). Therefore, the best achievable step forward in SDC seems to be the validation of the found cut-offs in an independent, prospectively treated, single-arm cohort.

Conclusions

In conclusion, we present methods to predict clinical benefit for CAB in recurrent and metastatic SDC. SRD5A1 expression analysis could be used to identify patients that will experience clinical benefit from CAB, with a PPV of 85.7%, and AR pathway activity scores could identify patients that will not experience clinical benefit, with an NPV of 93.3. Using AR pathway and SRD5A1 testing in clinical practice could therefore prevent the under- and overtreatment of SDC patients. Additionally, other tumor-driving signaling pathways (Notch and TGFβ) with predictive and prognostic value have been identified. Furthermore, the role of SRD5A1 in CAB response provides a rational basis for designing and conducting a clinical trial to assess the effectiveness of the SRD5A1-inhibitor dutasteride in the treatment of SDC.

References

1. El-Naggar A.K., Chan J.K.C., Grandis J.R., Takata T., Slootweg P.J. WHO classification of head and neck tumours, 4th edition. Lyon: IARC; 2017.
2. Boon E, Bel M, van Boxtel W, van der Graaf WTA, van Es RJJ, Eerenstein SEJ, et al. A clinicopathological study and prognostic factor analysis of 177 salivary duct carcinoma patients from The Netherlands. International journal of cancer. 2018;143(4):758-66.
3. Otsuka K, Imanishi Y, Tada Y, Kawakita D, Kano S, Tsukahara K, et al. Clinical Outcomes and Prognostic Factors for Salivary Duct Carcinoma: A Multi-Institutional Analysis of 141 Patients. Annals of surgical oncology. 2016;23(6):2038-45.
4. Nakaguro M, Tada Y, Faquin WC, Sadow PM, Wirth LJ, Nagao T. Salivary duct carcinoma: Updates in histology, cytology, molecular biology, and treatment. Cancer cytopathology. 2020;128(10):693-703.
5. Boon E, van Boxtel W, Buter J, Baatenburg de Jong RJ, van Es RJJ, Bel M, et al. Androgen deprivation therapy for androgen receptor-positive advanced salivary duct carcinoma: A nationwide case series of 35 patients in The Netherlands. Head & neck. 2018;40(3):605-13.
6. Lassche G, van Boxtel W, Ligtenberg MJL, van Engen-van Grunsven ACH, van Herpen CML. Advances and challenges in precision medicine in salivary gland cancer. Cancer Treat Rev. 2019;80:101906.
7. Schmitt NC, Kang H, Sharma A. Salivary duct carcinoma: An aggressive salivary gland malignancy with opportunities for targeted therapy. Oral oncology. 2017;74:40-8.
8. Uijen MJM, Lassche G, van Engen-van Grunsven ACH, Tada Y, Verhaegh GW, Schalken JA, et al. Systemic therapy in the management of recurrent or metastatic salivary duct carcinoma: A systematic review. Cancer Treat Rev. 2020;89:102069.
9. Takahashi H, Tada Y, Saotome T, Akazawa K, Ojiri H, Fushimi C, et al. Phase II Trial of Trastuzumab and Docetaxel in Patients With Human Epidermal Growth Factor Receptor 2-Positive Salivary Duct Carcinoma. Journal of clinical oncology : official journal of the American Society of Clinical Oncology. 2019;37(2):125-34.
10. Cornford P, van den Bergh RCN, Briers E, den Broeck TV, Cumberbatch MG, De Santis M, et al. EAU-EANM-ESTRO-ESUR-SIOG Guidelines on Prostate Cancer. Part II-2020 Update: Treatment of Relapsing and Metastatic Prostate Cancer. Eur Urol. 2020.
11. Fushimi C, Tada Y, Takahashi H, Nagao T, Ojiri H, Masubuchi T, et al. A prospective phase II study of combined androgen blockade in patients with androgen receptor-positive metastatic or locally advanced unresectable salivary gland carcinoma. Annals of oncology : official journal of the European Society for Medical Oncology. 2018;29(4):979-84.
12. Locati LD, Perrone F, Cortelazzi B, Lo Vullo S, Bossi P, Dagrada G, et al. Clinical activity of androgen deprivation therapy in patients with metastatic/relapsed androgen receptor-positive salivary gland cancers. Head & neck. 2016;38(5):724-31.
13. Viscuse PV, Price KA, Garcia JJ, Schembri-Wismayer DJ, Chintakuntlawar AV. First Line Androgen Deprivation Therapy vs. Chemotherapy for Patients With Androgen Receptor Positive Recurrent or Metastatic Salivary Gland Carcinoma-A Retrospective Study. Frontiers in oncology. 2019;9:701.
14. van Boxtel W, Verhaegh GW, van Engen-van Grunsven IA, van Strijp D, Kroeze LI, Ligtenberg

MJ, et al. Prediction of clinical benefit from androgen deprivation therapy in salivary duct carcinoma patients. International journal of cancer. 2020;146(11):3196-206.

15. van de Stolpe A, Holtzer L, van Ooijen H, Inda MA, Verhaegh W. Enabling precision medicine by unravelling disease pathophysiology: quantifying signal transduction pathway activity across cell and tissue types. Sci Rep. 2019;9(1):1603.
16. Wolff AC, Hammond MEH, Allison KH, Harvey BE, Mangu PB, Bartlett JMS, et al. Human Epidermal Growth Factor Receptor 2 Testing in Breast Cancer: American Society of Clinical Oncology/College of American Pathologists Clinical Practice Guideline Focused Update. Journal of Clinical Oncology. 2018;36(20):2105-22.
17. van de Stolpe A, Verhaegh W, Blay JY, Ma CX, Pauwels P, Pegram M, et al. RNA Based Approaches to Profile Oncogenic Pathways From Low Quantity Samples to Drive Precision Oncology Strategies. Front Genet. 2020;11:598118.
18. van Ooijen H, Hornsveld M, Dam-de Veen C, Velter R, Dou M, Verhaegh W, et al. Assessment of Functional Phosphatidylinositol 3-Kinase Pathway Activity in Cancer Tissue Using Forkhead Box-O Target Gene Expression in a Knowledge-Based Computational Model. Am J Pathol. 2018;188(9):1956-72.
19. Verhaegh W, van Ooijen H, Inda MA, Hatzis P, Versteeg R, Smid M, et al. Selection of personalized patient therapy through the use of knowledge-based computational models that identify tumor-driving signal transduction pathways. Cancer Res. 2014;74(11):2936-45.
20. Canté-Barrett K, Holtzer L, van Ooijen H, Hagelaar R, Cordo V, Verhaegh W, et al. A Molecular Test for Quantifying Functional Notch Signaling Pathway Activity in Human Cancer. Cancers (Basel). 2020;12(11).
21. Inda MA, Blok EJ, Kuppen PJK, Charehbili A, den Biezen-Timmermans EC, van Brussel A, et al. Estrogen Receptor Pathway Activity Score to Predict Clinical Response or Resistance to Neoadjuvant Endocrine Therapy in Primary Breast Cancer. Mol Cancer Ther. 2020;19(2):680-9.
22. Sieuwerts AM, Inda MA, Smid M, van Ooijen H, van de Stolpe A, Martens JWM, et al. ER and PI3K Pathway Activity in Primary ER Positive Breast Cancer Is Associated with Progression-Free Survival of Metastatic Patients under First-Line Tamoxifen. Cancers (Basel). 2020;12(4).
23. van de Stolpe A. Quantitative Measurement of Functional Activity of the PI3K Signaling Pathway in Cancer. Cancers (Basel). 2019;11(3).
24. van Lieshout L, van de Stolpe A, van der Ploeg P, Bowtell D, de Hullu J, Piek J. Signal Transduction Pathway Activity in High-Grade, Serous Ovarian Carcinoma Reveals a More Favorable Prognosis in Tumors with Low PI3K and High NF-κB Pathway Activity: A Novel Approach to a Long-Standing Enigma. Cancers (Basel). 2020;12(9).
25. van Weelden WJ, van der Putten LJM, Inda MA, van Brussel A, Snijders M, Schriever LMM, et al. Oestrogen receptor pathway activity is associated with outcome in endometrial cancer. British journal of cancer. 2020;123(5):785-92.
26. Akaike H. A new look at the statistical model identification. IEEE transactions on automatic control. 1974;19(6):716-23.
27. Heinlein CA, Chang C. Androgen receptor in prostate cancer. Endocr Rev. 2004;25(2):276-308.
28. Chandrasekar T, Yang JC, Gao AC, Evans CP. Mechanisms of resistance in castration-resistant prostate cancer (CRPC). Transl Androl Urol. 2015;4(3):365-80.
29. Watson PA, Arora VK, Sawyers CL. Emerging mechanisms of resistance to androgen receptor

inhibitors in prostate cancer. Nat Rev Cancer. 2015;15(12):701-11.

30. Hamid AR, Verhaegh GW, Smit FP, van Rijt-van de Westerlo C, Armandari I, Brandt A, et al. Dutasteride and enzalutamide synergistically suppress prostate tumor cell proliferation. J Urol. 2015;193(3):1023-9.

31. Orozco M, Valdez RA, Ramos L, Cabeza M, Segovia J, Romano MC. Dutasteride combined with androgen receptor antagonists inhibit glioblastoma U87 cell metabolism, proliferation, and invasion capacity: Androgen regulation. Steroids. 2020;164:108733.

32. Lassche G, van Boxtel W, Ligtenberg MJL, van Engen-van Grunsven ACH, van Herpen CML. Advances and challenges in precision medicine in salivary gland cancer. Cancer Treatment Reviews.

33. Ferrarotto R, Mitani Y, Diao L, Guijarro I, Wang J, Zweidler-McKay P, et al. Activating NOTCH1 Mutations Define a Distinct Subgroup of Patients With Adenoid Cystic Carcinoma Who Have Poor Prognosis, Propensity to Bone and Liver Metastasis, and Potential Responsiveness to Notch1 Inhibitors. Journal of clinical oncology : official journal of the American Society of Clinical Oncology. 2017;35(3):352-60.

34. Ho AS, Ochoa A, Jayakumaran G, Zehir A, Valero Mayor C, Tepe J, et al. Genetic hallmarks of recurrent/metastatic adenoid cystic carcinoma. J Clin Invest. 2019;129(10):4276-89.

35. Bray SJ. Notch signalling in context. Nat Rev Mol Cell Biol. 2016;17(11):722-35.

36. Ferrarotto R, Mitani Y, McGrail DJ, Li K, Karpinets TV, Bell D, et al. Proteogenomic Analysis of Salivary Adenoid Cystic Carcinomas Defines Molecular Subtypes and Identifies Therapeutic Targets. Clinical cancer research : an official journal of the American Association for Cancer Research. 2021;27(3):852-64.

37. Aldahl J, Yu EJ, He Y, Hooker E, Wong M, Le V, et al. A pivotal role of androgen signaling in Notch-responsive cells in prostate development, maturation, and regeneration. Differentiation. 2019;107:1-10.

38. Farah E, Li C, Cheng L, Kong Y, Lanman NA, Pascuzzi P, et al. NOTCH signaling is activated in and contributes to resistance in enzalutamide-resistant prostate cancer cells. J Biol Chem. 2019;294(21):8543-54.

39. Bai S, Cao S, Jin L, Kobelski M, Schouest B, Wang X, et al. A positive role of c-Myc in regulating androgen receptor and its splice variants in prostate cancer. Oncogene. 2019;38(25):4977-89.

40. Alame M, Cornillot E, Cacheux V, Tosato G, Four M, De Oliveira L, et al. The molecular landscape and microenvironment of salivary duct carcinoma reveal new therapeutic opportunities. Theranostics. 2020;10(10):4383-94.

41. Gargano SM, Senarathne W, Feldman R, Florento E, Stafford P, Swensen J, et al. Novel therapeutic targets in salivary duct carcinoma uncovered by comprehensive molecular profiling. Cancer Med. 2019;8(17):7322-9.

42. Ballman KV. Biomarker: Predictive or Prognostic? Journal of clinical oncology : official journal of the American Society of Clinical Oncology. 2015;33(33):3968-71.

Supplementary information

Supplementary file 1: Comparison of the AR pathway assay used by *Van Boxtel et.al.* comparted to a further optimized assay.

Compared to the study by Van Boxtel *et al.*, the target gene PCR amplification reactions and the subsequent algorithm for calculating the AR pathway activity score have been slightly modified (14). The average AR pathway activity score was 55.3 (standard deviation: 8.8) when the new algorithm was applied and 47.5 (standard deviation: 8.5) for the old algorithm. Although, an upward shift in mean AR pathway activity score was seen with the new algorithm, data obtained with both algorithms showed a very strong correlation (ρ=0.90, Figure 1). In addition, AR pathway activity score values calculated with the old algorithm showed a strong overlap in range (26.5-67.6) with the AR pathway activity score values in the study published by *Van Boxtel et al.* (33.1-65.6). For all subsequent analyses in this paper, the optimized assay and subsequently derived AR PAS was used, as this was in concordance with the algorithms used for the other pathways.

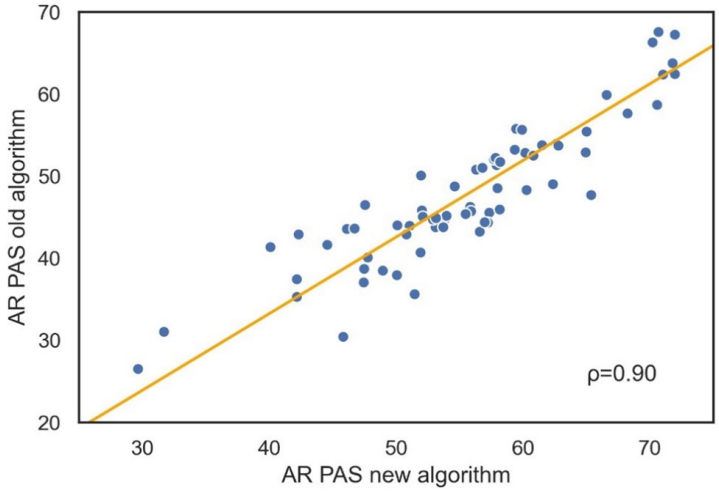

Supplementary File 1 Figure 1: Scatterplot of androgen receptor (AR) pathway activity score (PAS) calculated with two different algorithms, the AR PAS on the x-axis was used in this study, and the AR PAS on the y-axis was used in ref. 14 (Van Boxtel et al.). Regression line was fitted using Deming regression.

Supplementary Table 1: primer pairs used for *SRD5A1* expression quantification

Gene name	Primer Sequences (5' -> 3')	Amplicon size (basepairs)
SRD5A1	AGGAATCTCAGAAAACCAGGAGA	78
	GTTGGCTGCAGTTACGTATTCA	
HPRT1	CTGGAAAGAATGTCTTGATTGTGG	78
	GCCTGACCAAGGAAAGCAAAG	

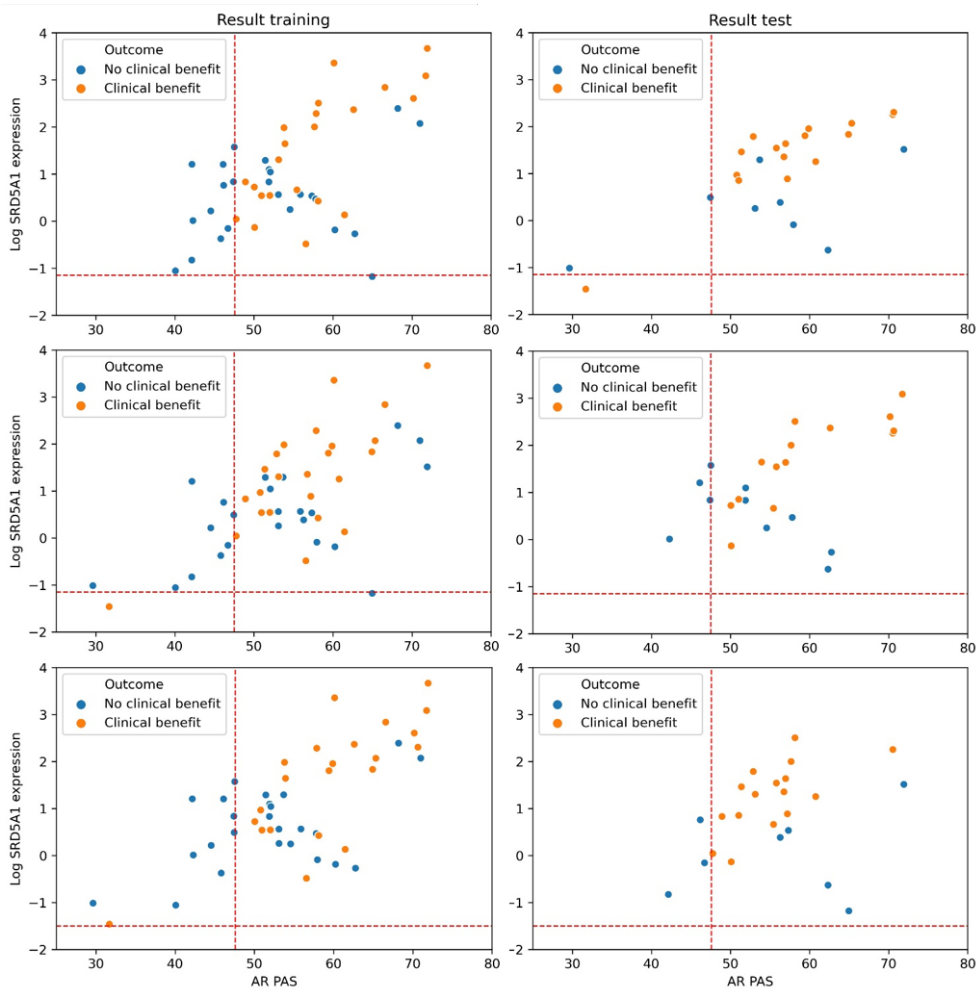

Supplementary Figure 1: Examples of the result of identification of cut-offs for androgen receptor (AR) pathway activity score (PAS) and *SRD5A1* expression using a loss function optimized towards identification of patients without clinical benefit. Cut-offs were calculated on a training set (left images), random sampling two-third of the total dataset and tested on the remaining one-third of the data (right images).

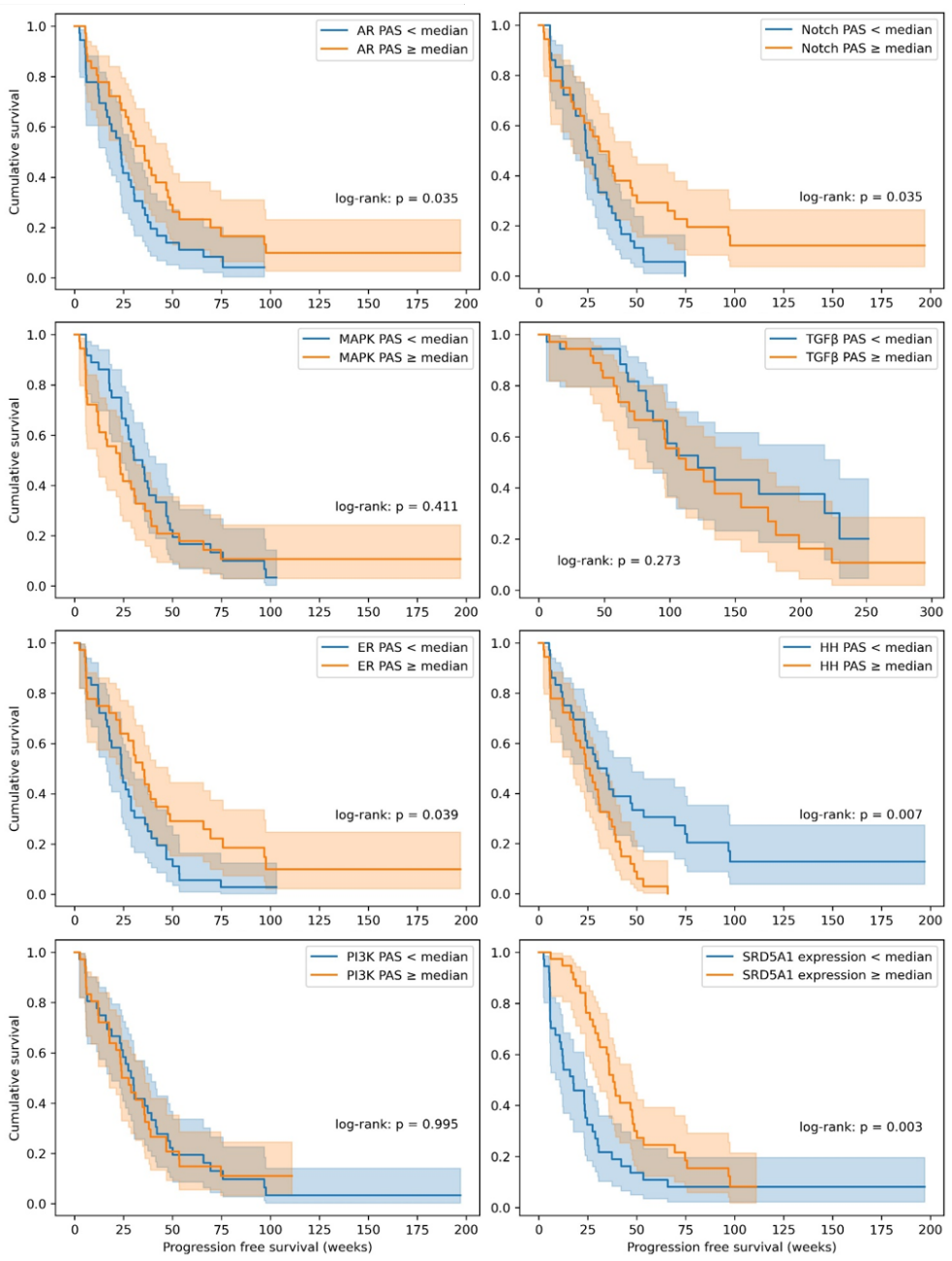

Supplementary Figure 2: Kaplan-Meier curves of progression-free survival for AR, Notch, MAPK, TGFβ, ER, HH, PI3K pathway activity scores (PAS) and *SRD5A1* expression, using median values as a cut-off.

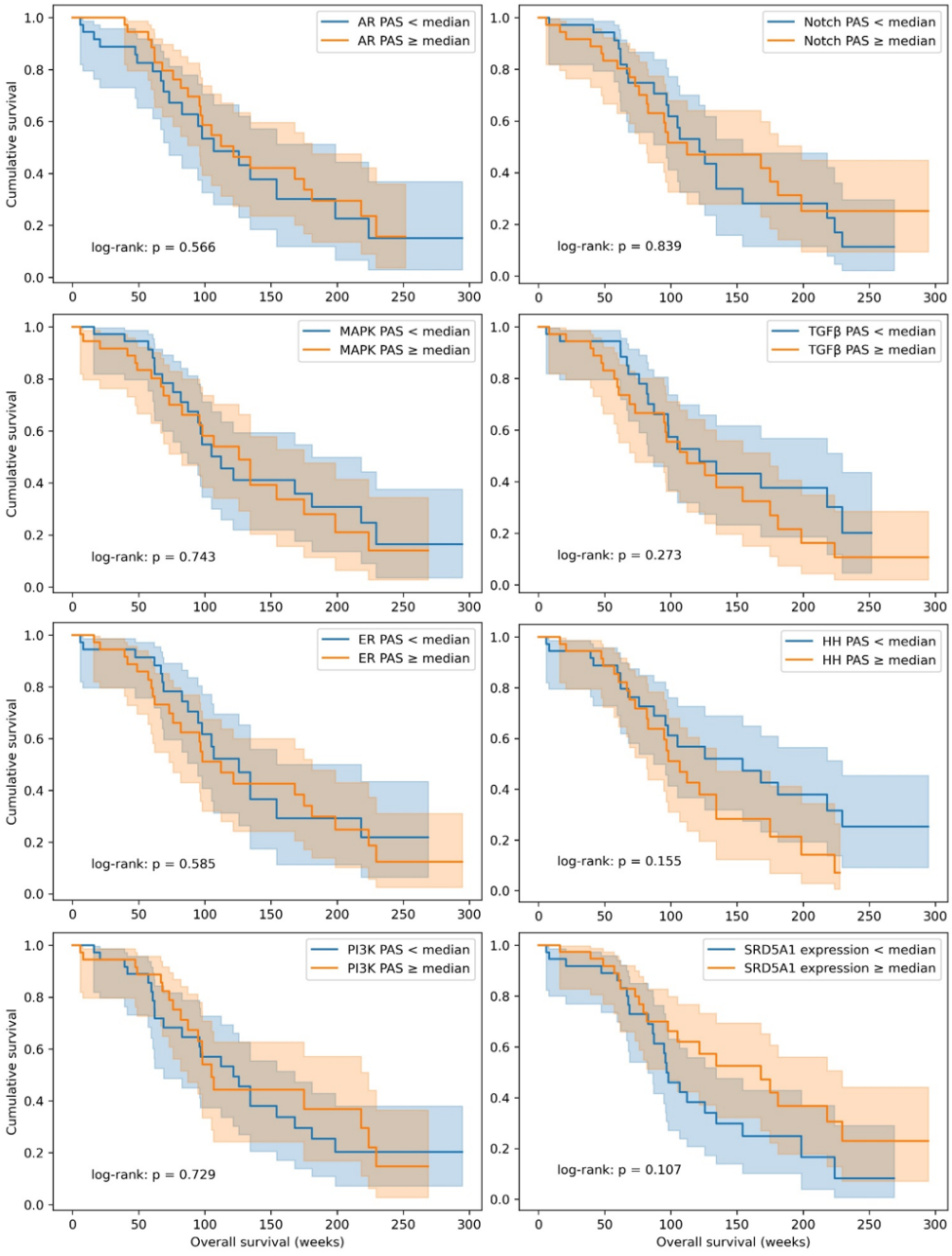

Supplementary Figure 3: Kaplan-Meier curves of overall survival for AR, Notch, MAPK, TGFβ, ER, HH, PI3K pathway activity scores (PAS) and SRD5A1 expression, using median values as a cut-off.

CHAPTER 5

Case series of docetaxel, trastuzumab, and pertuzumab (DTP) as first line anti-HER2 therapy and ado-trastuzumab emtansine (T-DM1) as second line for recurrent or metastatic HER2-positive salivary duct carcinoma

Maike J.M. Uijen*, Gerben Lassche*, Adriana C.H. van Engen-van Grunsven, Chantal M.L. Driessen, Carla M.L. van Herpen

* These authors contributed equally

Oral Oncoloyg 2022;125:105703

Abstract

Objective

Salivary duct carcinoma (SDC) overexpresses Human Epidermal growth factor Receptor 2 (HER2) in 29-46% of cases, favouring anti-HER2 therapy. Here, we present the results of patients with recurrent or metastatic HER2-positive SDC treated with docetaxel, trastuzumab, and pertuzumab (DTP) as first-line anti-HER2 therapy and subsequently ado-trastuzumab emtansine (T-DM1) in second-line. Furthermore, we searched for potential biomarkers.

Methods

Retrospective case series from a tertiary hospital. First-line anti-HER2 treatment consisted of DTP, after progression T-DM1 was considered for patients with an adequate performance status. Objective response rate (ORR), progression-free survival (PFS) and overall survival (OS) were assessed and related to mRNA-based PI3K and MAPK signalling pathway activity scores.

Results

Thirteen SDC HER2+ patients received DTP. In twelve evaluable patients, one complete response (CR) and six partial responses (PR) were observed (ORR 58%), with a median PFS of 6.9 months (95%-CI 5.3-8.5). Seven patients received subsequent T-DM1 in second-line, resulting in four PR (ORR 57%), with a median PFS of 4.4 months (95%-CI 0-18.8). Median OS after start of DTP was 42.0 months (95%-CI 13.8-70.1). Grade ≥3 toxicity on DTP was seen in 39% of patients, and 14% on T-DM1. Highest combined PI3K and MAPK signalling was seen in the patient with CR and lowest in the patient with progressive disease on DTP.

Conclusion

In R/M HER2-positive SDC patients DTP followed by T-DM1 upon progression are promising treatments, leading to responses in the majority (58%) of the patients at an acceptable toxicity profile.

Introduction

Salivary duct carcinoma (SDC) is an aggressive subtype of salivary gland cancer. It was first described by Kleinsasser *et al.* in 1968 as histologically highly similar to ductal carcinoma of the breast, and recently the resemblance of SDC to apocrine breast cancer has also been recognized regarding genetic background (1, 2). SDC most often occurs in the parotid gland, but it can also originate in other salivary glands in the head and neck region. Primary treatment consists of surgery, which is often combined with a lymph node neck dissection due to the high rates (49-72% of patients) of extensive lymph node involvement. Surgery is regularly followed by postoperative radiotherapy, and in a retrospective case control study with androgen receptor (AR) positive SDC (67-97% expresses AR) adjuvant androgen deprivation therapy (ADT) showed to be possibly effective, but it is not standard, yet (3). The prognosis of SDC is negatively affected by the high rates of distant metastases, and approximately half of the patients diagnosed with SDC are faced with metastatic disease during their disease course, with a median time of 16 months until the occurrence of distant metastases (4). This results in poor survival rates, with a median overall survival (OS) ranging between 48 to 79 months from diagnosis (4-6), and only 5 months in recurrent or metastatic disease when best supportive care is given (7).

In the case of recurrent and/or metastatic (R/M) disease, both androgen deprivation therapy and chemotherapy have previously shown clinical activity, with objective responses ranging from 18-53% and 10-50%, respectively (7-13). Additionally, 29-46% of the SDC tumours overexpress the Human Epidermal growth factor Receptor 2 (HER2), which could serve as a key to targeted therapy (4, 14, 15).

The transmembrane protein HER2 is a member of the epidermal growth factor receptor family and its overexpression is widely recognized to play a critical role in the initiation and maintenance of several malignancies, including SDC. HER2 dimerization leads to the activation of a complex interplay of several signal transduction cascades, which include the important PI3K/AKT/mTOR and RAS/RAF/MEK/ERK (MAPK) cascades (16-18). Currently, a wide palette of therapies aiming to interrupt this signalling exists, targeting at several levels. Small molecule tyrosine kinase inhibitors targeting the receptor pathway (e.g. lapatinib) are available as are agents inhibiting more downstream signalling. Most used are however monoclonal antibodies that upon binding to HER2 uncouple or block dimerization and thereby disrupt initiation of the signalling cascades, besides triggering antibody-dependent cell-mediated cytotoxicity. These include trastuzumab and pertuzumab, which both bind to different epitopes on HER2 and could therefore have synergistic effects (17, 18).

The efficiency of these HER2-targeted therapies has been investigated extensively in HER2-positive breast cancer, following the favourable results of chemotherapy and trastuzumab, and the addition of pertuzumab has shown even better outcomes. In a phase III study, progression-free survival (PFS) was 18.5 months (OS: 56.5 months) for the group with the addition of pertuzumab, compared to 12.4 months (OS: 40.8 months) for the control group (docetaxel, trastuzumab, placebo) (19, 20). In breast cancer, second-line HER2 targeted therapy with ado-trastuzumab emtansine (T-DM1) is available for patients who progressed on first-line HER2 targeted therapy, following the results of a phase III study in which objective responses were observed in 43.6% of the cases (21).

In SDC, agents targeting the HER2 pathway have shown impressive response rates (4, 14, 15). In the prospective phase II study of Takahashi *et al.,* 57 HER2-positive R/M SDC patients were treated with docetaxel and trastuzumab, which resulted in objective responses in 70% of the patients and a median PFS and OS of 8.9 and 39.7 months (22), respectively. However, in SDC patients, literature is scarce on the effects of the possible synergistic combination of docetaxel, trastuzumab, and pertuzumab (DTP) and subsequent T-DM1, that is used in breast cancer patients. Existing literature on these treatments mainly consist of case reports (23-28).

In this paper we therefore describe the results of SDC patients treated with DTP as first-line anti-HER2 therapy and T-DM1 in second-line in our tertiary referral hospital specialized in salivary gland cancer in the Netherlands. Besides this, we provide a preliminary analysis of possible biomarkers predicting response to these HER2 targeting agents, based on quantification of PI3K and MAPK pathway activities.

Methods

Patients

All HER2-positive SDC patients that were treated with DTP as first-line anti-HER2 therapy (and followed with T-DM1 in second-line in part of patients) at the Radboud University Medical Centre (a tertiary centre for recurrent and metastatic salivary gland cancer in the Netherlands), were retrospectively identified for this retrospective case-series. According to Dutch law, a review by a medical ethical committee was not required due to the retrospective nature of this research.

HER2 status

HER2 status was assessed a combination of immunohistochemistry (IHC) and in situ hybridization (ISH) and interpreted following the guidelines for HER2 assessment in breast cancer (29, 30). For IHC the HercepTest (Dako Agilent) was used (including a rabbit

anti-human HER2 monoclonal antibody). An experienced pathologist scored the staining intensity which ranged from 0 (no immunoreactivity) to 3+ (strong immunoreactivity in >10% of tumour cells). Fluorescence in situ hybridization (FISH) was performed with dual ERBB2 FISH probes (Z-2077-200; ZytoVision or KB-00007; Leica). An HER2-CEP17 ratio was calculated, tumours with a ratio of >2 were considered to be amplified.

Treatment

DTP consisted of the combination docetaxel, trastuzumab, and pertuzumab, administered every 3 weeks. After 6 dosages of docetaxel (75mg/m2), patients continued the combination of trastuzumab and pertuzumab until disease progression or intolerable toxicity. In the case of docetaxel-related toxicity, the dose of docetaxel could be reduced. Trastuzumab was given either intravenously (i.v., starting dose 8 mg/kg, with subsequent dosages of 6 mg/kg) or subcutaneously (s.c., 600mg). The starting dose of pertuzumab consisted of 840 mg with subsequent dosages of 420 mg, intravenously. Termination of treatment was at the discretion of the treating physician. In some cases, the treatment could have been continued despite progression according to Response Evaluation Criteria in Solid Tumours (RECIST) criteria (e.g. in case of the ongoing response of target lesions despite the occurrence of a new metastatic lesion).

After DTP treatment, second-line HER2 targeted therapy consisting of ado-trastuzumab emtansine (T-DM1) was considered for patients with an adequate performance status (Karnofsky ≥70). T-DM1 treatment consisted of 3.6 mg/kg intravenously, every 3 weeks. The dose could be adjusted in case of toxicity. T-DM1 was continued until disease progression or intolerable toxicity.

For both treatments, patients were evaluated approximately every 3 months, consisting of MR-scanning or CT of the head and neck area (in case of local recurrence or brain metastases) and CT-scan of the chest and abdomen. Patients could receive local treatment during or in between DTP or T-DM1 therapy, including stereotactic brain radiotherapy in case of brain metastases.

Outcomes

Treatment evaluation was performed according to the RECIST version 1.1 (31). Objective response rate (ORR) was defined as complete response (CR) or partial response (PR). Other response categories were stable disease (SD) and progressive disease (PD). Progression-free survival (PFS) was defined as the time between the start of HER2 targeted therapy and disease progression or death. Overall survival (OS) was defined as the time between the start of HER2 targeted therapy until the death of any cause or lost follow-up. Time on treatment was defined as the time between the start of HER2 targeted therapy and the last administration of that

treatment. Furthermore, treatment-related adverse events were retrospectively identified from medical files. Adverse events were scored according to the Common Terminology Criteria for Adverse Events, version 5.0 (32).

Signalling pathway activity quantification

If residual tumour tissue from regular diagnostics prior to DTP initiation was available, three 10 μm slices of formalin-fixated paraffin-embedded (FFPE) material were collected. These slices were annotated for the presence of tumour material on an adjacent haematoxylin and eosin slide. RNA was extracted using VERSANT Tissue Preparation Reagents kit (Siemens, Munich, Germany) according to the manufacturer's instructions. The Philips pathway activity profiling OncoSignal test (Philips Molecular Pathway Diagnostics, Eindhoven, The Netherlands, model version O4.4) was used to quantify the Phosphoinositide 3-Kinase pathway (PI3K, as the inverse of Forkhead Box-O (FOXO) signalling) and Mitogen-Activated Protein Kinase pathway (MAPK) activities. If enough RNA was available Androgen Receptor pathway (AR), Notch signalling pathway (Notch), Transforming Growth Factor beta signalling pathway (TGFβ), Estrogen Receptor pathway (ER) and Hedgehog signalling pathway (HH) activities were also quantified. For each of these pathways, output of this test is the odds of the transcription complex of this pathway being active vs. not active, expressed on a logarithmic scale and scaled to range from 0-100. This approach has previously been published and is validated in several tissue types for different pathways, which include AR pathway activity in SDC (33-37).

As both the PI3K and MAPK pathway are downstream signalling cascades for activated HER2 receptors, a composite metric of these two activity scores was used, defined as the sum of PI3K and MAPK scores.

Statistical analysis

Descriptive measures were summarized as medians with their respective ranges (minimum and maximum). Survival curves using Kaplan-Meier estimates were constructed, for OS and for PFS on both therapies. Kaplan-Meier curves were made for the entire cohort and after dichotomization was made using the median PI3K/MAPK scores. Using the Kaplan-Meier estimates, median survival with 95% confidence intervals (CI) were estimated. A log-rank test was performed to compare differences in survival. Analyses were performed in SPSS version 25. Graphical work was created using Python version 3.8 with Matplotlib, Pandas, Numpy, Seaborn and Lifelines packages and R Studio version 3.5.3.

Results

Patient characteristics

In total 13 patients received DTP as first-line anti-HER2 therapy and 7 patients T-DM1 as second-line. The first HER2-positive SDC patient started with DTP in 2015. The median age at the start of DTP therapy was 61 years (range 48-75). The majority of patients was male (77%). Most often the SDC tumour occurred in the parotid gland (92%), only in one patient (8%) the primary tumour was located in the submandibular gland. HER2 status was assessed on the primary tumour in 8/13 patients and on metastatic tissue in 5/13 patients. IHC staining intensity ranged from 2+ to 3+. All patients had HER2 amplified SDC tumours assessed with FISH. In addition, the tumours of all 13 patients were AR-positive. Prior systemic therapy included adjuvant ADT (23%), palliative ADT (46%) and chemotherapy (8%) (table 2). Additional information on baseline patient characteristics is listed in table 1. Median duration of follow-up, from start of DTP to current analysis, was 15.4 months (range: 5.5-55.0). Last data for this study was collected on 27 July 2021. Figure 1 graphically summarizes treatment and response information per individual patient.

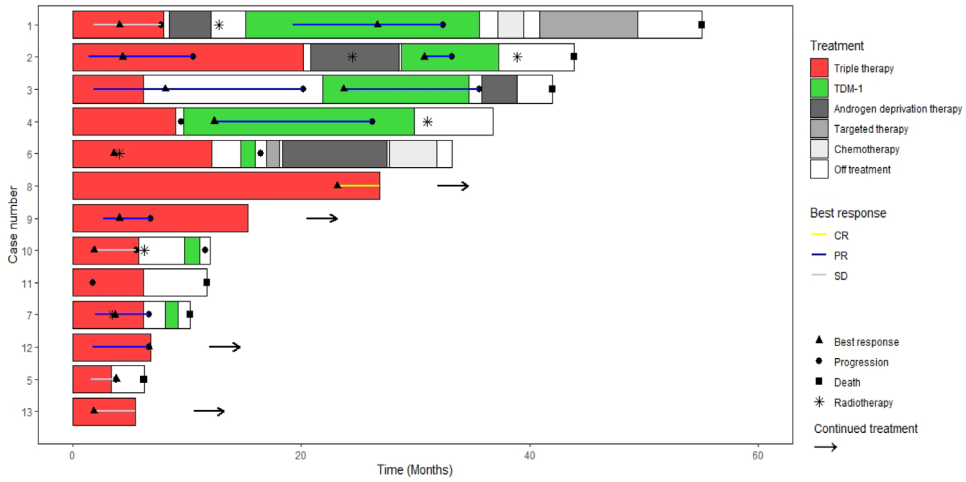

Figure 1: Swimmers plot, graphically summarizing treatment and response information per individual case.

Table 1: Baseline patient characteristics before start of HER2 targeted therapy

Patient No.	Age	Gender	Primary tumour	Prior treatments	Disease distribution	Sites of DM	HER2 status assessed on	HER2 IHC	HER2 FISH	AR IHC ‡
1	48	F	Parotid gland	Surgery + PORT	DM	Lung	Primary tumour	3+	amplified	positive
2	64	M	Parotid gland	Surgery + PORT Palliative ADT	DM	Lung, liver, lymph node	Primary tumour	3+	amplified	positive
3	54	M	Parotid gland	Surgery + PORT Palliative ADT	DM	Lung, liver, bone	Bone metastasis	3+	amplified	positive
4	59	M	Parotid gland	Surgery Palliative ADT	DM	Brain, bone, lymph node	Primary tumour	2-3+	amplified	positive
5	54	F	Parotid gland	Palliative ADT	LR + DM	Lung, liver, lymph node	Liver metastasis	2-3+	amplified	positive
6	51	M	Parotid gland	-	LR	-	Primary tumour	2-3+	amplified	positive
7	55	M	Parotid gland	Surgery	DM	Brain, lung, lymph node	Lung metastasis	3+	amplified	positive
8	66	F	Parotid gland	Surgery + PORT Adjuvant ADT	DM	Lung	Primary tumour	3+	amplified	positive
9	75	M	Submandibular gland	Surgery + PORT Adjuvant ADT	DM	Lung, lymph node	Primary tumour	3+	amplified	positive
10	64	M	Parotid gland	Palliative chemo† Palliative ADT	LR + DM	Lymph node	Lymph node metastasis	3+	amplified	positive
11	61	M	Parotid gland	Surgery + PORT Adjuvant ADT	DM	Liver	Liver metastasis	2-3+	amplified	positive
12	62	M	Parotid gland	Surgery + PORT Palliative Rx	LR + DM	Lymph node, brain	Primary tumour	3+	amplified	positive
13	67	M	Parotid gland	Surgery+ PORT Palliative ADT	LR + DM	Lung, pancreas	Primary tumour	3+	amplified	positive

ADT: androgen deprivation therapy, AR: androgen receptor, DM: distant metastases, F: female, FISH: fluorescence in situ hybridization, IHC: immunohistochemistry, LR: locoregional disease, M: male, PORT: Postoperative radiotherapy, Rx: radiotherapy.

†Cisplatin, etoposide and ifosfamide.

‡ AR status was assessed by an experienced pathologist through immunohistochemistry in routine clinical practice.

DTP therapy

All 13 patients received DTP, with a median duration of treatment of 6.9 months (range 3.4-26.8+). Six patients (46%) required a dose reduction of docetaxel during DTP treatment. Of the 13 patients, two patients consistently received trastuzumab i.v., seven patients consistently received trastuzumab s.c. and four patients have received trastuzumab both i.v. and s.c. during their treatment. Twelve patients were RECIST evaluable (one patient did not have target lesions). The ORR was 58%, 1 CR (8%) and 6 PR (50%). Furthermore, 4 patients (33%) had stable disease (SD) of which only one patient had SD with a response duration of >6 months (table 2). At the time of this report, four patients are still on DTP therapy. Median overall survival (calculated using Kaplan-Meier estimates) was 42.0 (95%-CI 13.8-70.1 months) after start of DTP (figure 2A). Median PFS on DTP was 6.9 months (95%-CI 5.2-8.5) (figure 2B). Three patients with brain metastases received DTP. All these patients received radiation therapy on the brain metastases prior to the start of DTP. The brain metastases of two patients showed a significant reduction in size over time; after the second treatment evaluation (several months after the start of DTP), the brain metastases decreased further than shown on the first treatment evaluation. In one other patient new brain metastases were detected on the second treatment evaluation scans.

T-DM1 therapy

Seven patients received T-DM1 after DTP therapy. The median time on treatment was 8.5 months (range 1.1-20.4). During T-DM1 treatment, three patients (43%) required a dose reduction. T-DM1 resulted in an ORR of 57%, 4 PR (57%), see table 2. The three other patients (43%) had progressive disease (PD) as best response. In figure 3 the response of a patient with pulmonary metastases on T-DM1 is visualized. Median PFS on T-DM1 after progression on DTP was 4.4 months (95%-CI 0-18.8) (figure 2C). Two patients with brain metastases received second-line T-DM1, one of these patients died before the first treatment evaluation, in the other patient a reduction in tumour size of the brain metastasis was observed (PR).

Table 2: Response to HER2 targeted therapy

Patient No.	First-line HER2 targeted treatment (DTP therapy)	Best response	Best percentage change in target lesions	Duration of response	Second-line HER2 targeted Treatment (T-DM1)	Best response	Best percentage change in target lesions	Duration of response
1	Docetaxel + trastuzumab + pertuzumab	SD	-17%	7.7 mo	T-DM1	PR	-78%	17.3 mo
2	Docetaxel + trastuzumab + pertuzumab	PR	-62%	10.6 mo	T-DM1	PR	-32%	4.4 mo
3	Docetaxel + trastuzumab + pertuzumab	PR	-100%	20.2 mo	T-DM1	PR	-42%	13.7 mo
4	Docetaxel + trastuzumab + pertuzumab	IR/SD*	N.A.	9.5 mo	T-DM1	PR	-40%	16.6 mo
5	Docetaxel + trastuzumab + pertuzumab	SD	-27%	3.8 mo	-	-	-	-
6	Docetaxel + trastuzumab + pertuzumab	PR	-33%	Unclear†	T-DM1	PD	+22%	1.8 mo
7	Docetaxel + trastuzumab + pertuzumab	PR	-45%	6.7 mo	T-DM1	PD	Unclear‡	Unclear‡
8	Docetaxel + trastuzumab + pertuzumab	CR	-100%	Ongoing at 26.8 mo	-	-	-	-
9	Docetaxel + trastuzumab + pertuzumab	PR	-78%	6.9 mo¶	-	-	-	-
10	Docetaxel + trastuzumab + pertuzumab	SD	+1%	5.6 mo	T-DM1	PD	+34%	1.8 mo
11	Docetaxel + trastuzumab + pertuzumab	PD	+38%	1.8 mo	-	-	-	-
12	Docetaxel + trastuzumab + pertuzumab	PR	-68%	6.7 mo¶	-	-	-	-
13	Docetaxel + trastuzumab + pertuzumab	SD	-2%	Ongoing at 5.5 mo	-	-	-	-

Abbreviations: CR: complete response, mo: months, PR: partial response, SD: stable disease.

*This patient had no RECIST measurable target lesions, based on non-target lesions the response is defined as: incomplete response/stable disease (IR/SD).

†This patient was treated for locally advanced disease, based on the good response on HER2 therapy, the patient received local radiotherapy with a curative intent. Therefore the duration of response could not be assessed.

‡Patient died before first treatment evaluation imaging.

¶ According to RECIST criteria, these patients have progressive disease. However, treatment in these patients is still ongoing; treatment discontinuation is at the discretion of the treating physician, as previously described in methods section.

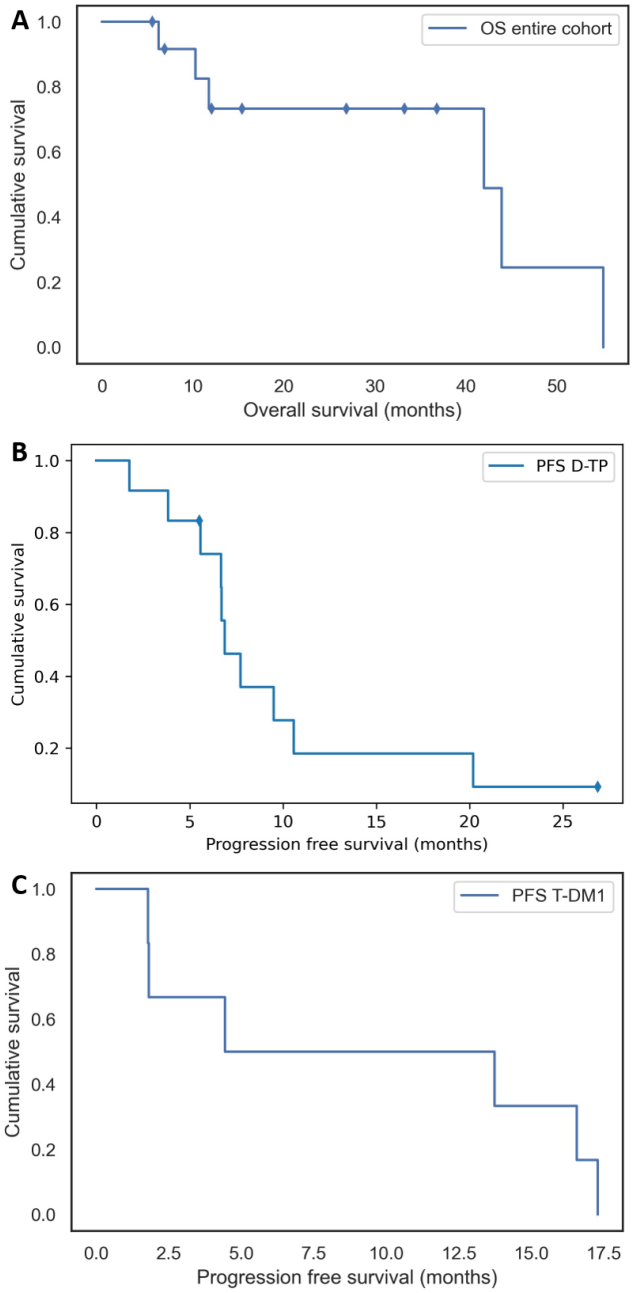

Figure 2: A: Kaplan-Meier curve of overall survival for the entire cohort. **B:** Kaplan-Meier curve of progression free survival on DTP therapy. **C.** Kaplan-Meier curve of progression free survival on T-DM1.

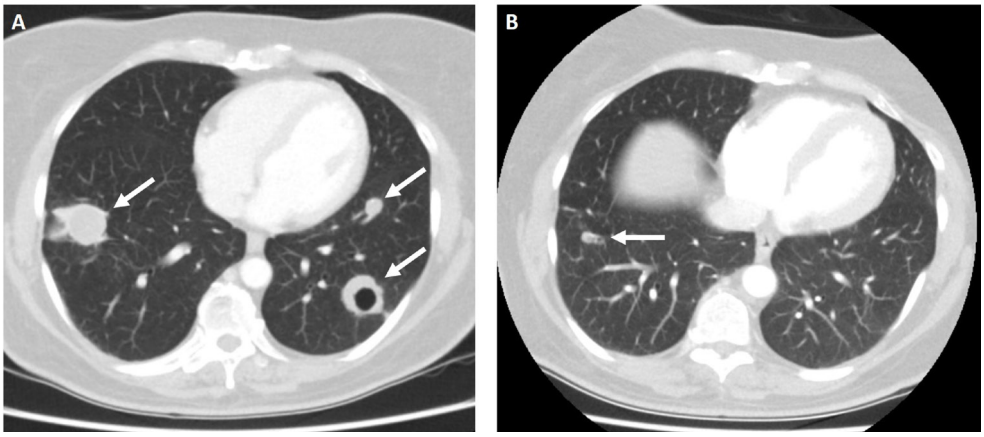

Figure 3: Visualization of response on T-DM1 therapy in SDC patient with pulmonary metastases, **A:** before start of T-DM1 therapy **B**: 1 year on treatment. Pulmonary metastases are indicated by white arrows.

Response prediction potential of pathway analysis

Of the 13 patients, material for RNA extraction was available in 11 cases (85%). RNA quantities were sufficient to assess PI3K and MAPK pathway activity scores in these 11 cases. In 10 cases AR, ER, HH, Notch and TGFβ pathway activity scores could also be assessed. The median MAPK pathway activity score was 62 (range 47-69) and PI3K pathway activity score 34 (range 27-48). Composite scores, summing these metrics ranged from 88-107 (median 94). Figure 4A summarizes pathway activity scores of the samples in which all pathways could be determined. In all patients, activity scores followed the same pattern, with a relatively narrow bandwidth of scores within a single pathway, with a range of usually <25 points (except for one outlier in the HH pathway, figure 4A). AR pathway activity scores ranged from 42-60, with a median of 51 (figure 4A).

The patient with the highest combined PI3K/MAPK score was the only patient experiencing CR and the patient with the lowest combined score was the only patient experiencing PD as best response upon DTP therapy (figure 4B). PR and SD scores ranged in between. No relation was observed between the combined PI3K/MAPK score and the response on T-DM1 (supplementary figure 1).

After dichotomization of the cohort on the median PI3K/MAPK score, OS and PFS did not differ significantly between the groups with a low and high score (p=0.15, p=0.59 and p=0.21, regarding OS, PFS on DTP therapy and PFS on T-DM1, respectively, Supplementary figure 2).

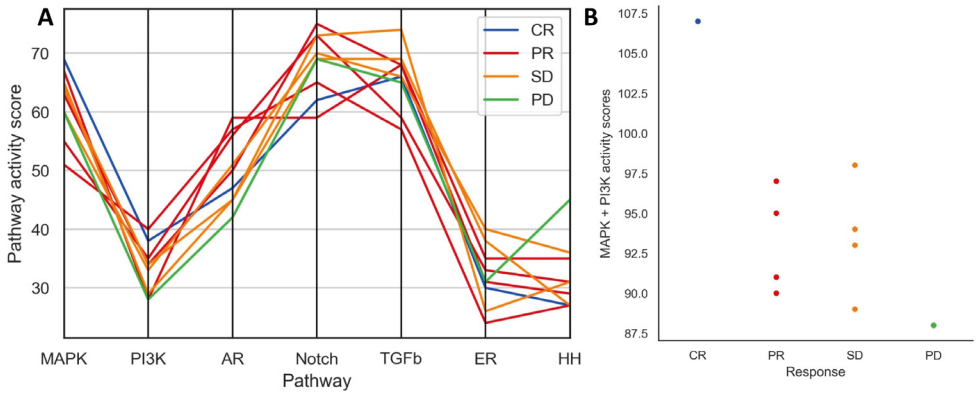

Figure 4: **A:** parallel coordinates plot of all seven pathway activity scores, color-coded for response on DTP therapy. **B:** Swarm plot of combined MAPK and PI3K score versus response on DTP therapy.

Toxicity

Regarding DTP therapy, most common toxicities were mainly docetaxel related and included haematological toxicity, gastrointestinal toxicity, fatigue, and peripheral sensory neuropathy. Five patients (39%) developed grade ≥3 toxicity on DTP, including infections (n=3), neutropenia (n=1), and heart failure (related to trastuzumab/pertuzumab) (n=1) (table 3, Supplementary table 1). Regarding T-DM1 therapy, often reported toxicities were fatigue, nausea, peripheral sensory neuropathy, and increasing levels of liver enzymes. One patient (14%) developed grade ≥3 hyponatremia during T-DM1 treatment, this was however deemed unrelated to T-DM1 treatment.

Table 3: Grade 3 and 4 treatment-related toxicity

	DTP therapy (N=13)	**T-DM1 therapy (N=7)**
Adverse events	Grade 3-4 N (%)	Grade 3-4 N (%)
Bone marrow toxicity		
White blood count decreased	1 (8)	-
Lymphocyte count decreased	1 (8)	-
Neutrophil count decreased	2 (15)	-
Gastrointestinal toxicity		
Pharyngeal mucositis	1 (8)	-
Infectious toxicity		
Skin infection	2 (15)	-
Enterocolitis infectious	1 (8)	-
Heart failure	1 (8)	-

Discussion

In this retrospective case series, the efficacy of two sequential HER2 targeted treatment strategies was evaluated in HER2-positive recurrent or metastatic SDC patients. The majority of the 13 patients treated with DTP responded to this therapy, with an objective response rate of 58%. Also on subsequent T-DM1 therapy, objective responses were observed for the majority of patients (4/7; 57%). Besides this, the PI3K and MAPK signalling pathway activity scores show potential in predicting response to DTP treatment, although numbers of patients in this study are too low to draw firm conclusions, so these findings should be considered as hypothesis generating rather than confirming.

The combination of docetaxel and trastuzumab has previously shown a comparable, even slightly better response rate in a prospective phase II study in SDC patients as compared to our DTP regimen that also includes pertuzumab, ORR 70% with median PFS of 8.9 (95%-CI 7.8-9.9) and OS of 39.7 months (95%-CI not reached) versus ORR of 58% with PFS of 6.9 months (95%-CI 5.2-8.5) and OS of 42.0 months (95%-CI 13.8-70.1), respectively (22). This might be due to selection bias, since generally prospective studies include a different patient population as compared to a routine clinical setting. For instance, brain metastases occurred in 5% of the patients in that study, compared to 23% in our study. This is also supported by other retrospective data, in which an OS for R/M SDC in case of best supportive care as low as 5 months and 17 months upon administration of ADT was seen, although these were not all HER2-positive patients (HER2 is probably not a prognostic factor in SDC) (4, 7). Besides this, the sample size in this study is relatively small, influencing robustness of the found ORR, as one response more or one response less substantially alters the ORR. Regarding efficacy of T-DM1 in salivary gland cancer, preliminary results of a recent phase II basket study in HER2-positive patients also reported high response rates (28). Although unclear how many of SDC subtype, the ORR in this basket study was higher than our results: 90% (9/10 patients) versus 57% (4/7 patients), but both results point towards efficacy of T-DM1 most patients (28). Interestingly, recent research also focusses on the efficacy of HER2 targeted treatments in adjuvant setting of HER2-positive SDC (38). A prospective study on adjuvant T-DM1 is currently recruiting patients (NCT04620187).

Given the histological and molecular similarity between breast cancer and SDC and the frequent overexpression of HER2 in breast cancer, achieved results on anti-HER2 therapy in breast cancer are of interest. The addition of pertuzumab to docetaxel and trastuzumab (DTP) has shown favourable results in HER2-positive breast cancer with a PFS of 18.5 months for DTP versus 12.4 for docetaxel and trastuzumab (19, 20). Also in HER2-positive gastric cancers, slightly better outcomes were seen upon addition of pertuzumab to trastuzumab

combined with chemotherapy: PFS 8.5 months (pertuzumab) versus 7.0 months (placebo) (39, 40).

Toxicity was on average bearable, highlighting the potential of this therapy for this aggressive cancer. Overall, the toxicity of docetaxel and trastuzumab seems comparable to DTP. However, in the prospective SDC trial of docetaxel and trastuzumab no grade ≥2 or higher heart failure was observed, yet one patient in our case series developed grade 3 heart failure. Cardiotoxicity is a known side-effect of trastuzumab treatment, but in larger clinical trials the addition of pertuzumab to trastuzumab did not result in higher rates of cardiotoxicity (19, 20, 39). It, therefore, seems unlikely that the case of heart failure in this case series is related to the addition of pertuzumab.

In our cohort, the treatment-related toxicity profile of T-DM1 was more favourable than that of DTP (grade ≥3 toxicity in 0% versus 39%). The relatively favourable toxicity profile of T-DM1 is also observed in phase III studies of HER2-positive breast cancer patients; adverse events are generally of low grade and manageable (41). This raises the question of whether T-DM1 should be considered as first-line treatment (before DTP). To date, no clinical study in metastatic breast cancer compared DTP to T-DM1 in the first-line setting. Yet, results of a retrospective multicentre study in early-relapsing breast cancer patients, suggests the superiority of DTP over T-DM1 (42). Therefore, first-line HER-2 therapy with DTP followed by T-DM1 remains probably the favourable choice.

In this study, PI3K and MAPK pathway signalling cascades were quantified at mRNA level to explore their potential as predictive or prognostic biomarkers based on the hypothesis that the high activity of these cascades is a result of HER2 activation and that tumour cells with high PI3K/MAPK signalling depend on these pathways for survival and proliferation. Inhibition of HER2, preventing downstream PI3K/MAPK signalling, would hit tumours with high scores harder than those with low activity scores.

Quantification of downstream HER2 signalling is however hard, given the complex nature of the involved and intertwined signalling cascades (17, 18). The summation of the MAPK and PI3K pathway activity scores, which are both optimized towards the quantification of the single pathway, might be a too simple representation of this complex biology. It is unknown which of these two pathways most, let alone in which amount, contributes to the pro-tumorigenic effect in SDC. It is however promising to see that despite these limitations, the combined PI3K/MAPK scores could still be of predictive value as the one patient in our small series experiencing PD on DTP had the lowest score and the only patient experiencing CR the highest score. For T-DM1 response prediction PI3K/MAPK pathway activity scores (Supplementary figure 1, 2C) might not be optimal biomarkers, as HER2 is mainly used as

a target to deliver the cytotoxic emtansine rather than to specifically inhibit downstream signalling.

Recently, the interplay between HER2 and AR signalling cascades is gaining increasing interest, and in models of other cancers reciprocal activation of these pathways has been observed (43, 44). However, the extent of this cross-talk in SDC and its clinical consequences still needs to be investigated. In our case series, all SDC patients were both HER2-positive and AR-positive. If HER2-targeted therapy influenced AR-targeted treatment and vice versa is difficult to deduce from our case series due to the limited patient numbers and heterogenous treatment strategies (e.g. in several patients HER2-directed therapy was administered before AR-directed therapy was given, and in other patients the other way around).

The aggressive nature and rarity of SDC hampers patient accrual in large clinical trials, and learning from advances made in more common cancers is therefore an appealing strategy. Although this study, translating the advances made in breast cancer to SDC patients, has several limitations, such as the retrospective nature and limited sample size, it may still be of great value to SDC patients given the abovementioned difficulties in clinical studies. The absence of a control cohort impedes the drawing of a robust conclusion about anti-HER2 therapy on PFS and OS, but our results seem promising in this patient group with dismal prognoses. This study leaves the question unanswered which sequence of anti-HER2 treatment strategies for HER2-positive SDC patients is optimal and what the additive effect pertuzumab onto trastuzumab and docetaxel is. As overall toxicity does not seem to be increased upon addition of pertuzumab, and synergy of trastuzumab/pertuzumab in blocking HER2 downstream signalling is to be expected both because of the working mechanisms of these agents and as a result of clinical trials in other cancers, we suggest the addition of pertuzumab to trastuzumab/docetaxel in SDC patients (18), realizing that a formal phase III study comparing both treatment arms could not be performed because of the rarity of the disease.
Furthermore, recent research in breast cancer indicates that Trastuzumab deruxtecan, a new antibody-drug conjugate targeting HER2, improved PFS when compared to T-DM1 as second-line HER2 targeted therapy. Trastuzumab deruxtecan might replace T-DM1 as second-line HER-2 treatment in the future (45, 46). This also encourages future research on Trastuzumab deruxtecan in SDC patients.

Conclusion

In R/M HER2-positive SDC patients, DTP followed by T-DM1 upon progression as second-line anti-HER2 therapy are promising treatment strategies, leading to responses in the majority of the patients at an acceptable toxicity profile.

Acknowledgements

We would like to thank Wim Verhaegh (Philips Research, Eindhoven, The Netherlands) and Diederick Keizer (Philips molecular pathway diagnostics, Eindhoven, The Netherlands) for performing the pathway analyses and critical revision of the manuscript.

References

1. Kleinsasser O, Klein HJ, Hubner G. [Salivary duct carcinoma. A group of salivary gland tumors analogous to mammary duct carcinoma]. Arch Klin Exp Ohren Nasen Kehlkopfheilkd. 1968;192(1):100-5.
2. Dalin MG, Desrichard A, Katabi N, Makarov V, Walsh LA, Lee KW, et al. Comprehensive Molecular Characterization of Salivary Duct Carcinoma Reveals Actionable Targets and Similarity to Apocrine Breast Cancer. Clinical cancer research : an official journal of the American Association for Cancer Research. 2016;22(18):4623-33.
3. van Boxtel W, Locati LD, van Engen-van Grunsven ACH, Bergamini C, Jonker MA, Fiets E, et al. Adjuvant androgen deprivation therapy for poor-risk, androgen receptor-positive salivary duct carcinoma. European journal of cancer (Oxford, England : 1990). 2019;110:62-70.
4. Boon E, Bel M, van Boxtel W, van der Graaf WTA, van Es RJJ, Eerenstein SEJ, et al. A clinicopathological study and prognostic factor analysis of 177 salivary duct carcinoma patients from The Netherlands. International journal of cancer. 2018;143(4):758-66.
5. Roh JL, Lee JI, Choi SH, Nam SY, Kim SO, Cho KJ, et al. Prognostic factors and oncologic outcomes of 56 salivary duct carcinoma patients in a single institution: high rate of systemic failure warrants targeted therapy. Oral oncology. 2014;50(11):e64-6.
6. Jayaprakash V, Merzianu M, Warren GW, Arshad H, Hicks WL, Jr., Rigual NR, et al. Survival rates and prognostic factors for infiltrating salivary duct carcinoma: Analysis of 228 cases from the Surveillance, Epidemiology, and End Results database. Head & neck. 2014;36(5):694-701.
7. Boon E, van Boxtel W, Buter J, Baatenburg de Jong RJ, van Es RJJ, Bel M, et al. Androgen deprivation therapy for androgen receptor-positive advanced salivary duct carcinoma: A nationwide case series of 35 patients in The Netherlands. Head & neck. 2018;40(3):605-13.
8. Fushimi C, Tada Y, Takahashi H, Nagao T, Ojiri H, Masubuchi T, et al. A prospective phase II study of combined androgen blockade in patients with androgen receptor-positive metastatic or locally advanced unresectable salivary gland carcinoma. Annals of oncology : official journal of the European Society for Medical Oncology. 2018;29(4):979-84.
9. Viscuse PV, Price KA, Garcia JJ, Schembri-Wismayer DJ, Chintakuntlawar AV. First Line Androgen Deprivation Therapy vs. Chemotherapy for Patients With Androgen Receptor Positive Recurrent or Metastatic Salivary Gland Carcinoma-A Retrospective Study. Frontiers in oncology. 2019;9:701.
10. Locati LD, Perrone F, Cortelazzi B, Lo Vullo S, Bossi P, Dagrada G, et al. Clinical activity of androgen deprivation therapy in patients with metastatic/relapsed androgen receptor-positive salivary gland cancers. Head & neck. 2016;38(5):724-31.
11. Okada T, Saotome T, Nagao T, Masubuchi T, Fushimi C, Matsuki T, et al. Carboplatin and docetaxel in patients with salivary gland carcinoma: A retrospective study. In Vivo. 2019;33(3):843-53.
12. Nakano K, Sato Y, Sasaki T, Shimbashi W, Fukushima H, Yonekawa H, et al. Combination chemotherapy of carboplatin and paclitaxel for advanced/metastatic salivary gland carcinoma patients: differences in responses by different

pathological diagnoses. Acta oto-laryngologica. 2016;136(9):948-51.

13. Uijen MJM, Lassche G, van Engen-van Grunsven ACH, Tada Y, Verhaegh GW, Schalken JA, et al. Systemic therapy in the management of recurrent or metastatic salivary duct carcinoma: A systematic review. Cancer Treat Rev. 2020;89:102069.
14. Takase S, Kano S, Tada Y, Kawakita D, Shimura T, Hirai H, et al. Biomarker immunoprofile in salivary duct carcinomas: clinicopathological and prognostic implications with evaluation of the revised classification. Oncotarget. 2017;8(35):59023-35.
15. Schmitt NC, Kang H, Sharma A. Salivary duct carcinoma: An aggressive salivary gland malignancy with opportunities for targeted therapy. Oral oncology. 2017;74:40-8.
16. Vu T, Claret FX. Trastuzumab: updated mechanisms of action and resistance in breast cancer. Frontiers in oncology. 2012;2:62.
17. Yarden Y, Pines G. The ERBB network: at last, cancer therapy meets systems biology. Nat Rev Cancer. 2012;12(8):553-63.
18. Arteaga CL, Engelman JA. ERBB receptors: from oncogene discovery to basic science to mechanism-based cancer therapeutics. Cancer Cell. 2014;25(3):282-303.
19. Baselga J, Cortes J, Kim SB, Im SA, Hegg R, Im YH, et al. Pertuzumab plus trastuzumab plus docetaxel for metastatic breast cancer. The New England journal of medicine. 2012;366(2):109-19.
20. Swain SM, Baselga J, Kim SB, Ro J, Semiglazov V, Campone M, et al. Pertuzumab, trastuzumab, and docetaxel in HER2-positive metastatic breast cancer. The New England journal of medicine. 2015;372(8):724-34.
21. Verma S, Miles D, Gianni L, Krop IE, Welslau M, Baselga J, et al. Trastuzumab emtansine for HER2-positive advanced breast cancer. The New England journal of medicine. 2012;367(19):1783-91.
22. Takahashi H, Tada Y, Saotome T, Akazawa K, Ojiri H, Fushimi C, et al. Phase II Trial of Trastuzumab and Docetaxel in Patients With Human Epidermal Growth Factor Receptor 2-Positive Salivary Duct Carcinoma. Journal of clinical oncology : official journal of the American Society of Clinical Oncology. 2019;37(2):125-34.
23. Park JC, Ma TM, Rooper L, Hembrough T, Foss RD, Schmitt NC, et al. Exceptional responses to pertuzumab, trastuzumab, and docetaxel in human epidermal growth factor receptor-2 high expressing salivary duct carcinomas. Head & neck. 2018;40(12):E100-e6.
24. van Boxtel W, Boon E, Weijs WLJ, van den Hoogen FJA, Flucke UE, van Herpen CML. Combination of docetaxel, trastuzumab and pertuzumab or treatment with trastuzumab-emtansine for metastatic salivary duct carcinoma. Oral oncology. 2017;72:198-200.
25. Almquist D, Umakanthan JM, Ganti AK. Sequential HER2-Targeted Therapy in Salivary Ductal Carcinoma With HER2/neu Overexpression and a Concomitant ERBB2 Mutation. JCO Precision Oncology. 2018(2):1-5.
26. Correa TS, Matos GDR, Segura M, Dos Anjos CH. Second-Line Treatment of HER2-Positive Salivary Gland Tumor: Ado-Trastuzumab Emtansine (T-DM1) after Progression on Trastuzumab. Case reports in oncology. 2018;11(2):252-7.
27. Swed BL, Cohen RB, Aggarwal C. Targeting HER2/neu Oncogene Overexpression With Ado-Trastuzumab Emtansine in the Treatment of Metastatic Salivary Gland Neoplasms: A Single-Institution Experience. JCO precision oncology. 2019;3.
28. Li BT, Shen R, Offin M, Buonocore DJ, Myers ML, Venkatesh A, et al. Ado-trastuzumab emtansine

in patients with HER2 amplified salivary gland cancers (SGCs): Results from a phase II basket trial. Journal of Clinical Oncology. 2019;37(15_suppl):6001-.

29. Wolff AC, Hammond MEH, Allison KH, Harvey BE, Mangu PB, Bartlett JMS, et al. Human Epidermal Growth Factor Receptor 2 Testing in Breast Cancer: American Society of Clinical Oncology/College of American Pathologists Clinical Practice Guideline Focused Update. Archives of pathology & laboratory medicine. 2018;142(11):1364-82.
30. Wolff AC, Hammond MEH, Hicks DG, Dowsett M, McShane LM, Allison KH, et al. Recommendations for Human Epidermal Growth Factor Receptor 2 Testing in Breast Cancer: American Society of Clinical Oncology/College of American Pathologists Clinical Practice Guideline Update. Journal of Clinical Oncology. 2013;31(31):3997-4013.
31. Eisenhauer EA, Therasse P, Bogaerts J, Schwartz LH, Sargent D, Ford R, et al. New response evaluation criteria in solid tumours: revised RECIST guideline (version 1.1). European journal of cancer (Oxford, England : 1990). 2009;45(2):228-47.
32. Sood S, McGurk M, Vaz F. Management of Salivary Gland Tumours: United Kingdom National Multidisciplinary Guidelines. The Journal of laryngology and otology. 2016;130(S2):S142-s9.
33. Lassche G, Tada Y, van Herpen CML, Jonker MA, Nagao T, Saotome T, et al. Predictive and Prognostic Biomarker Identification in a Large Cohort of Androgen Receptor-Positive Salivary Duct Carcinoma Patients Scheduled for Combined Androgen Blockade. Cancers (Basel). 2021;13(14).
34. van Boxtel W, Verhaegh GW, van Engen-van Grunsven IA, van Strijp D, Kroeze LI, Ligtenberg MJ, et al. Prediction of clinical benefit from androgen deprivation therapy in salivary duct carcinoma patients. International journal of cancer. 2020;146(11):3196-206.
35. van de Stolpe A. Quantitative Measurement of Functional Activity of the PI3K Signaling Pathway in Cancer. Cancers (Basel). 2019;11(3).
36. van de Stolpe A, Holtzer L, van Ooijen H, Inda MA, Verhaegh W. Enabling precision medicine by unravelling disease pathophysiology: quantifying signal transduction pathway activity across cell and tissue types. Sci Rep. 2019;9(1):1603.
37. van de Stolpe A, Verhaegh W, Blay JY, Ma CX, Pauwels P, Pegram M, et al. RNA Based Approaches to Profile Oncogenic Pathways From Low Quantity Samples to Drive Precision Oncology Strategies. Front Genet. 2020;11:598118.
38. Hanna GJ, Bae JE, Lorch JH, Haddad RI, Jo VY, Schoenfeld JD, et al. The Benefits of Adjuvant Trastuzumab for HER-2-Positive Salivary Gland Cancers. The oncologist. 2020;25(7):598-608.
39. Tabernero J, Hoff PM, Shen L, Ohtsu A, Shah MA, Cheng K, et al. Pertuzumab plus trastuzumab and chemotherapy for HER2-positive metastatic gastric or gastro-oesophageal junction cancer (JACOB): final analysis of a double-blind, randomised, placebo-controlled phase 3 study. The Lancet Oncology. 2018;19(10):1372-84.
40. Tabernero J, Hoff PM, Shen L, Ohtsu A, Shah MA, Siddiqui A, et al. 1423MO End-of-study analysis from JACOB: A phase III study of pertuzumab (P) + trastuzumab (H) and chemotherapy (CT) in HER2-positive metastatic gastric or gastro-esophageal junction cancer (mGC/GEJC). Annals of Oncology. 2020;31:S900-S1.
41. Kowalczyk L, Bartsch R, Singer CF, Farr A. Adverse Events of Trastuzumab Emtansine (T-DM1) in the Treatment of HER2-Positive Breast Cancer Patients. Breast Care (Basel). 2017;12(6):401-8.

42. Schettini F, Conte B, Buono G, De Placido P, Parola S, Griguolo G, et al. T-DM1 versus pertuzumab, trastuzumab and a taxane as first-line therapy of early-relapsed HER2-positive metastatic breast cancer: an Italian multicenter observational study. ESMO Open. 2021;6(2):100099.
43. Locati LD, Cavalieri S, Bergamini C, Resteghini C, Colombo E, Calareso G, et al. Abiraterone Acetate in Patients With Castration-Resistant, Androgen Receptor–Expressing Salivary Gland Cancer: A Phase II Trial. Journal of Clinical Oncology.0(0):JCO.21.00468.
44. Ho AL. Androgen Receptor Pathway in Salivary Gland Cancer. Journal of Clinical Oncology.0(0):JCO.21.01983.
45. J. Cortés SK, W. Chung, S. Im, Y.H. Park, R. Hegg, M.H. Kim, L. Tseng, V. Petry, C. Chung, H. Iwata, E. Hamilton, G. Curigliano, B. Xu, C. Lee, Y. Liu, J. Cathcart, E. Bako, S. Verma, S.A. Hurvitz. LBA1 - Trastuzumab deruxtecan (T-DXd) vs trastuzumab emtansine (T-DM1) in patients (Pts) with HER2+ metastatic breast cancer (mBC): Results of the randomized phase III DESTINY-Breast03 study. Annals of Oncology (2021) 32 (suppl_5): S1283-S1346. 10.1016/annonc/annonc741; 2021.
46. Perez J, Garrigós L, Gion M, Jänne PA, Shitara K, Siena S, et al. Trastuzumab deruxtecan in HER2-positive metastatic breast cancer and beyond. Expert Opin Biol Ther. 2021;21(7):811-24.

Supplementary information

Supplementary Table 1. All treatment related toxicity

	DTP therapy (N=13)		T-DM1 therapy (N=7)	
Adverse events	Grade 1 -2 N (%)	Grade 3-4 N (%)	Grade 1 -2 N (%)	Grade 3-4 N (%)
Bone marrow toxicity				
Anemia	11 (85)	-	2 (29)	-
White blood count decreased	2 (15)	1 (8)	-	-
Lymphocyte count decreased	4 (31)	1 (8)	-	-
Neutrophil count decreased	-	2 (15)	-	-
Platelet count decreased	1 (8)	-	3 (43)	-
Gastrointestinal toxicity				
Mucositis oral	5 (39)	-	-	-
Pharyngeal mucositis	-	1 (8)	-	-
Dysphagia	4 (31)	-	-	-
Dysgeusia	1 (8)	-	-	-
Nausea	3 (23)	-	4 (57)	-
Anorexia	2 (15)	-	3 (43)	-
Abdominal pain	4 (31)	-	-	-
Diarrhea	8 (62)	-	3 (43)	-
Constipation	1 (8)	-	1 (14)	-
Infectious toxicity				
Skin infection	1 (8)	2 (15)	1 (14)	-
Lung infection	-	-	1 (14)	-
Urinary tract infection	2 (15)	-	-	-
Enterocolitis infectious	-	1 (8)	-	-
Heart failure	-	1 (8)	-	-
Fatigue	9 (69)	-	5 (71)	-
Peripheral sensory neuropathy	9 (69)	-	4 (57)	-
Alopecia	8 (62)	-	-	-
Nail changes	8 (62)	-	-	-
Epistaxis	2 (15)	-	3 (43)	-
AST increased	1 (8)	-	4 (57)	-
ALT increased	1 (8)	-	4 (57)	-
Conjunctivitis	2 (15)	-	1 (14)	-
Rash acneiform	3 (23)	-	-	-
Weight loss	2 (15)	-	1 (14)	-
Bone pain	1 (8)	-	1 (14)	-
Dry eyes	1 (8)	-	-	-
Dyspnea	1 (8)	-	-	-
Radiation recall reaction	1 (8)	-	-	-
Edema limbs	1 (8)	-	-	-
Cough	1 (8)	-	-	-
Myalgia	1 (8)	-	-	-
Muscle cramp	1 (8)	-	-	-
Lymphedema	1 (8)	-	-	-
Headache	-	-	1 (14)	-

AST: Aspartate aminotransferase, ALT: Alanine aminotransferase.

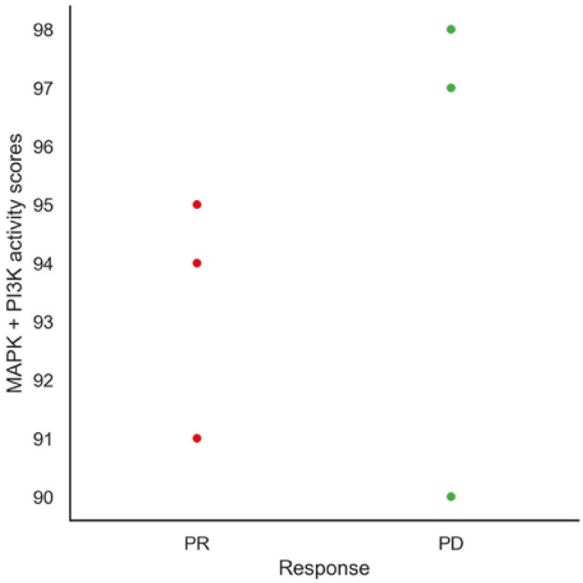

Supplementary figure 1: Swarm plot of combined MAPK and PI3K score versus response on T-DM1.

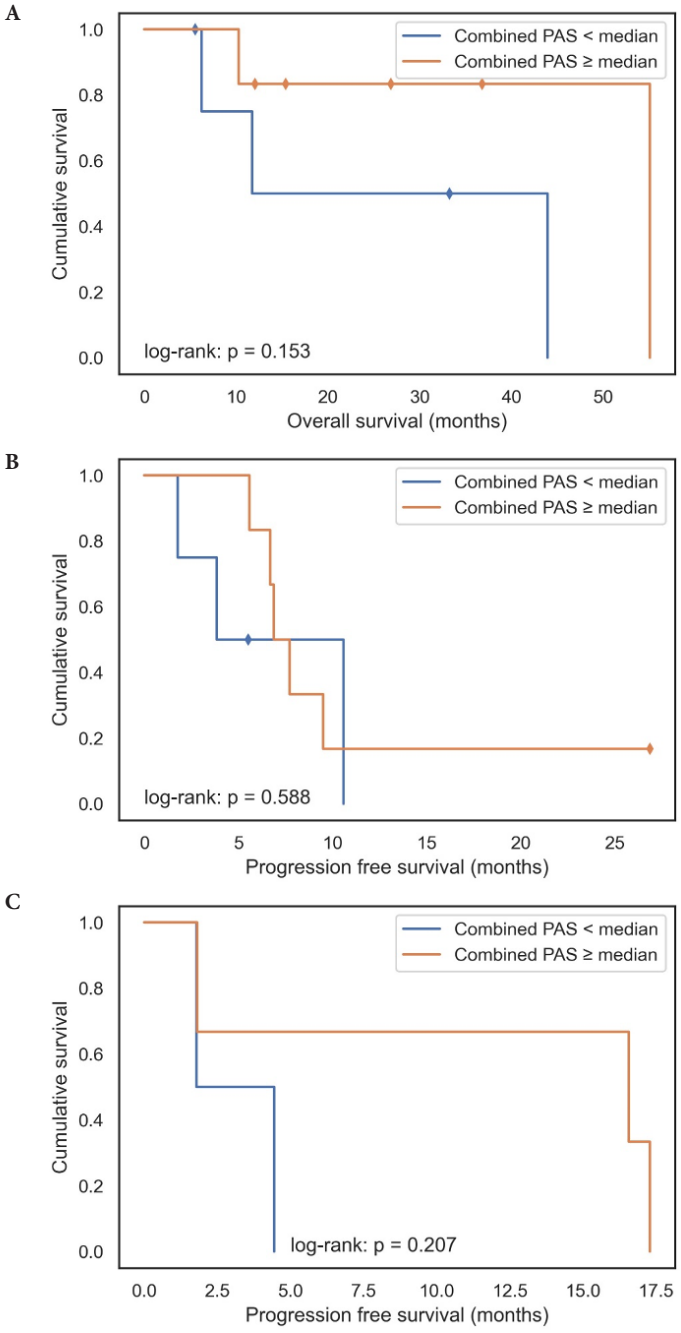

Supplementary figure 2: A: Kaplan-Meier curve of overall survival for the entire cohort, dichotomized on median PI3K/MAPK score. **B:** Kaplan-Meier curve of progression free survival on DTP therapy, dichotomized on median PI3K/MAPK score. **C:** Kaplan-Meier curve of overall survival on T-DM1, dichotomized on median PI3K/MAPK score. Abbreviation: PAS: pathway activity score.

PART 3:
Organoid models of salivary gland cancer

CHAPTER 6

Development and characterization of patient-derived salivary gland cancer organoid cultures

Gerben Lassche, Wim van Boxte1, Tilly W. Aalders, Onno van Hooij, Adriana C.H. van Engen-van Grunsven, Gerald W. Verhaegh, Carla M.L. van Herpen*, Jack A. Schalken*

* These authors share last authorship

Oral Oncol. 2022;135:106186

Abstract

Objective

Three-dimensional organoid cell cultures have been established for a variety of human cancers. For most rare cancers, including salivary gland cancer (SGC), these models are lacking, despite the great unmet need to study cancer biology in these diseases. Therefore, we aimed to develop patient-derived organoid (PDO) models for different subtypes of SGC.

Methods

Tumor samples of SGC patients were processed and embedded in Matrigel. Successful PDOs (expandable $>1*10^6$ cells) were phenotypically characterized using immunohistochemistry (IHC) and genotypically by gene fusion analysis and by targeted and whole-exome sequencing. Successfully established PDOs were subjected to small-scale drug screening.

Results

Out of 37 attempts, 7 viable short-term PDOs were established (19% success rate; 3 salivary duct carcinoma, 3 adenoid cystic carcinoma and 1 mucoepidermoid carcinoma). Each PDO showed close phenotypical mimicry to parental tissue. Genotypic characterization revealed that in each PDO >97.6% of all COSMIC annotated variants and all *MYB, MYBL1* and *NFIB* gene rearrangements were retained. Drug screening was proven feasible in all PDOs.

Conclusion

We present the first comprehensively characterized short-term SGC PDO models for three subtypes of SGC with close phenotypic and genotypic resemblance to parental tissue, which can be used for drug screening applications.

Introduction

Three-dimensional patient-derived stem cell-based tumor models, more commonly known as tumor organoids or tumoroids, have shown their value to study cancer biology and perform drug screenings. Compared to more conventional two-dimensional cancer cell line cultures and patient-derived xenografts, organoids have several advantages, including options to mimic the tumor immunological microenvironment, to study tumor and immune system interactions and to easily model and adapt tumor genetics (1-3). In the last decade, patient-derived organoid models of several cancer types have been described, including cancer of the intestinal tract, breast, prostate, lung, kidney, liver, head-and-neck, and bladder (1, 4-6).

For most cancers with a low incidence, organoid models are lacking, despite the great unmet need for ways to study cancer biology in these diseases. Salivary gland cancer (SGC) is such a rare cancer with an annual incidence rate of 0.4-2.6 cases/100,000 people, for which preclinical research has been scarce (7). A complicating factor to study this disease is its extensive heterogeneity, as evidenced by the 22 subtypes recognized in the most recent World Health Organization classification (7). Adenoid cystic carcinoma (AdCC) and salivary duct carcinoma (SDC) often progress to recurrent/metastatic (R/M) disease (in 42% and 54% of cases, respectively) (8, 9). Therefore, the demand for systemic treatment options is most pressing for AdCC and SDC patients.

In R/M AdCC patients, chemotherapy remains the cornerstone of treatment, although clinical trials with a variety of targeted therapies have been performed (10). Of all chemotherapy regimens studied, cyclophosphamide plus doxorubicin plus cisplatin (CAP) seems most effective with a response rate of 25%. Evidence for second-line therapy is lacking (11). For R/M SDC patients, an increasing number of therapeutic options have become available over the last 5 years. Combined Androgen Blockade (CAB) and HER2-targeted therapies (such as taxane + trastuzumab regimens) are well-established for androgen receptor (AR) positive (78-96%) and HER2-positive (29-46%) SDC patients, respectively (12, 13). Furthermore, subgroups of SDC tumors have other targets that may be amenable for systemic therapy (10). However, especially in HER2-negative patients, treatment options are scarce and the overall benefit of systemic therapy is often limited.

To enhance the development of tumor-specific treatment options based on characteristics such as intrinsic or acquired resistance mechanisms, tumor-immune system interactions or intra-tumor heterogeneity, we aimed to establish SGC patient-derived organoid (PDO) models. Such 3D models might eventually serve, for example, as platform for high-throughput drug screening applications. In this paper we describe the establishment of organoid models

for the AdCC, SDC, and mucoepidermoid carcinoma (MEC) SGC subtypes and small-scale drug screening using those PDO models.

Methods

Patients

Patients with planned surgical resection of (suspected) SGC or tissue sampling of metastatic lesions at the Radboud university medical center (Nijmegen, the Netherlands) were asked permission for secondary use of tumor tissue for medical research from March 2016 until October 2020. Of these patients, clinical data was retrieved from medical records. This study was approved by the institutional review board (Commissie Mensgebonden Onderzoek (CMO) Radboudumc, file number 2017-3697) and written informed consent was obtained.

PDO culture protocol

AR signaling plays an essential role in SDC (14, 15). Therefore, the prostate cancer PDO culture protocol described by Drost *et al.* was used (16, 17). In brief, tissue was mechanically and enzymatically digested, washed, resuspended in 100% growth factor reduced Matrigel (Corning) at a cell density of 1,000 cells/µl, plated in a 48-wells plate in drops of 20 µl Matrigel and supplemented with organoid medium (Supplementary Table 1). This medium was further optimized during this study and tailored to SGC subtypes (Supplementary Table 1, Supplementary File 1) (17). Medium was refreshed biweekly and cultures were passaged every 2 weeks, using TrypLE Express Enzyme (ThermoFisher) digestion, and re-seeding cells in Matrigel at a density of 1,000 cells/µl. Cultures were evaluated using brightfield microscopy. Detailed culture protocol and media formulations are described in Supplementary File 1.

PDO phenotypic characterization

To assess whether viable organoids originated from tumor cells and maintained their characteristics, the organoid phenotype was assessed using hematoxylin and eosin (HE) staining and AR, CK7, HER2, and p63 immunohistochemistry (IHC) (protocols in Supplementary File 1). All sections and stainings were assessed by an expert salivary gland pathologist (AvEvG).

PDO genotypic characterization

The genotypic resemblance between parental tissue and PDO was assessed using the TruSight Oncology 500 (TSO500) assay, targeting 523 pan-cancer related genes (covering 1.94Mb of the genome) (18). Organoid DNA of each successful PDO was whole-exome sequenced to a median coverage of 200X. Gene fusion analysis on parental tissue of AdCC PDOs was performed using a customized RNA-based targeted NGS panel, which allows detection of

fusion transcripts with clinical relevance for targeted therapy and recurrent fusion transcripts in SGC (Archer® FusionPlex panel RadboudV1). To confirm the presence of the identified gene fusions in the AdCC PDOs, reverse transcribed RNA was subjected to real-time PCR followed by Sanger sequencing. Detailed protocols can be found in Supplementary File 1.

Drug treatments

PDOs were treated with six different drugs that are frequently used in clinical treatment of SGC or that target tumor-specific gene or protein alterations: cisplatin, erlotinib (inhibiting epidermal growth factor receptor (EGFR) signaling), lapatinib (inhibiting HER2 and EGFR signaling), sunitinib (inhibiting vascular endothelial growth factor receptor and platelet-derived growth factor receptor signaling), crenigacestat (inhibiting NOTCH signaling) and monensin (inhibiting MYB signaling) (19). All PDOs were subjected to drug treatment experiments, in which drug treatment was started immediately after organoid cell seeding, and for a duration of 96 hours (detailed treatment protocol described in Supplementary File 1).

Results

Patients and tumor specimen characteristics

Tissue specimens of 37 SGC patients were brought into culture. Of these 37 samples, 15 were SDC, 12 AdCC, 7 MEC, 2 acinic cell carcinomas (AciCC) and 1 epithelial-myoepithelial carcinoma (EMC) (AciCC and EMC together called the miscellaneous group). These patients had a median age of 57 years, and 20/37 (54%) suffered from locally advanced, R/M disease. Ten out of 37 patients (27%) received systemic therapy prior to tissue acquisition (Supplementary Table 2). Surgical resection specimens were the tissue source in 57% of the cases, and 43% of the tissues were biopsy-derived (Supplementary Table 2).

In the first attempts, mostly including SDC tumor specimens, a low proliferation rate and fast transition into senescence was observed. The prostate cancer organoid-based medium was therefore depleted of several growth factors and further tailored to the SGC subtype (Supplementary Table 1, Supplementary File 1). Using adapted media formulations we were able to establish 7 successful PDO cultures (19%) out of 37 attempts in total (i.e. expandable to $>1*10^6$ cells) (Figure 1A-B). Of the successful PDOs, 5 out of 7 were cultured directly on this adapted medium formulation (Figure 1B), and the other 2 successful PDOs were established using this medium after thawing cryopreserved cells grown for 1 passage on the prostate cancer organoid-based medium. In the majority of culture attempts the prostate cancer organoid-based medium was initially used, indicating that indeed the adapted medium formulation led to higher success rates. All successful PDOs were derived from resection specimens. Overall, success rate differed between the distinct SGC subtypes, 3/15 (20%) for SDC, 3/12 (25%) for AdCC, 1/7 (14%) for MEC and in the miscellaneous group no cultures out of 3 attempts were successful (Figure 1C, Supplementary Table 2). In these successful cultures organoid formation was observed within 2 weeks after seeding. The successful cultures could initially be passaged at a split rate ranging from 1:2-1:7 every 1-2 weeks (seeding in the same cell density of 1000 cells/µl Matrigel after every passage), until passage 4 till 6, after which senescence was observed (Supplementary Table 2).

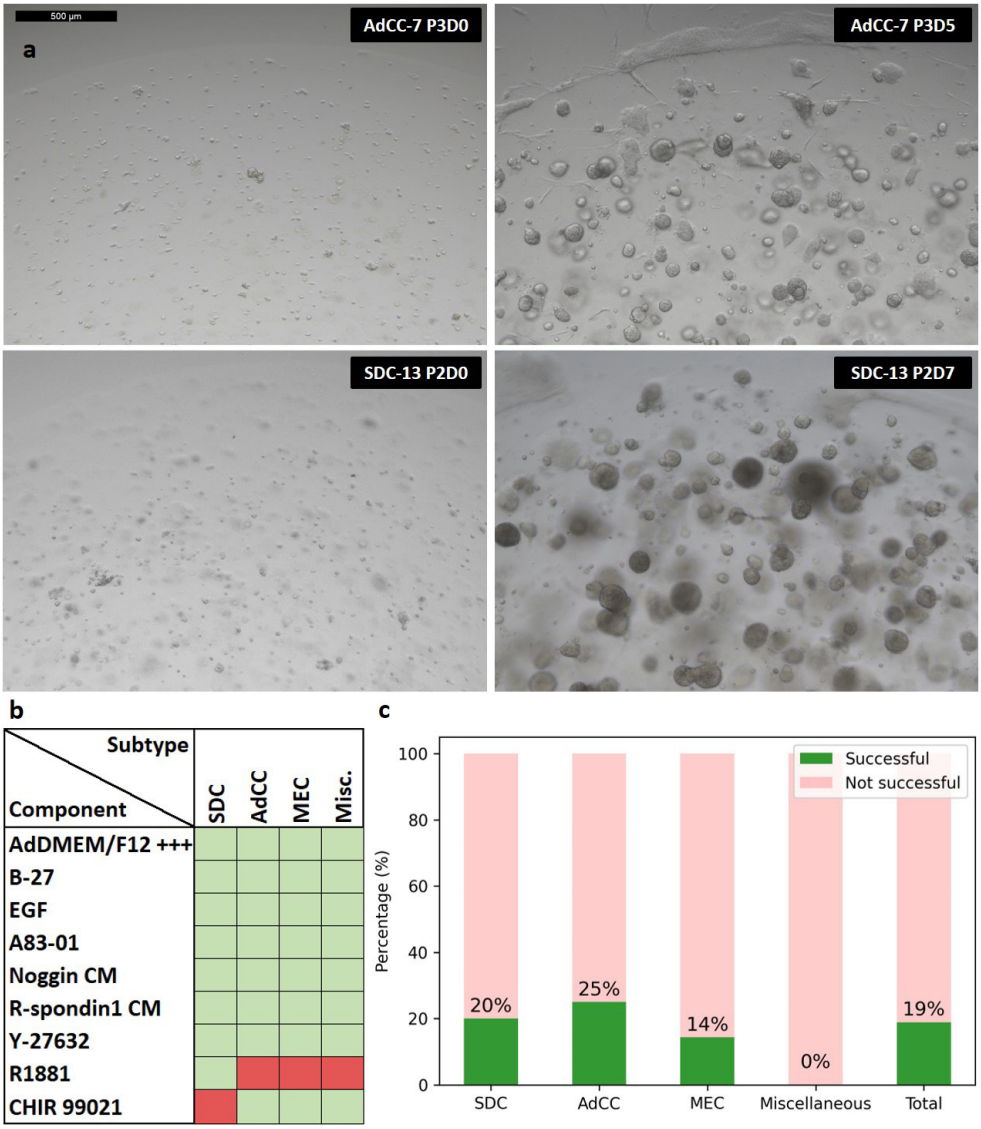

Figure 1: **A**: representative images of organoid cultures just after passaging (left column) and after 5-7 days in culture (right column). Single cells in Matrigel are visible, at a density of 1,000 cells/µl after passaging, and cell cluster formation after several days. Scale bar upper left corners: 500µm. **B**: overview of organoid medium formulation for several SGC subtypes. **C**: PDO establishment success rate per SGC subtypes.

Phenotypic resemblance of PDOs to parental tumor tissue

For all organoids, a cohesive growth-pattern was observed, except for one AdCC PDO (AdCC-3), which had a cystic growth pattern (Figure 2, Supplementary Figure 1). The SDC-derived organoids displayed overtly malignant features with large polymorphic nuclei and abundant eosinophilic cytoplasm as seen in the parental tumor tissue. The HE sections also confirmed that the organoids mainly consisted of tumor cells. Overall, organoids morphologically mimicked parental tissue and adequately recapitulated subtype characteristics (Figure 2, Supplementary Figure 1). All parental tissue and PDOs were CK7 positive in IHC analysis. The high-grade MEC-8 tissue was only focally CK7 positive and the MEC-8 PDO was completely CK7 positive, indicating outgrowth of the CK7 positive subclone. The biphasic architecture of AdCC, comprised of P63 negative ductal cells and P63 positive myoepithelial cells, was maintained in a significant proportion of the AdCC organoid structures (Supplementary Figure 1). In SDC PDOs AR expression was lost and in PDOs derived from HER2-positive parental tissue expression was lost or at least drastically diminished (Supplementary Figure 1). Alcian Blue staining for mucus in the parental tissue of MEC-8 was largely negative, due to the high-grade characteristics, but some mucus formation was seen in the MEC-8 PDO (Figure 2, Supplementary Figure 1).

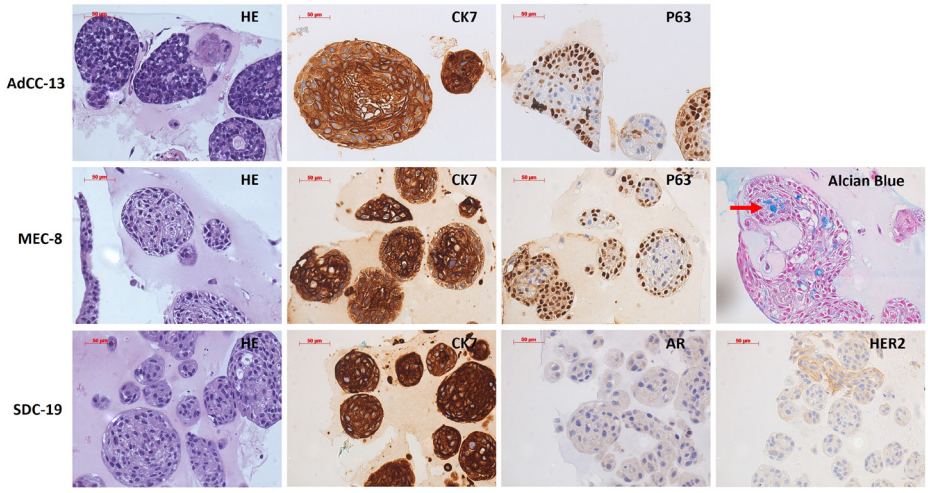

Figure 2: Phenotypic characterization of successful PDOs. Representative images of hematoxylin and eosin (HE) staining and immunohistochemistry (IHC) of a successful PDO of every subtype is shown (see Supplementary Figure 1 for images of all PDOs). Arrow: Alcian Blue positivity, indicating mucus producing cells.

Genotypic resemblance of PDOs to parental tissue

A molecular fingerprint of the tumor cells in the parental tissue was made using a targeted next generation sequencing (NGS) panel which contains 523 genes (TSO500®), which were sequenced to a median exon coverage ranging between 179-497X (average: 391X). On average 1212 (range 1144-1271) variants were called per parental tissue, of which on average 412 (range 400-424) were annotated in the Catalogue of Somatic Mutations in Cancer (COSMIC). WES of PDOs revealed that on average 56.6% of all variants found in parental tissue could be retrieved in the PDOs and at least 97.6% of the COSMIC variants were present in the PDOs (Figure 3B). A significant proportion of the single nucleotide variants (SNVs) in the parental tissue, consisting of a mix of tumor cells and normal cells, is therefore lost in the PDOs. The high percentage of COSMIC variants retained in the PDOs indicate that this lost proportion is largely attributable to the normal cells and confirms that PDO cultures consisted of tumor cells with excellent recapitulation of the genetic make-up of the parental tumor tissue.

Hierarchical clustering of the variant allele frequencies (VAF) of genetic alterations that are identified in the parental tissues and PDOs revealed that parental tissue and the thereof-derived PDO strongly cluster together. This intra-patient clustering was much stronger when only VAFs of COSMIC annotated variants were used. Samples of the same subtype did not cluster together (Figure 3C).

COSMIC variants in the parental tissue were assessed for their overlap between and within subtypes. This indicated that 35% of the COSMIC variants were present in all of the 7 SGC samples, and that 13% of all variants were unique to AdCC and 18% to SDC. Within the COSMIC variants identified in AdCC and SDC subtypes, significant overlap was also present (30% and 27% respectively), but approximately 15% of the variants remained unique to specific samples (Figure 3D). The vast majority of variants unique to AdCC and SDC subtypes were also unique to one of the samples within that subgroup.

Each AdCC parental tissue contained at least one gene fusion and one sample contained two gene fusions, all of which were in-frame fusions (Figure 3A). The detected fusion transcripts involved genes known to be frequently fused in AdCC, such as *MYB, MYBL1*, *NFIB* and the *EYA1* genes, the latter which is located in close proximity to *MYBL1* on chromosome 8. Polymerase chain reaction (PCR) and Sanger sequencing of PDO-derived cDNA confirmed the presence of these unique gene fusions in the corresponding organoid cultures (tested in passage 2).

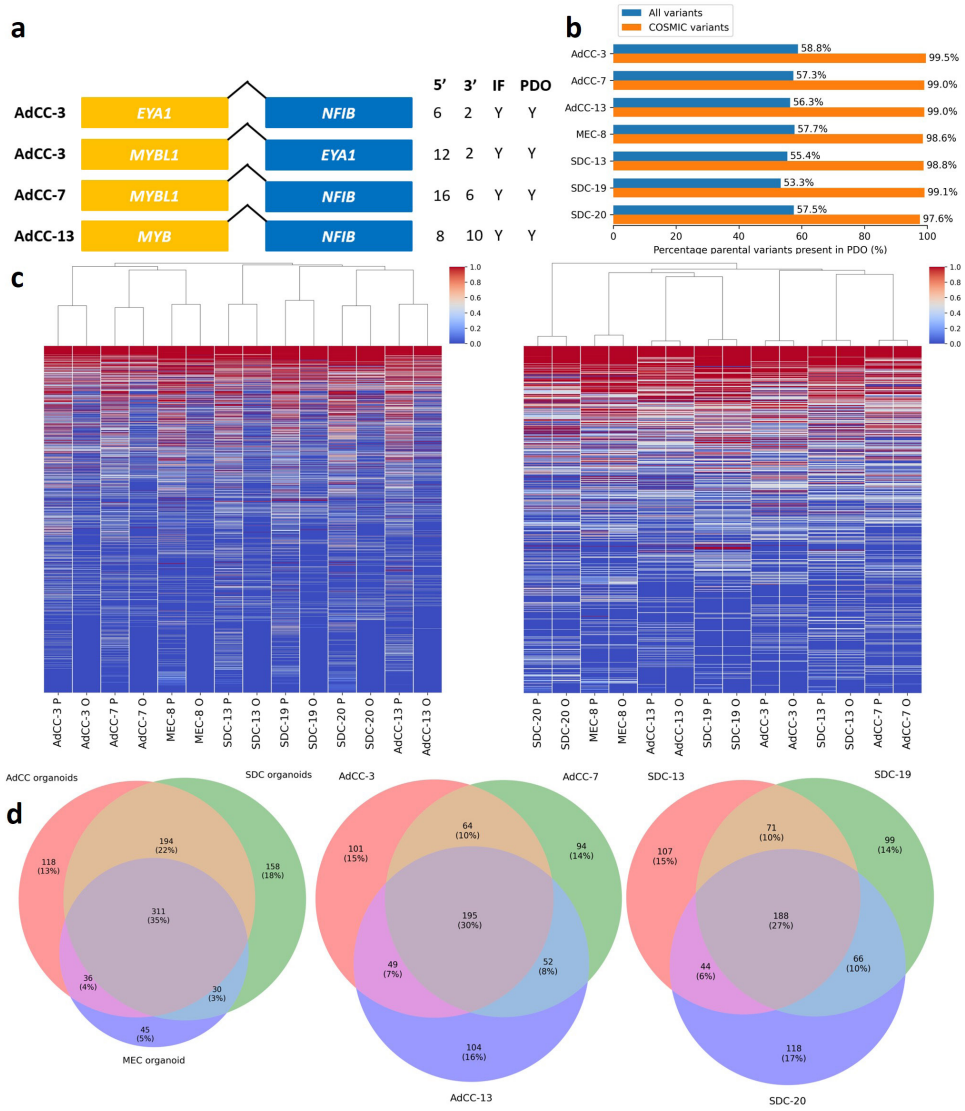

Figure 3: Genotypic characterization of parental tissue and PDOs. **A:** schematic overview of gene fusions present in AdCC parental tissue and PDOs. 5': fused exon of 5' partner gene; 3': fused exon of 3' partner gene; IF: in frame gene fusion (Y/N); PDO: gene fusion present in the PDO (Y/N). **B:** percentage variants identified by targeted sequencing in parental tissue that is also present in the PDOs (WES data), split for all variants (including SNPs) and only COSMIC-annotated variants. **C:** clustermap of all variants (left image) and all COSMIC-annotated variants (right image). Abbreviations: P: parental; O: PDO. **D:** overlap of the COSMIC variants between the PDOs of different subtypes (first Venn diagram), and within AdCC and SDC subtypes (second and third Venn diagram, respectively).

Drug sensitivity

In the established PDOs, differences in drug sensitivity of up to almost one order of magnitude were seen for cisplatin, erlotinib and lapatinib. None of the patients from whom the successful PDOs were derived of had received any of these treatments prior to sampling. The MEC PDO was most resistant to erlotinib and lapatinib and most sensitive to cisplatin compared to the AdCC and SDC PDOs (Figure 4). With respect to sunitinib, monensin and crenigacestat, no clear differences in sensitivity was observed between the PDOs. Regarding sunitinib sensitivity, molecular characterization revealed that none of the parental tissues harbored amplification of *PDGFRA*. Monensin appeared to be toxic in any PDO already at low concentrations, which makes specificity of this inhibitor questionable. No response to crenigacestat was seen, but molecular characterization revealed that none of the parental tissues harbored activating *NOTCH* mutations (Figure 4).

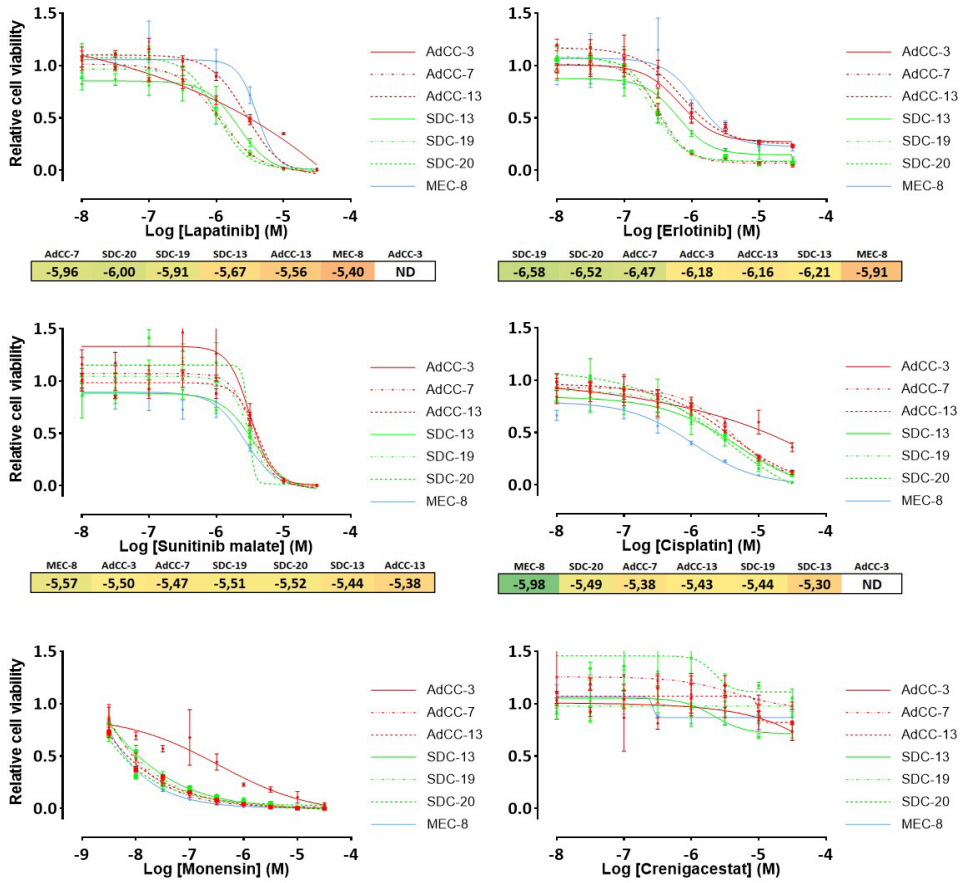

Figure 4: Drug screening of successful PDOs. Organoids were seeded as single cells in a 96-wells format and directly treated for 4 days, after which cell viability was assessed using CellTiter-Glo. For lapatinib, erlotinib, sunitinib and cisplatin IC50 values are depicted below the graphs. No valid IC50 values could be calculated for monensin and crenigacestat.

Discussion

In this article we present the successful development and characterization of SGC PDO cultures. An overall success rate of 19% was achieved for several different SGC subtypes (20% in SDC, 25% in AdCC and 14% in MEC). These PDOs can facilitate pre-clinical and pharmacological studies since we observed mimicry, regarding histology and genetic make-up, of organoids to the parental tumor, although some hallmarks , such as AR-negative SDC PDOs, were lost. Drug testing was feasible and differences in drug sensitivity between different PDOs were observed. Especially in this rare cancer type, in which *in vitro* models and preclinical knowledge are scarce, a reliable organoid culture method to study tumor biology fills a gap and entails chances to personalize treatment. Recently, when this manuscript was in preparation, a study describing the establishment of AdCC organoids as initial step to generate patient-derived xenograft models was published (20). In this study the established PDOs, however, were not characterized in-depth. The here presented work adds up to this study by describing the PDO culture protocol for other SGC subtypes and by comprehensively immunophenotyping and molecular characterizing the PDOs.

The observed success rate of 19% in this series can be considered as rather low compared to PDO culture attempts for other cancer types. For instance, in head and neck squamous cell carcinoma a biobank of 31 organoid cultures has been established with a reported success rate of approximately 60% (6). Urothelial cancer organoids have been established with a success rate of 50% and breast cancer organoids with a success rate of >80% (16, 21-23). The first prostate organoid cell lines were established with a success rate of 15-20% (growing for >6 months, 30-70% for 1-2 months). Recently, a pan-cancer organoid study by Larsen *et al.* reported a success rate, with the same definition as in our study (i.e. organoids expandable to $>1*10^6$ cells), of 24.11% in >1000 attempts, which ranged between 15-75% in the different cancer types (5). Our reported success rate is in the lower end of this range, but was negatively influenced by the initial attempts with some (potentially avoidable) technical failures. This led to markedly higher success rate in the later attempts, making the platform more robust than indicated by the success rate of 19%. The finite passaging capacity of our cultures however remains a limitation.

One of the explanations for the initial unsuccessful PDO culture attempts may have been the sub-optimal medium composition, as no successful PDO was cultured solely on the initially used prostate cancer-organoid based medium whilst 5 out of 7 successful PDOs were established using the altered SGC medium exclusively. We started with medium optimization for SGC as one entity, although it is a very heterogenous disease. This is one of the main challenges in SGC research in general, and in particular for organoid culturing. The evident differences in clinical behavior, morphology, cell types and mutational landscape between

these subtypes indicate that tumor biology is highly different between the subtypes (7, 10). These differences merit a more tailored approach regarding culture medium rather than a one-size-fits-all protocol. However, the rarity of SGC and of each single subtype limits the possibility to extensively optimize culture conditions due to the low number of available specimens. Especially regarding the longevity of cultures there is room for improvement, although this is not a necessity for drug screening applications, as for the latter enough PDOs can be generated.

Regarding further medium optimization, a diversity of additional growth factors has been described on top of the widely used basis of R-spondin (potentiating Wnt-signaling), Noggin (a bone morphogenic protein inhibitor), fibroblast growth factors (FGF) and epidermal growth factor (EGF) in epithelial organoid culture protocols (1, 24, 25). For normal mouse salivary gland tissue, organoids have been established using medium containing EGF, FGF-2, insulin, Rho-kinase inhibitor Y-27632 and Wnt-signaling agonists (most of these components are also present in the SGC medium in this study). Wnt-signaling was proven to be pivotal for adequate salivary gland stem cell expansion (26). The glycogen synthase kinase-3 (GSK3β) inhibitor CHIR99021 was therefore added to our medium, resulting in inhibition of β-catenin phosphorylation and thereby promoting canonical Wnt-signaling (27). Although addition of CHIR99021 led to better outgrowth of AdCC and MEC organoids, it did not improve SDC culture success. Further improvement of Wnt-signaling by medium alteration could be achieved by addition of a Wnt-agonist to the medium, rather than potentiators of the Wnt pathway such as R-spondin and CHIR99021. Recently, highly potent 'next-generation' surrogate Wnts have been described, which led to improved long-term expansion of organoid cultures in several cancers. These next-generation Wnts are therefore promising candidates to improve the SGC organoid protocol as in the current protocol organoids cannot be passaged indefinitely (28).

In SDC, AR is expressed in the vast majority of cases (8). Patients often benefit from androgen deprivation therapy, underlining the importance of androgens for tumor proliferation in SDC (15, 29). Therefore, androgens were added to the SDC culture medium, initially we added dihydrotestosterone, which was later replaced by the more stable synthetic androgen R1881. Despite abundant presence of androgens, SGC PDOs lost AR expression, even though the same culture protocol was used that preserved AR expression in several prostate cancer PDOs (16, 17). Not all SDC cells express AR, and therefore outgrowth of an AR negative subclone in our PDOs is likely, although significant downregulation of AR expression due to factors present in the medium cannot be ruled out. Future studies are required to test these hypotheses regarding SDC PDO AR-negativity. The AR-negativity limits the possibility to use the model for predicting *in vivo* responses to AR blocking agents, although it might enhance the utility to screen for new therapies in patients progressing upon (combined) androgen blockade. Both

of the abovementioned mechanisms, outgrowth of a negative subclone or downregulation due to medium components, could also explain loss of HER2 expression in the SDC PDOs. A possible alternative route to generate *in vitro* models to study AR-signaling in SDC could be by xenografting tumors in testosterone supplemented NSG mice and thereafter grow PDX-derived cells as organoids. This method has proven very successful for the establishment of AR-positive prostate cancer organoids (30). Xenografting the tumors could also possibly overcome the problem of culture longevity. Lack of contact of the tumor cells with the stroma might be a crucial missing component and engrafting in mice could serve to initially maintain this contact with the tumor-microenvironment.

The here presented protocol for establishing SGC-derived PDOs was proven suitable to create PDOs for drug screening applications. This entails the possibility to screen the patients' tumor on drug sensitivity prior to treating the patient, possibly preventing toxicity. This needs validation in a clinical study, especially since in other cancer types organoid drug screening could predict response to one chemotherapeutic agent but failed to predict it for others (31). In addition, the true representativeness of the SGC PDOs for the parental tissue with regard to drug susceptibility is uncertain, especially because some hallmark features have been lost. Furthermore, the culture protocol (*i.e.* medium composition) needs further improvement to achieve a higher success rate and establish long-term cultures that are suitable for, for example, genetic manipulation to study SGC tumor biology and co-culture experiments with immune cells.

In conclusion, we present the first established patient-derived organoid models for three different SGC subtypes that adequately recapitulate the phenotype and genotype of the parental tissue. This model can be of great value for future studies of SGC cancer biology and to screen for novel therapies.

References

1. Drost J, Clevers H. Organoids in cancer research. Nat Rev Cancer. 2018;18(7):407-18.
2. Neal JT, Li X, Zhu J, Giangarra V, Grzeskowiak CL, Ju J, et al. Organoid Modeling of the Tumor Immune Microenvironment. Cell. 2018;175(7):1972-88.e16.
3. Dijkstra KK, Cattaneo CM, Weeber F, Chalabi M, van de Haar J, Fanchi LF, et al. Generation of Tumor-Reactive T Cells by Co-culture of Peripheral Blood Lymphocytes and Tumor Organoids. Cell. 2018;174(6):1586-98.e12.
4. Bleijs M, van de Wetering M, Clevers H, Drost J. Xenograft and organoid model systems in cancer research. EMBO J. 2019;38(15):e101654.
5. Larsen BM, Kannan M, Langer LF, Leibowitz BD, Bentaieb A, Cancino A, et al. A pan-cancer organoid platform for precision medicine. Cell Rep. 2021;36(4):109429.
6. Driehuis E, Kolders S, Spelier S, Lohmussaar K, Willems SM, Devriese LA, et al. Oral Mucosal Organoids as a Potential Platform for Personalized Cancer Therapy. Cancer discovery. 2019;9(7):852-71.
7. El-Naggar AK CJ, Grandis JR, Takata T, Slootweg PJ. WHO classification of head and neck tumours. 4th ed: WHO; 2017; 236-7.
8. Boon E, Bel M, van Boxtel W, van der Graaf WTA, van Es RJJ, Eerenstein SEJ, et al. A clinicopathological study and prognostic factor analysis of 177 salivary duct carcinoma patients from The Netherlands. International journal of cancer. 2018;143(4):758-66.
9. van Weert S, Reinhard R, Bloemena E, Buter J, Witte BI, Vergeer MR, et al. Differences in patterns of survival in metastatic adenoid cystic carcinoma of the head and neck. Head & neck. 2017;39(3):456-63.
10. Lassche G, van Boxtel W, Ligtenberg MJL, van Engen-van Grunsven ACH, van Herpen CML. Advances and challenges in precision medicine in salivary gland cancer. Cancer Treat Rev. 2019;80:101906.
11. Laurie SA, Ho AL, Fury MG, Sherman E, Pfister DG. Systemic therapy in the management of metastatic or locally recurrent adenoid cystic carcinoma of the salivary glands: a systematic review. The Lancet Oncology. 2011;12(8):815-24.
12. Takahashi H, Tada Y, Saotome T, Akazawa K, Ojiri H, Fushimi C, et al. Phase II Trial of Trastuzumab and Docetaxel in Patients With Human Epidermal Growth Factor Receptor 2-Positive Salivary Duct Carcinoma. Journal of clinical oncology : official journal of the American Society of Clinical Oncology. 2019;37(2):125-34.
13. Uijen MJM, Lassche G, van Engen-van Grunsven ACH, Tada Y, Verhaegh GW, Schalken JA, et al. Systemic therapy in the management of recurrent or metastatic salivary duct carcinoma: A systematic review. Cancer Treat Rev. 2020;89:102069.
14. Dalin MG, Watson PA, Ho AL, Morris LG. Androgen Receptor Signaling in Salivary Gland Cancer. Cancers (Basel). 2017;9(2).
15. Fushimi C, Tada Y, Takahashi H, Nagao T, Ojiri H, Masubuchi T, et al. A prospective phase II study of combined androgen blockade in patients with androgen receptor-positive metastatic or locally advanced unresectable salivary gland carcinoma. Annals of oncology : official journal of the European Society for Medical Oncology. 2018;29(4):979-84.
16. Gao D, Vela I, Sboner A, Iaquinta PJ, Karthaus WR, Gopalan A, et al. Organoid cultures derived from patients with advanced prostate cancer. Cell. 2014;159(1):176-87.

17. Drost J, Karthaus WR, Gao D, Driehuis E, Sawyers CL, Chen Y, et al. Organoid culture systems for prostate epithelial and cancer tissue. Nat Protoc. 2016;11(2):347-58.
18. Kroeze LI, de Voer RM, Kamping EJ, von Rhein D, Jansen EAM, Hermsen MJW, et al. Evaluation of a Hybrid Capture-Based Pan-Cancer Panel for Analysis of Treatment Stratifying Oncogenic Aberrations and Processes. J Mol Diagn. 2020;22(6):757-69.
19. Yusenko MV, Trentmann A, Andersson MK, Ghani LA, Jakobs A, Arteaga Paz MF, et al. Monensin, a novel potent MYB inhibitor, suppresses proliferation of acute myeloid leukemia and adenoid cystic carcinoma cells. Cancer Lett. 2020;479:61-70.
20. Takada K, Aizawa Y, Sano D, Okuda R, Sekine K, Ueno Y, et al. Establishment of PDX-derived salivary adenoid cystic carcinoma cell lines using organoid culture method. International journal of cancer. 2021;148(1):193-202.
21. Mazzucchelli S, Piccotti F, Allevi R, Truffi M, Sorrentino L, Russo L, et al. Establishment and Morphological Characterization of Patient-Derived Organoids from Breast Cancer. Biol Proced Online. 2019;21:12.
22. Mullenders J, de Jongh E, Brousali A, Roosen M, Blom JPA, Begthel H, et al. Mouse and human urothelial cancer organoids: A tool for bladder cancer research. Proc Natl Acad Sci U S A. 2019;116(10):4567-74.
23. Sachs N, de Ligt J, Kopper O, Gogola E, Bounova G, Weeber F, et al. A Living Biobank of Breast Cancer Organoids Captures Disease Heterogeneity. Cell. 2018;172(1-2):373-86.e10.
24. Urbischek M, Rannikmae H, Foets T, Ravn K, Hyvonen M, de la Roche M. Organoid culture media formulated with growth factors of defined cellular activity. Sci Rep. 2019;9(1):6193.
25. Clevers H. Modeling Development and Disease with Organoids. Cell. 2016;165(7):1586-97.
26. Maimets M, Rocchi C, Bron R, Pringle S, Kuipers J, Giepmans BN, et al. Long-Term In Vitro Expansion of Salivary Gland Stem Cells Driven by Wnt Signals. Stem Cell Reports. 2016;6(1):150-62.
27. Zhan T, Rindtorff N, Boutros M. Wnt signaling in cancer. Oncogene. 2017;36(11):1461-73.
28. Miao Y, Ha A, de Lau W, Yuki K, Santos AJM, You C, et al. Next-Generation Surrogate Wnts Support Organoid Growth and Deconvolute Frizzled Pleiotropy In Vivo. Cell stem cell. 2020;27(5):840-51.e6.
29. Locati LD, Perrone F, Cortelazzi B, Lo Vullo S, Bossi P, Dagrada G, et al. Clinical activity of androgen deprivation therapy in patients with metastatic/relapsed androgen receptor-positive salivary gland cancers. Head & neck. 2016;38(5):724-31.
30. Risbridger GP, Clark AK, Porter LH, Toivanen R, Bakshi A, Lister NL, et al. The MURAL collection of prostate cancer patient-derived xenografts enables discovery through preclinical models of uro-oncology. Nat Commun. 2021;12(1):5049.
31. Ooft SN, Weeber F, Dijkstra KK, McLean CM, Kaing S, van Werkhoven E, et al. Patient-derived organoids can predict response to chemotherapy in metastatic colorectal cancer patients. Sci Transl Med. 2019;11(513).

Supplementary information

Supplementary File 1: extended methods

Culture protocol

Establishment of SGC PDO cultures has not yet been described. Because SDC mimics prostate cancer and similarly expresses AR, the prostate cancer organoid culture protocol described by Drost *et al.* was used as starting point (17). Briefly, fresh tissue of resection specimens or biopsies of primary tumors or metastases of SGC patients were collected in Advanced Dulbecco's Modified Eagle Medium/Ham's F-12 (AdDMEM/F12) supplemented with HEPES Buffer Solution 10mM, GlutaMAX Supplement 2mM, Primocin 100µg/ml, together called AdDMEM/F12+++, and fungizone. Time between biopsy or resection and collection in medium was usually <30 minutes and after collection in medium further processing usually started within 60 minutes, but at the latest within 24 hours, at room temperature. Tissue was mechanically digested by mincing with scalpels and enzymatically digested with collagenase type II (0.5mg/ml, specific activity 127.5U/ml) supplemented with Rho-kinase inhibitor Y-27632 (10 µM) for 20 minutes at 37°C (with frequent resuspension with a P1000 pipette) or overnight at room temperature under continuous rotation (direct or overnight digestion depending on time of arrival of the sample). When the majority of tissue was digested into single cells, cells were washed with AdDMEM/F12+++ and viable cells were counted using Trypan blue. Approximately 20,000 cells per 20 µl growth factor reduced Matrigel (VWR) were plated in the middle of a 48-wells plate. Organoid culture medium, freshly prepared on weekly basis, (200-300µl/well) was added and refreshed every 3-4 days. The organoid culture medium formulation that has been initially used, as described by Drost *et al.*, is listed in Supplementary Table 1 (17). After frequent evaluation of culture success and gaining new insights, medium composition was altered and tailored to each SGC subtype. Several components were left out, and *e.g.* CHIR99021 was added for non-SDC organoid cultures as this was proven pivotal for head and neck squamous cell organoid cultures (6). The medium used in the latest cultures consisted of AdDMEM/F12+++ supplemented with B-27 Supplement (1X), EGF (50ng/ml), A 83-01 (500nM), Noggin CM (12.5%), R-spondin1 CM (10%), Y-27632 (10µM), R1881 (1nM) for SDC tissue and CHIR99021 (0.3µM) for non-SDC tissue (Figure 1B, Supplementary Table 1).

Viable PDOs were passaged approximately every 2 weeks by mechanically disrupting the Matrigel with a pipette tip and TrypLE Express Enzyme treatment of the organoids until majority of cell clusters were digested into single cells (approximately 5-10 minutes at 37°C with frequent resuspension) and embedding cells in fresh Matrigel. In case sufficient cells could be harvested, organoids were cryopreserved in freezing medium (Supplementary Table

3) in liquid nitrogen. A successful PDO culture was defined as the ability to expand the content of the culture to at least $1*10^6$ cells, as this will often suffice for drug screening applications (5).

H&E and IHC

Organoids were fixated using 4% paraformaldehyde and processed for embedding in paraffin. Four micrometer thick sections were stained with H&E and Alcian Blue (for MEC PDOs) or used for IHC. HE and IHC was performed on the same tissue block. For IHC, antibodies targeting CK7 (OV-TL 12/30, Cell Marque / Sigma-Aldrich, diluted 1:800), P63 (4A4, Immunologic (a WellMed company), diluted 1:3000), AR (A9853, Sigma-Aldrich, diluted 1:500) and HER2 (HercepTest, DAKO / Agilent), were used. Detection was performed using EnVision Systems (DAKO / Agilent), except for AR for which Swine Anti-Rabbit Immunoglobulins/HRP were used (P0217, Dako / Agilent). IHC was assessed by an expert salivary gland pathologist (AvEvG).

Molecular characterization and gene fusion analysis

Formalin-fixed paraffin embedded (FFPE) tumor tissue was used for extraction of DNA and RNA of the parental tissue, using Chelex-100 extraction (VWR) for DNA and ReliaPrep FFPE Total RNA Miniprep System (Promega) for RNA isolation. The hybridization-capture based TruSight Oncology 500 (TSO500) panel, which contains 523 pan-cancer related genes (total genomic content of 1.94Mb), was used for the identification of variants present in the parental tissue, as published before (18). Variants were aligned to reference genome GRCh37/hg19 and annotated for presence in the Catalogue of Somatic Mutations in Cancer (COSMIC) using the COSMIC database v86. Gene fusion analysis on parental tissue of AdCC PDOs was performed using a customized RNA-based targeted NGS panel, which allows detection of fusion transcripts with clinical relevance for targeted therapy and recurrent fusion transcripts in SGC (Archer® FusionPlex RadboudV1).

PDO DNA of passage number 2 or 3 was isolated using the QIAamp DNA Mini Kit (Qiagen) and used for WES at GenomeScan B.V. (Leiden, The Netherlands), with a coverage aimed at 200X. Sample preparation and hybridization capture was performed according to SureSelectXT Target Enrichment System for Illumina Paired-End Sequencing Library protocol v.1.8. The Agilent SureSelectXT Human All Exon v7 capture library (5191-4006 Agilent Technologies) was used and clustering and sequencing was performed using a NovaSeq6000 (Illumina). Variant calling and analysis was based on the Illumina DRAGEN-GATK software, using reference genome GRCh37/hg19. Variants identified in the TSO500 analysis were compared to the WES data (all variants and variants annotated in the COSMIC database). Hierarchical clustering was performed for the VAFs of all variants and all COSMIC annotated variants using Manhattan distances and the complete linkage method. As input VAFs of all variants that were identified in at least one TSO500 dataset were used as input. Graphs and figures

for the characterization were created using Python version 3.8 with the Matplotlib, Pandas, Numpy and Seaborn packages.

AdCC PDO RNA was isolated using TRIzol Reagent (Thermo Fisher Scientific). Random-primed reverse transcribed RNA was used as input for real-time PCR using LightCycler 480 SYBR Green I Master (Roche Diagnostics) or PCR using Phusion High-Fidelity DNA Polymerase (Thermo Fisher Scientific) and primers listed in Supplementary Table 4. PCR products were purified after 2% agarose gel electrophoresis using QIAquick Gel Extraction Kit (Qiagen), and products were analyzed by Sanger sequencing to confirm the presence of gene fusions identified in the parental tissue.

Drug treatments

Organoids were harvested, digested into single cells using TrypLE Express Enzyme and counted using Trypan blue staining. Cells were subsequently seeded in 5µl discs of Matrigel diluted with AdDMEM/F12+++ (70/30 v/v%) in a 96-wells culture plate at a density of 2,000 cells/disc per well. Cells were treated with 6 different drugs that are frequently used in clinical treatment of SGC or that target tumor-specific gene or protein alterations (Supplementary Table 5). Immediately after cell seeding drug treatment (final concentration -8.5 to -4.5 log M, performed in triplicate) was commenced. After 4 days of incubation cell viability was determined using CellTiter-Glo Luminescent Cell Viability Assays (Promega) and luminescent activity was measured on a Victor^3 Multilabel Counter (PerkinElmer). Relative cell viability was calculated to vehicle-treated cells. A non-linear regression sigmoidal dose-response (variable slope) analysis was performed and the IC50 was calculated using Graphpad Prism 9.

Supplementary Table 1: Used chemicals and suppliers for organoid culturing

Name	Company	Catalog number	Final conc.	Drost *et al.* organoid medium	SGC organoid medium
Advanced DMEM/F12	Thermo Fisher Scientific	12634-010	NA	Yes	Yes
Penicillin/Streptomycin	Thermo Fisher Scientific	15140-122	1%	Yes	No
Primocin	Invivogen	Ant-pm-1	100µg/ml	No	Yes
HEPES Buffer Solution	Thermo Fisher Scientific	15630-056	10mM	Yes	Yes
GlutaMAX Supplement	Thermo Fisher Scientific	35050-038	2mM	Yes	Yes
B-27 Supplement	Thermo Fisher Scientific	17504-044	1x	Yes	Yes
Nicotinamide	Sigma-Aldrich	N0636	10mM	Yes	No
N-acetyl-L-cysteine	Sigma-Aldrich	A9165	1,25mM	Yes	No
EGF	PeproTech	AF-100-15	5ng/ml or 50ng/ml	Yes, 5ng/ml	Yes, 50ng/ml
A 83-01	Tocris Bioscience	2939	500nM	Yes	Yes
Noggin: CM recombinant HEK293T cells	-	-	12.5% (v/v) Conditioned medium	Yes	Yes
DHT	Sigma-Aldrich	A8380	1nM	Yes	No
R1881	Bioconnect	M8128	1nM	No	SDC only
FGF-2	PeproTech	100-18B	5ng/ml	Yes	No
FGF-10	PeproTech	100-26	10ng/ml	Yes	No
Prostaglandin E2	Tocris Bioscience	2296	1µM	Yes	No
SB202190	Selleckchem	S1077	10µM	Yes	No
Cultrex-HA-R-Spondin-1-Fc 293T cells	Amsbio	3710-001-01	10% (v/v) Conditioned medium	Yes	Yes
Y-27632 dihydrochloride	AbMole Bioscience	M1817	10µM	Yes	Yes
CHIR99021	Sigma-Aldrich	SML1046	0.3µM	No	Non-SDC only
Matrigel GFR, Phenol Red free	VWR	356321	-	NA	NA
Collagenase Type 2	Worthington	LS004176	-	NA	NA

Abbreviations: DMEM/F12: Advanced Dulbecco's Modified Eagle medium/Ham's F-12; EGF: Epidermal Growth Factor; CM: conditioned medium; DHT: Dihydrotestosterone; FGF: Fibroblast Growth Factor; GFR: Growth Factor Reduced.

Supplementary Table 2: clinical parameters and PDO characteristics

	Patient characteristics		Disease characteristics		Treatment information				PDO characteristics				
PDO ID	Gender	Age	Primary location	Recurrent/ metastatic	Pretreated with chemotherapy	Pretreated with hormonal therapy	Pretreated with anti-HER2 therapy	Prior treatment specification	Tissue specimen source	Sample taken from previously irradiated area	Culture success		Reason culture stopped*
Salivary duct carcinoma PDOs													
SDC-1	M	61	Submandibular gland	Yes	No	Yes	No	Bicalutamide	Lymph node excision	No	No	0	No initial growth
SDC-2	M	78	Parotid gland	Yes	No	Yes	No	Bicalutamide	Biopsy lymphangitis carcinomatosa	Yes	No	2	Growth arrest
SDC-3	M	52	Parotid gland	Yes	No	No	No		Biopsy of bone metastasis	No	No	1	Growth arrest
SDC-5	M	78	Parotid gland	No	No	No	No		Primary tumor resection	No	No	3	Growth arrest
SDC-6	M	53	Parotid gland	Yes	No	Yes	No	Bicalutamide	Biopsy of lymph node metastasis	No	No	0	Fungal infection
SDC-8	F	84	Parotid gland	No	No	No	No		Primary tumor resection	No	No	1	Technical problem
SDC-9	F	78	Parotid gland	No	No	No	No		Primary tumor resection	No	No	2	Growth arrest
SDC-10	F	53	Parotid gland	Yes	No	No	No		Biopsy of liver metastasis	No	No	1	Growth arrest
SDC-11	M	37	Parotid gland	Yes	No	Yes	No	Bicalutamide	Biopsy of skin metastasis	No	No	1	Growth arrest
SDC-13	M	81	Parotid gland	No	No	No	No		Primary tumor resection	No	Yes	4	Growth arrest
SDC-15	M	51	Parotid gland	Yes	Yes	No	Yes	Docetaxel/ trastuzumab/ pertuzumab	Biopsy of pulmonary metastasis	No	No	2	Growth arrest
SDC-16	F	73	Parotid gland	No	No	No	No		Primary tumor resection	No	No	3	Growth arrest

(Table continues on next page)

Supplementary Table 2: Continued

SDC-18	F	52	Parotid gland	Yes	Yes	Yes	Yes	1. Docetaxel/ trastuzumab/ pertuzumab 2. Goserelin/ bicalutamide 3. TDM-1 4. Trastuzumab/ capecitabine 5. Cabozantinib	Biopsy of pulmonary metastasis	No	No	1	Growth arrest
SDC-19	M	71	Parotid gland	No	No	No	No		Primary tumor resection	No	Yes	5	Growth arrest
SDC-20	M	35	Parotid gland	No	No	No	No		Primary tumor resection	No	Yes	5	Growth arrest
Adenoid cystic carcinoma PDOs													
AdCC-1a	F	57	Lacrimal gland	Yes	No	N.a.	N.a.		Biopsy of primary tumor	No	No	0	Fungal infection
AdCC-1b	M	58	Parotid gland	Yes	No	N.a.	N.a.		Biopsy of pulmonary metastasis	No	No	0	Fungal infection
AdCC-2	M	53	Minor gland nasopharynx	No	No	N.a.	N.a.		Primary tumor resection	No	No	2	Growth arrest
AdCC-3	M	46	Parotid gland	Yes	No	N.a.	N.a.		Kidney metastasis resection	No	Yes	6	Growth arrest
AdCC-4	F	47	Minor gland maxillary sinus	Yes	Yes	N.a.	N.a.	Cyclophosphamide/ doxorubicin/cisplatin	Biopsy of primary tumor	Yes	No	1	Growth arrest
AdCC-5	M	55	Lacrimal gland	Yes	No	N.a.	N.a.		Biopsy of local recurrent lesions	Yes	No	2	Growth arrest
AdCC-6	F	57	Main bronchus	Yes	No	N.a.	N.a.		Biopsy of skin metastasis	No	No	1	Growth arrest
AdCC-7	F	33	Parotid gland	No	No	N.a.	N.a.		Primary tumor resection	No	Yes	5	Growth arrest
AdCC-8	M	60	Minor gland tongue	Yes	Yes	N.a.	N.a.	1. Vinorelbine 2. Cabozantinib	Excision of skin metastasis	No	No	2	Growth arrest
AdCC-10	M	58	Main bronchus	Yes	Yes	N.a.	N.a.	Cyclophosphamide/ doxorubicin/cisplatin	Biopsy of soft tissue metastasis	No	No	2	Growth arrest

(Table continues on next page)

AdCC-12	F	67	Parotid gland	Yes	No	N.a.	N.a.		Biopsy of pleural metastasis	No	No	1	Growth arrest
AdCC-13	M	46	Submandibular gland	Yes	No	N.a.	N.a.		Primary tumor resection	No	Yes	4	Growth arrest
Mucoepidermoid carcinoma PDOs													
MEC-1	F	64	Minor gland tongue	No	No	N.a.	N.a.		Primary tumor resection	No	No	1	Growth arrest
MEC-2	M	57	Minor gland tonsil	Yes	Yes	N.a.	N.a.	1. Gemcitabine/ cisplatin 2. Gemcitabine/ carboplatin 3. Docetaxel/carboplatin 4. Olaparib 5. Cyclophosphamide/ doxorubicin/cisplatin	Biopsy of skin metastasis	No	No	1	Growth arrest
MEC-4	F	53	Trachea	No	No	N.a.	N.a.		Primary tumor resection	No	No	4	Growth arrest
MEC-5	F	48	Parotid gland	No	No	N.a.	N.a.		Primary tumor resection	No	No	1	Growth arrest
MEC-6	M	63	Minor gland tongue	No	No	N.a.	N.a.		Primary tumor resection	No	No	0	Growth arrest
MEC-7	M	57	Parotid gland	No	No	N.a.	N.a.		Primary tumor resection	No	No	0	Growth arrest
MEC-8	M	65	Parotid gland	No	No	N.a.	N.a.		Primary tumor resection	No	Yes	5	Growth arrest
Miscellaneous													
EMC-1	M	70	Minor gland cheeck	No	No	N.a.	N.a.		Primary tumor resection	No	No	1	Growth arrest
ACiC-2	F	64	Parotid gland	Yes	No	N.a.	N.a.		Biopsy subcutaneous metastasis	No	No	2	Growth arrest
ACiC-3	M	72	Parotid gland	No	No	N.a.	N.a.		Primary tumor resection	No	No	2	Growth arrest

Abbreviations: PDO=patient derived organoid, SDC=salivary duct carcinoma, AdCC=adenoid cystic carcinoma, MEC=mucoepidermoid carcinoma, EMC=epithelial-myoepithelial carcinoma, ACiC=acinic cell carcinoma.

* Definition of successful PDO: expandable to >1*10^6 cells.

Supplementary Table 3: Used chemicals and suppliers for organoid freezing medium

Components	Company	Concentration
Fetal Calf Serum	Sigma-Aldrich	90%
Dimethyl Sulfoxide (DMSO)	Merck	10%
Y-27632 dihydrochloride	AbMole Bioscience	10 µM

Supplementary Table 4: primers used to confirm gene fusion presence in AdCC PDOs

Gene name	Primer name	Primer Sequences (5' -> 3')
EYA1	EYA1-ex6-for	GGCTGCATATGGGCAAACAC
	EYA1-ex2-rev	AGAGTTACCGAGTTTGGGGC
MYB	MYB-ex7-8-for	CCGCAGCCATTCAGAGACAC
MYBL1	MYBL1-ex11-for	AGGAAACAACTCCCAAAGATCA
	MYBL1-ex15-for	AGGTGCAACTTGATTCCTGAAA
NFIB	NFIB-ex4-rev	GACTCCAGATTTTACAAAACTATCCTC
	NFIB-ex7-rev	CAGGTATTCCGGGATGGTGG
	NFIB-ex9-rev	GAACCAAGCTAGCCCAGGTA

Supplementary Table 5: Used chemicals and suppliers for drug treatment experiments

Drug	Supplier	Product cat. #
Lapatinib	SelleckChem	S1028
Erlotinib	SelleckChem	S1023
Sunitinib malate	SelleckChem	S1042
Cisplatin	Sigma-Aldrich	P4394
Monensin	Sigma-Aldrich	M5273
Crenigacestat	MedChemExpress	HY-12449

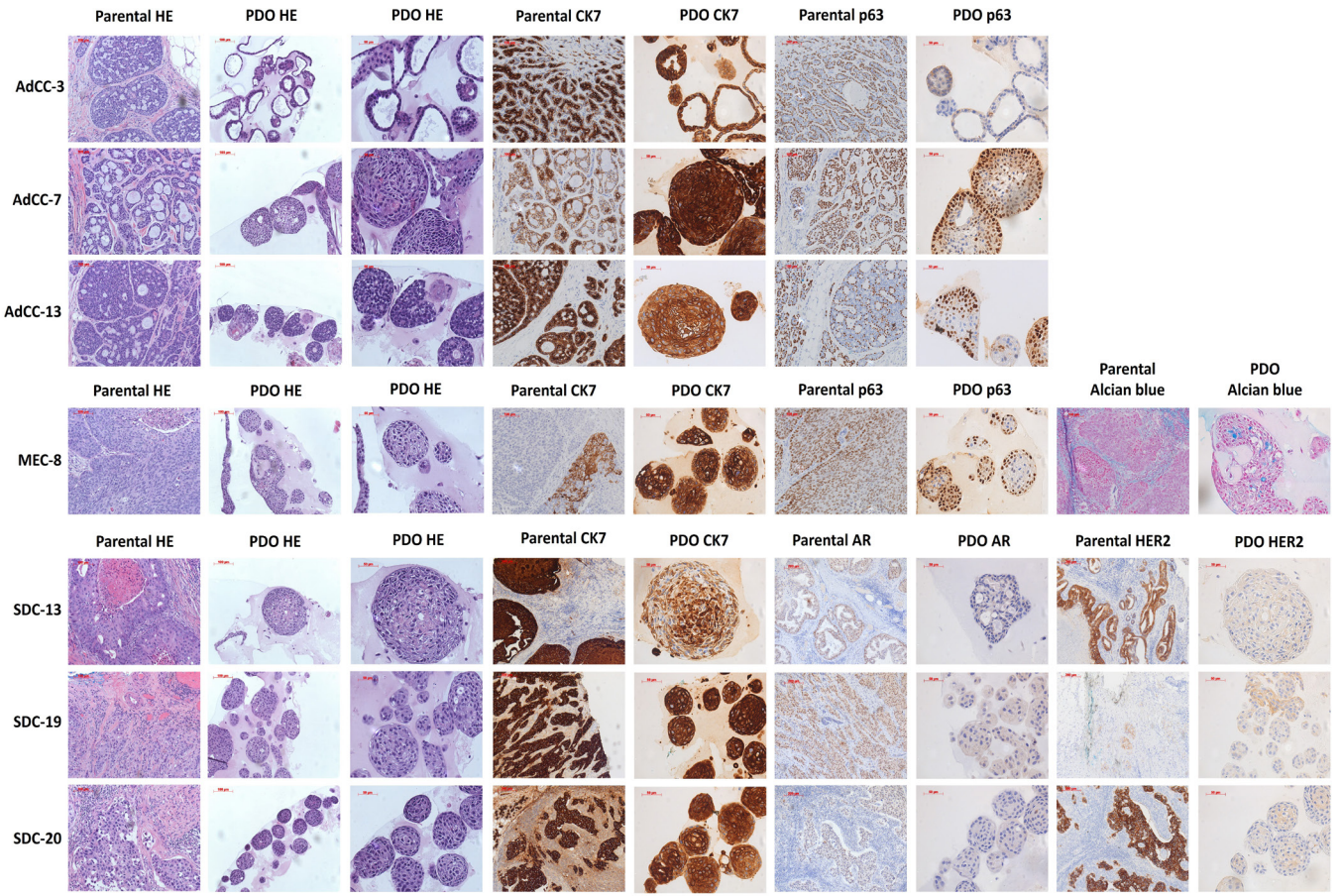

Supplementary Figure 1: Phenotype comparison between parental tissue and successful PDOs. All HE stainings and IHC was performed on the same tissue block, except for CK7 of MEC-8 in which a different tissue block was chosen demonstrating the focal positivity of the parental tissue.

CHAPTER 7

Precision oncology using organoids of a secretory carcinoma of the salivary gland treated with TRK-inhibitors

Gerben Lassche, Adriana C.H. van Engen-van Grunsven, Onno van Hooij, Tilly W. Aalders, Jetty A.M. Weijers, Emiliano Cocco, Alexander Drilon, Alexander Hoischen, Kornelia Neveling, Jack A. Schalken, Gerald W. Verhaegh*, Carla M.L. van Herpen*

*Shared last author

Under review

Abstract

The use of anticancer drugs targeting specific molecular tumor characteristics is rapidly increasing in clinical practice, but selecting patients to benefit from these remains a challenge. It has been suggested that organoid cultures would be ideally suited to test drug responses *in vitro*. Here we describe and characterize in depth a case of *ETV6-NTRK3* gene fusion-positive secretory carcinoma of the salivary glands and corresponding organoid cultures that responded and subsequently acquired resistance to TRK targeting therapy with larotrectinib. This case-culture-characterization illustrates the advances made in precision oncology, but also exposes important caveats in using organoids to predict treatment response.

Introduction

In oncological clinical practice precision medicine has gained great momentum (1). Actionable aberrations can be identified in significant proportions of tumors and patients do benefit from treatments with matching therapies, even when regular treatment options are exhausted (2,3). Nevertheless, not all patients treated with drugs that target what is considered the Achilles heel of their tumor will benefit from such treatments.

To prevent unnecessary exposure to ineffective medication, great research efforts have been made to predict treatment response. Drug screening using organoids, *i.e.* three-dimensional patient-derived stem-cell based cell cultures, can be used for this purpose (4,5). This is based on the concept that culturing and treating patients' tumor cells in a dish, while preserving genotype and phenotype, can predict *in vivo* responses.

We illustrate the potential of genetically matched therapy with the specific TRK-inhibitor larotrectinib in an *NTRK*-gene fusion positive secretory carcinoma of the salivary glands. Secretory carcinoma is a rare subtype of salivary gland cancer. It resembles secretory carcinoma of the breast and on top of that is characterized by the occurrence of an *ETV6-NTRK3* gene fusion. Usually prognosis is favorable and recurrent or metastatic disease is rare (estimated 10 year overall survival of 95%) (6,7).

We highlight important caveats in using tumor-derived organoids to predict treatment response, by correlating *in vitro* and *in vivo* responses in an *NTRK*-gene fusion positive secretory carcinoma case.

Case description

A 61-year-old man, with a medical history of recurrent pulmonary embolisms and sarcoidosis, underwent a partial parotidectomy after being referred for a lump in the left parotid region. Diagnostic pathology showed a radically excised secretory carcinoma harboring the *ETV6-NTRK3* gene fusion that is pathognomonic for this tumor (8). One-year postoperative, a dermal local recurrence was surgically removed, followed by radiotherapy (66Gy in 33 fractions). Six years hereafter, the patient presented with weight loss, headache, hemoptysis, lymph node adenopathy and subcutaneous nodules spread across the body. The diagnosis of metastatic *NTRK* gene fusion-positive secretory carcinoma in the brain, liver, lungs, skin, thyroid, bones, heart, peritoneum and lymph nodes was made. Thereupon treatment with the selective TRK inhibitor larotrectinib was initiated (compassionate use). Prior to larotrectinib treatment, a skin metastasis located at the right jaw was resected and brought into organoid

culture (hereafter referred to as pre-larotrectinib). Within two weeks after start of larotrectinib all visible skin metastases disappeared and the patient's wellbeing greatly increased. Two months after start of therapy grade 3 liver toxicity developed, which fully resolved after corticosteroid administration without larotrectinib dose adjustment. Three months after larotrectinib initiation a partial response was seen, including remission of the brain metastases (Supplementary Figure 1). Shortly hereafter, a progressive lesion in the soft tissue surrounding the right jaw was noted. In a biopsy of this lesion a high-grade transformation of the known secretory carcinoma was observed and next-generation sequencing (NGS, Radboudumc PATHv3D panel) revealed the presence of an acquired resistance mutation (*i.e. NTRK3* p.G623R) in 12.5% of tumor cells (9). This biopsy was also used for organoid culturing (hereafter referred to as post-larotrectinib progression). Palliative radiotherapy was initiated on this progressive lesion (10x3Gy). New imaging revealed progression of several metastases (lung, liver and lymph nodes). Larotrectinib treatment was however continued due to persistent remission of the brain metastases. Shortly hereafter, the patient died of respiratory insufficiency due to pulmonary lymphangitic carcinomatosis, approximately five months after start of larotrectinib therapy. The clinical course is summarized in Figure 1A.

Methods

Treatment and follow-up information

Larotrectinib treatment consisted of a twice daily oral dose of 100mg. Tumor response was monitored every 3 months. Response was scored according to RECIST version 1.1 (10). Toxicity was scored according to the Common Terminology Criteria for Adverse Events (CTCAE) version 5.0.

Organoid culturing and treatment experiments

Pre-larotrectinib and post-larotrectinib progression tumor material was processed into organoids. Organoids were digested to single cells and treated directly after seeding for 96 hours with larotrectinib and the second-generation TRK inhibitor repotrectinib. A detailed organoid culturing protocol can be found in Supplementary File 1 and Supplementary Table 1.

Phenotypic and molecular characterization of tumor material and organoids

Hematoxylin and eosin (H&E) staining was performed on 4-micron tumor sections and as well as P63, S100, GATA3 and pan-TRK immunohistochemical stainings (IHC, antibodies specified in Supplementary Table 2). Whole-exome sequencing (WES) and shallow whole-genome sequencing (sWGS) were performed on genomic DNA extracted from parental tissue and corresponding organoid cultures. For calling of somatic variants, WES of a healthy control sample of the patient was used as a reference (detailed methodology in Supplementary File

1). To validate the presence of the *ETV6-NTRK3* gene rearrangement, real-time polymerase chain reaction (RT-PCR) analysis was performed and ultra-high-molecular-weight genomic DNA of the pre-larotrectinib organoid culture was subjected to optical genome mapping (OGM, Supplementary File 1) as described previously (11).

RNA sequencing experiments

RNA sequencing was performed on ribodepleted total RNA from pre-larotrectinib parental tissue, corresponding untreated organoids and organoids treated with 1μM larotrectinib or 150nM repotrectinib for 24 hours (detailed methodology in Supplementary File 1).

Results

Organoid phenotype resemblance to parental tumor architecture

An organoid cell line could be established from the pre-larotrectinib tumor tissue (*i.e.* organoids growing for >15 passages). Unfortunately, no organoid cell line could be established from the post-larotrectinib progressive tumor tissue. The latter organoids went into senescence after 5 passages. Excellent histological mimicry was seen between both the pre-and post-larotrectinib organoids and corresponding parental tissue (Figure 1B). The H&E staining strongly suggested that organoids were derived from tumor cells. Protein expression patterns, however, diverged between parental tissues and organoids (Supplementary Figure 2). Organoid IHC profiles did not match the typical secretory carcinoma protein expression profile, as p63 was positive, S100 negative, GATA3 only weakly positive and pan-TRK negative.

Resemblance of tumor molecular background in organoids

The *ETV6-NTRK3* gene fusion that was present in both parental tissues was preserved in all 15 first passages of the pre-larotrectinib organoids, despite the negative pan-TRK IHC in the organoids (RT-PCR, Supplementary Figure 3). The *ETV6-NTRK3* gene fusion was absent in all passages of the post-larotrectinib progression organoids. Whole-exome sequencing revealed that most somatic variants matched between the pre-larotrectinib and post-larotrectinib progression parental tissues, but an *NTRK3* p.G623R resistance mutation arose in the latter. Genetic changes in organoids derived from the pre-larotrectinib tumor tissue closely resembled the parental tissue, but the organoids derived from the post-larotrectinib progression tumor tissue did not (Figure 2A). Genome-wide copy number variation (CNV) profiles showed the same close mimicry between pre-larotrectinib parental tissue and organoids and the post-larotrectinib progression parental tissue. Again, organoids derived from the post-larotrectinib progression tumor tissue were dissimilar (Figure 2B). The complex CNV profile with a large number of aberrations was largely similar to the profile detected by

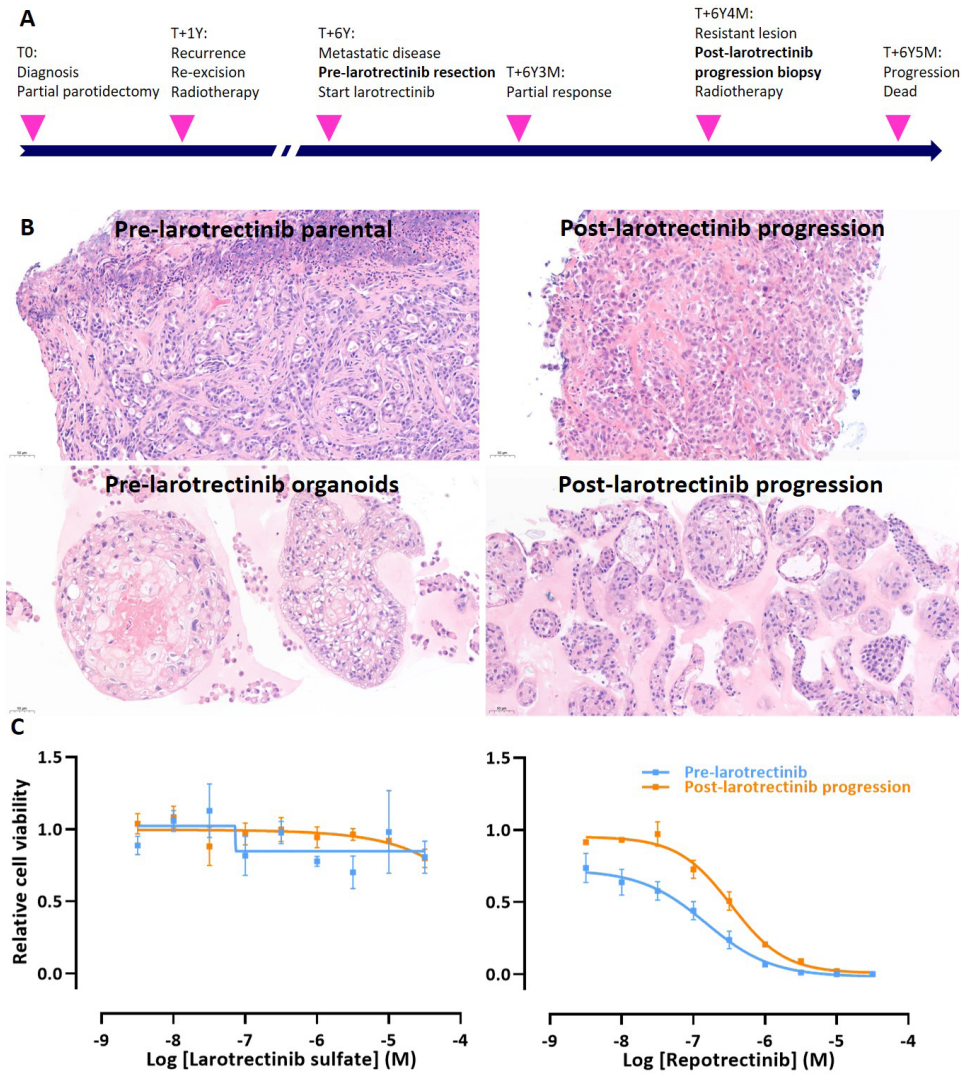

Figure 1: **A:** Timeline of the described secretory carcinoma case. **B:** Hematoxylin and Eosin (H&E) staining of pre- and post-larotrectinib progression parental tissue and corresponding organoids. The post-larotrectinib progression biopsy showed the known secretory carcinoma with high grade transformation (i.e. increased atypia, mitotic activity and proliferation index and more solid and less glandular architecture). Close phenotypic mimicry between parental tissue and organoids can be observed. **C:** Pre- and post-larotrectinib progression organoid drug screening with selective TRK inhibitor larotrectinib (left) and second generation TRK inhibitor repotrectinib (right).

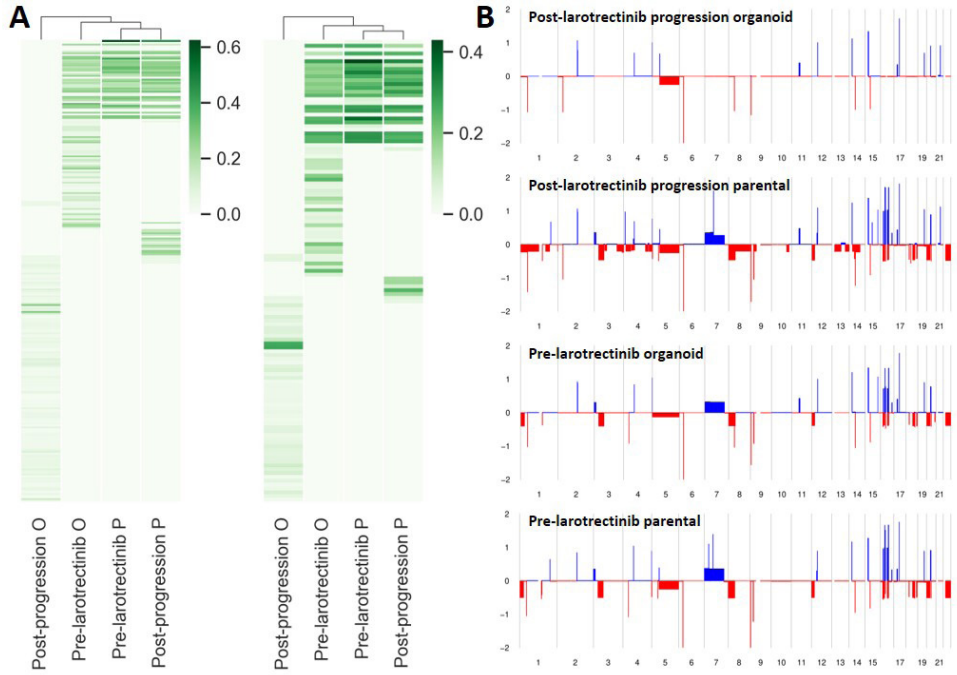

Figure 2: Molecular characterization of parental tissue and organoid cultures. **A:** Heatmap of variant allele frequencies of all somatic mutations (left) and variants with predicted moderate/high effect on protein structure (right) detected by whole-exome sequencing of pre- and post-larotrectinib progression parental tissue (P) and corresponding organoids (O). Majority of identified variants present in het pre-larotrectinib parental can be identified in the corresponding organoids, which is not the case for the post-larotrectinib progression organoid. **B:** Shallow whole-genome sequencing copy number variation (CNV) profiles of pre- and post-larotrectinib progression parental tissue and corresponding organoids. In the CNV profiles of both parental tissue and the pre-larotrectinib organoid cultures close mimicry can be seen, but the CNV profile of the post-larotrectinib progression organoid diverges.

OGM of pre-larotrectinib tumor tissue derived organoids. OGM also confirmed the presence of the rearrangement of chromosomes 12p13.2 and 15q25.3, leading to the *ETV6-NTRK3* gene fusion in the pre-larotrectinib organoids (insufficient post-larotrectinib progression organoids were available for OGM). Several other structural variants, such as chromothripsis of chromosome 18, and an overall complex karyotype were seen (Supplementary Figure 4). In total, the molecular characterization of the organoids indicates that the pre-larotrectinib culture has a very complex karyotype and that it closely resembled its parental tissue. The genome of post-larotrectinib progression organoids diverged despite tumor cell presence on H&E staining.

Organoid response to TRK-inhibition

Organoids derived from pre-larotrectinib and post-larotrectinib progression tumor tissue did not show any sensitivity to larotrectinib (Figure 1C). Both did show sensitivity to the multikinase inhibitor repotrectinib, with an approximately 2-fold lower half maximal inhibitory concentration (IC_{50}) for the pre-larotrectinib tissue derived organoids compared to the post-larotrectinib progression tissue derived organoids (IC_{50} of 151nM (95%-confidence interval (CI): 93-223nM) and 270nM (95% CI: 270-421nM), respectively) (Figure 1C).

Resemblance of tumor transcriptome and transcriptomic changes induced by TRK inhibition

In the principal component analysis of the RNA sequencing data, all organoid samples clustered together, apart from the parental tissue (Supplementary Figure 5A). This gross transcriptome dissimilarity between parental and corresponding organoids was also seen in the heatmaps including all genes or differentially expressed genes (DEGs) only (Supplementary Figures 5B-C).

Untreated organoids clustered together, as were TRK inhibitor-treated organoids, except for one repotrectinib treated outlier (Figures 3A-B, Supplementary Figure 5A). DEGs after larotrectinib treatment could be identified and did show overlap with DEGs after repotrectinib treatment (Figures 3C-D). These DEGs include cAMP response element-binding protein (CREB) target genes, which is a known downstream transcription factor of TRK (12,13). Removal of the repotrectinib outlier did not affect this (Supplementary Figures 6A-C). The overlap between repotrectinib and larotrectinib DEGs indicates that both TRK inhibitors partially induce the same early transcriptome changes. Pathways influenced by the common DEGs include pathways involved in system development, cell differentiation and cellular signaling (Supplementary Figure 6D). Combined with the treatment assays, these transcriptomic results indicate that larotrectinib and repotrectinib exert intracellular effects, but that the organoids do not depend on active TRK signaling. *In vitro* response to the multikinase inhibitor repotrectinib might be explained by off-target effects.

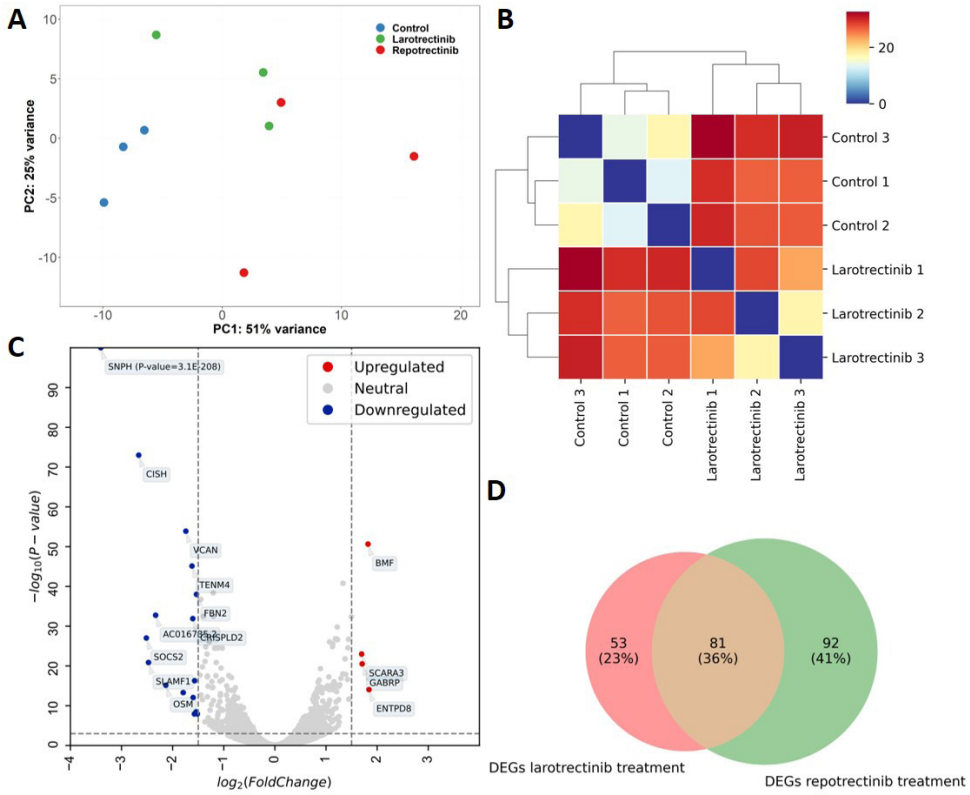

Figure 3: Transcriptome analysis of organoids derived from pre-larotrectinib tumor tissue, treated with TRK inhibitors larotrectinib or repotrectinib. **A:** Principal component analysis of RNA sequencing data of replicates of untreated (control) and larotrectinib or repotrectinib treated organoids. **B:** Heatmap of Euclidean distances between regularized log transformed count data of all genes for control and larotrectinib treated organoids. Group-wise clustering of larotrectinib treated and untreated organoids can be seen. **C:** Volcano plot, in which the log2 transformed fold-change on the x-axis is plotted against the log10 transformed adjust P-values on the y-axis. Genes in blue and red are differentially expressed (|log2 fold-change| ≥1.5, p-value <0.00001) upon treatment with larotrectinib. **D**: Venn diagram showing overlap in significant differentially expressed genes (DEGs) upon treatment with larotrectinib (left) or repotrectinib (right).

Discussion

Here we describe a clinical case that illustrates major advances made in recent oncological clinical practice: 1. histology agnostic treatment of a patient with a rare cancer using targeted therapy tailored to the molecular features of the tumor, and 2. using an *in vitro* organoid culture model to predict the *in vivo* drug response. To do so, the first *NTRK3* fusion positive organoid model for secretory carcinoma was established. On the other hand, this study also revealed some major challenges: 1. the acquisition of resistance under therapeutic pressure and 2. mismatches between clinical response and organoid response. The latter has been investigated in depth using a plethora of NGS techniques. The pitfalls revealed here, limits bench-to-bedside translation in this N=1 study.

A critical step prior to drug screening using organoids is evaluation of the presence of tumor cells and assessment of the organoid's resemblance to the parental tumor genome and phenotype (5). Selection of a specific subclone, either physically by culturing only the biopsied portion of a tumor or by selective pressure from growth factors in the culture medium, can compromise the required representativeness. Subclonal expansions can be detected in 95% of all cancers, and this may lead to sampling artefacts (14). Organoids derived from several single tumor cells from different tumor areas have been shown to reflect genetic tumor heterogeneity and, partly because of this, respond variably to chemotherapy and targeted therapy (15). In our study, the organoids derived from the pre-larotrectinib tissue effectively resembled the genome of the parental tissue, including the characteristic *ETV6-NTRK3* translocation. However, the post-larotrectinib progression organoids diverged and did not express the *ETV6-NTRK3* fusion transcript, possibly due to the selection of a genetically highly divergent gene fusion negative subclone.

Even though genomic mimicry was evident in pre-larotrectinib organoids, transcriptomic and phenotypic divergence was observed (*i.e.* expression of *ETV6-NTRK3* fusion transcript with negative TRK IHC). One explanation of the discrepant tumor and organoid transcriptomes is contamination of tumor tissue with benign cells, whilst organoids are typically composed of tumor cells only. A second explanation could be the influence of the microenvironment (in the organoid cultures the medium components) on the transcriptome. One report on an organoid-to-parental comparison in mouse gut organoids indeed indicated that the transcriptome is strongly influenced by culture conditions (16). Our used culture medium for instance contains supraphysiological levels of epidermal growth factor and components enhancing Wnt-signaling (R-Spondin and CHIR99021). These growth factors may induce survival pathways that bypass the need for NTRK signaling, and hence possibly explain the lack of larotrectinib sensitivity. Absent TRK expression in the presence of the *NTRK3* fusion transcript could also be the result of post-transcriptional or post-translational regulation.

Undoubtedly, the organoid culture protocol used in this study is not optimal. For TRK-driven tumors, earlier studies have demonstrated that it is possible to culture patient-derived cells (in 2D or in animal models) with excellent genomic mimicry and that corresponding responses to TRK-inhibition could be observed (17,18). Organoid models however have several advantages over 2D cell lines and animal models, which include their enhanced recapitulation of the tumor architecture and heterogeneity, their initiation success rate and their utility for high-throughput drug screenings (4,19). Organoid culturing protocols are often tailored to specific cancer types but individual tumors or tumor subtypes differ and may therefore require individualized culture conditions. Although obviously limited by the fact that in this study only one case is presented, shortcomings using this approach are exposed. These shortcomings can limit the use of organoids for response prediction, despite reported similarities between *in vivo* and organoid drug sensitivities in other studies (20,21).

Our study emphasizes the importance of thorough characterization of organoids before extrapolating *in vitro* reactions to possible clinical responses. Ideally, this should include a comparison of critical features in the genome, transcriptome and proteome.

References

1. Yates LR, Seoane J, Le Tourneau C, et al. The European Society for Medical Oncology (ESMO) Precision Medicine Glossary. Annals of oncology : official journal of the European Society for Medical Oncology 2018;29(1):30-35. (In eng). DOI: 10.1093/annonc/mdx707.
2. Larson KL, Huang B, Weiss HL, et al. Clinical Outcomes of Molecular Tumor Boards: A Systematic Review. JCO Precis Oncol 2021;5 (In eng). DOI: 10.1200/po.20.00495.
3. van der Velden DL, Hoes LR, van der Wijngaart H, et al. The Drug Rediscovery protocol facilitates the expanded use of existing anticancer drugs. Nature 2019;574(7776):127-131. (In eng). DOI: 10.1038/s41586-019-1600-x.
4. Drost J, Clevers H. Organoids in cancer research. Nat Rev Cancer 2018;18(7):407-418. (In eng). DOI: 10.1038/s41568-018-0007-6.
5. Driehuis E, Kretzschmar K, Clevers H. Establishment of patient-derived cancer organoids for drug-screening applications. Nat Protoc 2020;15(10):3380-3409. (In eng). DOI: 10.1038/s41596-020-0379-4.
6. Boon E, Valstar MH, van der Graaf WTA, et al. Clinicopathological characteristics and outcome of 31 patients with ETV6-NTRK3 fusion gene confirmed (mammary analogue) secretory carcinoma of salivary glands. Oral oncology 2018;82:29-33. (In eng). DOI: 10.1016/j.oraloncology.2018.04.022.
7. Lassche G, van Boxtel W, Ligtenberg MJL, van Engen-van Grunsven ACH, van Herpen CML. Advances and challenges in precision medicine in salivary gland cancer. Cancer Treat Rev 2019;80:101906. (In eng). DOI: 10.1016/j.ctrv.2019.101906.
8. Skalova A, Vanecek T, Sima R, et al. Mammary analogue secretory carcinoma of salivary glands, containing the ETV6-NTRK3 fusion gene: a hitherto undescribed salivary gland tumor entity. The American journal of surgical pathology 2010;34(5):599-608. (In eng). DOI: 10.1097/PAS.0b013e3181d9efcc.
9. Steeghs EMP, Kroeze LI, Tops BBJ, et al. Comprehensive routine diagnostic screening to identify predictive mutations, gene amplifications, and microsatellite instability in FFPE tumor material. BMC cancer 2020;20(1):291. (In eng). DOI: 10.1186/s12885-020-06785-6.
10. Eisenhauer EA, Therasse P, Bogaerts J, et al. New response evaluation criteria in solid tumours: revised RECIST guideline (version 1.1). European journal of cancer (Oxford, England : 1990) 2009;45(2):228-47. (In eng). DOI: 10.1016/j.ejca.2008.10.026.
11. Neveling K, Mantere T, Vermeulen S, et al. Next-generation cytogenetics: Comprehensive assessment of 52 hematological malignancy genomes by optical genome mapping. Am J Hum Genet 2021;108(8):1423-1435. (In eng). DOI: 10.1016/j.ajhg.2021.06.001.
12. Zhang X, Odom DT, Koo SH, et al. Genome-wide analysis of cAMP-response element binding protein occupancy, phosphorylation, and target gene activation in human tissues. Proc Natl Acad Sci U S A 2005;102(12):4459-64. (In eng). DOI: 10.1073/pnas.0501076102.
13. Cocco E, Scaltriti M, Drilon A. NTRK fusion-positive cancers and TRK inhibitor therapy. Nature reviews Clinical oncology 2018;15(12):731-747. (In eng). DOI: 10.1038/s41571-018-0113-0.
14. Dentro SC, Leshchiner I, Haase K, et al. Characterizing genetic intra-tumor heterogeneity

across 2,658 human cancer genomes. Cell 2021;184(8):2239-2254.e39. (In eng). DOI: 10.1016/j.cell.2021.03.009.

15. Roerink SF, Sasaki N, Lee-Six H, et al. Intra-tumour diversification in colorectal cancer at the single-cell level. Nature 2018;556(7702):457-462. (In eng). DOI: 10.1038/s41586-018-0024-3.
16. Lu J, Krepelova A, Rasa SMM, et al. Characterization of an in vitro 3D intestinal organoid model by using massive RNAseq-based transcriptome profiling. Sci Rep 2021;11(1):16668. (In eng). DOI: 10.1038/s41598-021-96321-8.
17. Cocco E, Lee JE, Kannan S, et al. TRK xDFG Mutations Trigger a Sensitivity Switch from Type I to II Kinase Inhibitors. Cancer discovery 2021;11(1):126-141. (In eng). DOI: 10.1158/2159-8290.Cd-20-0571.
18. Cocco E, Schram AM, Kulick A, et al. Resistance to TRK inhibition mediated by convergent MAPK pathway activation. Nat Med 2019;25(9):1422-1427. (In eng). DOI: 10.1038/s41591-019-0542-z.
19. Kopper O, de Witte CJ, Lõhmussaar K, et al. An organoid platform for ovarian cancer captures intra- and interpatient heterogeneity. Nat Med 2019;25(5):838-849. (In eng). DOI: 10.1038/s41591-019-0422-6.
20. Verduin M, Hoeben A, De Ruysscher D, Vooijs M. Patient-Derived Cancer Organoids as Predictors of Treatment Response. Frontiers in oncology 2021;11:641980. (In eng). DOI: 10.3389/fonc.2021.641980.
21. Wensink GE, Elias SG, Mullenders J, et al. Patient-derived organoids as a predictive biomarker for treatment response in cancer patients. NPJ Precis Oncol 2021;5(1):30. (In eng). DOI: 10.1038/s41698-021-00168-1.
22. Love MI, Huber W, Anders S. Moderated estimation of fold change and dispersion for RNA-seq data with DESeq2. Genome Biol 2014;15(12):550. (In eng). DOI: 10.1186/s13059-014-0550-8.

Supplementary information

Supplementary File 1: extended methods

Organoid culturing and treatment experiments

Tumor material was collected in Advanced Dulbecco's Modified Eagle Medium/Ham's F-12 (AdDMEM/F12) supplemented with HEPES Buffer Solution 10mM, GlutaMAX Supplement 2mM, Primocin 100µg/ml (AdDMEM/F12+++) and fungizone. Tissue was minced, enzymatically digested using Collagenase type 2 (0.5mg/ml, specific activity 127.5U/ml) and embedded in 100% Matrigel at a density of 1000 cells/µl. Culture medium, consisting of AdDMEM/F12+++ supplemented with B-27 (1X), epidermal growth factor (50ng/ml), A83-01 (500nM), 12.5% Noggin conditioned medium, 10% R-Spondin conditioned medium, CHIR99021 (0.3µM) and Y-27632 dihydrochloride (10µM) was refreshed biweekly. Organoids were passaged by enzymatic digestion with TrypLE Express Enzyme into single cells approximately every 1-3 weeks in a split rate ranging from 1:1-1:7, depending on the growth rate.

For treatment experiments, organoids were digested to single cells using TrypLE Express Enzyme and subsequently seeded at a density of 400 cells/µl in 5µl discs of 70% Matrigel (diluted with AdDMEM/F12+++) in a 96-wells culture plate. Directly after seeding treatment commenced for 96 hours in a concentration ranging from -8.5 to -4.5 log(M). Cells used for transcriptome analysis were treated with 1µM larotrectinib or 150nM repotrectinib for 24 hours. Cell viability was determined using CellTiter-Glo Luminescent Cell Viability Assays (Promega). Relative cell viability was calculated to vehicle (DMSO) treated cells and a non-linear regression sigmoidal dose-response (variable slope) analysis was performed using Graphpad Prism 9. All used chemicals and suppliers are listed in Supplementary Table 1.

Immunohistochemistry

Organoids were fixated using 4% paraformaldehyde and processed for embedding in paraffin. Four micrometer thick sections of parental tissue and paraffin embedded organoids were used for IHC. For IHC, antibodies targeting P63, GATA3, S100 and pan-TRK (Supplementary Table 2), were used on a semi-automatic Labvision Immunostainer 480/360 (Thermo Fisher Scientific). Immunohistochemistry was assessed by an expert salivary gland pathologist (AvEvG).

Whole-exome sequencing

Whole-exome sequencing (WES) was performed on a peripheral blood (buffy coat) sample as germline control, snap frozen tissue of the two tumor samples used for organoid culturing and both the pre- and post-larotrectinib progression organoid cultures (second or third passage). DNA was isolated using the QIAamp DNA Mini Kit, according to the manufacturers'

protocol (Qiagen). Sample preparation and hybridization capture was performed according to SureSelectXT Target Enrichment System for Illumina Paired-End Sequencing Library protocol v.1.8, using the Agilent SureSelectXT Human All Exon v7 capture library (5191-4006 Agilent Technologies). Sequencing was performed using a NovaSeq6000 (Illumina). Median autosomal sequencing depth ranged from 280-337X. Variant calling was performed using the Illumina DRAGEN v3.8.4 Somatic Variants workflow, using genome hg19 and the germline sample as references. Called variants were annotated using the Ensembl Variant Effect Predictor (VEP) tool and only variants both covered in the VEP read-out and Agilent SureSelect Human All Exon V7 gene panel were further processed. Heatmaps of VAFs of all variants that passed quality control and variants with predicted high or moderate impact on protein function (assessed by VEP) were created using Python version 3.8 with the Matplotlib, Pandas, Numpy and Seaborn packages.

Shallow whole-genome sequencing

The same parental tissue and organoid DNA samples as used for WES were used for shallow whole-genome sequencing. Samples were processed using the NEBNext® Ultra® II DNA Library Prep Kit for Illumina, according to the manufacturers' protocol (New England Biolabs). Sequencing was performed using a NovaSeq6000 (Illumina). After read mapping using genome hg19 as reference, QDNAseq v1.32 was used to call CNV events and create plots, with a bin size of 10kb. Median autosomal sequencing depth over the genome ranged from 1.67-2.62X.

Optical genome mapping and real-time polymerase chain reaction

For optical genome mapping (OGM) ultra-high-molecular-weight (UHMW) genomic DNA (gDNA) was extracted out of $1.5x10^6$ organoid cells derived from the pre-larotrectinib tissue sample using the Bionano Prep SP Blood a Cell Culture DNA Isolation Kit following manufacturers' instructions (Bionano Genomics). UHMW gDNA was subsequently fluorescently labelled using the Bionano Prep Direct Label and Stain kit (Bionano Genomics). Fluorescently labeled gDNA samples were loaded on a Saphyr Chip and read out on a Saphyr System (Bionano Genomics) to generate 1200 gigabase of data (effective molecule coverage of 303X). Bioinformatic processing was performed using the rare variant pipeline of Bionano Solve v3.6.1, following earlier published protocols (11). A panel of control samples was used to filter unique variants in the organoid sample, as described previously (11). All structural variants were visualized in a circos plot.

For real-time polymerase chain reaction, total RNA was isolated using TRIzol Reagent (Thermo Fisher Scientific). Random-primed reverse transcribed RNA was used as input for real-time PCR using LightCycler 480 SYBR Green I Master (Roche Diagnostics) and 5'- ACCACATCATGGTCTCTGTCTCCC-3' as *ETV6* forward primer and 5'-

CAGTTCTCGCTTCAGCACGATG-3' as *NTRK3* reverse primer. PCR products were purified after 2% agarose gel electrophoresis using QIAquick Gel Extraction Kit (Qiagen), and products were analyzed by Sanger sequencing.

RNA sequencing

Total RNA was isolated using TRIzol™ Reagent (Invitrogen) and column purified using the RNeasy Plus Mini Kit (Qiagen). Libraries were prepared using the NEBNext Ultra II Directional RNA Library Prep Kit for Illumina and depleted from ribosomal RNA using NEBNext® rRNA Depletion Kit, both according to manufacturers' instructions (New England Biolabs). Sequencing was performed using a NovaSeq6000 (Illumina), aimed at a yield of 20 million paired-end reads of 150 bps per sample. Base calling, and quality check was performed with the Illumina data analysis pipeline RTA3.4.4 and Bcl2fastq v2.20. Trimmed reads were mapped to reference genome GRCh37.75. DESeq2 v1.34.0 in R version 4.1.2 was used to identify differentially expressed genes (DEGs) between parental, untreated organoids and larotrectinib or repotrectinib treated organoids (22). Principal component analysis was performed using DESeq2. Heatmaps for sample-to-sample comparison were created using Euclidean distances between regularized log transformed count data of all genes and the complete linkage method. To create heatmaps of DEGs, z-scores of regularized log transformed count data, calculated using DESeq2, were used. The 50 genes with a 2-log fold change ≤-1 or ≥1 with the lowest adjusted p-value were used as input. Heatmaps, volcano plots and Venn diagrams were created using the matplotlib, seaborn, pandas, numpy, matplotlib venn and bioinfokits packages in Python v3.8.8.

For pathway analysis, common DEGs after larotrectinib and repotrectinib treatment were used as input. The online application programming interface of g:Profiler (part of the ELIXIR infrastructure) was used for pathway analysis.

Supplementary Table 1: Chemicals and suppliers used for organoid culturing

Chemical	Company	Catalog number
Matrigel GFR, Phenol Red free	Corning	356321
Collagenase Type 2	Worthington	LS004176
Advanced DMEM/F12	Thermo Fisher Scientific	12634-010
Primocin	Invivogen	Ant-pm-1
HEPES Buffer Solution	Thermo Fisher Scientific	15630-056
GlutaMAX Supplement	Thermo Fisher Scientific	35050-038
B-27 Supplement	Thermo Fisher Scientific	17504-044
EGF	PeproTech	AF-100-15
A 83-01	Tocris Bioscience	2939
Noggin: CM recombinant HEK293T cells	-	-
Cultrex-HA-R-Spondin-1-Fc 293T cells	Amsbio	3710-001-01
Y-27632 dihydrochloride	AbMole Bioscience	M1817
CHIR99021	Sigma-Aldrich	SML1046
TrypLE Express Enzyme	Thermo Fisher Scientific	12605-010
Larotrectinib (LOXO-101)	Selleck Chemical	S7960
Repotrectinib (TPX-0005)	Selleck Chemical	S8583
CellTiter-Glo® Luminescent Cell Viability Assay	Promega	G7573

Supplementary Table 2: Antibodies used for immunohistochemistry

Antibody	Product number	Supplier	Dilution used
P63	4A4	Immunologic	1:3000
GATA3	L50-823	Cell Marque	1:100
S100	GA504	DAKO Agilent	Ready-to-use
Pan-TRK	EPR17341	Abcam	1:25

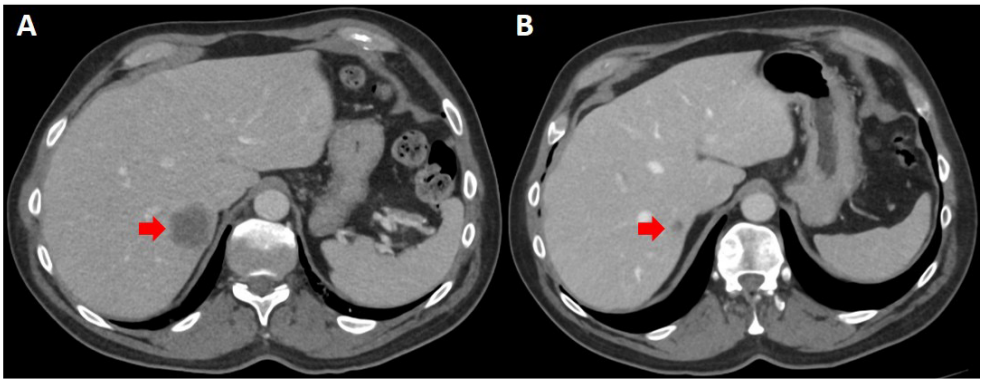

Supplementary Figure 1: Computed tomography scans of the liver prior to start treatment (**A**) and 3 months after therapy (**B**). Red arrows indicate the location of a liver metastasis. A partial response according to RECIST was observed.

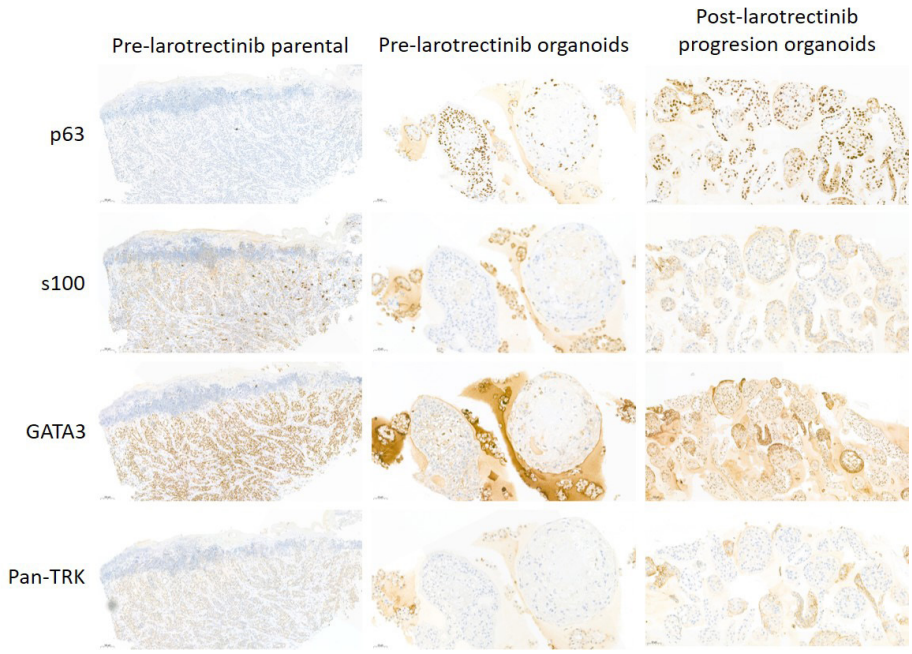

Supplementary Figure 2: Immunohistochemical stains for P63, S100, GATA3 and pan-TRK in organoid cultures (derived from pre- and post-larotrectinib progression tissue) and the pre-larotrectinib parental tissue. Pre-larotrectinib parental tissue showed a staining pattern as expected in a secretory carcinoma, *i.e.* positive for GATA3, S100, and pan-TRK (moderately positive). P63 staining was negative. In the corresponding organoids p63 was positive, S100 negative, GATA3 only weakly positive and pan-TRK negative. Post-larotrectinib progression parental tissue IHC could not be performed due to tissue shortage after the molecular analysis, but corresponding organoids did also not match an expression profile as expected in a secretory carcinoma.

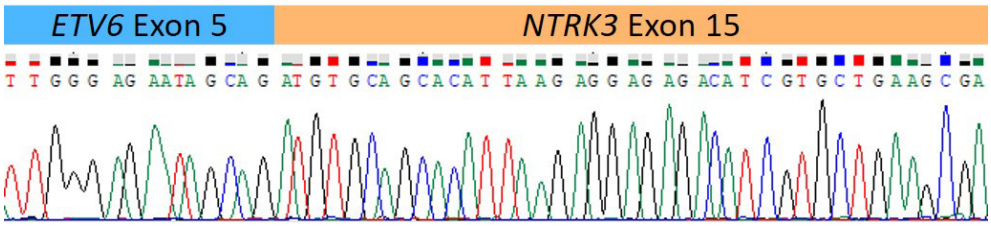

Supplementary Figure 3: Histogram of a Sanger sequenced PCR product, generated using a forward primer in *ETV6* and a reverse primer in *NTRK3*. The expected gene fusion transcript of *ETV6* exon 1-5 (NM_001987) and *NTRK3* exons 15-19 (NM_002530) is detected.

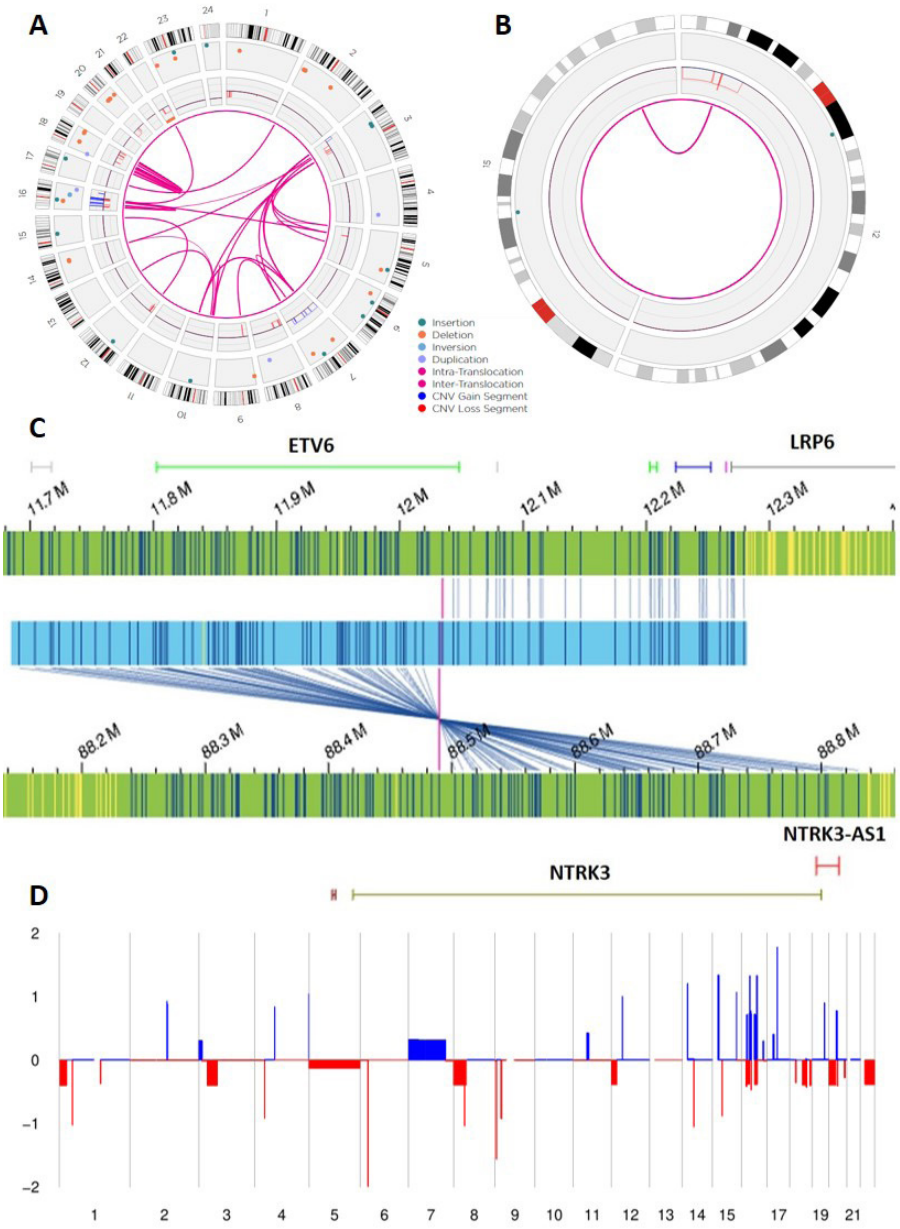

Supplementary Figure 4: Optical genome mapping (OGM) of ultra-high-molecular-weight genomic DNA of organoids derived from pre-larotrectinib tumor tissue. **A**: Circos plot of all chromosomes. Outer circle: chromosome G-banding patterns, second circle: structural variants, third circle: copy number variations (CNV), inner circle: translocations. A complex genome regarding structural variants can be observed, with chromothripsis on chromosome 18. **B**: Circos plot zooming in on chromosome 12 and 15. The *ETV6-NTRK3* gene fusion is preserved **C**: Genome map of chromosome 12 and 15 showing the *ETV6-NTRK3* translocation. Green bars: reference genome, blue bar, sample genome map. **D**: CNV pattern of the pre-larotrectinib organoids derived from shallow whole-genome sequencing. The CNV patterns matches the CNV pattern identified in OGM.

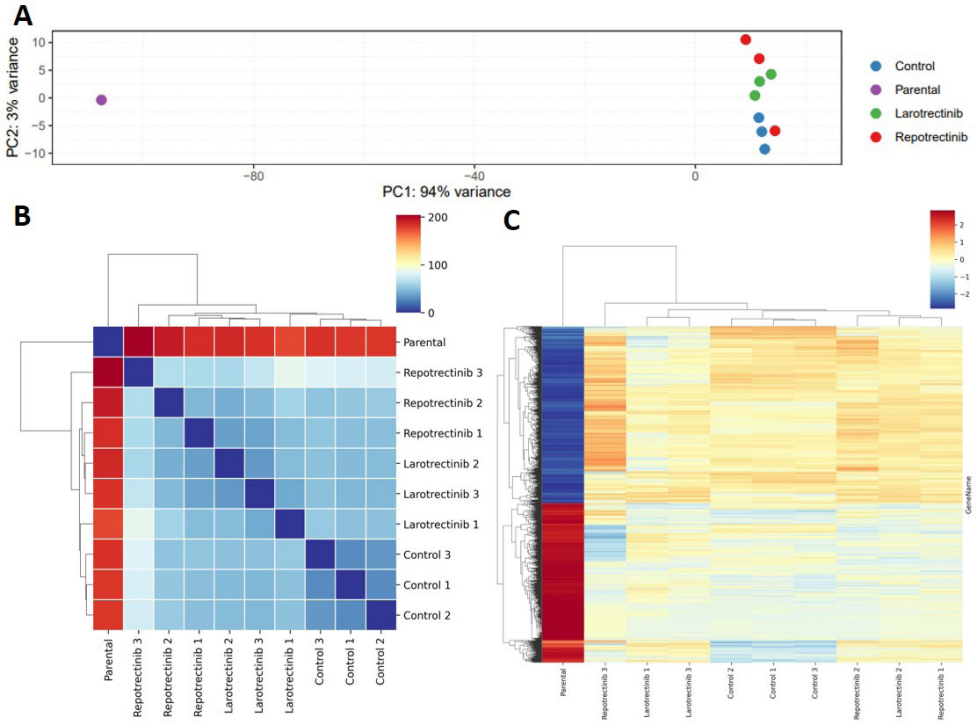

Supplementary Figure 5: Transcriptome analysis of pre-larotrectinib parental tissue and untreated and larotrectinib/repotrectinib treated organoids. **A**: principal component analysis of RNA sequencing data of the parental tissue and the organoids. The organoid conditions cluster together, although one repotrectinib replicate does not cluster to the other replicates. The parental tissue is distinct from each of the organoid samples. **B**: Heatmap of Euclidean distance between regularized log transformed count data of all genes. Parental tissue expression profile differs greatly from expression profiles in the treated and untreated organoids. **C**: Heatmap of Z-scores of differentially expressed genes (|2log fold change| >1) that significantly differed between each of the samples ($p<0.00001$). Parental tissue differs from all other samples and replicates of other conditions cluster together.

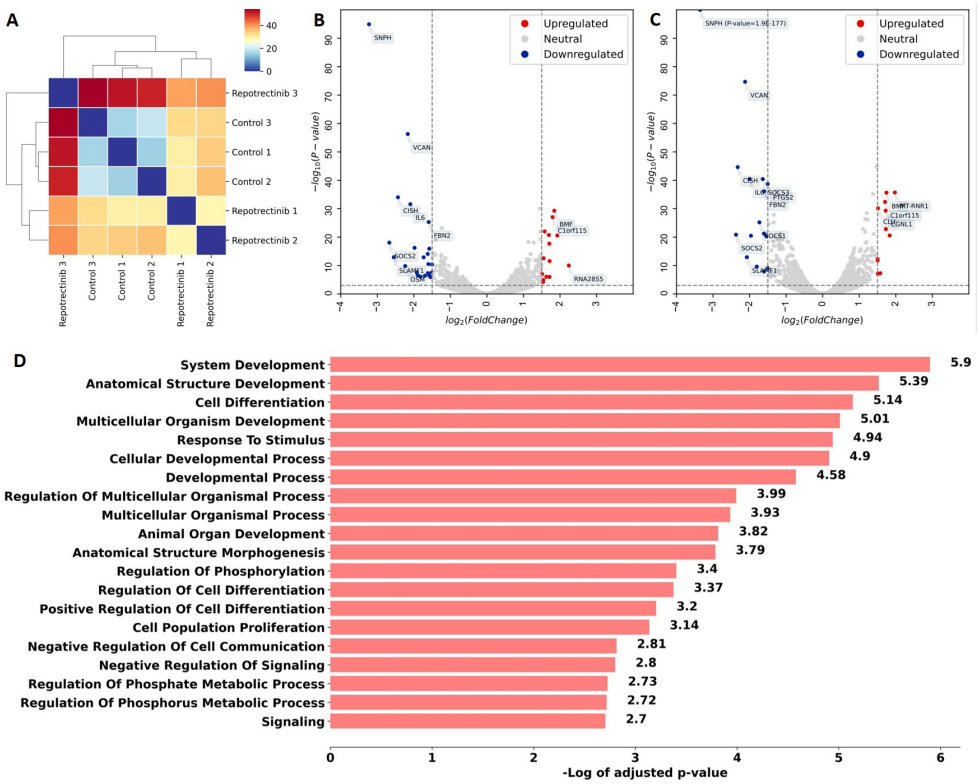

Supplementary Figure 6: Transcriptome analysis of repotrectinib treated organoids. **A**: Heatmap of Euclidean distance between regularized log transformed count data of all genes. One repotrectinib replicate differs from the other replicates (repotrectinib 3). **B**: Volcano plot, in which the log2 transformed fold-change on the x-axis is plotted against the log10 transformed adjust P-values on the y-axis. Genes in blue and red are differentially expressed (|log2 fold-change| ≥1.5, p-value <0.00001) upon treatment with repotrectinib. **C** Volcano plot as described in **B**, with exclusion of outlier 'repotrectinib 3'. **D**: Top 20 most significant biological processes regulated by genes that are differentially expressed upon treatment with TRK inhibitors, larotrectinib or repotrectinib.

PART 4:
General discussion, future perspectives and summaries

CHAPTER 8

General discussion and future perspectives

Introduction

The results described in this thesis aimed to translate salivary gland cancer (SGC) tumor biological insights to the clinic. SGC is a rare cancer, and the systemic treatment of SGC is challenging due to its heterogeneous nature. SGC can be subdivided into 22 subtypes that differ regarding tumor biology (1). Systemic treatment options are therefore limited, and it is difficult to perform clinical studies for rare cancers (2). By studying the SGC cancer biology, SGC patients may benefit from the advances made in common cancers. This thesis expands the current knowledge on tumor genetics of different SGC subtypes, pathway analysis to predict treatment response in salivary duct carcinoma (SDC) and it describes the development, characterization and utility of organoid models in SGC. The different parts of this thesis have their strengths and limitations, which will be discussed in this chapter and will be put in the perspective of the current literature. Besides this, perspectives for future research and implementation in the clinic will be given.

Part 1: Unraveling tumor genetics of salivary gland cancer

In chapter 2 of this thesis, differences in tumor genetics between SGC subtypes and actionable aberrations have been described. For this, DNA and RNA was extracted out of 121 SGC samples. Gene fusion analysis was performed using a customized RNA-based targeted next-generation sequencing (NGS) panel and DNA was sequenced using a targeted NGS panel that includes 523 cancer related genes. Gene fusion analysis led to detection of a fusion transcript in half of all SGC cases. Gene fusions are considered to be important drivers of cancer and several subtypes of SGC depend on this type of genetic aberration for their proliferation (3). Gene fusions are notoriously hard to detect, as almost all chromosomal breaking points occur in intronic regions and can consequently not be detected by NGS panels sequencing exonic DNA regions. RNA-based sequencing panels can overcome this, which was used in the work described. However, the targeted approach used by us can only detect gene fusions if probes for one of the 5' or 3' partner genes is present in the panel. The identified fraction by us is thus an underestimation of the true fraction of SGCs with gene fusions in their genome. Besides this, the relative short reads obtained in regular NGS cannot always capture the complexity of the gene fusions present. For instance, in one adenoid cystic carcinoma (AdCC) case described in chapter 3 a triple gene fusion has been detected (*MYBL1-EYA1-NFIB)*, a novelty not earlier described in literature. Due to the short reads, two individual breaking points or NGS reads were identified. Their coherence could be substantiated by means of long-range qPCR analysis, a step requiring a more laborious rational design on a case-by-case basis. Newer techniques, such as optical genome mapping, which uses ultra-long genomic DNA

as input, can overcome this (4). This technique was used in chapter 7 and showed that it can identify several structural variants at a high resolution in a complex genome.

Detection of gene fusions can be of diagnostic importance and is regularly used in the clinic to distinguish different subtypes. Indeed, the majority of gene fusions that have been identified were pathognomonic to distinct SGC subtypes: *MYB-NFIB* for AdCC, *CRTC1-MAML2* for mucoepidermoid carcinoma (MEC), and *ETV6-NTRK3* for secretory carcinoma. However, the biological functional relation between different gene fusions and the putative role in cancer development and/or progression needs further investigation. For instance, due to the loss of the last exons of *MYB* in the *MYB-NFIB* gene fusion, the negative regulatory domain (NRD) of *MYB* is lost, while the DNA-binding and transactivation domains are preserved. But not in all cases the NRD is lost, suggesting other mechanisms of *MYB* activation are in play. A mechanistic study suggests that juxtaposition of super-enhancers located at the *NFIB* locus adjacent to *MYB* seem to drive *MYB* overexpression (5). In contrast to *MYB-NFIB* gene fusions, in which the 5' fusion partner is overexpressed, *ETV6-NTRK3* fusions mainly involve active signaling activity of the 3' fusion partner. Homodimerization of the chimeric fusion protein encoded by this gene fusion or heterodimerization with wildtype ETV6 leads to ligand-independent constitutively active TRK-signaling (although *ETV6* does not contain a typical dimerization domain) (6, 7). These examples underline that detection of recurring gene fusions should be followed by biological functional research into process that are deregulated by the fusion proteins or truncated proteins.

In this light, two recurring gene fusions detected in chapter 2 are of interest. The *CRTC1-MAML2* gene fusions that were found in MEC cases and the fusions involving *RAD51B* in SDC cases. The *MAML2* fusions have been previously detected in MEC and could lead to activated epidermal growth factor receptor (EGFR) signaling (8, 9). EGFR is indeed frequently overexpressed (in immunohistochemistry studies) in MEC (10). EGFR is a putatively actionable target in MEC. Effects of the *RAD51B* gene are more speculative and should be further studied. In the four cases in which such a fusion was present, bi-allelic loss of this gene (*i.e.,* loss of the second wild-type allele) could not be detected, but due to haploinsufficiency homologous recombination (HR) deficiency still may occur (11). HR-deficient tumors can be targeted with poly (ADP-ribose) polymerase (PARP) inhibitors, such as olaparib, which are interesting drugs for future clinical studies in *RAD51B*-affected tumors.

The abovementioned speculation on actionability of genetic aberrations illustrates why the clinically most relevant finding of chapter 2, the fraction of patients with actionable aberrations, should be interpreted with caution. Overall, targeted NGS (at the RNA and DNA level) could detect these actionable aberrations in 54% of the cases, although this differed per subtype (ranging between 82% in SDC and 28% in AdCC). This number is however

speculative, as novel insights might alter this number and not every patient with such an aberration will benefit from therapy. Another trial on actionable aberrations in rare cancers however detected the same fraction of 53% by using whole-genome sequencing (12). This supports use of routine testing for these actionable aberrations in recurrent or metastatic (R/M) SGC.

The search for actionable aberrations should include detection of gene fusions. Several gene fusion products now can be treated with matched therapies. For example, NTRK-containing fusion products can be targeted by larotrectinib, entrectinib, and repotrectinib, RET fusions by selpercatinib, ALK fusions by alectinib, crizotinib, entrectinib and lorlatinib, and ROS1 fusions by crizotinib, entrectinib and lorlatinib (6, 13, 14). Some of these fusions also have been described in SGC, such as *NTRK3* rearrangements in secretory carcinoma and in our study one SDC patient harbored a *RET* rearrangement. In AdCC *MYB* or *MYBL1*-containing gene fusions occur very frequently (in approximately 88% of the cases), but unfortunately no therapies for these fusions have been registered, yet (15). One phase 1 trial combining programmed cell death protein 1 (PD-1) inhibition with a vaccine containing a *MYB* cDNA plasmid vector is active (NCT03287427) (16).

An important problem with the approach of treating patients with genetically matched therapies is that not every patient has an actionable aberration in their tumor genome. If such an aberration is present the matched therapy is not always available, and if the therapy is given not every patient will benefit. In approximately 62% of all cancer patients an actionable aberration can be detected (using whole-genome sequencing), whereas only in approximately 13% of the cases drugs can be used off-label. Of these treated patients, 33% will experience clinical benefit (12, 17). Out of a hypothetical cohort of 1000 patients for whom tumor DNA sequencing would have been performed, 27 would eventually experience benefit after receiving such genetically matched treatment. This number can be increased by new drug development (*i.e.* creating more actionable targets) or expand the off-label use of existing drugs (*i.e.* treating more patients with the genetically matched therapy). Addressing the problem of patients not responding to therapy, what is believed to be the tumor's Achilles heel, is however more challenging.

One major explanation for patients not responding to therapy is intra-tumor heterogeneity (ITH). ITH arises as a result of evolutionary dynamics that are present in every cancer (18). The complex process of metastasis adds significantly to ITH (19). An ideal anticancer medicine targets all tumor cells and not healthy cells. It should therefore be aimed at a (molecular) feature that drives the tumor and is exclusively present in tumor cells. Evolutionary dynamics in tumors and subsequent occurrence of ITH raise the question whether such a common

molecular feature does exist in every tumor cell. Mapping of ITH is therefore crucial to understand mechanisms behind therapy failure.

Mapping of spatial ITH requires samples of different disease sites. In living patients sampling of many locations is impossible or undesirable, but deceased patients can be extensively sampled during autopsy (20). The preliminary results of an autopsy protocol to study ITH in SGC is described in chapter 3. Bodies were directly cooled after death. DNA extracted during subsequent autopsy was of sufficient quality to perform whole-genome sequencing. This shows that the protocol is feasible. Future bioinformatic processing of the WGS data will reveal the extent of heterogeneity between tumor lesions from different locations (3-7 per patient). Based on the outcome, targeted sequencing on all sampled locations (9-53 per patient) will be performed and is expected to lead to robust assessment of ITH in SGC. This will tell something about subclonality of these single-nucleotide variants (SNVs) and insertions/deletions (INDELS) but will not yield information on copy-number variations (CNVs) in all these disease locations. This could be cost-effectively assessed on this great number of locations by low-pass whole-genome sequencing. As SNV/INDELS and CNVs are probably driven by independent mutational processes, this could give valuable additional information (21).

Mapping ITH gives information about fundamental biological processes but can also directly have an impact on the clinical treatment of patients. It can assess the representativeness of a biopsied location for other disease locations. It can for instance answer the question whether a biopsy of a skin metastasis sufficiently recapitulate the genetic background of a brain metastasis in the same patient, a location that is notoriously hard to sample. Besides this, it can give information about (targeted) therapy failure. For example, if activating *NOTCH* mutations are present in a minority of metastases, targeting these mutations with selective NOTCH-inhibitors is less rational. However, a limitation in this extrapolation to clinical treatment is the small number of patients included in this autopsy study, which warrants further research.

This autopsy study results in assessment of spatial ITH but will not provide information about temporal ITH. A recent report on whole-genome sequencing on paired biopsies (almost all coming from metastatic lesions) indicated that actionable aberrations are stable over time in the vast majority of cases (median time of 6.4 months between the 2 biopsies) (22). Addition of circulating tumor DNA and/or biopsies sampled ante-mortem to samples taken during autopsy can reveal some of the temporal ITH and will answer whether these samples will be representative for the total burden of disease.

Part 2: Biomarkers to predict response to systemic therapy in salivary duct carcinoma

The second part of this thesis addresses the selection of patients that will benefit or will not benefit from treatment. Specifically, the response of SDC patients to combined androgen blockade (CAB) or therapy aimed at the human epidermal growth factor receptor 2 (HER2) has been investigated. SDC expresses the androgen receptor (AR) in 78-96% of cases and HER2 in 29-46% of cases, suggesting effectiveness of CAB or anti-HER2 therapy for the majority of SDC cases (23-25). Survival in untreated SDC is poor, 5 months in a historical cohort when best supportive care is given. CAB leads to responses in 42% of the cases, with a median progression-free survival of 8.8 months (26). Since not all patients responded to CAB, identification of responders and non-responders would be of added value (27).

Quantification of 7 different signal transduction pathways activities (Oncosignal) and correlation to the response data in a large cohort of SDC patients with CAB did reveal both predictive and prognostic potential of these analyses (28). The activity of the AR and Notch pathways significantly differed between the group with or without clinical benefit (i.e., high AR and Notch activities in the group that experienced clinical benefit). The observation that active AR signaling correlates to more clinical benefit upon CAB fits the hypothesis that tumors with active AR signaling will be inhibited more from androgen deprivation therapy than tumors without active AR signaling. However, the role of active Notch signaling in CAB response is puzzling.

Activating *NOTCH* mutations are of importance in AdCC, where they define a distinct subgroup with poor prognosis, but aberrations in these genes are not frequently found in SDC (29, 30). In chapter 2 of this thesis, none of these activating mutations were identified in SDC patients, although *NOTCH1* amplifications have been described in 2 SDC cases in another study (31). Activating *NOTCH* mutations thus do not seem to explain these observations, but downstream Notch-signaling might be activated in the absence of such mutations. Transcriptome/proteome analysis indeed indicate that Notch signaling is activated in SDC (32). Response to CAB in tumors with active Notch signaling might be explained by interplay between AR-signaling and Notch-signaling, as was found in prostate cancer (33). Nevertheless, the importance of Notch-signaling in SDC warrants future research, as this might become an additional, and novel, therapeutic target.

Expression levels of *SRD5A1* had better prognostic and predictive value than the activity scores of the 7 different pathways (Oncosignal). *SRD5A1* encodes the 5α-reductase type A1 enzyme that converts testosterone into the more potent androgen dihydrotestosterone (DHT). Therefore, we hypothesize that elevated levels of *SRD5A1* are indicative for tumors with a high

dependency on androgens and that CAB treatment will therefore lead to higher response rates compared to patients with low *SRD5A1* expression levels. *SRD5A1* expression can not only be a prognostic and predictive biomarker, but the SRD5A1 enzyme encoded by this gene can serve as therapeutic target. SRD5A1 can be selectively inhibited with dutasteride, a drug that is frequently prescribed to patients suffering from benign prostatic hyperplasia (BPH). In patients with BPH this drug is well tolerated and relieves symptoms (34). Furthermore, dutasteride combined with the AR antagonist enzalutamide synergistically inhibit prostate tumor cell proliferation and anecdotal evidence of response of abiraterone-resistant prostate cancer patients after addition of dutasteride have been published (35, 36). These data provide a rationale for combining dutasteride with CAB in AR-positive SDC patients. Currently, preparations for a randomized phase 2 trial testing CAB with and without dutasteride in SDC patients are being made in the Radboudumc, Nijmegen.

Ultimately, the abovementioned biomarkers (*SRD5A1* expression and pathway activity scores) can be used in the clinic to select patients that will or may benefit from CAB. Especially, excluding patients that are likely not to respond to CAB is of clinical value, because of the poor prognosis of untreated R/M SDC. Prior to implementation in the clinic, a validation study should be performed in an independent cohort, using the cut-offs for the pathway activity scores and *SRD5A1* expression levels as defined in the study described in chapter 4.

For SDC patients in which *HER2* gene amplification is (also) present, anti-HER2 therapy is a rational approach and the promising results of triple therapy using docetaxel, trastuzumab and pertuzumab in SDC patients are presented in chapter 5. Second line trastuzumab-emtansine (T-DM1), an antibody drug conjugate targeting HER2, is a reasonable approach after progression on first-line DTP. Both treatment regimens have an acceptable toxicity profile.

Pivotal pathways involved in downstream HER2 signaling, after dimerization of the HER2 receptor, are the PI3K and MAPK signaling cascades (37). In order to select patients that will eventually benefit form anti-HER2-based therapy these signaling cascades were quantified using the same approach as in chapter 4. The small number of patients included in this study limits the interpretation of the pathway analysis, but the only patient experiencing a complete response had the highest combined PI3K and MAPK activity score and the only patient that experienced progressive disease had the lowest combined score. These promising data warrant further validation, although this will be hampered by the small number of HER2 positive SDC patients.

Besides this, it is unknown to which extent either of these 2 signaling cascades contribute to the tumor cell proliferation in SDC and whether a summation of both scores adequately

summarize activity of the complex HER2 signaling. Further fundamental research in HER2 signaling cascades in SDC is needed to elaborate on this. In these future fundamental studies on the role of HER2-signaling in SDC, the complex interplay between AR and HER2 signaling should be taken into account, as there is a known interaction between these pathways (38). From a clinical perspective, it is unknown whether patients co-expressing AR and HER2 should be treated with CAB or anti-HER2 therapy first, or with a combination of both. Future clinical studies on the optimal sequence of these therapies in patients with both AR and HER2 expression is warranted.

Part 3: Organoid models of salivary gland cancer

The fundamental questions raised above require adequate models to perform functional studies. For example, the role of gene fusions and HER2-signaling in SGC can be investigated in preclinical research models. Such models are very scarce in SGC and mostly restricted to AdCC, MEC and SDC (chapter 1). For most subtypes, only few 2D cell lines and xenograft models are available. Recently, AdCC patient-derived organoids (PDOs) have been described, although they have been poorly characterized (39). For other subtypes PDO models are lacking.

The results described in chapter 6 show that it is possible to establish short-term PDOs for AdCC, MEC and SDC (in general, limited to about 5 passages). Therefore, establishing organoid cultures is promising, but requires additional optimization in terms of success rate and culture longevity. Besides this, in SDC organoid cultures the signature AR expression was also lost, and phenotypic mimicry to parental tissue was thus suboptimal in these cultures. Potentially, these problems arise due to lack of a yet unidentified factor from the tumor microenvironment (TME) in the organoid culture (medium). Cancer cells, in particular cancer stem cells (CSCs), interact with the tumor microenvironment (TME) (40). This TME contains numerous cell types, including fibroblasts, immune cells, and endothelial cells, and various factors including signaling molecules and extracellular matrix (41). A specialized group of fibroblasts, cancer-associated fibroblasts (CAFs) are of unusual importance for tumor development. CAFs can support formation of cancer stem cell niches, tumor growth, and metastasis, and mediate drug resistance by directly interacting with cancer cells or secreting a panel of (growth) factors (41-43). The clinical significance of CAFs in disease progression, therapeutic response, and patient outcome has been widely reported in various types of cancer (44, 45). This includes AdCC, in which CAFs have been shown to promote tumor cell proliferation (46). In several more common tumor types it has been feasible to co-culture CAFs with organoids to study the tumor-stroma interaction (47-50).

For prostate cancer, which is also a cancer type that is notoriously hard to culture as AR-positive organoids (own observations), xenografting tumor tissue prior to culturing cells in a 3D-scaffold has been shown to greatly enhance the success rate of establishing AR-positive organoids (51). This further indicates that potentially unidentified factors from the TME could alter the culture success regarding longevity and phenotypic mimicry, as the cells initially remain into contact with their TME in the mouse host. The organoid model therefore could benefit from either co-culturing tumor cells with CAFs in 3D or by first xenografting tumors in immune deficient mice.

The organoid culturing method and their characterization as described in chapter 8 can be considered a proof of concept for SGC, albeit improvement of the model is needed. Using an identical culture protocol as described in chapter 6, an organoid cell line was established in 1 out of 2 tumor samples of the same patient. This indicates that culture success is unpredictable. Besides this, genotypic mimicry with parental tumor tissue was evident in one organoid and close to absent in the other. This organoid culture study is insidious, as on first glance the culture seems an adequate recapitulation of the parental tissue. On hematoxylin and eosin staining the tumor phenotype was retained and whole-exome and whole-genome sequencing results revealed identity between the organoid and the tumor. Moreover, the signature *ETV6-NTRK3* gene fusion was retained in the organoids. *In vivo* and *in vitro* drug responses do however not correspond and at the transcriptome level divergence between organoids and parental tumor tissue is evident. This emphasizes that extensive molecular characterization is required before extrapolation of *in vitro* data to the clinic can be made.

In the literature however, several reports on matches between drugs screens in organoids and responses in patients have been reported, although some reports also mention mismatches (52). Publication bias cannot be ruled out, and possibly negative results of organoid drug screens correlated to clinical response exist. Nevertheless, caution is advised when extrapolating organoid drug screening results to the clinic. This should only take place in a trial setting and after careful characterization of the organoid models that have been used.

A possible approach to enhance the transcriptome mimicry is again to co-culture organoids with cells from the TME. Co-culturing tumor cells with CAFs and with immune cells is feasible (53, 54). Such co-culture models could be used to study the interaction of the tumor cells with the immune system and could also enable drug screens with agents that require immune effector cells to exert their effect, such as monoclonal antibodies.

Conclusion

In this thesis several translational studies have been described that aim to improve systemic treatment options for patients with SGC. Firstly, gene fusions and actionable aberrations have been identified in several SGC subtypes. Secondly, the feasibility of mapping ITH in SGC patients using autopsy-derived material has been presented. Thirdly, biomarkers to select SDC patients that will benefit from CAB and/or anti-HER2 therapy have been identified. Finally, patient-derived organoid models for SGC have been established and characterized. Several suggestions to translate hypotheses generated in this thesis to future clinical studies or patient-tailored treatment strategies have been made. Altogether, the better understanding of the tumor biology of SGC can and will improve clinical outcome, *i.e.* treatment response and survival, of patients suffering from this rare cancer.

References

1. El-Naggar A.K., Chan J.K.C., Grandis J.R., Takata T., Slootweg P.J. WHO classification of head and neck tumours, 4th edition. Lyon: IARC; 2017.
2. de Heus E, Duijts SFA, van der Zwan JM, Kapiteijn E, Nieveen van Dijkum EJM, van Herpen CML, et al. The gap between rare and common cancers still exists: Results from a population-based study in the Netherlands. European journal of cancer (Oxford, England : 1990). 2022;167:103-11.
3. Mertens F, Johansson B, Fioretos T, Mitelman F. The emerging complexity of gene fusions in cancer. Nat Rev Cancer. 2015;15(6):371-81.
4. Mantere T, Neveling K, Pebrel-Richard C, Benoist M, van der Zande G, Kater-Baats E, et al. Optical genome mapping enables constitutional chromosomal aberration detection. Am J Hum Genet. 2021;108(8):1409-22.
5. Drier Y, Cotton MJ, Williamson KE, Gillespie SM, Ryan RJ, Kluk MJ, et al. An oncogenic MYB feedback loop drives alternate cell fates in adenoid cystic carcinoma. Nature genetics. 2016;48(3):265-72.
6. Cocco E, Scaltriti M, Drilon A. NTRK fusion-positive cancers and TRK inhibitor therapy. Nature reviews Clinical oncology. 2018;15(12):731-47.
7. Wai DH, Knezevich SR, Lucas T, Jansen B, Kay RJ, Sorensen PH. The ETV6-NTRK3 gene fusion encodes a chimeric protein tyrosine kinase that transforms NIH3T3 cells. Oncogene. 2000;19(7):906-15.
8. Luk PP, Wykes J, Selinger CI, Ekmejian R, Tay J, Gao K, et al. Diagnostic and prognostic utility of Mastermind-like 2 (MAML2) gene rearrangement detection by fluorescent in situ hybridization (FISH) in mucoepidermoid carcinoma of the salivary glands. Oral surgery, oral medicine, oral pathology and oral radiology. 2016;121(5):530-41.
9. Chen Z, Chen J, Gu Y, Hu C, Li JL, Lin S, et al. Aberrantly activated AREG-EGFR signaling is required for the growth and survival of CRTC1-MAML2 fusion-positive mucoepidermoid carcinoma cells. Oncogene. 2014;33(29):3869-77.
10. Cros J, Sbidian E, Hans S, Roussel H, Scotte F, Tartour E, et al. Expression and mutational status of treatment-relevant targets and key oncogenes in 123 malignant salivary gland tumours. Annals of oncology : official journal of the European Society for Medical Oncology. 2013;24(10):2624-9.
11. Date O, Katsura M, Ishida M, Yoshihara T, Kinomura A, Sueda T, et al. Haploinsufficiency of RAD51B causes centrosome fragmentation and aneuploidy in human cells. Cancer Res. 2006;66(12):6018-24.
12. Hoes LR, van Berge Henegouwen JM, van der Wijngaart H, Zeverijn LJ, van der Velden DL, van de Haar J, et al. Patients With Rare Cancers in the Drug Rediscovery Protocol (DRUP) benefit from Genomics - Guided Treatment. Clinical cancer research : an official journal of the American Association for Cancer Research. 2022.
13. Schram AM, Chang MT, Jonsson P, Drilon A. Fusions in solid tumours: diagnostic strategies, targeted therapy, and acquired resistance. Nature reviews Clinical oncology. 2017;14(12):735-48.
14. Drilon A, Hu ZI, Lai GGY, Tan DSW. Targeting RET-driven cancers: lessons from evolving preclinical and clinical landscapes. Nature reviews Clinical oncology. 2018;15(3):151-67.
15. Fujii K, Murase T, Beppu S, Saida K, Takino H, Masaki A, et al. MYB, MYBL1, MYBL2 and NFIB gene alterations and MYC overexpression in salivary gland adenoid cystic carcinoma. Histopathology. 2017;71(5):823-34.

16. Pham T, Pereira L, Roth S, Galletta L, Link E, Akhurst T, et al. First-in-human phase I clinical trial of a combined immune modulatory approach using TetMYB vaccine and Anti-PD-1 antibody in patients with advanced solid cancer including colorectal or adenoid cystic carcinoma: The MYPHISMO study protocol (NCT03287427). Contemp Clin Trials Commun. 2019;16:100409.
17. Priestley P, Baber J, Lolkema MP, Steeghs N, de Bruijn E, Shale C, et al. Pan-cancer whole-genome analyses of metastatic solid tumours. Nature. 2019;575(7781):210-6.
18. McGranahan N, Swanton C. Clonal Heterogeneity and Tumor Evolution: Past, Present, and the Future. Cell. 2017;168(4):613-28.
19. Hunter KW, Amin R, Deasy S, Ha NH, Wakefield L. Genetic insights into the morass of metastatic heterogeneity. Nat Rev Cancer. 2018;18(4):211-23.
20. Iacobuzio-Donahue CA, Michael C, Baez P, Kappagantula R, Hooper JE, Hollman TJ. Cancer biology as revealed by the research autopsy. Nat Rev Cancer. 2019;19(12):686-97.
21. Dentro SC, Leshchiner I, Haase K, Tarabichi M, Wintersinger J, Deshwar AG, et al. Characterizing genetic intra-tumor heterogeneity across 2,658 human cancer genomes. Cell. 2021;184(8):2239-54.e39.
22. van de Haar J, Hoes LR, Roepman P, Lolkema MP, Verheul HMW, Gelderblom H, et al. Limited evolution of the actionable metastatic cancer genome under therapeutic pressure. Nat Med. 2021;27(9):1553-63.
23. Gilbert MR, Sharma A, Schmitt NC, Johnson JT, Ferris RL, Duvvuri U, et al. A 20-Year Review of 75 Cases of Salivary Duct Carcinoma. JAMA otolaryngology-- head & neck surgery. 2016;142(5):489-95.
24. Takase S, Kano S, Tada Y, Kawakita D, Shimura T, Hirai H, et al. Biomarker immunoprofile in salivary duct carcinomas: clinicopathological and prognostic implications with evaluation of the revised classification. Oncotarget. 2017;8(35):59023-35.
25. Boon E, Bel M, van Boxtel W, van der Graaf WTA, van Es RJJ, Eerenstein SEJ, et al. A clinicopathological study and prognostic factor analysis of 177 salivary duct carcinoma patients from The Netherlands. International journal of cancer. 2018;143(4):758-66.
26. Fushimi C, Tada Y, Takahashi H, Nagao T, Ojiri H, Masubuchi T, et al. A prospective phase II study of combined androgen blockade in patients with androgen receptor-positive metastatic or locally advanced unresectable salivary gland carcinoma. Annals of oncology : official journal of the European Society for Medical Oncology. 2018;29(4):979-84.
27. Boon E, van Boxtel W, Buter J, Baatenburg de Jong RJ, van Es RJJ, Bel M, et al. Androgen deprivation therapy for androgen receptor-positive advanced salivary duct carcinoma: A nationwide case series of 35 patients in The Netherlands. Head & neck. 2018;40(3):605-13.
28. van de Stolpe A, Holtzer L, van Ooijen H, Inda MA, Verhaegh W. Enabling precision medicine by unravelling disease pathophysiology: quantifying signal transduction pathway activity across cell and tissue types. Sci Rep. 2019;9(1):1603.
29. Ferrarotto R, Mitani Y, Diao L, Guijarro I, Wang J, Zweidler-McKay P, et al. Activating NOTCH1 Mutations Define a Distinct Subgroup of Patients With Adenoid Cystic Carcinoma Who Have Poor Prognosis, Propensity to Bone and Liver Metastasis, and Potential Responsiveness to Notch1 Inhibitors. Journal of clinical oncology : official journal of the American Society of Clinical Oncology. 2017;35(3):352-60.

30. Ho AS, Ochoa A, Jayakumaran G, Zehir A, Valero Mayor C, Tepe J, et al. Genetic hallmarks of recurrent/metastatic adenoid cystic carcinoma. J Clin Invest. 2019;129(10):4276-89.
31. Gargano SM, Senarathne W, Feldman R, Florento E, Stafford P, Swensen J, et al. Novel therapeutic targets in salivary duct carcinoma uncovered by comprehensive molecular profiling. Cancer Med. 2019;8(17):7322-9.
32. Alame M, Cornillot E, Cacheux V, Tosato G, Four M, De Oliveira L, et al. The molecular landscape and microenvironment of salivary duct carcinoma reveal new therapeutic opportunities. Theranostics. 2020;10(10):4383-94.
33. Aldahl J, Yu EJ, He Y, Hooker E, Wong M, Le V, et al. A pivotal role of androgen signaling in Notch-responsive cells in prostate development, maturation, and regeneration. Differentiation. 2019;107:1-10.
34. Roehrborn CG, Boyle P, Nickel JC, Hoefner K, Andriole G. Efficacy and safety of a dual inhibitor of 5-alpha-reductase types 1 and 2 (dutasteride) in men with benign prostatic hyperplasia. Urology. 2002;60(3):434-41.
35. Hamid AR, Verhaegh GW, Smit FP, van Rijt-van de Westerlo C, Armandari I, Brandt A, et al. Dutasteride and enzalutamide synergistically suppress prostate tumor cell proliferation. J Urol. 2015;193(3):1023-9.
36. Lian JP, Gao YY, Tang JJ, Chen X, Liu Y, Wu DL, et al. Response of prostate cancer to addition of dutasteride after progression on abiraterone. Asian J Androl. 2021;23(2):222-3.
37. Yarden Y, Pines G. The ERBB network: at last, cancer therapy meets systems biology. Nat Rev Cancer. 2012;12(8):553-63.
38. Ho AL. Androgen Receptor Pathway in Salivary Gland Cancer. Journal of clinical oncology : official journal of the American Society of Clinical Oncology. 2021;39(36):4069-72.
39. Takada K, Aizawa Y, Sano D, Okuda R, Sekine K, Ueno Y, et al. Establishment of PDX-derived salivary adenoid cystic carcinoma cell lines using organoid culture method. International journal of cancer. 2021;148(1):193-202.
40. Prager BC, Xie Q, Bao S, Rich JN. Cancer Stem Cells: The Architects of the Tumor Ecosystem. Cell stem cell. 2019;24(1):41-53.
41. Giraldo NA, Becht E, Remark R, Damotte D, Sautès-Fridman C, Fridman WH. The immune contexture of primary and metastatic human tumours. Curr Opin Immunol. 2014;27:8-15.
42. Kalluri R. The biology and function of fibroblasts in cancer. Nat Rev Cancer. 2016;16(9):582-98.
43. Multhaupt HA, Leitinger B, Gullberg D, Couchman JR. Extracellular matrix component signaling in cancer. Adv Drug Deliv Rev. 2016;97:28-40.
44. Ebbing EA, van der Zalm AP, Steins A, Creemers A, Hermsen S, Rentenaar R, et al. Stromal-derived interleukin 6 drives epithelial-to-mesenchymal transition and therapy resistance in esophageal adenocarcinoma. Proc Natl Acad Sci U S A. 2019;116(6):2237-42.
45. Hu G, Wang S, Xu F, Ding Q, Chen W, Zhong K, et al. Tumor-Infiltrating Podoplanin+ Fibroblasts Predict Worse Outcome in Solid Tumors. Cell Physiol Biochem. 2018;51(3):1041-50.
46. Kong J, Zhao H, Shang Q, Ma Z, Kang N, Tan J, et al. Establishment and characterization of a carcinoma-associated fibroblast cell line derived from a human salivary gland adenoid cystic carcinoma. Cell Commun Adhes. 2018;24(1):11-8.
47. Nakamura H, Sugano M, Miyashita T, Hashimoto H, Ochiai A, Suzuki K, et al. Organoid culture containing cancer cells and stromal cells reveals that podoplanin-positive cancer-associated fibroblasts enhance proliferation of lung cancer

cells. Lung cancer (Amsterdam, Netherlands). 2019;134:100-7.

48. Zhao H, Jiang E, Shang Z. 3D Co-culture of Cancer-Associated Fibroblast with Oral Cancer Organoids. J Dent Res. 2021;100(2):201-8.

49. Tsai S, McOlash L, Palen K, Johnson B, Duris C, Yang Q, et al. Development of primary human pancreatic cancer organoids, matched stromal and immune cells and 3D tumor microenvironment models. BMC cancer. 2018;18(1):335.

50. Seino T, Kawasaki S, Shimokawa M, Tamagawa H, Toshimitsu K, Fujii M, et al. Human Pancreatic Tumor Organoids Reveal Loss of Stem Cell Niche Factor Dependence during Disease Progression. Cell stem cell. 2018;22(3):454-67.e6.

51. Risbridger GP, Clark AK, Porter LH, Toivanen R, Bakshi A, Lister NL, et al. The MURAL collection of prostate cancer patient-derived xenografts enables discovery through preclinical models of uro-oncology. Nat Commun. 2021;12(1):5049.

52. Liu L, Yu L, Li Z, Li W, Huang W. Patient-derived organoid (PDO) platforms to facilitate clinical decision making. J Transl Med. 2021;19(1):40.

53. Neal JT, Li X, Zhu J, Giangarra V, Grzeskowiak CL, Ju J, et al. Organoid Modeling of the Tumor Immune Microenvironment. Cell. 2018;175(7):1972-88.e16.

54. Dijkstra KK, Cattaneo CM, Weeber F, Chalabi M, van de Haar J, Fanchi LF, et al. Generation of Tumor-Reactive T Cells by Co-culture of Peripheral Blood Lymphocytes and Tumor Organoids. Cell. 2018;174(6):1586-98.e12.

CHAPTER 9

Summary

Salivary gland cancer (SGC) is a rare malignancy consisting of 22 subtypes with different histological, clinical and genetic characteristics. This rarity and heterogeneity makes systemic treatment of recurrent or metastatic (R/M) disease challenging. The use of chemotherapy is scarcely studied and chemotherapy at best has moderate effects. New therapeutic strategies are therefore needed, but advances made in SGC are lagging those in more common cancers. Unraveling of the tumor biology of SGC can help closing this gap. By doing so, rationales for use of existing treatments for other cancers can be investigated, i.e. treatments can be better tailored to specific patients. Besides this, with the use of tumor models new treatment options can be investigated. The work described in this thesis focused on translating SGC tumor biological characteristics to clinically meaningful applications.

Chapter 1 provides a general introduction on tumor characteristics that are putatively actionable with targeted therapy in different SGC subtypes, compiles evidence on treatment options in salivary duct carcinoma (SDC) and outlines scarcity in tumor models for SGC.

In **part 1** of this thesis research unraveling (part of) the tumor genetics of SGC is presented. In **chapter 2** RNA and DNA was extracted from archival tumor material from 121 SGC patients suffering from various SGC subtypes and subjected to next-generation sequencing (NGS). The goal of this study was to identify actionable genomic aberrations that can be targeted with genetically matched therapies. Besides this, the diagnostic utility of pan-TRK immunohistochemistry for *NTRK* gene fusion detection was assessed, as *NTRK* gene fusions are highly relevant for therapy selection, and these fusions are pathognomonic for secretory carcinoma, one of the 22 SGC subtypes. NGS of the RNA revealed presence of gene fusion in half of all SGC cases. Known fusions were identified, such as *MYB(L1)-NFIB* gene fusions in adenoid cystic carcinoma (AdCC), *CRTC1-MAML2* fusions in mucoepidermoid carcinoma (MEC) and *PLAG1* fusions in carcinoma ex pleomorphic adenoma. Besides this, several fusions not earlier described in SGC were identified, including fusions involving *BRAF, RAD51B* and *RET.* Only one *NTRK* gene fusion was detected in a secretory carcinoma case. In 74% of the cases the pan-TRK IHC was however false positive, which limits its utility to detect *NTRK* gene fusions in SGC. On the DNA level actionable aberrations were frequently seen in the *PIK3CA, ERBB2, HRAS* and *NOTCH* genes. Overall, in 53.7% of all cases one or more actionable aberrations were seen, although this highly differed between subtypes, being lowest in AdCC and highest in SDC, with 28.3% and 81.8% of the cases harboring a putatively actionable aberration, respectively.

In **chapter 3**, a more fundamental question regarding SGC molecular biology is addressed. In this chapter preliminary results of an autopsy study are presented. Data from this study can eventually map spatial intra-tumor heterogeneity (ITH) and clonal evolution, *i.e.* the process by which (epi)genetic changes create diversity. This is important because ITH contributes to

failure of therapy and, unfortunately, little is known about this process in SGC. Every cancer, and probably every patient has its own evolutionary narrative, and this study tells the stories of 4 patients that died from metastatic SGC. In these 4 patients elaborate post-mortem imaging was performed, followed by autopsy between 12-56 hours after death. During autopsy, 169 tumor samples of several different disease locations in these 4 patients were taken. In 138 of these 169 samples tumor presence was confirmed and libraries of sufficient quality for subsequent whole-genome sequencing (WGS) could be prepared in all these 138 samples. WGS was performed in 19 of these samples of which the bioinformatic processing has yet to be performed. In one patient somatic variants in samples taken from the right and left lung could already be compared, revealing significant differences between these two locations (61% of the variants were unique to one of the samples). This chapter shows feasibility of this autopsy approach, and provides first the indications of the existence of tumor heterogeneity in SGC.

Part 2 of this thesis specifically focuses on SDC. This aggressive SGC subtypes expresses the androgen receptor (AR) in the vast majority of cases and the human epidermal growth factor receptor 2 (HER2) in 29-46% of cases. Hence, treatment with androgen deprivation therapy and/or anti-HER2 therapy can be considered. A significant proportion of SDC patients will however not respond to such therapies. The utility of pathway analysis to predict treatment responses to these agents in SDC patients were presented.

In **chapter 4**, the activity of the AR, Notch, MAPK, TGFβ, estrogen receptor (ER), Hedgehog (HH), and PI3K signaling pathways was determined based on the expression levels of target genes in RNA derived from archival tissue. For this purpose, tumor material and data of 76 SDC patients were collected in several hospitals in Japan by collaborating partners. In this tumor material also the expression of *SRD5A1,* a gene encoding for an enzyme that intracellularly converts testosterone in the more potent dihydrotestosterone, was determined. Expression levels of *SRD5A1* and the abovementioned pathway activity scores were related to clinical benefit (*i.e.* complete response (CR), partial response (PR) or stable disease ≥6 months) upon treatment with combined androgen blockade (CAB). Regarding response prediction, *SRD5A1* expression had the highest positive predictive value (85.7%), and the AR pathway activity score had the highest negative predictive value (93.3%). High *SRD5A1* expression and low AR pathway activity score were positively and negatively related to benefit from CAB therapy, respectively. Combined, *SRD5A1* expression and the TGFβ and Notch scores provided the most predictive combination. Several pathways as well as *SRD5A1* expression had prognostic relevance for progression-free survival (PFS), but only *SRD5A1* expression had prognostic value for overall survival (OS).

In **chapter 5** the results of a case series on first line anti-HER2 therapy with docetaxel, trastuzumab and pertuzumab (DTP) followed by second-line anti-HER2 therapy with trastuzumab-emtansine (T-DM1) are presented. Pathway analysis (as described in chapter 4) was also performed in search for potential biomarkers to predict response to this treatment. Thirteen SDC patients with HER2-positive tumors were selected for DTP therapy. In total 12 patients were evaluable, of which 1 experienced CR and 6 experienced PR, leading to an objective response rate of 58% (median PFS 6.9 months, OS 42.0 months). Subsequent T-DM1 given in 7 patients after progressive disease on DTP led to 4 PRs (median PFS 4.4 months). Toxicity profiles of both treatments were acceptable, making this promising treatments for HER2-positive SDC patients. Combined PI3K and MAPK pathway activity scores, both pathways which are involved in downstream HER2 signaling, may have predictive potential. The highest combined score was seen in the one patient experiencing CR on DTP and the lowest score in the one patient with direct progressive disease at the first evaluation.

In **part 3**, of this thesis experiences in establishment and use of three-dimensional patient-derived stem-cell based organoid models of SGC are presented. Appropriate tumor models to perform fundamental and translational research in SGC are very scarce and we therefore attempted to establish an organoid model for several SGC subtypes. This is described in **chapter 6**. To establish organoid models, fresh tumor material of 37 SGC patients (15 SDC, 12 AdCC, 7 MEC, 2 acinic cell carcinomas and 1 epithelial-myoepithelial carcinoma) was embedded in Matrigel, an extracellular matrix scaffold, supplemented with organoid medium. Out of these 37 organoid attempts 7 viable short-term patient-derived organoid cultures (PDO) could be established (3 SDC, 3 AdCC and 1 MEC). Each PDO showed close phenotypical mimicry to tumor tissue it was derived from, although AR expression was lost in the SDC PDOs. Genotypic characterization using a combination of targeted sequencing and whole-exome sequencing revealed that in each PDO >97.6% of all variants that have annotations in the catalogue of somatic mutations in cancer (COSMIC) and all *MYB, MYBL1* and *NFIB* gene rearrangements were retained. These 7 viable PDOs were used for small-scale drug screenings, which was proven feasible in all PDOs. Although only short-term organoid cultures could be established, this is the first description of PDO establishment in SGC.

In **chapter 7** the next step in organoid research is made and the research described in this chapter builds a bridge between different parts of this thesis. In this chapter, organoids out of tumor material of a patient suffering from metastasized *ETV6-NTRK3* gene fusion positive secretory carcinoma have been established. This patient received treatment with the selective TRK-inhibitor larotrectinib and prior to systemic treatment initiation and after progression on this treatment tumor material was obtained and brought into culture. Long-term organoids could be propagated out of the pre-treatment tumor material and short-term cultures of the post-progression tumor material, using the protocol described in chapter 6 of

this thesis. Phenotypic and elaborate genotypic characterization of the tumor material and the corresponding organoid cultures was performed using whole-exome sequencing, shallow whole-genome sequencing, RNA sequencing and optical genome mapping. Hematoxylin and eosin staining of the tumor and the PDOs revealed excellent phenotypic mimicry, but immunohistochemical expression patterns of marker proteins diverged. Based on the hypothesis that culturing and treating the patient's specific tumor in a dish can predict the *in vivo* response, drug treatments were performed. This revealed that *in vivo* (patient) and *in vitro* drug sensitivities did not correlate. On genomic level excellent mimicry was seen between the tumor tissue and organoids of the pre-treatment sample but not for the post-progression sample. Transcriptome analysis of the pre-treatment parental tissue and corresponding organoids revealed divergence of the parental to the organoids. Besides this, this study revealed that, in this patient, TRK inhibitors exerted molecular effects on the target tumor cells but the cells are no longer dependent on TRK signaling for their survival. This TRK-independency possibly explains the lack of correlation between the *in vivo* and *in vitro* drug response. Altogether this highlights important caveats in using organoids culture drug screens as predictive biomarker.

In conclusion, better understanding of the tumor biology of SGC can and will improve clinical outcome of patients suffering from this rare cancer. The studies described in this thesis take a first step in this translation of the tumor biology to clinical meaningful applications.

APPENDICES

Nederlandse samenvatting

Speekselklierkanker is een zeldzame vorm van kanker, die opgedeeld kan worden in 22 verschillende subtypes. Deze subtypes verschillen wat betreft de histologische, klinische en genetische kenmerken. De zeldzaamheid en heterogeniteit van speekselklierkanker maakt systemische behandeling van patiënten met een recidief of gemetastaseerde speekselklierkanker lastig. Er is weinig onderzoek naar de rol van chemotherapie en over het algemeen is het effect van chemotherapie maar matig. Nieuwe behandelingen zijn dus hard nodig, maar de vooruitgang in de ontwikkeling van nieuwe effectieve geneesmiddelen voor speekselklierkanker gaat minder snel dan bij niet-zeldzame vormen van kanker. Het ontrafelen van de tumorbiologie van speekselklierkanker kan helpen om de achterstand ten opzichte niet-zeldzame vormen van kanker in te lopen. Op deze manier kunnen we targets identificeren waartegen therapieën bestaan die voor andere vormen van kanker geregistreerd zijn of onderzocht worden, en die mogelijk ook patiënten met speekselkierkanker ten goede kunnen komen. Door de tumorbiologie te bestuderen kunnen behandelingen toegespitst worden op specifieke kenmerken van de tumor, waarvan de patiënt dan profijt kan hebben. Daarnaast kunnen we in het laboratorium nieuwe behandelopties onderzoeken met behulp van nieuwe tumormodellen. Het werk dat in dit proefschrift beschreven is, spitst zich toe op het bestuderen van de tumorbiologie van speekselklierkanker, zodat dit vertaald kan worden naar betekenisvolle toepassingen in de klinische praktijk. Het uiteindelijke doel hiervan is de zorg, prognose en kwaliteit van leven te verbeteren van patiënten met speekselklierkanker.

Hoofdstuk 1 geeft een algemene inleiding op tumorkenmerken van verschillende subtypes van speekselklierkanker die mogelijk kunnen responderen op doelgerichte therapie. Daarnaast worden specifiek voor het subtype salivary duct carcinoom (SDC) alle studies naar behandelopties samengevat en wordt er ingegaan op de schaarste aan tumormodellen voor speekselklierkanker.

Deel 1 van dit proefschrift gaat over het ontrafelen van tumorgenetische aspecten van speekselklierkanker. In **hoofdstuk 2** werd RNA en DNA geïsoleerd uit archiefmateriaal van tumoren van 121 speekselklierkankerpatiënten, van verschillende subtypes. Op dit RNA en DNA werd next-generation sequencing (NGS) toegepast. Het doel hiervan was om tumorkenmerken (mutaties, inserties, deleties, copynumbervariaties of genfusies) te identificeren die mogelijk een aangrijpingspunt zijn voor doelgerichte therapie. Daarnaast werd de diagnostische waarde van pan-TRK immuunhistochemie voor het detecteren van *NTRK*-genfusies onderzocht. Dit laatste omdat *NTRK* genfusies pathognomonisch zijn voor het secretoir carcinoom, één van de 22 subtypes van speekselklierkanker, en recent zijn voor tumoren die gedreven worden door *NTRK*-genfusies zeer effectieve medicijnen geregistreerd.

Als *NTRK*-genfusies ook bij andere subtypes voor zouden komen zou dat van grote waarde zijn voor deze patiënten.

NGS op het RNA liet zien dat in de helft van alle speekselkliertumoren een genfusie gevonden kon worden, zoals *MYB(L1)-NFIB*-genfusies in adenoïd cysteus carcinoom (AdCC), *CRTC1-MAML2*-fusies in mucoepidermoïd carcinoom (MEC) en *PLAG1*-fusies in carcinoom ex pleiomorf adenoom. Daarnaast werden verschillende fusies gevonden die niet eerder beschreven zijn in speekselklierkanker, waaronder fusies in de genen *BRAF, RAD51B* en *RET*. In deze studie was één patient met een secretoir carcinoom geïncludeerd. In deze casus werd een *NTRK*-genfusie gedetecteerd. In andere subtypes van speekselklierkanker werden geen *NTRK*-genfusies gevonden. In 74% van de gevallen was de pan-TRK immuunhistochemie vals positief, waardoor de diagnostische waarde te beperkt is om zinvol te zijn. Op DNA-niveau werden afwijking in de genen *PIK3CA*, *ERBB2*, *HRAS* en *NOTCH* vaak gezien. In totaal werd in 53,7% van de gevallen een tumorkenmerk geïdentificeerd wat mogelijk geïnhibeerd kan worden met doelgerichte therapie. Dit verschilde echter wel sterk tussen de verschillende subtypes. Deze fractie was het laagst in AdCC (28,3%) en het hoogst in SDC (81,8%).

In **hoofdstuk 3** wordt een meer fundamentele vraag op het gebied van de tumorbiologie van speekselklierkanker onderzocht. In dit hoofdstuk worden de eerste resultaten van een obductiestudie in 4 patiënten gepresenteerd. Bij deze 4 patiënten heeft na overlijden uitgebreide beeldvorming van de tumor en diens metastasen plaatsgevonden, waarna binnen 12-56 uur na overlijden obductie plaatsvond. Bij die obductie werden 169 tumorsamples afgenomen op verschillende locaties in het lichaam van deze 4 patiënten. In 138 van deze 169 samples werd daadwerkelijk tumorweefsel aangetroffen. Al deze samples waren van voldoende kwaliteit voor whole-genome sequencing. Whole-genome sequencing is vervolgens ook daadwerkelijk uitgevoerd op 19 van deze samples.

De data die in deze studie zijn gegenereerd zullen uiteindelijk leiden tot het in kaart brengen van de mogelijke intra-tumorale heterogeniteit tussen verschillende ziektelocaties. Daarnaast kan hiermee de klonale tumorevolutie in kaart worden gebracht. Klonale tumorevolutie is het proces waardoor (epi)genetische veranderingen in een tumor leiden tot genetische diversiteit. Het is belangrijk om te weten hoe uitgebreid dit voorkomt, omdat intra-tumorale heterogeniteit uiteindelijk kan leiden tot het falen van behandelingen. Hierover is weinig bekend in speekselklierkanker. Elke kankersoort, en zo ook elke kankerpatiënt, heeft zijn eigen evolutionair verhaal. Na analyse zal deze studie dit evolutionaire verhaal van deze 4 patiënten vertellen.

De bioinformatische analyse hiervan moest bij het schrijven van dit proefschrift nog plaatsvinden. In één patiënt konden al wel de somatische varianten in 2 samples die uit

de linker- en rechterlong genomen zijn, worden vergeleken. Hierin werden significante verschillen gezien (61% van de varianten waren uniek in één van beide samples). In dit hoofdstuk wordt aangetoond dat de aanpak met een obductiestudie haalbaar is, en dat intratumorale heterogeniteit in speekselklierkanker daadwerkelijk kan optreden, maar de meeste data moeten nog geanalyseerd worden.

Deel 2 van dit proefschrift gaat specifiek over het SDC. Dit agressieve subtype van speekselklierkanker kenmerkt zich door de expressie van de androgeenreceptor (AR) in de overgrote meerderheid van de gevallen. In 29-46% van de gevallen brengt het ook de humane epidermale groeifactor receptor 2 (HER2) tot expressie. Daarom wordt bij deze patiënten vaak behandeling met androgeendeprivatie-therapie en/of anti-HER2 therapie gegeven. Een deel van alle SDC-patiënten zal hier echter geen baat of slechts een beperkte tijd baat van ondervinden. In dit proefschrift wordt gekeken of zogenaamde pathway-analyse kan voorspellen wie van de SDC-patiënten zal responderen op deze therapieën en wie niet.

In **hoofdstuk 4** wordt de activiteit van de AR, Notch, MAPK, TGFβ, oestrogeenreceptor (ER), HedgeHog (HH) en PI3K pathways bepaald, gebaseerd op de expressieniveaus van de doelwitgenen van deze pathways. Dit werd gedaan op RNA wat uit het archiefmateriaal was gehaald van 76 SDC patiënten, die behandeld waren in Japan. Dit materiaal werd in samenwerking met Japanse oncologen naar ons toegestuurd en door ons geanalyseerd. In dit tumormateriaal werd ook het expressieniveau van *SRD5A1* bepaald. Dit gen codeert voor een eiwit dat zorgt voort de intracellulaire conversie van testosteron in het krachtigere dihydrotestosteron. Expressieniveaus van *SRD5A1* en van de bovengenoemde pathway-activiteiten werden vervolgens gerelateerd aan de kans dat patiënten een complete of partiële respons of stabiele ziekte ≥6 maanden hadden (klinisch voordeel) na de behandeling met gecombineerde androgeen blokkade. Voor wat betreft responspredictie had *SRD5A1* expressie de hoogste positief voorspellende waarde (85.7%) en de AR pathway activiteit de hoogste negatief voorspellende waarde (93.3%). Hierbij was een hoge *SRD5A1* expressie en een lagere AR pathway-acitiviteit positief en negatief gecorreleerd aan klinisch voordeel voor de patiënt, respectievelijk. De *SRD5A1* expressie samen met de TGFβ en Notch scores was de beste predictieve combinatie voor klinisch voordeel. Daarnaast hadden verschillende pathway-activiteitscores en *SRD5A1* expressie ook een prognostische waarde voor wat betreft progressievrije overleving, maar alleen *SRD5A1* expressie had prognostische waarde met betrekking tot de overleving.

In **hoofdstuk 5** wordt een patiëntenserie over eerstelijns anti-HER2 behandeling met docetaxel, trastuzumab en pertuzumab (DTP) gevolgd door tweedelijns anti-HER2 therapie met trastuzumab-emtansine (T-DM1) beschreven. Op tumormateriaal van deze patiënten werd ook pathway-analyse uitgevoerd, net zoals in hoofdstuk 4 beschreven. Het doel hiervan

was om predictieve biomarkers te identificeren. Dertien SDC-patiënten met een HER2-positieve tumor kregen DTP-behandeling. Bij 12 behandelde patiënten kon de respons geëvalueerd worden. Eén patiënt had een complete respons en 6 patiënten een partiële respons. In totaal had dus 58% een respons, met een mediane progressievrije overleving van 6.9 maanden en een mediane overleving van 42 maanden. De T-DM1 behandeling die hierop volgde na progressieve ziekte bij 7 patiënten gaf in 4 gevallen een partiële respons. Beide behandelingen werden goed verdragen, met een beperkte toxiciteit, waardoor dit dus een veelbelovende behandeling is voor HER2-positieve SDC-patiënten. Gecombineerde PI3K en MAPK pathway-activiteitscores, beide betrokken bij de intracellulaire HER2-signaalcascade, lijken mogelijk predictief te zijn. De hoogste gecombineerde score werd namelijk gezien in de enige patiënt met een complete respons en de laagste score in de enige patiënt met progressieve ziekte bij de eerste evaluatie van de DTP-behandeling.

In **deel 3** van dit proefschrift worden ervaringen met het opzetten van zogenaamde patient-derived organoids (PDO) beschreven. PDOs zijn driedimensionale op stamcellen gebaseerde celkweekmodellen die van tumoren van patiënten zijn afgeleid. Tumormodellen om fundamenteel en translationeel onderzoek te verrichten naar speekselklierkanker zijn zeer schaars, en daarom hebben we gepoogd om PDO modellen voor verschillende subtypes van speekselklierkanker op te zetten. Dit wordt in **hoofdstuk 6** beschreven. Om deze organoïdemodellen op te zetten werd vers tumormateriaal van 37 speekselklierkankerpatiënten (15 SDC, 12 AdCC, 7 MEC, 2 acinuscelcarcinomen en 1 epitheliaal-myoepitheliaal carcinoom) ingebed in Matrigel, een extracellulaire matrix die de tumorcellen ondersteunen bij de groei. Daarbij werd organoïde-groeimedium gebruikt. Deze 37 pogingen resulteerden in 7 PDO-kweken die gedurende enige tijd levensvatbaar waren (3 SDC, 3 AdCC en 1 MEC). Qua fenotype leken deze PDOs sterk op de tumor waar ze uit gekweekt waren, hoewel de AR expressie in de SDC organoïdekweken verloren was gegaan. Genotypische karakterisering liet zien dat in elke PDO >97.6% van alle mutaties, die voorkomen in een database met somatische mutaties (de COSMIC database), behouden bleven. Daarnaast bleven alle fusies tussen de *MYB, MYBL1* en/of *NFIB* genen behouden in de PDOs. De 7 levensvatbare PDOs werden gebruikt voor experimenten waarin op kleine schaal behandelingen werden getest. Deze experimenten waren succesvol in al deze 7 kweken. Hoewel alleen organoïdekweken konden worden opgezet die slechts een beperkte duur van levensvatbaarheid hadden, is dit de eerste stap in het kweken van en testen van medicijnen in organoïden voor speekselklierkanker.

In **hoofdstuk 7** wordt voortgeborduurd op dit organoïdeonderzoek. Dit hoofdstuk slaat een brug tussen de verschillende delen van dit proefschrift. In dit hoofdstuk wordt beschreven dat organoïden werden gekweekt uit tumormateriaal van een patiënt met een gemetastaseerd secretoir carcinoom met een *ETV6-NTRK3*-genfusie. Deze patiënt werd behandeld met de selectieve TRK-inhibitor larotrectinib. Voordat hiermee begonnen werd en nadat bij de patiënt

progressieve ziekte optrad werd tumormateriaal afgenomen en tot PDO's gekweekt, waarbij hetzelfde protocol als in hoofdstuk 6 werd gebruikt. Uit het materiaal dat voor start van de behandeling werd afgenomen konden organoïden gekweekt worden die ook na een langere periode nog groeiden. Van het materiaal dat na progressie op larotrectinib werd afgenomen konden alleen kweken gemaakt worden die gedurende een korte periode groeiden. Fenotypische en uitgebreide genotypische karakterisering van het tumor materiaal en de bijbehorende organoïdekweken werd uitgevoerd met behulp van whole-exome sequencing, shallow whole-genome sequencing, RNA-sequencing en optical genome mapping. Hematoxyline en eosine kleuringen van de tumor en de PDOs lieten zien dat de organoïden qua fenotype sterk leken op de tumor waar ze uit gekweekt waren, maar immuunhistochemische expressie van belangrijke proteïnes verschilde. Op genoomniveau werd uitstekende gelijkenis gezien tussen de tumor en de organoïden die gekweekt waren uit het weefsel dat voor start van de behandeling afgenomen was. Dat gold niet voor het weefsel, en de bijbehorende organoïden, dat na progressie afgenomen was. Gebaseerd op de hypothese dat als de tumor van een patiënt in kweek wordt gebracht, dit de respons *in vivo* (in de patiënt) kan voorspellen, werden er ook behandelexperimenten op de organoïden uitgevoerd. Dit liet zien dat de *in vivo* en *in vitro* (in de organoid) respons niet correleerden. Om de paradoxale uitkomsten van deze behandelexperimenten te verklaren werd transcriptoomanalyse verricht (RNA-sequencing). De transcriptoomanalyse van het weefsel dat voor start van de behandeling afgenomen werd, liet zien dat het transcriptoom in dit weefsel sterk afweek van het transcriptoom in de organoïden. Daarnaast liet dit zien dat de TRK-inhibitors wel degelijk een effect hadden op het transcriptoom, maar dat de cellen waarschijnlijk niet langer strikt afhankelijk waren van de TRK-signaalcascade voor hun overleving. Dit is een mogelijke verklaring voor het gebrek aan correlatie tussen de *in vivo* en *in vitro* respons zoals hierboven beschreven. Al met al laat deze studie belangrijke valkuilen en mogelijk beperkingen zien in het gebruik van organoïden voor behandelexperimenten. Voor gebruik van zulke organoïdemodellen als predictieve test voordat een behandeling ingezet gaat worden zal nog meer klinisch onderzoek verricht moeten worden, waarbij het een cruciale stap is de organoïden uitvoerig te karakteriseren.

Concluderend kan en zal een beter begrip van de tumorbiologie van speekselklierkanker de klinische uitkomsten van patiënten die lijden aan deze zeldzame vormen van kanker in de toekomst verbeteren. De studies die zijn beschreven in dit proefschrift vormen een eerste stap in het ontrafelen van de tumorcelbiologie en het vertalen van deze kennis naar zinvolle toepassingen voor de patiënt.

List of publications

Precision oncology using organoids of a secretory carcinoma of the salivary gland in a secretory carcinoma case treated with TRK-inhibitors
Lassche G, Van Engen - van Grunsven ACH, Van Hooij O, Aalders TW, Weijers JAM, Cocco E, Drilon A, Hoischen A, Neveling K, Schalken JA, Verhaegh GW* , Van Herpen CML*
Under Review

Cutaneous Lymphangitis Carcinomatosa in Salivary Duct Carcinoma
Uijen MJM*, Weijers JAM*, **Lassche G**, Van Ravensteijn SG, Van Rijk MC, Lubeek SFK, Van Engen - Van Grunsven ACH, Amir A, Driessen CML, Van Herpen CML
J Clin Pathol. Published online first: 2022 Nov 8;jcp-2022-208564. DOI: 10.1136/jcp-2022-208564.

Development and characterization of patient-derived salivary gland cancer organoid cultures
Lassche G, Van Boxtel W, Aalders TW, Van Hooij O, Van Engen - Van Grunsven ACH, Verhaegh GW, Van Herpen CML*, Schalken JA*
Oral Oncol. 2022;135:106186. DOI: 10.1016/j.oraloncology.2022.106186.

Identification of fusion genes and targets for genetically matched therapies in a large cohort of salivary gland cancer patients
Lassche G, Van Helvert S, Eijkelenboom A, Tjan MJH, Jansen EAM, Van Cleef PHJ, Verhaegh GW, Kamping EJ, Grünberg K, Van Engen - Van Grunsven ACH, Ligtenberg MJL*, Van Herpen CML*
Cancers (Basel). 2022;27;14(17):4156. DOI: 10.3390/cancers14174156.

Case series of docetaxel, trastuzumab, and pertuzumab (DTP) as first line anti-HER2 therapy and ado-trastuzumab emtansine (T-DM1) as second line for recurrent or metastatic HER2-positive salivary duct carcinoma
Uijen MJM*, **Lassche G***, Van Engen - Van Grunsven ACH, Driessen CML, Van Herpen CML
Oral oncology. 2022;125:105703. DOI: 10.1016/j.oraloncology.2021.105703

Predictive and Prognostic Biomarker Identification in a Large Cohort of Androgen Receptor-Positive Salivary Duct Carcinoma Patients Scheduled for Combined Androgen Blockade
Lassche G, Tada Y, Van Herpen CML, Jonker MA, Nagao T, Saotome T, Hirai H, Saigusa N, Takahashi H, Ojiri H, Van Engen - Van Grunsven ACH, Schalken JA, Fushimi C, Verhaegh GW
Cancers (Basel). 2021;14;13(14):3527. DOI: 10.3390/cancers13143527

Systemic therapy in the management of recurrent or metastatic salivary duct carcinoma: A systematic review
Uijen MJM, **Lassche G**, Van Engen - Van Grunsven ACH, Tada Y, Verhaegh GW, Schalken JA, Driesen CML, Van Herpen CML.
Cancer Treat Rev. 2020;89:102069. DOI: 10.1016/j.ctrv.2020.102069

Het speekselkliercarcinoom: een klinische les
Lassche G, Van Engen - Van Grunsven ACH, Honings J, Dijkema T, Weijs WLJ, Van Herpen CML
Ned Tijdschr Geneeskd. 2020;164:D4760.

Thermal distribution, physiological effects and toxicities of extracorporeally induced whole-body hyperthermia in a pig model.
Lassche G*, Frenzel T*, Mignot MH, Jonker MA, Van der Hoeven JG, Van Herpen CML, Scheffer GJ
Physiol Rep. 2020;8(4):e14366. DOI: 10.14814/phy2.14366

Advances and challenges in precision medicine in salivary gland cancer
Lassche G, Van Boxtel W, Ligtenberg MJL, Van Engen - Van Grunsven ACH, Van Herpen CML
Cancer Treat Rev. 2019;80:101906. DOI: 10.1016/j.ctrv.2019.101906

Whole-body hyperthermia in combination with systemic therapy in advanced solid malignancies
Lassche G, Crezee J, Van Herpen CML
Critical reviews in oncology/hematology. 2019;139:67-74. DOI: 10.1016/j.critrevonc.2019.04.023

Use of the Child-Pugh score in anticancer drug dosing decision making: proceed with caution - Authors' reply
Krens SD, **Lassche G**, Jansman FGA, Desar IME, Lankheet NAG, Burger DM, Van Herpen CML, Van Erp NP
The Lancet Oncology. 2019;20(6):e290. DOI: 10.1016/S1470-2045(19)30349-3

Dose recommendations for anticancer drugs in patients with renal or hepatic impairment
Krens SD, **Lassche G**, Jansman FGA, Desar IME, Lankheet NAG, Burger DM, Van Herpen CML, Van Erp NP
The Lancet Oncology. 2019;20(4):e200-e7. DOI: 10.1016/S1470-2045(19)30145-7

* shared authorship.

Research Data Management

Data derived from human material and patient charts were used for this thesis, all in accordance with the principles of Good Clinical Practice (GCP) and the Declaration of Helsinki. For chapter 3, 6 and 7 material was prospectively collected and for chapter 2, 4 and 5 material was retrospectively collected.

All studies were approved by the institutional review board (Commissie Mensgebonden Onderzoek Radboudumc). Patients provided written informed consent for participation in the studies, if required. For chapters 2, 3, 5, 6 and 7 the consent and procedures of the Radboud biobank salivary gland cancers was used (file number 2017-3679). Separate submissions to the institutional review board have been made to use material from the biobank or for approval in patients not participating in the biobank (file number 2019-5476 for chapter 2 and 2019-5089 for chapter 3). For chapter 4 approval was granted by the Institutional Review Board of the International University of Health and Welfare, Mita hospital in Tokyo, Japan (file number 5-19-6).

The protocol for the systematic review used in adapted form for chapter 1 was registered in the international Prospective Register of Systematic Reviews in Health and Social Care (PROSPERO, ID: CRD42020142540).

All data used in this thesis are stored in accordance with Findable, Accessible, Interoperable and Reusable (FAIR) principles:

Findable – Clinical data is stored on the server of the department of Medical Oncology (\\umcfs074\Hoofd-hals onderzoek\Gerben\Speekselklier) as Excel or SPSS files. Clinical data from chapter 2 is also available in CASTOR, a cloud-based clinical data management platform (project name: NTRK gene fusion analysis in salivary gland cancer). Sequencing data of the TruSight Oncology 500 panel described in chapter 2 are uploaded and available in the European Genome-Phenome Archive (BAM and VCF files, study ID EGAS00001006232). Whole-genome sequencing data described in chapter 3 is stored at the servers of the Radboudumc Center for Molecular and Biomolecular Informatics cluster (narrativum.umcn.nl/mnt/rtc/projects/gerben_lassche/). Raw sequencing data described in chapter 6 and 7 is stored at two separate external hard drives, stored at the department of experimental urology and medical oncology (whole-exome sequencing, shallow whole-genome sequencing and RNA-sequencing data). Data from organoid studies described in chapter 6 and 7 are stored in the Labguru e-Notebook of the Radboudumc (Urology account). Hematoxylin and eosin stainings and Immunohistochemistry stainings used in chapter 3, 4, 5, 6 and 7 are stored in the archives at the department of experimental urology. All fresh tumor material, gDNA, RNA

and cDNA are stored in -196°C, -80°C or -20°C freezers at the department of experimental urology and samples are registered in corresponding databases (located on \\umcfs063\urodata$\expurologie).

Accessible – upon reasonable request and fulfillment of legal obligations all data described in this thesis are available to the wider research community. All data is accessible for members of the salivary gland cancer research team have access to the data. For the data stored in the European Genome-Phenome Archive a data committee has been installed (prof. dr. C.M.L. van Herpen and prof. dr. M.J.L. Ligtenberg).

Interoperable – all data is stored in English. All used syntaxes (Python, R and SPSS) are stored together with the data.

Reusable – all data will be stored for at least 10 years after publication and is available for future studies upon reasonable request. For the data described in chapter 2, stemming from several different databases, an elaborate database description has been written, which is stored with the data.

PhD Portfolio

Institute for Health Sciences
Radboudumc

Name PhD candidate:	G. Lassche	**PhD Period:**	1-1-2019 until 1-6-2022
Department:	Medical Oncology	**Promotors:**	Prof. dr. C.M.L. van Herpen Prof. dr. J.A. Schalken
Graduate School:	Radboud Institute for Health Sciences	**Copromotor:**	Dr. G.W. Verhaegh

Training activities	**Year(s)**	**ECTS**
a) Courses & Workshops		
- Introduction day Radboudumc	2018	0.25
- Basiscursus Regelgeving en Organisatie Klinisch onderzoekers (eBROK)	2018	1.5
- RIHS introduction day	2019	0.75
- Advanced conversation course	2019	1.5
- Data Science in Health - Jheronimus academy of data science	2019-2020	7
- Scientific integrity course	2020	1
- Statistics for PhD's using SPSS	2020	2
b) Seminars & lectures		
- Radboud Research Rounds*	2019-2021	0.4
- Research Integrity Rounds	2021	0.2
- Multidisciplinary oncology education	2019-2021	0.5
c) Symposia & Congresses		
- RIHS PhD Retreat	2019	0.5
- Roche Oncology Update	2019	0.2
- Jonge oncologenavond	2019	0.2
- Annual meeting American Assocation for Cancer Research (AACR, virtual)	2021	1.25
- Annual meeting American Assocation of Clinical Oncology (ASCO) #	2021	0.4
- Research meeting hoofd-halswerkgroep (HHWG)*	2019 & 2022	0.2
d) Other		
- Medical Oncology journal club (monthly)	2019-2022	2
- Medical Oncology labmeeting (weekly)	2020-2022	6
- Experimental Urology journal club (weekly)	2019-2022	4
- Experimental Urology work in progress meeting (weekly)	2019-2022	4
- Experimental Urology PCA3 meeting (every other week)	2020-2022	3
- Medical Oncology research meeting (monthly)	2020-2021	1
- Peer review scientific paper	2021	0.2

Teaching activities	Year(s)	ECTS
a) Supervision of internship students		
- Bachelor internship biomedical sciences Amy Heeren	2020	2
- Bachelor internship laboratory sciences Daniëlle Rijbroek	2020-2021	2
- Bachelor internship laboratory sciences Luna van Merkestein	2021	2
- Master internship medical biology Alet van der Leeuw	2021-2022	2
- Funding proposal writing biomedical sciences students	2021	0.5
b) Teaching & Organization		
- Lecture for oncology nurses (research in oncology)	2019	0.3
- Lecture for honours students (research in rare cancers)	2019 & 2020	0.3
Total		**47.15**

Oral and poster presentations are indicated with a * and # after the name of the activity, respectively.

Radboud University Radboudumc university medical center

Dankwoord (acknowledgements)

Het werk dat in dit proefschrift beschreven is, heb ik zeker niet alleen uitgevoerd. Het is het resultaat van de inspanning van velen. Ik ben erg dankbaar voor iedereen die hier een bijdrage aan geleverd heeft. Ik hoop die dankbaarheid de afgelopen jaren al kenbaar te hebben gemaakt. Maar ik wil ook deze plek nog gebruiken om daar uiting aan te geven.

Op de eerste plaats wil ik de patiënten bedanken die meededen aan de studies in dit proefschrift. In het bijzonder de vier patiënten en hun families die deelnamen aan de obductiestudie. Ik vond het heel bijzonder en een groot voorrecht dat ik in een kwetsbare en moeilijke tijd met jullie op kon trekken. Dank daarvoor! Ook wil ik hier de patiëntenvereniging speekselklierkanker benoemen. **Joost, Mark, Frans†, Saskia, Margriet (en familie!)** en **Eline**: ik waardeer ontzettend hoe jullie je inzetten voor de patiënten met speekselklierkanker. Fijn dat ik ook meermaals aan mocht sluiten bij de ledenbijeenkomsten, dat was altijd ontzettend inspirerend. Zonder jullie zou dit proefschrift er niet hebben gelegen!

Prof. dr. C.M.L. van Herpen, **Carla,** jij was het die naast mij stond bij mijn eerste stappen in de wetenschap. En het eerste deel van de weg die we samen aflegden was hobbelig, maar daarin heb ik je leren kennen als integer en betrouwbaar. Ik heb me altijd door jou gesteund gevoeld. En toen we de aandacht verlegden naar speekselklierkanker was dat echt een schot in de roos. Je gaf me veel vertrouwen en je liet me vrij om te doen wat ik leuk vond: het lab ontdekken. De vrijheid die je me gaf heeft me veel goeds gebracht, en als ik je hulp nodig had kon ik op je rekenen. Jouw hart voor het speekselklierkankeronderzoek is groot, en je gedrevenheid is iets waar ik veel van geleerd heb. Bedankt voor je begeleiding!

Prof. dr. J.A. Schalken, **Jack**, jij bent een sterke man. Je hebt veel sterke vakinhoudelijke kennis, sterke meningen en sterke verhalen. En daarmee heb je mij gedurende mijn tijd op het lab verbeterd, verrijkt en vermaakt, niet per se respectievelijk. Ik zal niet vergeten dat ik ooit een journal club gaf over een – mijns inziens – redelijk ingewikkelde paper, waarbij jij nadien aangaf dat ik het 'best aardig uitgelegd had voor een MD'. En dat vat wel zo'n beetje samen welke ontwikkeling ik doormaakte onder jouw hoede: voor wat betreft labwerk zo groen als gras, tot redelijk ingevoerd. Dank voor alles wat jij daarin voor mij betekend hebt!

Dr. G.W. Verhaegh, **Gerald,** in het Duits wordt een promotor een 'Doktorvater' genoemd. En dat dekt veel beter hoe ik jou de afgelopen jaren gezien heb: als mijn wetenschappelijke voorbeeld. Ik heb je leren kennen als iemand die gedreven wordt door weinig anders dan nieuwsgierigheid en de wil de data te begrijpen. In de samenwerking met jou was het geheel meer dan de som der delen, zowel aan de labtafel als aan de koffietafel. Ik verwacht een carrière lang plezier te hebben van de encyclopedische moleculairbiologische kennis die je

ruimschoots met me deelde. Daarnaast heeft je grote beschikbaarheid mij veel ontzorgd en vooral ook veel plezier gegeven. Bedankt daarvoor!

I would like to express my gratitude to the members of the thesis committee, **prof. dr. M.M. van den Heuvel, prof. dr. V.L.M. Vander Poorten** and **prof. dr. A. Skálová**, for their reviewing of my manuscript. Many thanks for the fast processing.

Prof. dr. N.P. Riksen, beste Niels, bedankt dat jij mij hebt begeleid als mentor. Gelukkig heb ik niet veel ad hoc gebruik hoeven maken van je aangeboden hulp, maar bij onze geplande overleggen heb je me waardevol advies gegeven.

Prof. dr. I.J.M. de Vries, beste Jolanda, toen ik aan dit promotietraject begon had ik niet vermoed dat het proefschrift eruit kwam te zien zoals het nu is. Het immunologisch onderzoek is wat uitgesteld, maar zeker niet afgesteld. Ik vond het fijn dat je bij mijn traject betrokken was en nog zult zijn. Dank daarvoor!

Heel veel van het labwerk dat beschreven is in dit proefschrift heb ik niet zelf uitgevoerd. En als ik het al zelf gepipetteerd heb, dan werd ik daar met raad en daad fors bij ondersteund. **Tilly,** jij was daarin leidend. Jij begeleidde me bij mijn eerste stapjes en leerde mij zelf organoids te kweken. En daar heb je een hele kluif aan gehad, gezien het feit dat ik over een - op z'n best - matige hoeveelheid pipetteertalent bleek te beschikken. Toch is het gelukt. En buiten dat heb ik ook genoten van de verhalen die jij altijd met je meebracht. Om met Ilja Leonard Pfeijffer te spreken: 'verhalen geven zin aan het leven'. Ik vind het een mooie bekroning van onze samenwerking dat jij paranimf bent bij de verdediging! **Onno,** jouw precisie en zorgvuldigheid verhouden zich tot de mijne als een BMW-cabriolet tot een Peugeot 206. Daar kan ik niet aan tippen, heel erg bedankt voor de eindspurt die jij aan het organoidproject gaf. **Mirjam, Jeanette, Dorien, Kees, Elze, Marion, Egbert, Nicoline, Dick** en **Renate** bedankt voor jullie hulp tijdens mijn PhD en bedankt voor het feit dat ik me altijd zo welkom heb gevoeld op jullie 'URL'. Dat geldt ook voor de andere PhD's bij de urologie: **Levi, Melissa, Elle, Iris, Manon, Cléo, Charlotte, Rayna, Sieb** en mijn U-genoot **Hossein.** De interne geneeskunde en de urologie zijn 'two worlds apart', desondanks heb ik ervan genoten met jullie op te trekken! And **Anglita,** many thanks for all your wonderful Indonesian lunches!

Amy, Daniëlle, Luna en **Alet**, door jullie als student te begeleiden heb ik zelf ook ontzettend veel geleerd. Bedankt voor jullie werk!

Beste **Wim,** dankzij jou ben ik echt met een vliegende start aan mijn promotietraject begonnen. Ik voelde me bevoorrecht dat ik op jouw werk kon voortborduren en heb zeker aan het begin veel aan je gehad. Ontzettend bedankt dat ik samen met je heb op kunnen trekken, met als kers

op de taart dat ik je paranimf mocht zijn! **Maike,** ook aan de samenwerking met jou heb ik veel gehad. We startten bijna gelijktijdig en zijn ook bijna gelijk klaar met ons onderzoek. Het was leuk om jou als maatje te hebben in het speekselklierkankeronderzoek. Je daadkracht heb ik bewonderd, het was verbazingwekkend hoe snel jij van een idee een paper wist te maken. Succes met je verdere loopbaan buiten het ziekenhuis! **Jetty,** veel succes bij het voortzetten van het speekselklierkankeronderzoek. Knap hoe jij je op de nieuwe klinische studies hebt gestort. Ik heb er alle vertrouwen in dat het goed gaat komen met die studies! **Vicky, Minke, Sarah, Dide, Martine, Wouter, Maarten, Sandra, Kim, Marije, Sophie, Lotte, Jorien, Iris, Stefan** en **Ilse:** bedankt voor de gezelligheid. Ook al was ik soms nogal veel aan de andere kant van het ziekenhuis, ik voelde me altijd welkom bij jullie!

Halverwege mijn promotietraject werden de labmeetings geïntroduceerd, daar heb ik van genoten. **Henk**, veel dank voor het initiëren hiervan. Ik vond het leuk met je te discussiëren, het heeft mijn tijd in het Radboudumc verrijkt. Also, many thanks to **Dennis** and **Kirti** for their advices regarding organoids! En **Nielka,** als ik advies op het gebied van de farmacologie nodig had kon ik altijd bij je aankloppen, bedankt daarvoor!

Bijna al het tumormateriaal dat nodig was voor het uitvoeren van de studies in dit proefschrift is binnengekomen via de biobank speekselklierkanker. Ik wil de betrokken **hoofd-halschirurgen** daarvoor hartelijk dank. En **Chantal,** veel dank voor de vele inclusies die jij gedaan hebt.

Dr. Tada, dear **Yuichiro,** during our work on the pathway analysis in SDC we had a lot of contact. I've always enjoyed working together with you. I admire your passion for your patients and I'm grateful for all your very thorough work and your trust in us. Thanks a lot! And this gratitude extends to all the co-authors in Japan.

Ik wil alle medewerkers van **Philips molecular pathway diagnostics** die betrokken waren bij de studies in deel 2 van dit proefschrift bedanken. In het bijzonder **Diederick Keizer** en **Wim Verhaegh,** jullie waren nauw betrokken, laagdrempelig te bereiken en altijd bereid mijn vragen te beantwoorden. Dank daarvoor!

Marianne, hartelijk bedankt voor jouw hulp bij diverse statistiekvragen! Ik vond het fijn dat je niet alleen vertelde wat de beste aanpak was, maar ook uitgebreid de tijd nam mij uit te leggen waarom dat het beste was. Jij loste daarmee niet alleen mijn statistiekvragen op, maar vijzelde vooral mijn kennis en kunde op dat gebied op. Daar heb ik veel plezier van gehad!

Ilse, jij was onmisbaar bij bijna alle studies die ik gedaan heb. Jouw speekselklierkankerexpertise heeft mij veel gebracht. En ook al was je druk, je nam altijd de tijd voor me en was altijd vol enthousiasme over mijn project. Bedankt voor al je hulp!

Het uitvoeren van de studie die in hoofdstuk 2 beschreven staat (de *NTRK*-studie) was erg arbeidsintensief. En het leeuwendeel van dat werk is verricht op de afdeling tumorgenetica en pathologie: **Marjolijn, Astrid, Katrien, Eveline, Erik en Patricia** heel veel dank voor wat jullie hierin betekend hebben. En in het bijzonder wil ik **Sjoerd** bedanken, het was ontzettend fijn dat jij uitgebreid bij dit project betrokken was. Ik heb je veel mails gestuurd en jij hebt me altijd uitgebreid te woord gestaan, daar heb ik veel van geleerd. Zonder jouw harde werk en precisie was het nooit zo'n mooi resultaat geworden. Ik heb heel plezierig met je samengewerkt. **Martijn,** jij ook bedankt voor jouw hulp in de controle van de data.

The work on *NTRK* gene fusion positive organoids described in chapter 7 was critically reviewed by **dr. Emiliano Cocco** and **dr. Alexander Drilon.** I am thankful for their excellent suggestions to improve the manuscript.

Bij het uitvoeren van de obductiestudie heb ik veel hulp gehad. **Willemijn,** bedankt dat jij altijd klaarstond om de beeldvorming te verrichten, ook buiten kantoortijden. En dank ook voor je hulp bij de interpretatie daarvan, dat was ontzettend waardevol! **Pui-Yuen,** bedankt voor jouw betrokkenheid bij de obducties zelf en de histopathologische analyse van de samples. Fijn dat je uitgebreid de tijd nam daarvoor. **Sander** en **Charlotte**: een groot deel van het werk ligt nog voor ons. De bioinformatica van dit project is tot nu toe niet makkelijk gegaan, maar ik ben blij dat jullie je expertise en tijd in willen zetten voor dit project.

Sander, Dorien en **Nori,** het was leuk om met elkaar op te trekken gedurende onze promotietrajecten. Hoewel de onderwerpen veel van elkaar verschilden, was de overeenkomst tussen onze vragen en frustraties groot. Ontzettend waardevol dat we dat met elkaar konden delen!

Wouter, Edward, Rick, Jan Dirk en **Arnout,** waarde Bazaleanen, jullie ontkenning van mijn wetenschappelijke vermogens was een grote drijfveer de afgelopen vier jaar. Ik hoop dat deze (E)HBO'er jullie ongelijk heeft bewezen met dit proefschrift. Ik twijfel er niet aan dat jullie dat ruimschoots toe zullen geven. Immers, jullie zullen als echte academici begrijpen dat je op basis van nieuwe informatie altijd eerder getrokken conclusies in twijfel moet trekken en je mening moet herzien. Toch?

De aanwezigheid van **vrienden** is onmisbaar in mijn leven, en dus ook de afgelopen jaren toen ik dit onderzoek uitvoerde. Zonder iedereen bij naam te noemen: bedankt voor de rijkdom die jullie aan mijn leven geven!

Ook kan ik niet zonder de steun van mijn familie, die is erg waardevol voor mij. **Teun** & **Juliëtte, Eliane** en **Sophie, Wouter** & **Judith, Lieneke** & **Ruben, Arne, Ad** & **Anja** en **Naomé, Jasper** & **Maaike, Dorine** & **Sjoerd, opa's** en **oma's, schoonouders:** ik ben ontzettend blij en gezegend met jullie als familie, niet alleen de afgelopen vier jaar. **Lien,** het is bijzonder dat we samen voor een groot deel dezelfde weg hebben bewandeld. Ik voel me vereerd dat jij mijn paranimf wil zijn!

Pa en **ma,** jullie hebben mij altijd uitgedaagd het maximale uit mijn 'cerebrale capaciteit' te halen. Dat heeft me veel gebracht. Maar het meest belangrijke is dat ik mij ontzettend bevoorrecht voel dat ik uit zo'n warm nest kom. Ik zeg dat niet vaak, maar bedankt daarvoor, dat doen jullie goed.

Henrike, zonder de stabiele basis die ik thuis elke dag vind had ik dit nooit zo goed en zo snel af kunnen ronden. Je bent onmisbaar voor mij. Ik ben gezegend met jou in mijn leven!

Sarah, jij hebt het laatste jaar van mijn promotietraject behoorlijk op z'n kop gezet. Jouw relativerende glimlach promoveert mij elke dag tot een gelukkig mens!

Curriculum Vitae

Gerben Lassche werd op 2 mei 1994 geboren te Arnhem. In 2011 behaalde hij het gymnasiumdiploma aan het Greijdanus College te Zwolle (cum laude). In datzelfde jaar begon hij met de studie geneeskunde aan het Radboud universitair medisch centrum in Nijmegen. In het voorjaar van 2018 behaalde hij het artsexamen (cum laude).

Direct hierna startte hij als arts-onderzoeker op de afdeling Medische Oncologie met een project naar hyperthermie als oncologische therapie (supervisor: prof. dr. C.M.L. van Herpen). Na driekwart jaar onderzoek naar deze therapie te hebben gedaan deed de mogelijkheid zich voor om dit te vervolgen met een promotieonderzoek naar speekselklierkanker met als (co)promoteren prof. dr. C.M.L. van Herpen, prof. dr. J.A. Schalken en dr. G.W. Verhaegh. Dit translationele onderzoek vond grotendeels plaats in het laboratorium voor experimentele urologie. De resultaten van dit onderzoek zijn beschreven in dit proefschrift. Gedurende zijn promotieonderzoek volgde hij de opleiding Data Science in Health aan de Jheronimus Academy of Data Science (JADS) in Den Bosch, die hij in 2020 afrondde.

Op 1 augustus 2022 is hij in het Canisius-Wilhemina Ziekenhuis te Nijmegen gestart met het eerste deel van de opleiding tot internist (opleider: dr. B.A.J. Veldman). Het tweede deel van die opleiding zal plaatsvinden in het Radboudumc (opleiders Radboudumc: dr. G.M.M. Vervoort en dr. E.M. Klappe).

Gerben is getrouwd met Henrike Lassche-Grunewald. Samen hebben zij een dochter, Sarah (2021).

Radboudumc
university medical center

Radboud University